Investigation of the Role of Asprosin and Downstream Glycolytic Molecules in Ovarian Cancer

A thesis submitted for the degree of Philosophy Doctor

by

Rachel KERSLAKE

College of Health and Life Sciences

BRUNEL UNIVERSITY LONDON

Abstract

Ovarian Cancer (OvCa) affects over 313,000 women globally, and is consistently defined as the most lethal form of gynaecological malignancy. Despite improvements to cancer biology and therapeutics, the arsenal to tackle OvCa has limitations, and there is still scope for better understanding of the disease. Augmented glycolysis and conversion of glucose to lactate within the tumour microenvironment (TME) is a process required for cell proliferation and long-term maintenance.

Through investigation of the novel glucogenic hormone asprosin, this work presents evidence of a possible regulator of glycolysis within the TME and assesses the biomarker potential of glycolytic molecules in OvCa detection and the monitoring of progression. Asprosin is expressed in OvCa of varying stage and subtype, with high expression of predicted receptors OR4M1 and TLR4 also evident. OR4M1 shows promise as a biomarker of early stage OvCa with significant decline seen in later stages ($p < 0.04$). Similarly, both receptors were detected in cancer-associated circulating cells with a decline recorded for OR4M1 as treatment progressed ($p < 0.0069$). In addition, olfactory receptors were seen to co-localise in cancer with cell entry mediators for SARS-CoV-2 and their distraction might be implicated in the anosmia seen in many COVID-19 patients.

Transcriptomic analyses revealed that asprosin can potentially influence integral cancer progressing pathways such as TGF-β, ROS and angiogenesis, plus the phosphorylation of the signalling molecule ERK 1/2 ($p < 0.01$). Additional work, highlights the biomarker potential of lactate; a signalling molecule and product of glycolysis in OvCa. Significantly elevated levels of lactate at rest were recorded, above the normal range of 0.2–2 mmol/L, in OvCa patients compared with controls ($p<0.0001$); with an area under curve (AUC) of 0.96. High lactate is seen regardless of treatment, age or BRCA status in OvCa patients. Moreover, RNA expression of the lactate receptor hydroxycarboxylic acid receptor 1 (HCAR1) is significantly upregulated in OvCa compared to controls ($p < 0.001$). HCAR1 showed widespread protein expression in OvCa patients including clear cell carcinoma (CCC), high grade serous carcinoma (HGSOC), low grade serous carcinoma (LGSOC), endometrioid adenocarcinoma (EAC), mucinous adenocarcinoma (MAC), lymph node metastasis (MET), and normal adjacent tissue (NAT).

Concluding investigations sought the current landscape of OvCa models in the literature. Focusing on 3D culture it was found that OvCa cells grown in this manner were more representative of *in vivo* systems compared with conventional monolayer cultures. In addition, 3D OvCa culture showed an enhanced ability to mimic complex processes such as angiogenesis, drug resistance and cell signalling.

This study provides novel evidence for the expression of an intact asprosin signalling pathway in OvCa both at tissue and liquid biopsy level. Additional evidence of the clinical utility of resting lactate levels for OvCa patients is also presented. Future studies should concentrate on the understanding of asprosin-receptor-mediated mechanisms, its role in metabolic changes and the potential biomarker utility of asprosin-related genes as well as lactate.

List of Abbreviations

ACE2	**A**ngiotensin **C**onverting **E**nzyme **2**
AUC	**A**rea **U**nder **C**urve
AgRP	**A**gouti **R**elated **P**rotein
BC	**B**reast **C**ancer
BRCA	**BR**east **CA**ncer gene
BER	**B**ase **E**xcision **R**epair
cAMP	**c**yclic **A**denisine **M**ono **p**hosphate
CA125	**C**ancer **A**ntigen **125**
CCC	**C**lear **C**ell **C**arcinoma
CCs	**C**irculating **C**ells
CTC	**C**irculating **T**umor **C**ell
DM	**D**iabetes **M**ellitus
EAC	**E**ndometrioid **A**deno **C**arcinoma
ECM	**E**xtra **C**ellular **M**atrix
EMT	**E**pithelial to **M**esenchymal **T**ransition
EpCAM	**E**pithelial **C**ell **A**dhesion **M**olecule
FBN1	**Fi**b**rilli**n **-1**
FBN2	**Fi**b**rilli**n **-2**
FDA	**F**ood and **D**rug **A**dministration
FSH	**F**ollicle **S**timulating **H**ormone
FIGO	**F**ederation of **G**ynecology and **O**bstetrics
GDM	**G**estational **D**iabetes **M**ellitus
GPCR	**G** **P**rotein **C**oupled **R**eceptor
HCAR1	**H**ydroxy **C**arboxylic **A**cid **R**eceptor **1**
HGSOC	**H**igh **G**rade **S**erous **O**varian **C**ancer
HR	**H**omologous **R**epair
IR	**I**nsulin **R**esistance
IUGR	**I**ntra **U**terine **G**rowth **R**estriction
GLOBOCAN	**Glob**al **Can**cer Observatory
JNK	**J**un **N**-terminal **K**inase
LH	**L**uteinizing **H**ormone
LGSOC	**L**ow **G**rade **S**erous **O**varian **C**ancer
LPS	**Li**p**o**poly**s**acharide
MAC	**M**ucinous **A**deno **C**arcinoma
MAPK	**M**itogen **A**ctivated **P**rotein **Kinase**

MET	**Met**astasis
MMP	**M**atrix **M**etallo **P**roteinases
NAT	**N**ormal **A**djacent **T**issue
NCI	**N**ational **C**ancer **i**nstitute
NPS	**N**eonatal **P**rogeroid **S**yndrome
OOC	**O**rgan **O**n a **C**hip
OR	**O**lfactory **R**eceptor
OR4M1	**O**lfactory **R**eceptor **4** **M**ember **1**
OS	**O**verall **S**urvival
OvCa	**Ov**arian **Ca**ncer
OXPHOS	**Ox**idative **Phos**phorylation
PARP	**P**oly **A**DP **R**ibose **P**olymerase
PARPi	**P**oly **A**DP **R**ibose **P**olymerase **i**nhibitor
PCOS	**P**oly**c**sytic **O**varian **S**yndrome
PDX	**P**atient **D**erived **X**enografts
PFS	**P**rogression **F**ree **S**urvival
PKA	**P**rotein **K**inase **A**
POMC	**P**ro **O**pio **M**elano **C**ortin
PTPRD	**P**rotein **T**yrosine **P**hosphatase **R**eceptor **T**ype **D**
STAT3	**S**ignal **T**ransducer **A**ctivator **T**ranscription **3**
T2DM	**T**ype **2** **D**iabetes **M**ellitus
TAU	**Tau**opathy
TBI	**T**raumatic **B**rain **I**njury
TCGA	**T**he **C**ancer **G**enome **A**tlas
TF	**T**ranscription **F**actor
TGF-β	**T**ransforming **G**rowth **F**actor **B**eta
TLR4	**T**oll **L**ike **R**eceptor **4**
TME	**T**umour **M**icro **E**nvironment
TMPRSS2	**T**ransmembrane **P**rotease **R**eceptor **S**erine **2**
TMPRSS4	**T**ransmembrane **P**rotease **R**eceptor **S**erine **4**
VEGF	**V**ascular **E**ndothelial **G**rowth **F**actor
WAT	**W**hite **A**dipose **T**issue
WHO	**W**orld **H**ealth **O**rganization

Contents

List of Figures

List of Tables

Acknowledgements

Firstly, I want to express my wholehearted thanks to the patients who kindly donated their samples for this research and to the amazing NHS staff who supported the project in addition to the Cancer Treatment and Research Trust (CTRT) and University Hospitals Coventry and Warwickshire NHS Trusts.

Dr Emmanouil Karteris I cannot thank you enough, your guidance throughout this PhD has been invaluable. Thank you so much for letting me be a part of your lab and for supporting me through numerous publications and failed experiments as well as a pandemic! And for helping me grow as a researcher, I will forever be in your debt and cannot wait to see what future collaborations hold. Dr Cristina Sisu thank you so very much for all that you have taught me, especially the "for loops", you've led me to my dream career and I shall never forget all of your support.

CBCEL it's been an honour to be a member and I will miss you all terribly. Suzana, thank you so much for everything, you will always be the Queen of the western blots and I owe my sanity to you and cannot wait for our next project together!

To my mam thank you for sharing your love of science with me and setting me on this path. To my family, thank you so much for always being there to support me and keep me going even if you think I'm crazy most of the time. Carys thank you for always being just a phone call away, our early morning calls kept me going so often when I felt like giving up, I could not have done this without your support. And lastly Becky, thank you so much for putting up with all of my ranting and raving about blots and qpcrs over the years, I owe a large chunk of this work to you (along with all the commas) and would never have finished without you calling out all of my procrastination, pouring me a cuppa and telling me to get on with it.

Declaration of Authorship

I, Rachel KERSLAKE, declare that this report titled, "Investigation of the Role of Asprosin and Downstream Glycolytic Molecules in Ovarian Cancer" and the work presented within are my own.
I confirm that:

- This work was done while in candidature for a research degree at Brunel University.
- Where the published work of others has been consulted, it is always clearly attributed.
- Where I have quoted from the work of others, the source is always given. With the exception of such quotations, this thesis is entirely my own work.
- I have acknowledged all main sources of help.
- Where the thesis is based on work jointly with others, I have acknowledged those responsible and noted their contributions.
- Unless stated otherwise all figures within this work were created in part using stock components from SMART - smart.servier.com and complied by myself.

Signed: Rachel Kerslake

Date: 09.11.2022

Chapter 1

Introduction

Ovarian Cancer (OvCa) is continuously characterized as one of the most lethal forms of gynaecological malignancy. With over 313,000 cases of OvCa recorded globally and a five-year survival rate of less than 30%, OvCa is one of the most lethal forms of female cancer (Sung et al., 2021; Siegel, Miller, and Jemal, 2019).

Despite increasing rates of incidence, and associated high mortality, the molecular mechanisms that influence the development and progression of OvCa are poorly defined. Exploring OvCa aetiology is imperative for furthering advancements in disease prevention and improved outcome (Reid, Permuth, and Sellers, 2017). In order to understand the mechanisms involved in the development and progression of OvCa, an understanding of associated molecular mechanisms and the tumour microenvironment (TME) is required. Current research however is limited in accurately modelling the complex metabolic landscape of OvCa (Matulonis et al., 2016).

Elevation of energy metabolites such as glucose, lactate, and associated hormones can drive an efflux of aerobic glycolysis. This shift in energy metabolism from mitochondrial oxidative phosphorylation (OXPHOS), to an incomplete process, that is quicker, yet requires higher levels of glucose, is known as the Warburg effect (Vander Heiden, Cantley, and Thompson, 2009). Deregulation of cellular energetics, is considered a hallmark of cancer and is implicit in OvCa prognosis and severity; as such investigations seek to therapeutically target pathways involved in the mediation of aerobic glycolysis (Kellenberger et al., 2010; Hanahan and Weinberg, 2011).

Considering the detriment OvCa presents to female health, influencing factors associated with energy metabolism warrant investigation for a thorough approach towards elucidation of disease aetiology. The glucogenic hormone asprosin, is therefore a promising candidate for exploration given its ability to regulate glucose homeostasis, and its association with disorders classified by their augmented energy profiles (Hoffmann, Xie, and Chopra, 2020). Since discovery, this relatively novel hormone has presented as dysregulated in insulin resistance (IR), diabetes, obesity, polycystic ovarian syndrome (PCOS), and pathological pregnancy related disorders (Hoffmann, Xie, and Chopra, 2020; Hoffmann et al., 2022; Groener et al., 2019).

Of note, many asprosin related metabolic disorders are also considered risk factors of OvCa i.e., obesity and insulin resistance (Craig et al., 2016). As such investigation of the role of asprosin, associated receptors and metabolites within the TME may provide pathological insight into unknown metabolic pathways associated with OvCa.

In order to recapitulate the TME, OvCa models must also be considered; in addition to conventional monolayer tissue culture emerging technologies using 3D culture techniques may provide deeper insight into the physiological mechanisms exerted by hormones and glycolytic metabolites such as asprosin and lactate, within the TME.

1.1 Female Reproductive Tissue Disease

The female reproductive system is regulated by a series of hormonal interactions, locally and peripherally, through feedback mechanisms such as the hypothalamic – pituitary axis (Messinis, Messini, and Dafopoulos, 2014). The tightly regulated interactions of hormonal pathways and molecular signals coordinate reproductive homeostasis and fertility. The major organs of the female reproductive system are outlined in Figure 1.1.

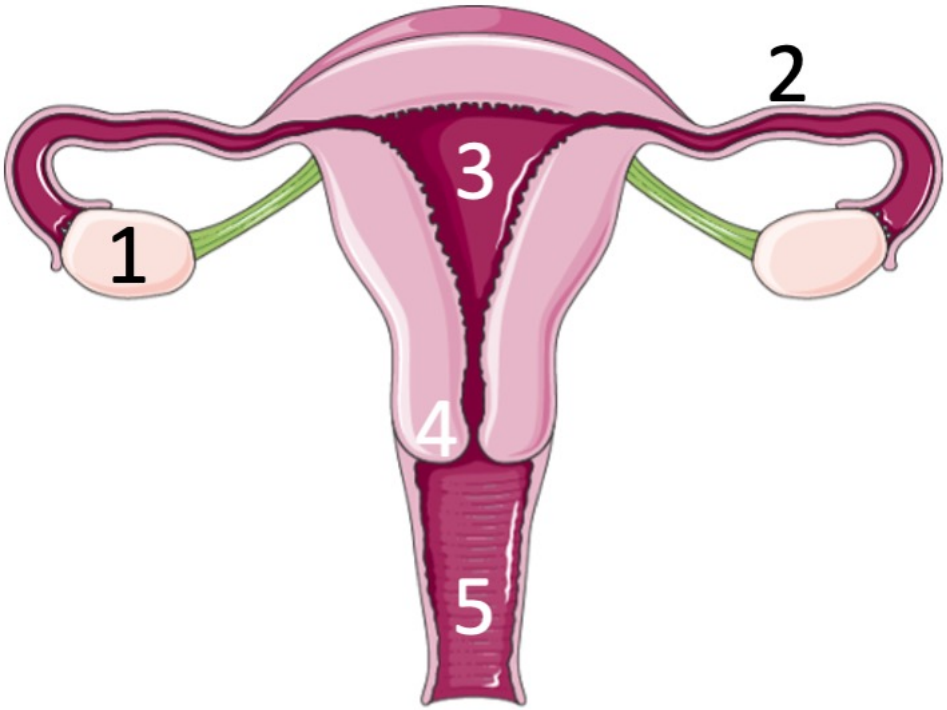

FIGURE 1.1: Female Reproductive System
Schematic of the primary organs of the female reproductive tract, showing: 1, The ovaries; 2, Fallopian tubes; 3, Uterus; 4, Cervix and 5, Vagina.

1.2 Ovarian Cancer

1.2.1 The Ovary in Health and Disease

The ovaries are primary sex organs responsible for the homeostasis of female reproductive hormonal axes (Messinis, Messini, and Dafopoulos, 2014). Development of the ovaries takes place around day 34 of gestation. Arising from the intermediate mesoderm, they are comprised of theca cells, stromal components, granulosa, follicular and epithelial cells, in addition to primary oocytes (Rimon-Dahari et al., 2016). The ovaries are vital for steroidal hormone production and the homeostasis of molecular mechanisms pertinent to fertility and reproduction; tightly regulated fluctuations of hormones from the ovaries during menarche mediate the onset of menstruation and peripheral organ development, including breast tissue growth.

Menstruation, depicted in Figure 1.2, is mediated via steroidal sex hormones such as oestrogen, Follicular Stimulating Hormone (FSH), Luteinizing Hormone (LH) and progesterone. All of which are regulated locally via the ovarian follicles and peripherally via the hypothalamic-pituitary-ovarian axis (Messinis, Messini, and Dafopoulos, 2014). This balance of feedback mechanisms contributes to a process of follicular release and transition of ova into the fallopian tubes, and the potential maintenance of pregnancy.

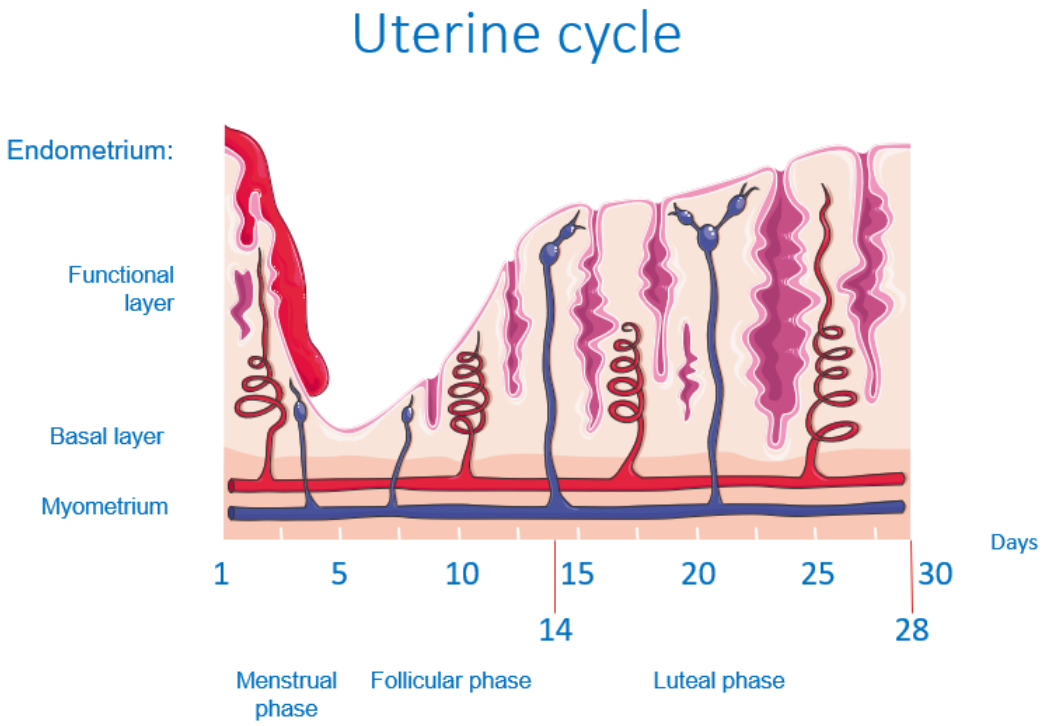

FIGURE 1.2: The Uterine Cycle
Diagram depicting changes of the uterine lining throughout the menstural phase, follicular phase and luteal phases of the menstrual cycle. Created with Servier Medical Art.

At birth, follicular cells contain a finite number of haploid gametes, ova, many of which perish or pass through the Fallopian tubes to be expelled along with the uterine lining during menstruation (Lindheim et al., 2018).

Over a life time roughly 300 - 400 of the 1 million ova present at birth are released. The remaining undergo atresia, perishing within the follicle, causing fertility to decline as age progresses (Lindheim et al., 2018). If fertilised however, an ova develops into a zygote, which then embeds within the endometrial lining of the uterus in preparation of the gestational process of foetal growth and development.

1.2.2 Reproductive Disease

Many women shy away from discussing their reproductive health due to societal and/or cultural stigma, however conditions affecting the female reproductive system are increasingly common (Lindsay and Vitrikas, 2015; Sims et al., 2021).

Fertility, is perhaps the most commonly thought of when reproductive health comes into question, with 15% of couples globally, struggling to conceive, the cause is not always known (Sun et al., 2019). There are a number of known conditions that can however have a detrimental effect on general health and in some cases decrease a woman's chance of pregnancy (Lindsay and Vitrikas, 2015).

One of the most common female reproductive disorders, affecting 1 in 10 women globally, is polcystic ovary syndrome (PCOS) (Cadagan, Khan, and Amer, 2016). This condition results in the production of excess androgen, which causes the ovaries to enlarge and in many cases develop multiple fluid-filled follicles. Additional symptoms include irregular menses and potential infertility.

Uterine fibroids are non-cancerous growths that can cause, pain, discomfort and heavy menstrual bleeding. Over 80% of women over the age of 50, are thought to develop at least one fibroid in their lifetime, regardless of ethnicity (Yaryari et al., 2022). Although less frequent, uterine fibroids can also develop in young women. They are often benign and go away on their own but in extreme cases can result in infertility and require surgical ablation (Piekos et al., 2022).

Endometriosis, is an increasingly common painful metabolic disorder characterised by endometrial cell growth outside of the uterus (Mackenzie and Cohn, 2022). Each month the womb lining is expelled vaginally. However, peripheral endometrial cells, cannot leave this way and instead break down within the body, causing inflammation and scarring. Affecting at least 10% of the global female population, diagnosis of this disorder is often probelmatic as medical confirmation may only take place following surgery (Schliep et al., 2022).

Additional non-hereditary disorders include sexually transmitted diseases as well as common yeast, bacterial and viral infections, such as: thrush, bacterial vaginosis, and human papilloma virus (HPV); the latter of which is associated with an increased risk of cervical cancer development (Liu et al., 2022; Keddem et al., 2022; Pache et al., 2022).

Breast Cancer (BC) is one of the most common forms of cancer to affect women, with 99% the the 2,261,419 BC cases recorded in 2020 affecting women (Sung et al., 2021). Diagnosis of other female cancers including those of reproductive origin, are also increasing in recognition (Table 1.1). Cervical and uterus cancer show the highest incidence with 604,127 and 417,367 cases detected in 2020, respectively (Zhang et al., 2019a; Sung et al., 2021).

TABLE 1.1: Incidence rates of cancers of female reproductive origin.

Cancer	**Global Cases**
Endometrial	382,069
Cervical	417,367
Uterus	604,127
Vagina	17,908
Vulva	45,240
Ovarian	313,959

The aetiology of many cancers from female reproductive tissues remains poorly defined (Lheureux et al., 2019). Despite not being the most frequent, OvCa has remained the most lethal of gynaecological malignancies over the decades, and continues to see an upward trend in cases, with 313,959 women diagnosed worldwide in 2020 (Lheureux et al., 2019). As such further research is imperative for early detection and advancements in therapeutics.

1.2.3 Epidemiology of Ovarian Cancer

There are many metabolic diseases and disorders associated with the ovaries such as endometriosis, PCOS, and OvCa (Lheureux et al., 2019). Many female reproductive disorders are associated with unspecific symptoms and are often misdiagnosed; with treatment and management delayed (Fotopoulou et al., 2017).

Owing to the unspecific nature of symptoms and societal stigma surrounding female health in many countries, disorders such as OvCa are often diagnosed at a late stage, leading to poor prognosis and survival outcomes (Slatnik and Duff, 2015). As such the literature remains unchanged over the decades in defining OvCa as one of the most lethal forms of gynaecological malignancies.

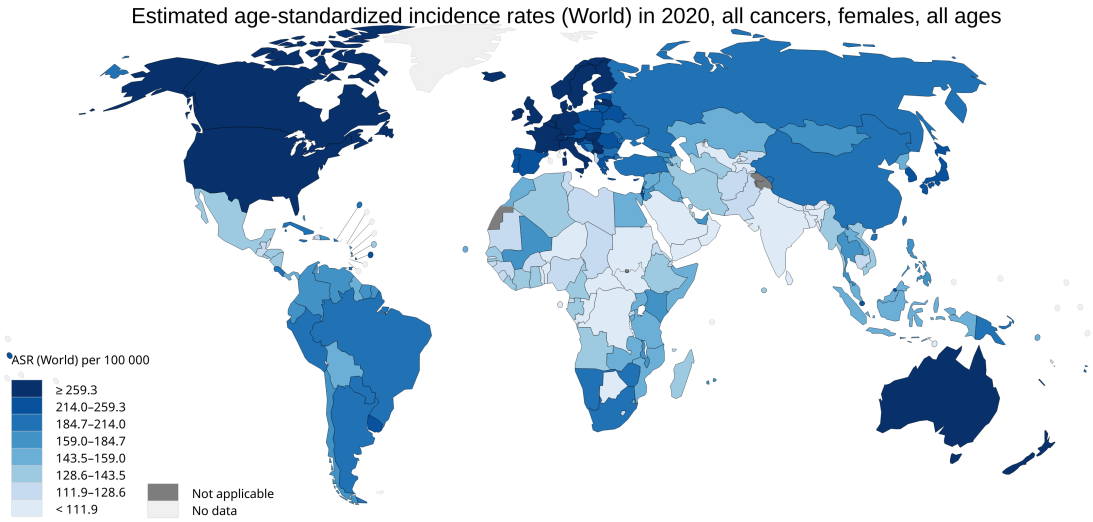

FIGURE 1.3: Global Incidence of Ovarian Cancer
Gradient map depicting OvCa incidence. Highest age standardised incidence rates (ASR) recorded in the Northern hemisphere as well as Australia, with lower incidences recorded in Africa (International Agency for Research on Cancer, 2020).

In 2020 the Global Cancer Observatory (GLOBOCAN) recorded over 313,959 cases of OvCa worldwide, with an annual death rate of 184,779 (Sung et al., 2021). Estimated incidences of OvCa are thought to be higher in Europe and North America compared to Asia and Africa (Figure 1.3). Despite medical advancements, incidence rates of OvCa, continue to see an upward trend year on year (Jessmon et al., 2017). Therefore this thesis will seek to further the understanding of metabolic pathways associated with the development, progression and prognosis of OvCa with hopes to further advancements in early-stage biomarker detection.

1.2.4 Histology of Ovarian Cancer

OvCa may arise from the sex cord stromal, germ or epithelial cells of the ovary (Kaku et al., 2003). Epithelial OvCa is the most prevalent form of OvCa, accounting for around 90% of cases and consists of the following histological sub types (Figure 1.4); high grade serous carcinoma (HGSOC), endometroid (EAC), clear cell (CCC), mucinous carcinoma (MAC) and low grade serous carcinoma (LGSOC) (Matulonis et al., 2016). The remaining 10% of OvCa's arise evenly from germ line (5%) and sex cord stromal (5%) origin.

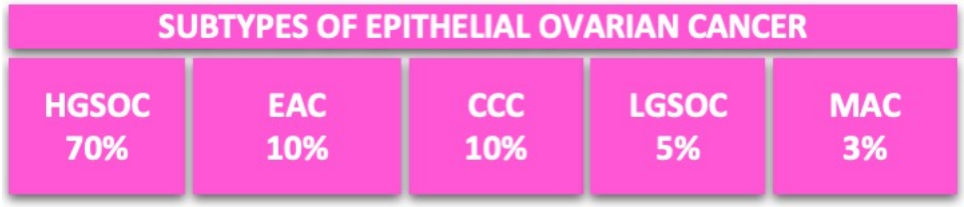

FIGURE 1.4: Histological Subtypes of Epithelial Ovarian Cancer
Sub types of epithelial OvCa. High Grade Serous (HGSOC), 70%; Endometroid Adenocarcinoma (EAC), 10%; Clear Cell (CCC), 10%; Low Grade Serous (LGSOC), 5%; Mucinous Adenocarcinoma (MAC), 3%.

High grade serous OvCa (HGSOC) accounts for 70% of epithelial OvCas, making it the most common of histological sub types (Kurman and Shih, 2016). Despite a detailed understanding of the morphological traits associated with epithelial OvCa, the aetiology is not clearly elucidated.

1.2.5 Ovarian Cancer Detection and Diagnosis

Cancer stages are a standardised set of parameters used to clinically define the status of a specific tumour type at the point of diagnosis, often in terms of cell type, size, grade, and status of metastasis (Table 1.2)(Berek et al., 2021). Around 80% of epithelial OvCas are detected during the later stages (III and IV) of disease, where long term survival is around 29%. This is a stark contrast to the 92% survival rate of those diagnosed at stages I – II (Elias, Guo, and Bast, 2018).

(see Table 1.2).

TABLE 1.2: Ovarian Cancer stages as defined by the Federation of Gynecology and Obstetrics (FIGO)

Stages	**Description**
Stage I	
Stage IA	Tumour is confined to a single ovary with no surface expression.
Stage IB	Both ovaries, in addition to the fallopian tubes, yet no acetic involvement or lymphatic spread.
Stage IC	Tumour is confined to one/both ovaries with signs of the tumour on the ovary surface, rupture of tumour capsule before or during surgery and/or malignant cells in ascites.
Stage II	
Stage IIA	Metastasis outside the ovaries in the uterus or fallopian tubes.
Stage IIB	Metastasis to organs of the pelvic cavity i.e., the bladder.
Stage IIC	The tumour has protruded into other tissues of the peritoneum with cancer cells in ascitic fluid.
Stage III	
Stage IIIA	Lymphatic spread or microscopic malignancy found outside of the pelvis.
Stage IIIB	Tumour < 2cm outside the pelvic cavity including surface of liver and/or spleen.
Stage IIIC	Tumour > 2cm outside the pelvic cavity.
Stage IV	
Stage IVA	Pleural effusion positive for malignant cells.
Stage IVB	Metastasis to distant sites including extra-abdominal as well as liver or spleen.

Delays in diagnosis are in part due to the asymptomatic and often vague nature symptoms, as well as limitations in current screening methods and technology, used for detection globally (Fotopoulou et al., 2017). Associated symptoms may include bloating, constipation, increased frequency of urination as well as pelvic/abdominal pain, and are often dismissed as menopausal symptoms (Sims et al., 2021).

Diagnosis typically requires trans-vaginal sonography as well as computerised tomography (CT) and a carbohydrate antigen 125 (CA125) protein biomarker test (Ebell, Culp, and Radke, 2016). CT uses x-ray imaging techniques and computerised systems to create a detailed profile inside the human body and is capable of detecting physical lesions and abnormalities (Engbersen et al., 2021). Positron

emission tomography (PET) scans are a more complex form of imaging that utilises radioactive glucose to produce a three-dimensional image of areas that consume high levels of glucose such as cancer (Yu et al., 2023). PET is becoming increasingly common in cancer detection; however, it is not currently used for the primary detection of OvCa owing to often indistinguishable results between benign and cancerous ovarian growths, with elevated absorption of glucose also seen in follicular cysts of pre-menopausal patients as well as those with endometriosis (Engbersen et al., 2021). PET also struggles to detect MAC due to the low uptake of radioactive glucose seen in this subtype of OvCa (Dejanovic, Hansen, and Loft, 2021). As such it is often used to monitor progression and cancer recurrence (Cengiz et al., 2019).

Over the last four decades, the detection of elevated CA125 levels in the blood (>35 U/ml), have proven useful for diagnostic referral, as such CA 125 has remained a constant in primary diagnostics of OvCa (Dochez et al., 2019). There are however drawbacks to this method; elevated levels may also indicate other gynaecological disorders such as endometriosis and PCOS and are also indicative of smoker status; rendering CA125 alone, problematic (Lycke et al., 2021). As such efforts to detect novel biomarkers to enhance the criteria used in OvCa screening are underway.

1.2.6 Treatments of Ovarian Cancer

Depending on stage, invasion and status of metastasis, a treatment plan is comprised accordingly. This may include partial or full removal of the ovaries (oophorectomy), along with a full hysterectomy (Xie, Meng, and Liao, 2022).

Adjuvant platinum-based chemotherapy such as cisplatin is often favoured in treatment (Tchounwou et al., 2021). Cisplatin targets DNA replication through the cross linking of purine bases, not only preventing replication, but also disrupting repair mechanisms triggering apoptosis (Dasari and Tchounwou, 2014). As cancer cells replicate at an increased rate, they are more susceptible to the effects of chemotherapeutics, however other cells are affected resulting in undesirable side effects such as kidney damage, numbness and vomiting (Yanagawa et al., 2022).

Additional targeted drug therapies including Poly ADP Ribose Polymerase inhibitors (PARPi) such as niraparib and olaparib, are often used in advanced cases (Lheureux et al., 2019). PARPi's are particularly effective in OvCa and BC classified with BRCA1 and 2 mutation (Bryant et al., 2005). In patients with BRCA mutations the

repair mechanism known as Homologous Repair (HR), is rendered inaccessible, as such an alternate pathway, base excision repair (BER) is used (Ray-Coquard et al., 2019). The protein Poly ADP Ribose Polymerase (PARP), is integral for the stabilisation of replication forks within BER. PARPi however suppress BER through preferentially binding to the active sites of PARP, which inhibits NAD+ mediated activation (Rose et al., 2020; Bryant et al., 2009). Inhibition of PARP then causes down regulation of the cystine transporter SLC7A11, and depletion of glutathione biosynthesis, which consequently promotes lipid peroxidation and ferroptosis (iron dependent cell death) (Hong et al., 2021). PARPi's have also proven effective when used in combination with platinum-based therapies, with studies recording improved survival in 10% of cases (González-Martín et al., 2019).

Bevacizumab may also be used in treatment, especially during instancies of relapse (Hall et al., 2020). Bevacizumab is a mono-clonal antibody that inhibits circulating vascular endothelial growth factor (VEGF), limiting the growth of blood vessels, consequently interrupting nutrient supply to the tumour (Wu et al., 2020; Ribatti, 2022). Unfortunately, chemotherapy resistance in advanced stage and relapse is increasingly common, as such new avenues of mechanistic exploitation are continually under investigation (Pokhriyal et al., 2019).

1.2.7 Liquid Biopsy

A novel area of investigation, with diagnostic and prognostic potential, includes the use of liquid biopsy for the detection of biological markers in fluids such as blood, urine, cerebrospinal fluid, or sputum (Alix-Panabières and Pantel, 2021). Samples may be screened for entities such as cancer associated circulating cells (CCs), circulating tumour DNA and cell-free RNA, as well as tumour specific proteins (i.e. CA 125) and other molecular biomarkers (Lianidou and Pantel, 2019). Additional research also explores the potential of molecules released from tumour cells such as extracellular vesicles as markers of diseases such as cancer (Pink et al., 2022). Liquid biopsy is a non-invasive technique that offers increased potential for sequential monitoring of disease progression, overcoming the limitations of tissue biopsies such as surgical risk, feasibility and cost. Application of liquid biopsy analysis in clinical settings is being explored in a wide range of cancer types including, ovarian, lung, colon, esophageal and thyroid (Kumar et al., 2019).

1.2.8 Cancer Associated Circulating Cells

In the last decade CCs in particular have received growing interest for prognostic and clinical application. CCs are thought to arise from primary tumour sites following the loss of cellular adhesion during epithelial to mesenchymal transitioning (EMT) (Kalluri and Weinberg, 2009). These cells become suspended within the circulation (Figure 1.5), where they are transported to secondary sites to act as important prerequisites for tumour metastasis (Paterlini-Brechot and Benali, 2007). As such this increased cellular mobility is thought to aid the development of secondary metastases including bowel and abdominal cancers in OvCa (Hong, Fang, and Zhang, 2016).

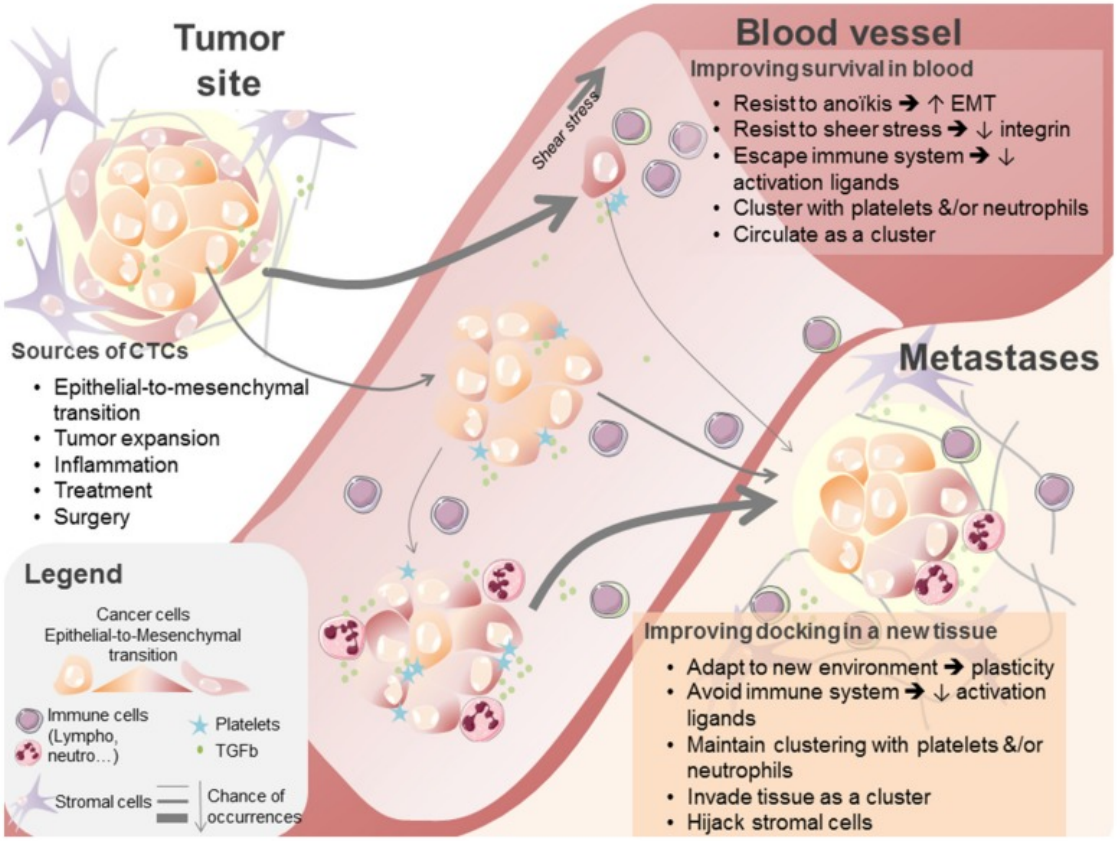

FIGURE 1.5: Origin and Transition of Cancer Associated Circulating Cells

CCs lose adhesion during epithelial to mesynchymal transition, and are subsequently released into the blood. Here they circulate and are shown to evade the immune system and spread to distant sites of secondary metastasis (Image taken from: Mari et al., 2019).

Studies show that elevated CCs in cancers such as lung and OvCa correlate negatively with therapeutic response and are indicative of poor survival (Botteri et al., 2010; Chudasama et al., 2019a). It has therefore been suggested that CCs have the potential to provide insight into the heterogenic landscape of malignant tumours, and the possible identification of therapeutic targets (Krebs et al., 2010; Chudasama et al., 2019a; Kumar et al., 2019). The detection of CCs can be achieved using multiple different techniques, with the application of methodology specific to research question and/or clinical relevance (Table 1.3)(Yang, Giret, and Cote, 2021).

Of current methods, the affinity based CellSearch (Janssen Diagnostics) proves the

TABLE 1.3: Techniques used for the separation and identification of CCs

Function	**Platform**
Label Free	
Gradient/Centrifugation	Ficoll-Paque RareCyte
Size Based	Circulogix ISET ScreenCell Parsortix
Dielectrophoresis	ApoSTream DEPArray
Affinity Based	
Immunomagnetic	CellSearch Adna Test MACS
Microfluidic	GEDI Chip OncoCEE Clearbridge BioMedics
Surface Based	ImageStream HD Imaging

most reliable/consistent in a clinical setting. CellSearch has recieved U.S. Food and Drug Administration (FDA) approval for the enumeration of epithelial based CCs in the blood of metastatic breast, prostate and colon cancer patients (Tu et al., 2015). Translation to other cancers however is not necessarily straight forward. The standardised cellular markers used in affinity based CC detection include epithelial cell adhesion molecule (EpCAM), CD45 hematopoietic marker and an array of cytokeratins (Andree, Dalum, and Terstappen, 2016).

However the expansive phenotypic landscape and loss of adhesion seen in cancers

such as OvCa render many markers inconsistent (Yang, Giret, and Cote, 2021). Cellular markers such as EpCAM for example are unable to capture cells that have lost adhesion during EMT, rendering this marker problematic (Wicha and Hayes, 2011). As such results obtained are non-comparable. The most efficient tool for CC detection is therefore dependant on the research question at hand and the nature of the cancer cells. Therefore, refined methods and improved biomarkers are necessary for accurate detection and clinical application of CCs in additional cancers.

1.2.9 Heritability, Heterogenicity and Risk Factors

OvCa is considered a heterogenous disease and is influenced by a number of genetic and environmental risk factors (Andrews and Mutch, 2017). OvCa typically presents in postmenopausal women, and is associated with a family history of ovarian and breast cancers (Paul and Paul, 2014).

Around 20% of cases are thought to be linked to heritable germ line mutations of genes, including BRCA1 and BRCA2 (Flaum et al., 2020). Both BRCA genes are involved in the DNA repair mechanism known as homologous recombination (HR); BRCA1 is involved in both detection and repair of double strand breaks, while BRCA2 is a core mediator of repair through the recruitment of proteins such as RAD51 (Roy, Chun, and Powell, 2011; Filipe et al., 2022). Mutations in BRCA genes can increase lifetime risk of developing OvCa by 11 - 68% (Kuchenbaecker et al., 2017). As such those with a family history of BRCA related OvCa or BC are often closely monitored (Elias, Guo, and Bast, 2018). Of note mutation of the tumour suppressor gene TP53, is considered one of the most frequent genomic alterations in malignant transformation and is also recorded in over 90% of OvCas (Ahmed et al., 2010; Bell et al., 2011).

Ethnicity may also contribute to risk, with Caucasian women presenting the highest risk and Chinese women appearing on average to develop OvCa roughly 10 years earlier than the average age of 60 (Shen et al., 2017; Webb and Jordan, 2017). Other risk factors include nulliparity, weight and a diet high in fat (Beral, 2007; La Vecchia, 2017).

Increased lifetime risk of developing OvCa has also been recorded for individuals exposed *in-utero* to the now banned, and since proven ineffective, anti-miscarriage, synthetic hormone diethylstilbestrol (Koushik et al., 2017). There is an abundance of

data showing that this xenoestrogen increases oestrogenic action *in utero*, with the national cancer institute (NCI) characterising it as a carcinogen capable of increasing the risk of cancers such as breast, cervical, and pancreatic. Thereby, implying that *in utero* exposure to xenoestrogens, and transgenerational risk factors, are also capable of influencing the development female reproductive malignancies (Troisi et al., 2018).

Metabolic disorders such as PCOS, insulin resistance (IR) and diabetes mellitus (DM) are also implicated with increased risk and a negative effect on overall outcome in patients with OvCa (Sun et al., 2016; Ding et al., 2018). Endometriosis, is also associated with a significant increase in the risk of developing sub-type specific forms of OvCa such as: CCC, LGSOC and EAC (Pearce et al., 2012). Furthermore, pathologically elevated levels of glucose, and obesity, are also complicit in the development of OvCa (Kellenberger et al., 2010).

1.2.10 Menopause and Cancer risk

Menopause is a natural stage in biological aging that marks the cessation of menstruation permanently, and the end of fertility (Hall, 2015). Typically, menopause takes place between the ages of 45 and 55, lasting 10 - 15 years, and is accompanied by a decline in oestrogen and progesterone as well as an elevation of LH and FSH (Hall, 2015; Dunneram, Greenwood, and Cade, 2019). Cancer is often more prevalent during later stages of life (Sung et al., 2021). However, this is thought to be owed to the accumulation of life-time exposure to hormones such as oestrogen, and not the decline that takes place during menopause (Liang and Shang, 2013). Obese women and those with diets high in fat are seen to have elevated oestrogen levels post menopause, as oestrogen's primary source becomes white adipose tissue (Qiu et al., 2016). As such women who undergo late menopause and have diets high in fat are seen to have an increased risk of OvCa, endometrial and breast cancer; owing prolonged exposures to elevated oestrogen (N et al., 2012). As such many women often present with these tumours when they are post-menopausal as this stage in life is accompanied by a higher age.

The fluctuating levels of hormones during menopause can however cause emotional unbalance, vasomotor menopausal symptoms i.e. hot-flashes and mental distress, in addition to an increased risk of osteoporosis (Vigneswaran and Hamoda, 2022).

Symptoms may be managed in the form of treatment with Hormone Replacement Therapy (HRT), a combination of oestrogen and progesterone based therapeutics. However prolonged use for 5 or more years, has been linked to an increase in ovarian, breast and endometrial cancers (Liu et al., 2019; Zhang et al., 2021).

1.2.11 Ovarian Cancer and Reduced Risk

Delayed onset of menarche and early menopause, as well as breast feeding, and multiple pregnancies are factors considered to lower the risk of OvCa development (Moorman et al., 2016). Long-term use of progesterone based oral contraception, is also an established protective factor against OvCa (Ferris et al., 2014). These protective factors are all associated with lower lifetime exposure to the endogenous hormone, oestrogen, a critical modulator of fertility, tissue development and bone density; yet a known carcinogen when exposed long term to high levels (Kamani, Akgor, and Gültekin, 2022).

Physical activity is also thought to lower risk, with exercise being explored in numerous pilot studies for cancers, including ovarian (Maurer et al., 2020). Many of these factors are related in their ability to regulate hormonal homeostasis as well as nutrient and hormone supply to the TME. The molecular mechanisms, exerted by these influencing factors however, are yet to be fully elucidated.

1.3 The Tumour Microenvironment

The tumour microenvironment is a complex heterogenic network of structural and stromal components formed of immune cells, endothelial cells and fibroblasts. Encompassing signalling molecules such as hormones, growth factors and extra cellular vesicles are required for the growth, development, differentiation and dissemination of cancer cells (Luo et al., 2021).

1.3.1 Immune response and inflammation in the TME

The escape of immune destruction by tumour cells is a recognised hallmark of cancer (Hanahan, 2022). Whereby signalling between immune cells and OvCa cells in

the TME is a complex process that can alter immune response either limiting or promoting disease progression depending immune cell composition and phenotypic state (Luo et al., 2021).

55% of Epithelial OvCa's present with anti-tumour response in the form of tumour associated antigen presentation, and the recruitment of T lymphocytes. Antibodies such as Folate Receptor α, Mucin-1 and mutant TP53 are common in OvCa, correlating with increased immune response and a higher rate of survival (Salas-Benito et al., 2020). Elevated CD4 and CD8 positive T cells are also associated with improved overall and progression free survival in OvCa through enhanced detection of cancer cells (Silveira et al., 2020). As such advances in OvCa understanding and cancer immune interaction have led to the development of immunotherapies such as the anti-angiogenic agent Bevacizumab which instigates VEGF inhibition via the innate immune system (Macpherson et al., 2020).

Conversely epithelial OvCa cells also produce pro-inflammatory cytokines during early stages of disease which may also instigate malignant progression through elevated interleukin (IL-1 and IL-6) signalling cascades (Singh et al., 2019). This prolonged state of chronic inflammation results in elevated production of reactive oxygen species (ROS), cytokines, and growth factors (Macpherson et al., 2020). Despite the elevation of pro-inflammatory cytokines the signalling required for specific and sustained immune response is often absent; while OvCa cells are seen to recruit various white blood cells (WBCs) including t-cells, b-cells, natural killer cells, as well as macrophages, function is often impaired (Macpherson et al., 2020). With elevated presentation of surface proteins such as PD-L1 and CD9, masking OvCa cells from immune detection through the deactivation of natural killer cells and macrophages respectively (Gonzalez et al., 2021). B-cells are also seen to produce an augmented array of growth factors in addition to anti-inflammatory cytokines such as IL-4 and IL-10, which are also seen to further support immunosuppression while instigating growth and metastatic progression (Batchu et al., 2021). Evidence also suggests that OvCa cells dampen T cell function through sequestering T cell glucose uptake via the expression of microRNA101 and microRNA26a (Zhao et al., 2016).

1.3.2 Glucose in the TME

Glucose is a dietary metabolite vital for the production of adenosine triphosphate (ATP), a molecule which provides energy to living cells. Thus driving metabolic pathways required for a number of essential biological processes (Alberts et al., 2018).

Glucose levels are tightly regulated, with dysregulation implicated in metabolic syndrome and cancer (Simmons, 2005). Over the last decade research focusing upon glucose regulation within the TME has grown, with studies implicating elevated levels of glucose with unfavourable disease outcome in cancers such as epithelial OvCa (Baczewska et al., 2022). The association of hyperglycemia in insulin-independent OvCa is also seen in patients with comorbidities such as diabetes and obesity (Baczewska et al., 2022).

Further supporting evidence implicates the dysregulation of glycolytic enzymes and transmembrane glucose transporters, such as GLUT-1, with the promotion of glycolysis through an increased rate of glucose entry into cancer cells (Xintaropoulou et al., 2018; Pizzuti et al., 2018). The consequent increased cellular glucose is often correlated with poor outcomes in OvCa (Lamkin et al., 2009). In addition, to GLUT1 elevation, CCC and HGSOC also show an increased affinity for glucose through elevated expression of glycolytic enzymes such as hexokinase II and pyruvate dehydrogenase kinase 2 and 4. These glycolytic molecules augment respiration through amplified conversion of glucose to glucose 6-phosphate and the suppression of mitochondrial OXPHOS respectively; resulting in an increase of glycolysis (Kobayashi, 2022).

Under normal conditions excess cellular glucose is converted to glycogen and stored in the liver for future use or used to produce cellular ATP (Alberts et al., 2018). In normoxic conditions, ATP is generated through glycolysis (Figure 1.6) in addition to downstream mitochondrial Krebs and oxidative phosphorylation (OXPHOS), in a process known as aerobic respiration (Lunt and Vander Heiden, 2011).

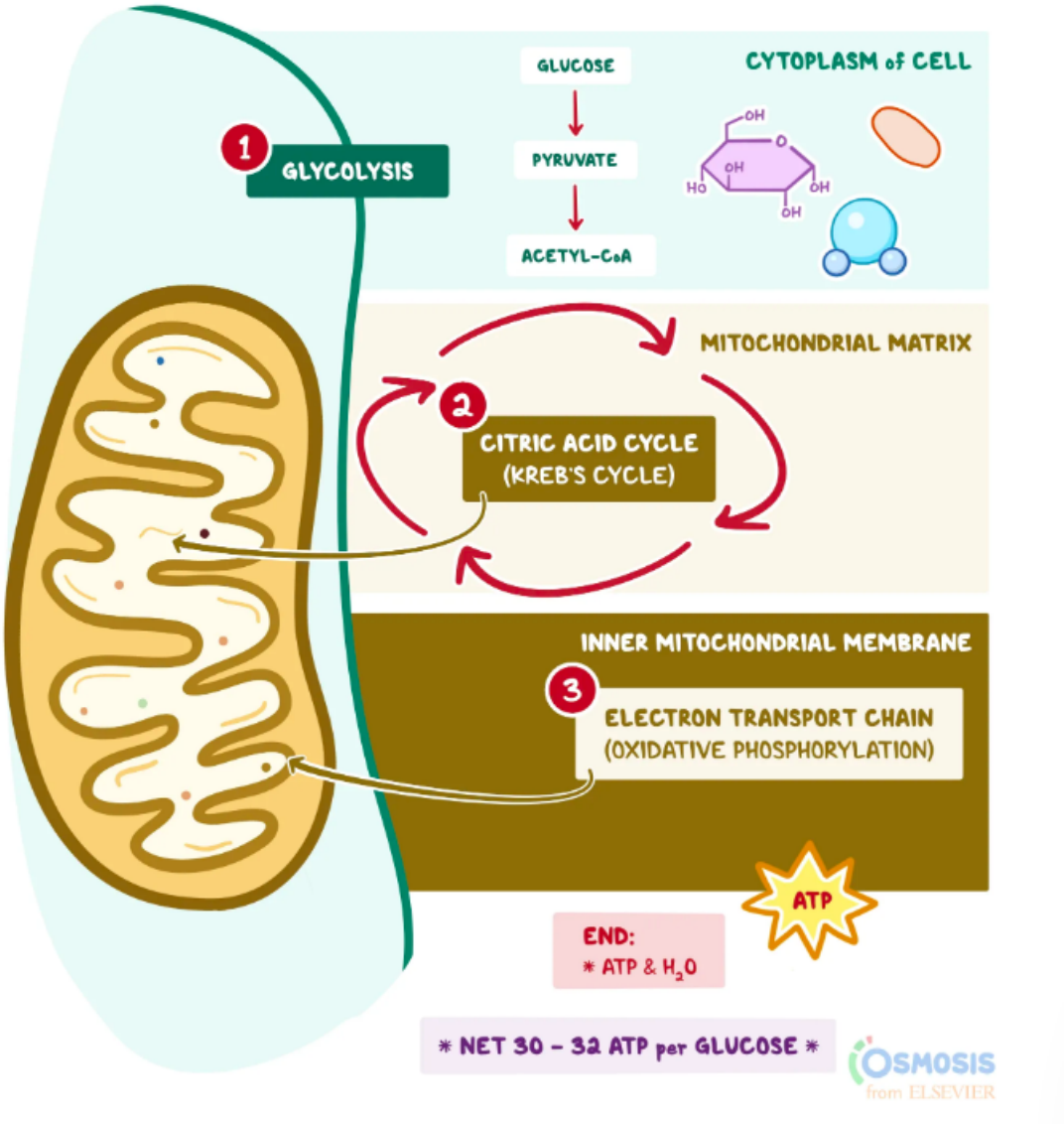

FIGURE 1.6: Cellular Respiration
Graphic depicting the key processes of cellular respiration. 1. Glucose is converted to pyruvate within the cytoplasm during the process of glycolysis; 2. Pyruvate is then transported to the mitochondrial matrix and converted to acetyl-CoA which undergoes a series of enzyme catalysed reactions throughout the Krebs cycle to generate CO2 and NADH; 3. NADH is subsequently used by the electron transport chain to generate ATP during oxidative phosphorylation (Image used under consent of Osmosis from Elsevier).

In hypoxic conditions however, glucose metabolism favours the route of glycolysis alone, where there is less available oxygen to complete the required reactions. This

results in the generation of less ATP per molecule of glucose due to the incomplete conversion of glucose to pyruvate (Alberts et al., 2018). Thus a lower energy yield per molecule of glucose is obtained; in addition to accumulation of lactate, which is explored further in subsequent sections (Xie et al., 2014).

1.3.3 The Warburg Effect

In the 1920's, Otto Warburg discovered that cancer cells appear to favour the route of anaerobic ATP generation through the process of glycolysis (Figure 1.7) (Warburg, Wind, and Negelein, 1927). At the time it was believed that this process was instigated by hypoxic conditions or damaged mitochondria (Vander Heiden, Cantley, and Thompson, 2009).

However, ensuing research indicates that utilisation of the glycolytic pathway in cancer cells is a controllable process, favoured by growth factor signalling, and that mitochondria often retain functional potential (Liberti and Locasale, 2016). Therefore, this preferential use of glycolysis despite the presence of oxygen in cancer, is frequently prefixed with "aerobic" in place of "anaerobic", and is often termed the Warburg Effect (Hanahan, 2022).

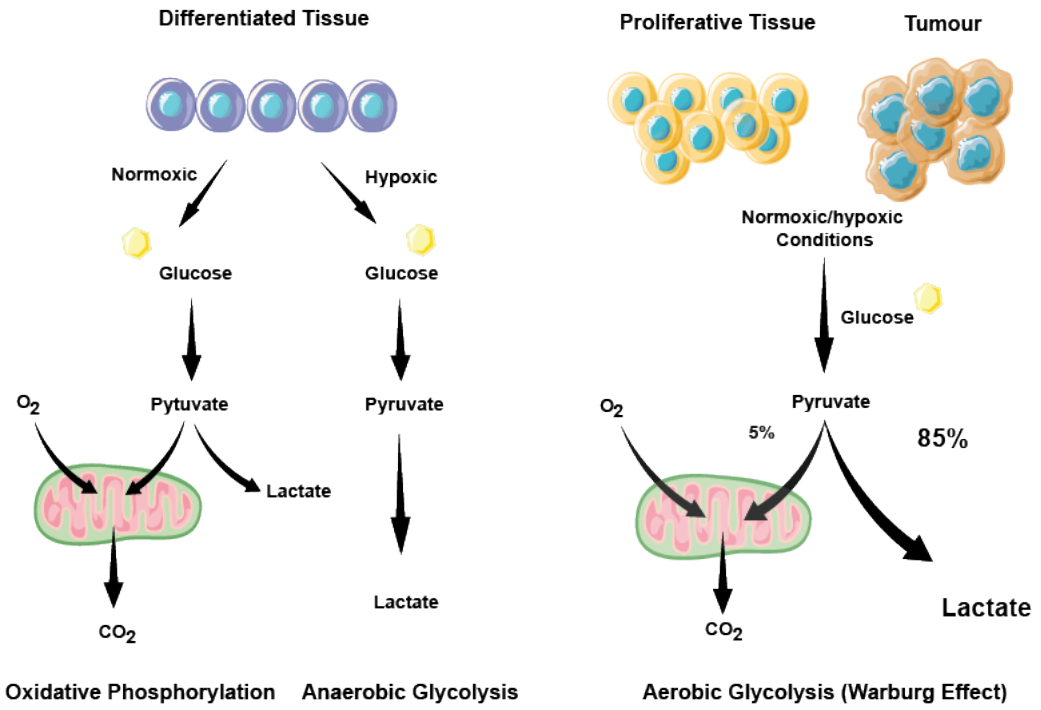

FIGURE 1.7: Warburg Effect
Process of oxidative phosphorylation and anaerobic glycolysis in differentiated tissues in normoxic and hypoxic environments respectively. Highly proliferative tissues and malignancies (right) favour glycolysis despite the presence of oxygen (in 85% of incidences), resulting in a lower yield of ATP and a higher lactate concentration. Image adapted from (Lunt and Vander Heiden, 2011).

Dysregulation of glycolytic pathways, within the TME, are thought vital for meeting the energy demands of cancers such as OvCa (Kellenberger and Petrik, 2018). Where, despite a lower yield of ATP per molecule of glucose (relative to OXPHOS), ATP is produced at an increased rate through glycolysis, rendering plasma glucose concentration, a limiting factor (Shestov et al., 2014; Liberti and Locasale, 2016).

This dysregulation of energy production is associated with a poorer prognosis through the promotion of cellular proliferation, growth and disease progression (Li et al., 2019). Cellular reprogramming of energy metabolism is therefore, considered an emerging hallmark of cancer with the Warburg effect retaining complex roles in these processes (Hanahan and Weinberg, 2011).

Tumour glycolysis is thought to enhance immune evasion and disrupt tissue architecture through alteration of the TME (Jiang et al., 2019). Glycolytic fuelling,

mediated by the Warburg effect, is also implicated in the activation of oncogenes and tumour suppressor genes such as MYC and TP53; as well as the mediation of biosynthetic pathways through the diversion of glycolytic intermediates, such as lactate and reactive oxygen species (ROS) (Liberti and Locasale, 2016).

1.3.4 Lactate in the Tumour Microenvironment

Lactate is a well established product of anaerobic respiration, often associated with energy production in hypoxic tissues or those with an energy deficit (Li et al., 2022b). In exercise lactate is increased and can be used as a measure of intensity and as a performance marker (Nalbandian, Radak, and Takeda, 2018). There are two biological lactate isomers. Bacteria produce D-lactate, while the endogenous lactate produced by humans is an L isomer (Larsen, 2017). Both present with different binding affinities, with the receptor of human lactate thought to be the G-protein coupled receptor, HCAR1. Lactate is routinely measured in hospitals during screening for bacterial induced sepsis, where levels rise beyond the normal range of of 0.2 - 2 mmol (Wacharasint et al., 2012). Initially dismissed as a by-product of incomplete pyruvate breakdown to nicotinamide adenine dinucleotide (NAD+) and ATP, lactate is receiving traction as a signalling molecule in its own right (Figure 1.8). Recent studies indicate an intrinsic role for lactate in tumour progression, inflammation and evasion of immune response (Pérez-Tomás and Pérez-Guillén, 2020).

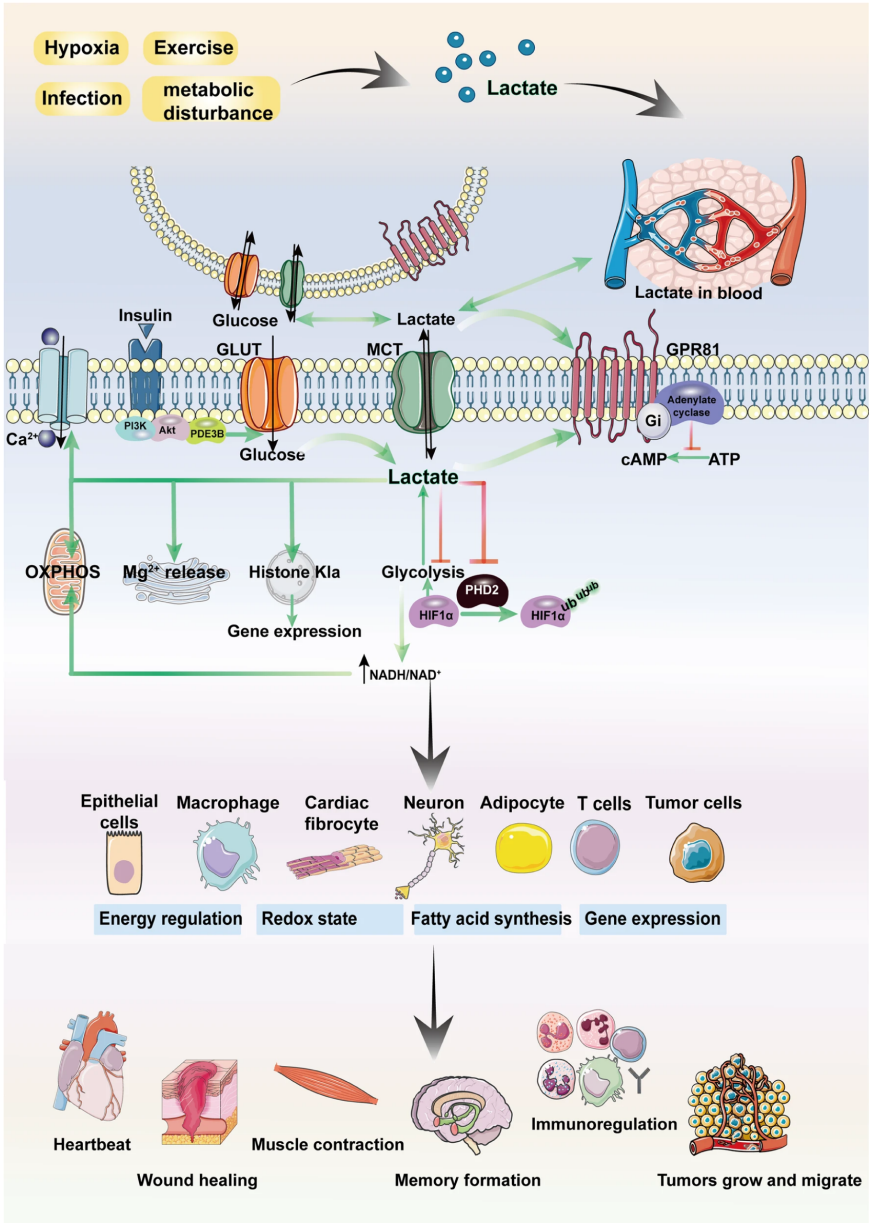

FIGURE 1.8: Lactate Metabolism
Inter cellular mediation via Monocarboxylate transporter 1 (MCT1), allows lactate to enter the cell. Here lactate can act as a metabolic substrate or signalling molecule. Processes influenced by lactate include fatty acid synthesis, glucose metabolism and oxidative phosphorylation. Lactate exerts effect as a signalling molecule through HCAR1 (alias GPR81) activation. Consequent lactate signalling is implicated in muscle contraction, wound healing, memory, and tumourigenesis. (Image taken from Li et al., 2022b)

As tumours progress and increase in size, their cores support hypoxic environments, where oxygen diffusion through cell layers is limited, consequently increasing lactate production within the TME (Muz et al., 2015). Sub-populations of normoxic tumour cells appear to import and utilise lactate produced by neighbouring cells, driving energy production through mitochondrial OXPHOS increasing growth (Xie et al., 2014).

When lactate production exceeds lactate clearance, H^+ ions are increased, lowering cellular pH, resulting in lactate acidosis (Davern et al., 2022). This process can deplete immune checkpoint expression and inhibit natural killer cell action. In addition, lactate is seen to influence mitochondiral dysfunction in oesophageal adenocarcinoma and colon cancer (Harmon et al., 2019).

As previously mentioned, lactate is not only a product of anaerobic conditions in cancer, but is also a product of glycolysis, i.e. the Warburg effect (Hanahan, 2022). Lactate is thought to aid tumorigenesis through the enhancement of TGF-β signalling in regulatory T-cells (Gu et al., 2022). In addition lactate has been shown to promote inflammation through activation of NF-κB and HIF-1α signalling instigating an increase in pro-inflammatory cytokines (Manosalva et al., 2021).

Emerging data supports the potential of blood lactate as a biomarker of cancer. Levels elevated above 2 mmol, are recorded in non-glial brain tumours and bladder cancers; with additional studies associating high levels in cancer stem cells, and poor prognosis in colorectal cancer (Bharadwaj et al., 2015; Liu et al., 2022).

A collective study of patients with solid tumours admitted to the emergency room in the USA, recorded elevated blood lactate in over 1,837 patients with solid tumours of varying site of origin, stage and grade (Maher et al., 2018). This retrospective data showed a significant increase in mortality, in cancer patients with elevated lactate. Unfortunately, data on serum lactate levels in female cancers of reproductive tissue origin are yet to be obtained. However, given the metabolic profile of OvCa, lactate proves a promising molecule to explore for prognostic and therapeutic targeting.

1.4 Fibrillin-1 Precursor Gene

Located at chromosome 15q21.1, FBN1 encodes the precursor protein, pro-fibrillin-1 (Lee et al., 1991). Proteolytic cleavage of profibrillin-1, at the 65th exon, by the enzyme furin, results in the production of two functional proteins (Figure 1.9)(O'Neill et al., 2007). The smaller of the two proteins was recently discovered, and is an adipokine termed asprosin (Romere et al., 2016). The larger protein, Fibrillin-1, is a 350kDa glycoprotein that functions primarily as a structural component of the calcium-binding microfibrils within the extracellular matrix (ECM).

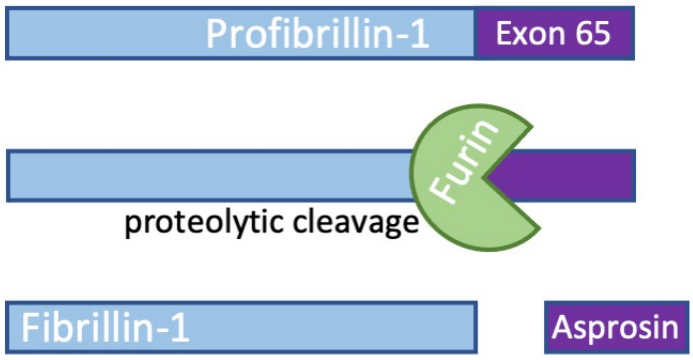

FIGURE 1.9: Clevage of Profibrillin-1
Proteolytic cleavage of profibrillin-1 by the enzyme furin, produces the 350kDa fibrillin-1 and a smaller 30kDa protein, asprosin. (Milewicz et al., 1995; Romere et al., 2016).

Fibrillin-1 primarily mediates the localisation of Transforming Growth Factor beta (TGF-β) (Chaudhry et al., 2007; Thériault and Nachtigal, 2011). The cytokine, TGF-β, is imperative for many biological processes including inflammation and T-cell regulation, as well as stem cell differentiation (Rimon-Dahari et al., 2016). TGF-β is also a key influencing factor of oocyte follicular development (Hao, Baker, and Dijke, 2019).

Mutation of FBN1 is associated with Neonatal Progeroid Syndrome (NPS), a connective tissue disease related to a state of reduced insulin, despite maintenance of euglycemia, and characterised by extreme leanness and partial lipodystrophy (O'Neill

et al., 2007). Genetic screening of patients with NPS revealed heterozygous truncation within a 71-bp segment of the 3' end of FBN1, and resultant premature protein ablation (Romere et al., 2016). Further investigation revealed that this truncation attenuates the production of asprosin.

Of note, FBN1 mutation has been associated with malignancies such as colon, lung and OvCa (Zhou et al., 2021; Li et al., 2015; Wang et al., 2015). In OvCa, increased stimulation of FBN1, by wild type BRCA2, is also believed to decrease the expression of E-cadherin and increase expression of matrix metalloproteases (MMPs) through dysregulation of tumour suppressor protein P53, supporting OvCa metastasis (Wang et al., 2015). However, with limited data, and investigation primarily focusing on FBN1 gene expression and *in-silico* analysis, there is a scarcity of distinguishable data between the protein expression of fibrillin-1 and asprosin (Zhai et al., 2017).

1.5 Asprosin

The recently discovered asprosin is an orexigenic, fasting induced hormone, involved in the modulation of hepatic glucose release and glucose homeostasis (Romere et al., 2016). Elevated levels of asprosin stimulate appetite through the activation of neuronal Agouti-related protein receptors (AgPRs), and subsequent inhibition of Pro-opiomelanocortin (POMC), thus driving adiposity and weight gain (Duerrschmid et al., 2017). Owing to its recent discovery, understanding of asprosin and associated signalling mechanisms is limited. However, emerging studies implicate dysregulated asprosin with an increasing magnitude of metabolic disorders.

1.5.1 Asprosin in Metabolic Disorders

Asprosin's canonical functions are listed as the activation of orexigenic neurons (AgRP) in appetite stimulation, and the regulation of hepatic glucose release during fasting (Duerrschmid et al., 2017). Both *in vivo* and *in vitro* studies, show elevated asprosin in fasting and postprandial serum measurements (Romere et al., 2016). In studies combining males and females, normal plasma asprosin levels range between 8 - 16 ng/ml (Güven and Kafadar, 2022; Zhang et al., 2019a). While fasted levels are seen to elevate above 20 ng/ml (Yaryari et al., 2022). Recently, asprosin was shown to exhibit a sexually dimorphic profile, with a lower levels detected in women regardless of fasting state (Mazur-Bialy, 2021).

TABLE 1.4: Asprosin in Metabolic Disease

Disorder	**Description**	**Levels**
Insulin Resistance	In response to elevated glucose, insulin inhibits glucose release, increasing storage. In IR, cells become resistant to insulin (Wang et al., 2018).	Elevated
Obesity	Characterised by an excess of adipose tissue, obesity is affects 2 in 5 adults and is considered an epidemic.	Elevated
NPS	A metabolic disorder characterised by extreme leanness and lipodystrophy.	Decreased
Nephropathy	A deterioration of kidney function often associated with DM.	Elevated
Liver disease (LD)	Non-alcoholic fatty LD often develop in patients with prolonged obesity, and can result in cirrhosis (Ke et al., 2020a).	Increased
Metabolic Syndrome	A medical condition arising from a combination of obesity, DM and hypertension (Ugur et al., 2022).	Elevated
Cardiovascular Disease (CVD)	Disorders affecting the heart and blood vessels, increasing the risk of blood clots, stroke and myocardial infarction. CVD accounts for 32% of global deaths (Roth et al., 2020; Güven and Kafadar, 2022).	Elevated
Sleep Apnea	Cessation of breathing multiple times during sleep. Associated with dysregulated supply of oxygen to cells (Ding et al., 2018).	Elevated
Acromegaly	Arising from an excess of growth hormone from pituitary dysfunction; rare condition causing unregulated growth in tissues and bones (Ke et al., 2020b).	Decreased
Cancer cachexia	A side effect of cancer growth, characterised by a loss of >5% body weight over 6 months, accompanied by fatigue and reduced strength (Du et al., 2021).	Elevated

Under normal conditions, oral glucose tests reveal an inverse relationship between glucose and asprosin; while those with T2DM however show elevation of both asprosin and glucose, suggesting a disruption to normal oscillation (Zhang et al., 2019a). Not only is asprosin present in circulating blood, recent studies have also detected asprosin within urine, breast milk and saliva; with possible influence over cartilage degradation (Morcos et al., 2022). Continued elevation of blood plasma asprosin has been detected in IR, DM, and obesity as well as a growing list of diseases (Table 1.4). Despite these associations, the exact role of asprosin in these disorders remains unclear (Duerrschmid et al., 2017; Zhang et al., 2019b).

IR and DM are the most widely studied in conjunction with asprosin. In 2019, Wang et al., established a link between the impairment of glucose homeostasis, elevation of asprosin and increased incidence of IR (Wang et al., 2019). IR affects glucose homeostasis and presents with symptoms of thirst, fatigue and frequent infection, in addition to elevated blood sugar (Rodríguez-Gutiérrez, Salcido-Montenegro, and González-González, 2018). IR is a defining feature of prediabetes and T2DM, another metabolic disorder correlated with elevated plasma asprosin (Zhang et al., 2019b).

Not only is elevated asprosin associated with obesity, IR and DM in adults, similar trends are also present in children, with higher levels in females (Corica et al., 2021b; Corica et al., 2021a; Alsaif et al., 2022). Given that dysregulation of asprosin in obesity also extends to children, there is cause to study the prolonged effects of elevated asprosin over an individuals lifetime (Wang et al., 2020; Long et al., 2019).

Emerging research investigating circulating asprosin in cancer shows elevated levels in cancer patients presenting with anorexia (Du et al., 2021). However, as an adiopkine, produced primarily by WAT, more research must be sought to determine if the decline of asprosin in patients with anorexia is a consequence of cancer, or simply reduction of body mass; and if this decline has any effect within the TME (Duerrschmid et al., 2017). Additional work has since shown high expression of asprosin in breast and pancreatic cancers, with higher expression correlated with non-metastatic early staging in the pancreas (Akkus et al., 2022a; Nam et al., 2022). Asprosin therefore shows a potentially emerging role in cancer aetiopathogenesis.

1.5.2 Asprosin in Female Metabolism

Since initial description five years ago, asprosin has emerged as a hormone increasingly related to the female metabolic profile, in both health and disease state (Figure 1.10). The sexually dimorphic relationship viewed between asprosin and women also extends to exercise; where asprosin levels increase in women following anaerobic exercise, yet remain consistent in males (Wiecek et al., 2018). Leonard et al., also show that asprosin fluctuates throughout the stages of the menstrual cycle; with lower levels seen in women taking the progesterone only pill (Leonard et al., 2021a). Asprosin is highest in the mid-luteal phase of the cycle, following ovulation, where oestrogen is also at it's highest (Lindheim et al., 2018).

Additionally, asprosin fluctuates at a higher rate during menstruation in women who do not exercise, suggesting that exercise influences the regulation of this hormone throughout a woman's fertile life. Changes in adipose microRNA expression are also evident throughout the menstrual cycle, perhaps influencing the production of asprosin, an adipokine of WAT (Messinis, Messini, and Dafopoulos, 2014).

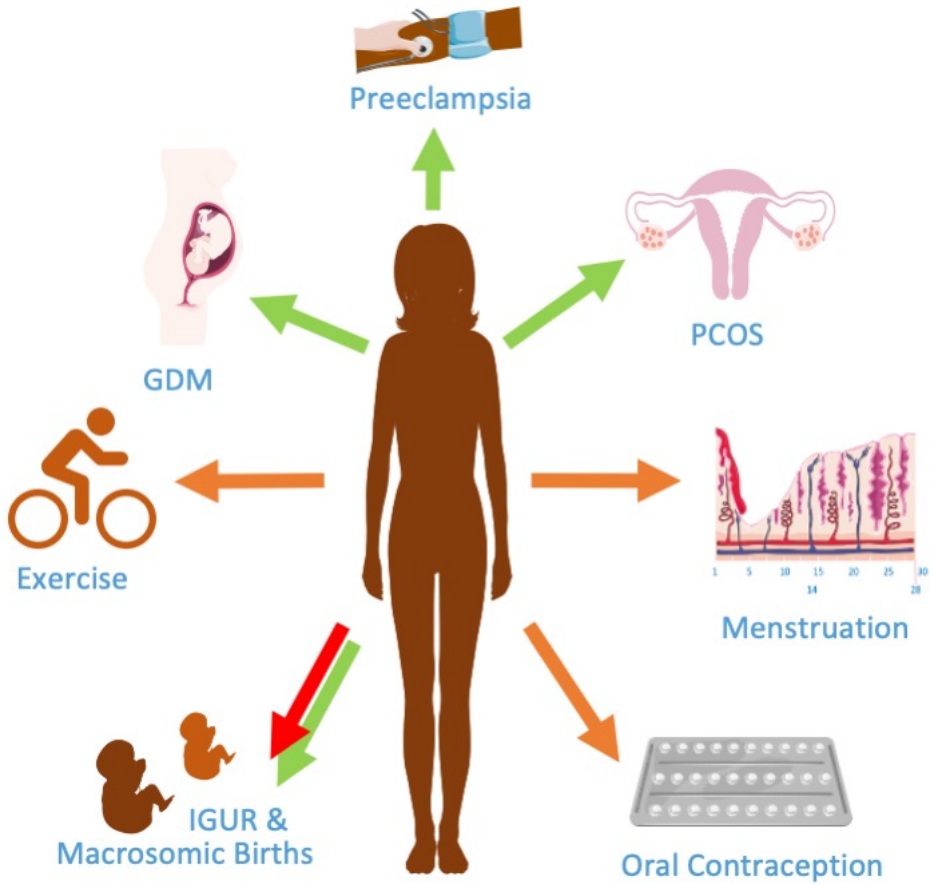

FIGURE 1.10: Female Metabolic Profile of Asprosin
Asprosin regulation in female pathology. Elevated (green arrow) levels are seen in polycystic ovarian syndrome (PCOS), preeclampsia, gestational diabetes (GDM) and macrosomic births. Decreased (red arrow) in intrauterine growth restriction (IGUR). Plasma levels also fluctuate (orange arrow) in line with exercise state and menstruation as well as the use of oral contraception.

Evaluation of asprosin in pregnancy related disorders reveals significant elevation in cases of preeclampsia, gestational diabetes (GDM) and macrocosmic births, with levels reflected in postpartum mothers and umbilical cord levels (Baykus et al., 2019). How long asprosin remains elevated postnatally is undetermined, with no indication of follow up examination in the literature, circa 2022.

Decreased levels of maternal asprosin in cases of intrauterine growth restriction (IUGR), a disorder resulting in foetal growth below the 10th percentile, along with

the increase in macrosomic births, suggests transplacental influence of asprosin in foetal growth (Baykus et al., 2019). Recently a homologous protein structurally similar to fibrillin-1 known as fibrillin-2 (FBN2), was also shown to produce a functional c-terminal product similar to asprosin, termed placensin (Yu et al., 2020). The discovery of an additional glucogenic hormone in the placenta, suggests a complex role of the fibrillin family of proteins in glucose homeostasis.

Given the fluctuations in the regulatory profile of asprosin during menstruation, exercise and metabolic disorders in women, a strong argument can be made that asprosin plays an intrinsic role in the female metabolic profile (Figure 1.10). Interestingly, many of these disorders associated with asprosin and the female metabolic profile, are also noted risk factors of OvCa. Obesity, IR, T2DM, pregnancy, PCOS as well as exercise, for example were all mentioned previously in the section covering "Heritability, Heterogenicity and Risk Factors" (Craig et al., 2016). This association between glucose homeostasis and asprosin, with known metabolic disorders implicated in OvCa, presents a unique opportunity to further metabolic understanding.

1.6 Promiscuous Ligand - Asprosin and Its' Predicted Receptors

Until five years ago the scientific community remained blissfully unaware of asprosins' existence (Romere et al., 2016). It is therefore unsurprising that the cognate receptor of this elusive hormone carries debate. Emerging studies implicate the activation of Toll like Receptor Member 4 (TLR4), and Protein Tyrosine Phosphatase Receptor Delta (PTPRD), with apsrosin mediated signalling in insulin resistance and orexigenesis respectively (Lee et al., 2019; Mishra et al., 2022).

Glucose homeostasis, through the instigation of hepatic glucose release, is thought however, to be the primary function of asprosin; with literature suggesting that the orphaned Olfactory Receptor Family 4 Member 1 (OR4M1), is responsible for this response (Maylem et al., 2022). Although uncommon, evidence of ligands that retain multi specific properties albeit at a lower binding affinity, exist (Chen, Almo, and Wu, 2017). Thus far the literature suggests that asprosin may behave in a similar manner with tissue specific receptors (Figure 1.11). It must be noted that investigations surrounding asprosin and associated receptors and signalling mechanisms are

still at an early stage. Therefore, whether asprosin is classified in a multi-specific manner, or if OR4M1 is the true primary receptor of asprosin, remains to be determined.

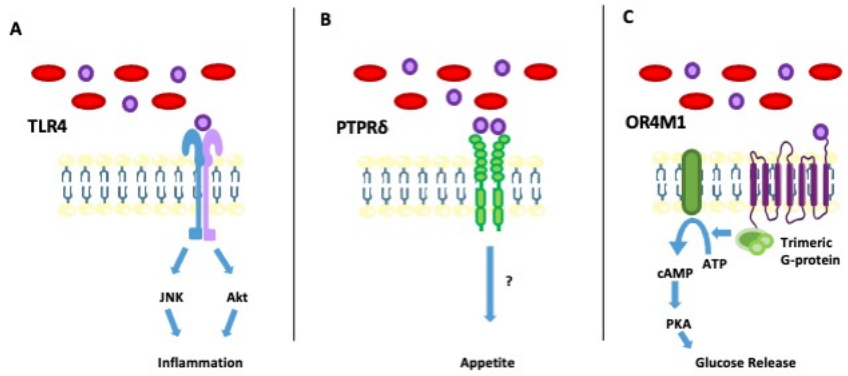

FIGURE 1.11: Predicted Receptors of Asprosin
Asprosin (purple) mediated signalling. A. Activation of Toll Like Receptor 4 (TLR4) instigating downstream inflammation; B. Stimulation of Protein Tyrosine Phosphatase Receptor Delta (PTPRD) and associated increase in appetite; C. Olfactory Receptor 4 Member 1 (OR4M1) mediated cAMP increase and consequent downstream glucose release.

Given the emergence of asprosin as a regulator of glucose homeostasis as well as metabolic disorders such as IR and T2DM (aforementioned with OvCa risk), the predicted receptors of asprosin and their expression profiles in OvCa warrant further investigation in light of disease.

1.6.1 Protein Tyrosine Phosphatase Receptor Delta

One of the first characteristics noted of asprosin was its orexigenic nature in humans i.e., ability to stimulate appetite (Duerrschmid et al., 2017). A recent publication by Mishra et al., presented Protein Tyrosine Phosphatase Receptor Delta (PTPRD) as the receptor responsible for asprosin's mediation of appetite (Mishra et al., 2022).

PTPRD is a member of the protein tyrosine phosphatase family, involved in cell growth, differentiation and mitotic cycle, in addition to oncogenic transformation (Tomita et al., 2020). Showing localised expression, this molecule is a key regulator of the central nervous system. Located primarily within the hypothalamus, PTPRD is highly expressed by appetite regulating Agouti-related peptide (AgRP) neurons,

aiding axon regulation and neuronal cell adhesion (Tomita et al., 2020). Inhibition of PTPRD in the AgRP neurons of mice limits appetite in a cell-autonomous manner and sequesters plasma asprosin (Mishra et al., 2022).

PTPRD is often inactivated in cancers including lung, colorectal and breast, with low expression correlating negatively with survival (Yu et al., 2017). Additional studies, show that PTRPD deactivates aurora-kinase A in neuroblastoma, a mediator of FBN1 signalling (Meehan et al., 2012; Wang et al., 2015). In cases of depleted expression, an increase in proliferation, invasion, and migration are seen (Wu et al., 2019).

PTRPD is thought to mediate effect through phosphorylation of Signal Transducer and Activator of Transcription 3 (STAT3). Conversely inactivation of PTPRD promotes angiogenesis through inhibition of STAT3 and ERK1/2; consequently increasing IL-8 activity as well as inflammation in gastric cancers (Bae et al., 2019). Integrated bioinformatic analysis also correlates PTPRD loss with OvCa diagnosis and poor prognostic outcome (Wang, Li, and Li, 2021; Zou et al., 2022).

1.6.2 Toll Like Receptor 4

Toll-like receptors (TLRs) are a part of the pattern recognition family of transmembrane receptors that regulate the innate immune system; TLRs direct and initiate response to exogenous pathogens (Kanzler et al., 2007). TLR4 is widely studied with expression detected in a plethora of tissues from the digestive tract through to reproductive tissues such as the testis and ovaries (Vaure and Liu, 2014).

TLR4 is responsible for recognising infections caused by bacteria such as lipopolysaccharide (LPS), and coordinating response through instigation of pro-inflammatory cytokines. Polymorphisms of this gene influence susceptibility to bacterial infection (Rehli, 2002).

Until recently, the endogenous ligand of TLR4 remained elusive. One study from 2019, however, implicates TLR4 with asprosin mediated IR. Here asprosin was seen to increase TLR4 mediated downstream signalling of JNK, and inflammation of pancreatic beta cells (Lee et al., 2019). Upon silencing of TLR4 in beta cells, asprosin exerts no effect (Lee et al., 2019). This work provides a possible mechanistic explanation for asprosin mediated IR through pancreatic inflammation, with further research needed to assess similar response in other tissues.

Augmented expression of TLR4 in cancer leads to an increased rate of angiogenesis through elevation of p38 Mitogen Activated Protein Kinase (MAPK) signalling which triggers cytokine production, and instigates vascular endothelial growth factor (VEGF) production (Kashani et al., 2021). In BC elevated expression of TLR4 is also associated with increased susceptibility to relapse (Ahmed, Redmond, and Wang, 2013). Additionally, TLR4 expression in OvCa is shown to exacerbate the rate of tumour growth and progression, and increase drug resistance through aggravated TLR4/IL-6/IRF1 signalling cascades (Zhao et al., 2022a; Huang et al., 2021).

1.6.3 Olfactory Receptor Family 4 Member 1

Olfactory Receptor Family 4 Member 1 (OR4M1) was the first receptor of asprosin to be identified (Li et al., 2019; Maurya and Singh, 2022). Prior to association with asprosin this receptor was characterised as orphaned (a receptor with no known ligand); with less than 10 publications listed within the NCBI database (PubMed.gov, circa 2022). As such there are few detailed studies on the expression and signalling of OR4M1.

Circulating asprosin has however shown repeated affinity for OLFR743, the murine ortholog of OR4M1, in the liver and testis of mice (Li et al., 2019; Maurya and Singh, 2022). Upon binding within the liver, asprosin instigates a G-alpha-s (Gas) protein signalling cascade, increasing cyclic-adenosine monophosphate (cAMP) production, consequently activating Protein Kinase A (PKA) and associated down stream signalling (Li et al., 2019). As mentioned previously, this increases transcriptional activity and consequently elevates hepatic glucose release into the circulation, which subsequently instigates insulin production (Romere et al., 2016).

Interestingly male fertility is also associated with elevated OLFR734 expression in murine reproductive tissues (testis and ovaries). Asprosin-OLFR734 activation in males influences sperm motility and restores functionality in older mice (Wei, Long, and Wang, 2019). Recently, OR4M1 was also detected in the ovaries of heifers with elevated asprosin-OR4M1 concurrent with follicular development (Maylem et al., 2021). Further exploration is required however, to elucidate expression and associated signalling of OR4M1 in human ovaries.

OR4M1 has also appeared once, as a potential biomarker of Traumatic Brain Injury (TBI), with decreased expression linked to TBI-induced tauopathy (Zhao et al.,

2013). Of note, the dysregulation of ORs in disease profiling, has received growing traction over the last decade; leading to the phenotypic classification of many ORs as disease biomarkers. Whether or not OR4M1 is the canonical receptor of asprosin, its status as a peripherally expressed OR deserves investigation in its own light.

1.7 Peripheral Olfactory Receptors in Health and Disease

Olfactory receptors such as OR4M1, are a collection of transmembrane receptors involved in the regulation of response to chemical stimuli and odorants (Veitinger and Hatt, 2017). ORs comprise one of the largest subtypes of G-protein coupled receptor (GPCR) families; and are structurally characterised by their seven transmembrane domains, intracellular carboxyl and extracellular amino termini (Kobilka, 2007).

There are over 800 ORs encoded by the human genome; roughly 400 present with open reading frames, and subsequent potential for functional expression. However, the corresponding ligands of over 80% of ORs and their associated roles are either yet to be elucidated, or are poorly understood (Mainland et al., 2014). Thus assigning many ORs the prefix orphan.

Initially ORs were assumed to be locally expressed by the olfactory epithelium of the nasal cavity (Figure 1.12). The primary function was believed to be the detection of chemical odorants and initiation of neurological response (Zozulya, Echeverri, and Nguyen, 2001).

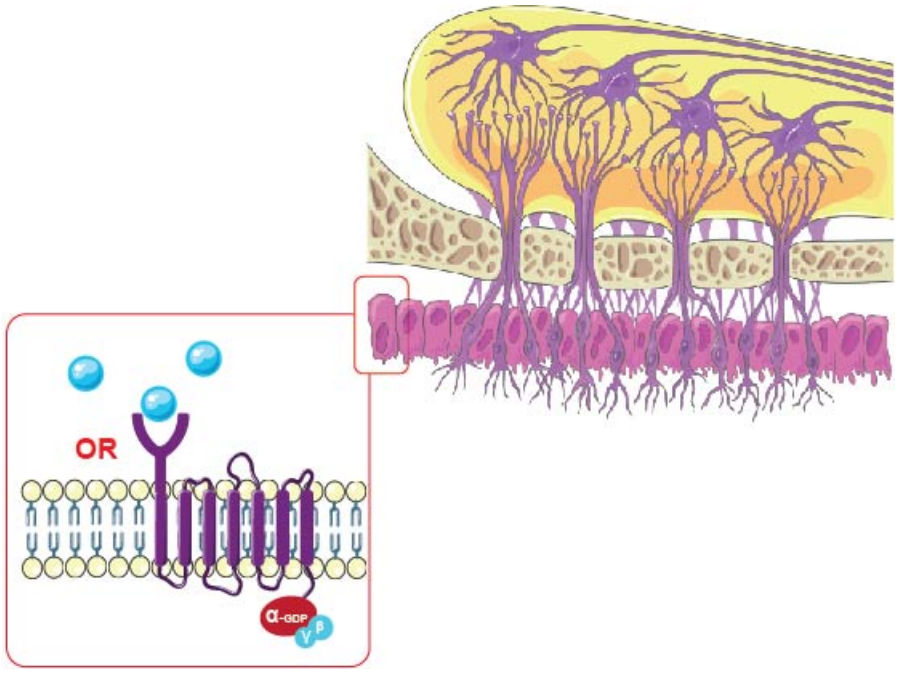

FIGURE 1.12: Olfactory Receptor Signalling
Upon binding to an Olfactory Receptor (OR), the corresponding ligand activates g-protein coupled receptor (GPCR) signalling resulting in the disassociation of the heterotrimeric g protein complex. G alpha then goes on to initiate adenylyl cyclase mediated catalytic conversion of ATP to cAMP. PKA is then activated resulting in downstream signalling. Within the nasal epithelium these cascades are linked to oderant response.

Increasing evidence however, supports the notion that OR expression peripherally to the nasal epithelium mediates complex roles in chemosensory and molecular pathways throughout mammalian tissues (Spehr and Munger, 2009). Peripheral ORs have been detected in over 45 human tissues, with implications in the regulation of sperm chemotaxis, obesity and diabetes (Maßberg and Hatt, 2018). As such, the detection of OR4M1 in tissues peripheral to the nasal epithelium should come as no surprise. Many studies also present a growing number of functional roles belonging to ORs in the lungs and airways. For example, OR51E2 and OR2W3 expression in airway smooth muscle influences proliferation and instigation of bronchodilation in respiratory disorders such as asthma (Aisenberg et al., 2016; Huang et al., 2020).

1.7.1 Olfactory Receptors in Cancer

Despite the orphaned status of a large percentage of ORs, many have shown differential expression in cancers and association with myogenesis, proliferation and apoptosis (Maßberg and Hatt, 2018). Elevated expression of OR51E2 and OR51B4, recently showed biomarker potential for tumorigenicity in prostate and colon cancer respectively (Weber et al., 2017; Neuhaus et al., 2009; Morita et al., 2016). Additionally, targeted activation of the orphaned, OR51B4, in colon cancer was shown to induce phosphorylation of p38, which led to a decline in Akt phosphorylation and consequent inhibition of proliferation and migration (Romere et al., 2016). The data therefore, provides evidence of ORs as therapeutic targets in cancer research.

Increased OR expression is also evident in breast cancer. The receptor OR5B21 is shown to drive BC metastasis through epithelial to mesenchymal transition via the STAT3/NF-kB/CEBP-β signalling axis (Li et al., 2021). OR2B6 and OR2W3 are also being explored for biomarker potential, with over expression detected in BC (Masjedi, Zwiebel, and Giorgio, 2019). Functional roles of these abundantly expressed, orphaned ORs in cancer and their corresponding ligands remain to be determined. However, as emerging data increases to associate ORs with an ever increasing number of cancers; their use as therapeutic targets requires attention (Zhao et al., 2013; Masjedi, Zwiebel, and Giorgio, 2019). Prior to this thesis, the expression of ORs in female gynaecological malignancies remained fairly unexplored.

1.7.2 Anosmia, ORs and Covid-19

In 2019, the first global pandemic for over a century struck (Cucinotta and Vanelli, 2020). In a matter of months severe acute respiratory syndrome coronavirus 2 (SARS-CoV-2), the virus responsible for Covid-19, disrupted the whole planet (Cucinotta and Vanelli, 2020). Covid-19 presented with an array of indistinguishable flu-like symptoms, such as fever, migraine, cough, diarrhoea, fatigue and shortness of breath (Sohrabi et al., 2020).

During the pandemic, many researchers sought to focus on the expression of SARS-CoV-2 cell entry mediators, in a collective effort to aid understanding, so that the pandemic may end (Li et al., 2022c). Surface proteins such as ACE2, TMPRSS2 and TMPRSS4, were found to mediate host cell entry of SARS-CoV-2, through binding of

the viral spike protein and consequent engulfment of the virus through endocytosis (Figure 1.13) (Dimitrov, 2004; Zhao et al., 2022b).

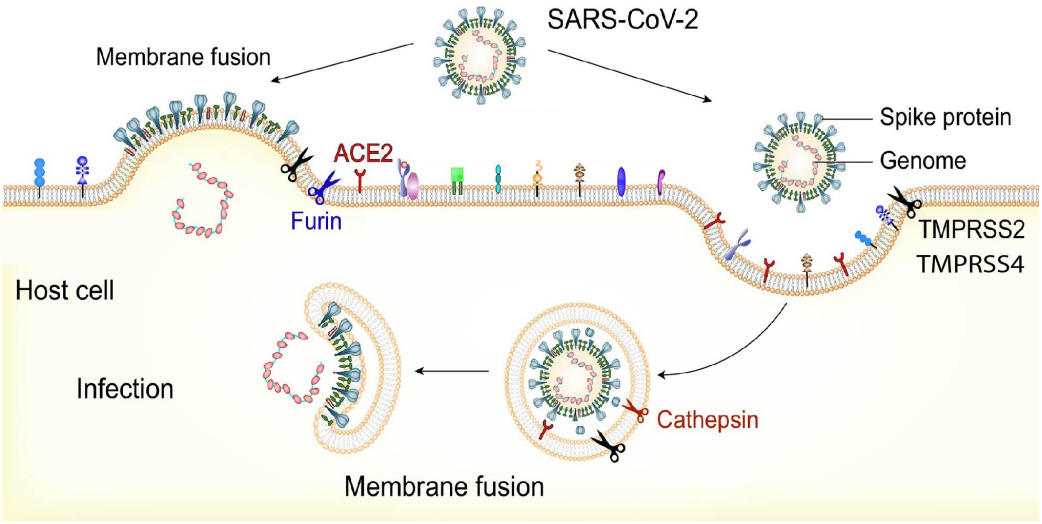

FIGURE 1.13: Cell Mediated Entry of SARS-CoV-2
Host cellular membrane proteins angiotensin-converting enzyme 2 (ACE2) and transmembrane protease serine 2 (TMPRSS2) and TMPRSS4, along with potential auxiliary receptors facilitate SARS-CoV-2 viral membrane spike protein binding, triggering membrane fusion. The consequent endocytosis, results in cellular entry and host infection (Image adapted from Peng et al., 2021).

Progressive illness during the early stages of outbreak, in many cases developed into respiratory failure as well as neurological complications, and resulted in the death of over 15 million globally (Taylor, 2022). Prior to vaccine administration, people with respiratory disorders, as well as metabolic conditions such as obesity, diabetes and cancer, were at an increased risk of contracting SARS-CoV-2 and were more susceptible to fatal outcomes (Loosen et al., 2022; Kompaniyets et al., 2021).

As of 2020, additional symptoms were added to define Covid-19 infection, ageusia and anosmia, also known as a loss of taste and smell (Pellegrino et al., 2020). The most frequent cause of anosmia became the spread of SARS-CoV-2, with dysfunctional olfactory function affecting 70% of early Covid-19 cases (Villarreal et al., 2021). Anosmia is characterised by attenuated oderant receptor (OR) response within the nasal epithelium (Li et al., 2022a). Interestingly, many co-morbidity factors associated with poor Covid-19 outcomes, such as the aforementioned, asthma, diabetes,

obesity, and cancer, are also associated with increased OR expression (Maßberg and Hatt, 2018).

Many studies correlated an increase in the mortality of patients with cancer in the first 7 days following Covid-19 diagnosis (Russell et al., 2021). While, further studies also implicated increased risk in patients with metastatic malignancies (Gupta et al., 2021). It should be noted that increased immunosuppression in cancer patients receiving radiation and or chemotherapeutics, can render patients susceptible to infectious disease, as white blood cells are depleted and immune response compromised (Preston et al., 2011). Delays in both diagnosis and surgery were prevalent during the pandemic also affecting mortality (Maringe et al., 2020); with patients requiring ovarian debulking surgery for example, experiencing delays due to the profound effects Covid-19 presented to health care services (Mandato and Aguzzoli, 2020).

Emerging studies however, sought to investigate causal links, beyond immune suppression and delayed treatment, between increased SARS-CoV-2 infection and cancer (Xia and Dubrovska, 2020). Here it was discovered that entry mediator proteins such as ACE2, TMPRSS2, TMPRSS4 and CTSL were elevated in peripheral tissues afflicted with cancers including lung and those of gastrointestinal origin (Katopodis et al., 2020; Kerslake et al., 2022b; Katopodis et al., 2021). Elevated expression of these mediators was also identified in the nasal epithelium, a tissue known for its prolific OR expression (Sungnak et al., 2020). Nevertheless, proximal expression of ORs to SARS-CoV-2 entry mediator proteins and their host tissues remained unexplored.

Despite the acceptance of anosmia as a symptom of Covid-19, studies have neglected to explore the mechansims associated with this dysfunction. It is important to note that as GPCRs, many ORs show potential for a magnitude of signalling pathways, triggering inflammation, immune response, proliferation, as well as cell death (Alberts et al., 2018). Given that many mammalian ORs are orphaned (unknown/no endogenous ligand), many studies show that these GPCRs are still responsive when stimulated (Nakashima et al., 2013; Veitinger and Hatt, 2017). Indeed, the activation of OR51E2 in cancer by the exogenous beta-ionone can result in cell death (Neuhaus et al., 2009). Therefore, SARS-CoV-2's ability to potentially disrupt the function of ORs, and the consequences of subsequent downstream signalling, warrant further investigation (Brann et al., 2020). Whether SARS-CoV-2 compromises signalling in ORs past those expressed in the nasal epithelium still remains unclear. However

the proximal expression of ORs to SARS-CoV-2 cell entry mediators in cancers associated with poor prognosis in those with Covid-19 infection cannot go unnoticed (Chung et al., 2022; Husain et al., 2022). Investigation of ORs in peripheral tissues could on that account provide novel insight into the mechanisms associated with increased susceptibility to Covid-19, in patients with cancer.

1.8 Disease Models

The tumour microenvironment (TME) is a complex network of nutrients and signalling molecules from encompassing cells, secreted factors and ECM, imperative for sustained cancer growth (Anderson and Simon, 2020). In order to study the effects of augmented receptor expression and glucogenic hormones such as asprosin within the TME, a suitable model must first be established.

A disease model is a system capable of representing disease processes and molecular response in order to further biomedical understanding (Budhwani et al., 2022). Models used in cancer typically include the use of *in vivo* animal studies, *ex vivo* analysis using patient biopsies, as well as *in vitro* tissue cultures. There are thousands of commercially available cell lines, with over 100 established OvCa cell lines available for purchase (Kaur and Dufour, 2012). However, many early cell lines are poorly defined and lack proper histological, and molecular annotation (Beaufort et al., 2014).

Disease models are vital for the translation of research to clinical settings (Kamb, 2005). Nevertheless, tightly regulated legislation surrounds the use of animals as disease models; and ethical considerations must be made for their justifiable use in testing, with UK and EU legislation dictating, where possible alternatives are to be used (Neuhaus et al., 2022). As an alternative emerging advancements in the form of *In silico* modelling also prove useful in disease modelling (McLean and Mehta, 2017; Medina, 2018). Computerised models are now often used by pharmaceutical companies for early development screening of therapeutic molecules to predict stereochemistry (Balani, Nguyen, and Eaves, 2017). *In vitro*, *in vivo* and *in silico* models provide a unique angle for addressing disease aetiology and together, are imperative for building a complex arsenal of research against cancer (Cekanova and Rathore, 2014).

1.8.1 Mouse Modelling

For over 100 years, animals have provided invaluable insight, in biomedical research. There is no disputing that advances in disease understanding and therapeutics would be where they are today without the use of animals such as mice in research (Budhwani et al., 2022). Their physiological similarities in relation to anatomy and genome structure, as well as their ability to closely predict pharmacological activity (including pharmacodynamics, pharmacokinetics, and toxicological response), make them useful candidates for modelling certain biological processes (Toutain, Ferran, and Bousquet-Mélou, 2010; Tratar, Horvat, and Cemazar, 2018).

Cancer cell lines and patient derived xenografts (PDXs), when grown in mice, provide physiological and molecular insight of the TME in an environment, that unlike *in vitro* culture, vastly resembles the origin (Franco, 2013); thus, allowing scientists to study tumour growth, natural tumour progression and metastasis in a translational model, within an accelerated time frame (Cekanova and Rathore, 2014; Robinson et al., 2019). In addition to PDX's, genetically engineered mouse models of OvCa are used to assess and predict therapeutic response (including the development of resistance), as well as metastasis and growth (Tsang et al., 2022). The use of PDX's provides a robust analytical model, although often accompanied by a compromised immune system and lack of tumour-stromal interaction (Qin et al., 2022). As such, predicted response is not always accurate (Flisikowska et al., 2022). The use of animals in testing is under constant refinement within the scientific community. Ethical considerations, such as those set out by the Medical Research Council of the 3R's, also seek to promote the reduction, refinement and replacement of animal use in modern day research (McGonigle and Ruggeri, 2014).

Additional limitations arise from species specific variation; with molecular mechanisms and associated metabolic responses sometimes differing from predicted response (Toutain, Ferran, and Bousquet-Mélou, 2010). A classic example of this is the toxicity of acetaminophen (paracetamol), a widely used analgesic. In mice, physiologically relevant doses of acetaminophen result in immediate liver damage. However in humans, prolonged or high exposure (overdose) is required to succumb to a similar effect (Jeong et al., 2019). Variation in gene expression and protein function, such as cytochrome P450, as well as hormone regulation and metabolic signalling contribute to varied species response (Jeong et al., 2019; Van Norman, 2019). Resultant differential responses from predicted data can greatly hinder clinical translation

of research from the lab to human based trials, and adoption of practices in medical settings (Cekanova and Rathore, 2014). As such *in vivo* models are not always the most appropriate to accurately recapitulate the complexity of human physiology.

1.8.2 3D Ovarian Culture

Conventional tissue culture is a well-established *in vitro* technique, that has contributed vastly towards advancements in cancer, ever since the establishment of the first immortalised cell line, HeLa, from the cervical tumour of Henrietta Lacks in 1951 (Jordan, 2021). Cell culture involves the growth of cells in a controlled environment outside of the body to further physiological, morphological and biochemical understanding of *in vivo* cell behaviour (Kapałczyńska et al., 2018). Nevertheless, conventional culture often fails to recapitulate the complex microenvironment, molecular gradients and cellular characteristics associated with an *in vivo* system (Pelizzoni and Scaglione, 2023). Thus, leading to variation from predicted response achieved through animal modelling and clinical testing (Duval et al., 2017).

Advancing techniques have led to the development of 3D culture and systems with higher capacities to emulate complex biophysical and biochemical factors of an *in vivo* tissue (Pelizzoni and Scaglione, 2023). 3D culture has proven superior to standard monolayer culture through recapitulation of diffusion gradients, ECM support and enhanced cell-cell communication (table 1.5). Differentiation and growth of cells in 3D are achieved through the embedding of culture in a scaffold enriched medium that resembles the ECM (Zhang et al., 2018). The protein rich scaffolds and physiological spatial arrangements captured in 3D support enhanced gene and protein expression as well as the development of tissues specific architecture (Ornell et al., 2019; Bär, Biersack, and Schobert, 2022). Organoid cultures have proven effective in recapturing disease environments with numerous cancer models under continued refinement.

Use of 3D models representing cancers such as colon, breast and lung cancer are increasing in frequency and continue to show improved response to chemical and physical stimuli in a similar manner to *in vivo* response (Monzer et al., 2022; Marchese and Silva, 2012; Mishra et al., 2012). Augmented glycolytic profiles are often evident in these 3D cultures, with 3D colorectal and pancreatic cancer cells for example

TABLE 1.5: Comparison of cells grown in monolayer and 3D culture.

Monolayer (2D) culture	**3D Culture**
Biologically simple	Complex aggregates, spheroids or organoids
Simplistic phenotypic expression	Gene and protein expression closer to *in vivo*
Uniform exposure to stimuli; resistance not accurately depicted	Nonuniform growth results in toxicity profiles and diffusion gradients closely related to *in vivo*
Uniform oxygen diffusion, not reflective of *in vivo* structures; thus, augmenting ROS production and mitochondrial function	Oxygen distribution graduated, hypoxic cores are evident; mimicking *in vivo* variation
Culture is often long term resulting in epigenetic and morphological changes caused by genetic drift	Short term growth, minimizing genetic drift
Often less complex and easily recapitulated	Additional reagents required
Established protocols	Scarcity in established protocols

exhibiting augmented ATP production and increased production of glycolytic intermediates (Ikari et al., 2021; Tidwell et al., 2022).

In contrast to monolayer culture, 3D OvCa cell models also show enhanced gene expression and increased signalling involved in angiogenesis, migration, and proliferation, similar to an *in vivo* environment i.e. mice and clinical settings (Kapałczyńska et al., 2018). A reduced rate in proliferation has also been observed in multiple epithelial OvCa cell lines of varying subtype grown in 3D, with exception to the EAC IGROV-1. Myungjin-Lee et al., also record a pattern of proliferative and apoptotic zones throughout these OvCa spheroids Where core cells show comparatively reduced proliferation and increased apoptosis (Myungjin Lee et al., 2013).

Thus far 3D OvCa models prove particularly useful as models of therapeutic resistance; with studies capturing the development of resistance to platinum-based

therapeutics similar to *in vivo* OvCa response (L'Espérance et al., 2008; Lin et al., 2020). Additional studies show enhanced representation of *in vivo* OvCa in 3D, with 3D epithelial OvCa cells shown to retain histological features characteristic of the primary tumour and the associated sub type (Zietarska et al., 2007). The complex modelling offered by 3D culture therefore provides a more robust *in vitro* insight into *in vivo* tumour biology.

1.8.3 3D Ovary on a Chip

3D cultures vary in complexity, from static single cell 3D culture to co-cultures, and pulsatile systems with the application of organ-on-a-chip (OOC) technology (Lengyel et al., 2014). *In vitro* modelling often overlooks the complex signalling and mechanical stresses offered by the tissue-tissue and cell type specific interactions experienced *in vivo* (Zhang et al., 2018).

Organs, tissues and cells of the human body are not isolated entities, they instead form a complex network of tissues and cell types mediated locally and peripherally via paracrine, autocrine and endocrine signalling (Alberts et al., 2018). The ovary for example, consists of interacting granulosa, stromal and epithelial cells, and is part of an even wider network of tissues and endocrine signalling events (Rimon-Dahari et al., 2016). To recapture the complexities of tissue specific signalling seen *in vivo* the incorporation of co-culture within a 3D OOC system could be used (Figure 1.14).

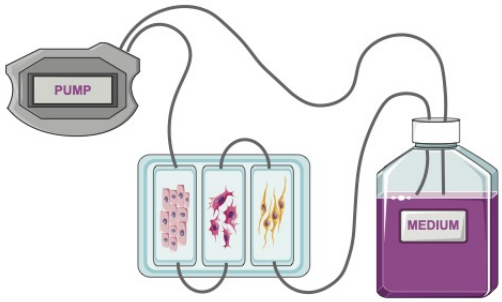

FIGURE 1.14: Organ on a Chip (OOC)
Schematic of a close loop circuit OOC comprised of a programmable pump attached to a series of chambers each containing different cell types grown on a scaffold (e.g. hydrogel) to form a series of 3D co-cultures. The system is complete with a medium reservoir for the circulation of nutrients.

One of the most complex gynaecological OOC systems to date is the EVATAR (Xiao et al., 2017). This system comprises of cells from the ovary, fallopian tubes, uterus, cervix and liver, and is complete with accompanying endocrine loops, capable of modelling the female reproductive tract and the 28-day menstrual cycle (White, Kenny, and Lengyel, 2014; Xiao et al., 2017). Many studies fail to capture the complex inter-play of female reproductive hormones, and instead neglect them for simplicity, with male counterparts in trials dominating past research (Zucker and Beery, 2010). However, with complex metabolic disorders such as OvCa, the influx of hormones can present a risk to disease development and outcome (Kamani, Akgor, and Gültekin, 2022).

Given the evidence, integration of 3D epithelial OvCa cells, relevant co-cultures i.e. WAT and fibroblasts, and hormonal loops using an OOC may therefore provide deeper molecular understanding of disease aetiology (Messinis, Messini, and Dafopoulos, 2014). In particular, novel hormones such as asprosin, that express sexual dimorphism, and fluctuation alongside hormones such as oestrogen and progesterone, may benefit from a complex system; thus providing a better overview of asprosin's physiological role in health and disease (Wiecek et al., 2018).

1.9 Aims and Objectives

1.9.1 General Hypothesis

It is well accepted that ovarian cancer cells undergo a metabolic "rewiring" to favour growth and cell proliferation. Augmented glycolysis and lactate production in cancer cells are accepted hallmarks of tumour development. This work investigates the potential of glucose related metabolites in the tumour microenvironment to increase understanding of metabolic processes associated with cancer glycolysis. In addition this work hypothesises that the newly discovered glucogenic hormone asprosin, may also be implicated in ovarian cancer signalling processes.

1.9.2 Aims

This project is structured around the following areas of research:

1. Study the expression of FBN1 (the gene encoding for asprosin), asprosin and its suggested receptors OR4M1, TLR4 in OvCa. Expression will be studied at mRNA and protein level comparing patients with OvCa and healthy controls. For this, both lab-based (RT-qPCR, immunofluorescence, and immunohistochemistry) and *in silico* tools (databases such as The Cancer Genome Atlas (TCGA) and Genotype Tissue Expression Project (GTEx)), will be used.

2. Study the expression of asprosin receptors in liquid biopsies (i.e. blood) of OvCa patients in order to assess their clinical utility as prognostic biomarkers. This will be achieved measuring protein expression in cancer-associated circulating cells using high-affinity imaging flow cytometry (ImageStream).

3. Gain a deeper understanding of transcriptomic and signalling changes exerted by asprosin in OvCa using an *in vitro* model and RNA sequencing, followed by gene enrichment analyses of the differentially expressed genes. Western blotting will also determine post-translational modifications of key kinases, following treatment with asprosin.

4. Explore circulating lactate levels from blood, in patients with high grade serous ovarian cancer (HGSOC) and elucidate the expression of the lactate receptor hydroxycarboxylic acid receptor 1 (HCAR1) in OvCa using tissue microarrays.

5. In light of the recent pandemic, and characterisation of anosmia as a symptom of SARS-CoV-2 infection, the expression of ORs in cancer (a comorbidity of Covid-19), in relation to SARS-CoV-2 entry mediators will also be explored.

Chapter 2

A pancancer overview of FBN1, asprosin and its cognate receptor OR4M1 with detailed expression profiling in ovarian cancer

Statement of Contribution

For the completion of the presented manuscript I contributed towards the following:

- Data curation
- Methodology
- Formal analysis
- Writing—original draft
- Writing—review and editing
- Referencing

A pancancer overview of FBN1, asprosin and its cognate receptor OR4M1 with detailed expression profiling in ovarian cancer

RACHEL KERSLAKE[1], MARCIA HALL[1,2], PAOLA VAGNARELLI[1], JEYAROOBAN JEYANEETHI[1], HARPAL S. RANDEVA[3,4], GEORGE PADOS[5], IOANNIS KYROU[3,4,6,7*] and EMMANOUIL KARTERIS[1,8*]

[1]Department of Life Sciences, Division of Biosciences, College of Health, Medicine and Life Sciences, Brunel University London, Uxbridge UB8 3PH; [2]Mount Vernon Cancer Centre, Northwood, Middlesex HA6 2RN, UK; [3]Warwickshire Institute for the Study of Diabetes, Endocrinology and Metabolism (WISDEM), University Hospitals Coventry and Warwickshire NHS Trust, Coventry CV2 2DX; [4]Warwick Medical School, University of Warwick, Coventry CV4 7AL, UK; [5]First Department of Obstetrics and Gynaecology, Aristotle University of Thessaloniki, School of Medicine, Thessaloniki 54124, Greece; [6]Centre for Sport, Exercise and Life Sciences, Research Institute for Health and Wellbeing, Coventry University, Coventry CV1 5FB; [7]Aston Medical Research Institute, Aston Medical School, College of Health and Life Sciences, Aston University, Birmingham B4 7ET; [8]Division of Thoracic Surgery, The Royal Brompton and Harefield NHS Foundation Trust, Harefield Hospital, Harefield UB9 6JH, UK

Received May 17, 2021; Accepted June 23, 2021

DOI: 10.3892/ol.2021.12911

Correspondence to: Dr Ioannis Kyrou, Centre for Sport, Exercise and Life Sciences, Research Institute for Health and Wellbeing, Coventry University, Priory Street, Coventry CV1 5FB, UK
E-mail: kyrouj@gmail.com

Dr Emmanouil Karteris, Department of Life Sciences, Division of Biosciences, College of Health, Medicine and Life Sciences, Brunel University London, Heinz Wolff Building, Kingston Lane, Uxbridge UB8 3PH, UK
E-mail: emmanouil.karteris@brunel.ac.uk

*Contributed equally

Abbreviations: ACC, adrenocortical carcinoma; BLCA, bladder urothelial carcinoma; BRCA, breast invasive carcinoma; CESC, cervical squamous cell carcinoma and endocervical adenocarcinoma; CHOL, cholangiocarcinoma; COAD, colon adenocarcinoma; DLBC, lymphoid neoplasm diffuse large B cell lymphoma; ESCA, oesophageal carcinoma; GBM, glioblastoma multiforme; HNSC, head and neck squamous cell carcinoma; KICH, kidney chromophobe; KIRC, kidney renal clear cell carcinoma; KIRP, kidney renal papillary cell carcinoma; LAML, acute myeloid leukaemia; LGG, brain lower grade glioma; LIHC, liver hepatocellular carcinoma; LUAD, lung adenocarcinoma; LUSC, lung squamous cell carcinoma; MESO, mesothelioma; OV, ovarian serous cyst-adenocarcinoma; PAAD, pancreatic adenocarcinoma; PCPG, pheochromocytoma and paraganglioma; PRAD, prostate adenocarcinoma; READ, rectum adenocarcinoma; SARC, sarcoma; SKCM, skin cutaneous melanoma; STAD, stomach adenocarcinoma; TGCT, testicular germ cell tumours; THCA, thyroid carcinoma; THYM, thymoma; UCEC, uterine corpus endometrial carcinoma; UCS, uterine carcinosarcoma and UVM, uveal melanoma

Key words: fibrillin-1, asprosin, cancer, ovarian cancer, olfactory receptor, olfactory receptor 4M1

Abstract. Ovarian cancer affects >295,000 women worldwide and is the most lethal of gynaecological malignancies. Often diagnosed at a late stage, current research efforts seek to further the molecular understanding of its aetiopathogenesis and the development of novel biomarkers. The present study investigated the expression levels of the glucogenic hormone asprosin [encoded by fibrillin-1 (*FBN1*)], and its cognate receptor, olfactory receptor 4M1 (OR4M1), in ovarian cancer. A blend of *in silico* open access The Cancer Genome Atlas data, as well as *in vitro* reverse transcription-quantitative PCR (RT-qPCR), immunohistochemistry and immunofluorescence data were used. RT-qPCR revealed expression levels of *OR4M1* and *FBN1* in clinical samples and in ovarian cancer cell lines (SKOV-3, PEO1, PEO4 and MDAH-2774), as well as the normal human ovarian surface epithelial cell line (HOSEpiC) . Immunohistochemical staining of a tissue microarray was used to identify the expression levels of OR4M1 and asprosin in ovarian cancer samples of varying histological subtype and grade, including clear cell carcinoma, serous ovarian cancer and mucinous adenocarcinoma. Immunofluorescence analysis revealed asprosin expression in SKOV-3 and HOSEpiC cells. These results demonstrated the expression of both asprosin and OR4M1 in normal and malignant human ovarian tissues. This research invokes further investigation to advance the understanding of the role of asprosin and OR4M1 within the ovarian tumour microenvironment.

Introduction

The tumour microenvironment has received growing interest owing to its role in metabolic dysregulation and tumorigenesis. Recent studies have associated dysregulation of extra cellular matrix (ECM) proteins, such as fibrillin-1, with tumorigenesis. The structural glycoprotein, fibrillin-1, is one of two cleavage

products encoded by the *FBN1* gene (1). *FBN1* encodes a 66 exon proprotein known as profibrillin-1, that is proteolytically cleaved within the 65th exon at the consensus sequence X-Arg-X-Lys/Arg-Arg-X by the enzyme furin (1,2). Cleavage produces the 320 kDa glycoprotein fibrillin-1 and the recently discovered 30 kDa glucogenic hormone, asprosin (3).

Asprosin was recently identified by Romere *et al* (3) through an investigation of Neonatal Progeroid Syndrome (NPS); a disorder characterised by reduced insulin despite maintenance of euglycemia, extreme leanness and partial lipodystrophy (4). The pathogenesis of NPS is attributed to premature ablation of profibrillin-1 as a result of a truncation mutation within the *FBN1* gene (3). Investigation of NPS pathophysiology led to the classification of asprosin - the c-terminal cleavage product of profibrillin 1 - as a novel orexigenic and glucogenic hormone, involved in the regulation of glucose homeostasis (3).

Elevated circulating levels of asprosin are present in patients with metabolic syndrome manifestations, such as insulin resistance and type 2 diabetes mellitus (T2DM), and are associated with obesity (5-7). Adipose tissue is the primary source of asprosin secretion, with recent data showing that patients with cancer-related anorexia exhibit significantly lower asprosin plasma levels compared to control counterparts (8,9). There is increasing evidence associating the expression of asprosin with metabolic disorders and complications during pregnancy, such as gestational diabetes, and preeclampsia, as well as intra-uterine growth restriction (10). Additionally, elevated circulating asprosin levels have been noted in women with polycystic ovarian syndrome (PCOS), although further research is required to clarify the relevant role of obesity in this population (11).

Olfactory Receptor 743, an orphan G protein-coupled receptor (GPCR), was recently identified as one of the possible receptors of asprosin in mice, whilst the human ortholog, olfactory receptor 4M1 (OR4M1), is considered to be the primary asprosin receptor in humans (12).

Detection of peripherally expressed olfactory receptors (ORs) is now well-documented; despite initial beliefs for localised expression of these receptors solely within the olfactory epithelium of the nasal cavity (12). Existing data suggest that expression of OLFR734 (and its orthologue OR4M1) may involve the testis, whilst emerging evidence further indicates that expression may also extend to other reproductive tissues, such as the ovaries, with further implications for fertility in mammals (13,14). Recent data present expression of this receptor in the ovaries of murine and bovine samples, supporting an auto/paracrine circuit between asprosin and OR4M1 which may be implicated in female fertility, as well as healthy ovarian follicular function (14). However, expression of OR4M1 is yet to be explored in human tissues past the testis, with the exception of peripheral blood mononuclear cell expression in cases of traumatic brain injury (15).

Ovarian cancer is one of the most lethal gynaecological malignancies, affecting over 295,000 women worldwide (16). Dysregulation of *FBN1* [which is expressed within the theca interna and stroma of healthy ovarian tissue (17)], in ovarian cancer, through Aurora A and BRCA 2 signalling, is associated with invasion and metastasis of tumour cells (18). Moreover, *FBN1* is linked with worse overall survival, as well as advanced stage of disease in high grade serous ovarian cancer (19). However, studies have yet to investigate the expression of asprosin in reproductive tissues in both healthy women and those with ovarian cancer.

The regulation of glucose metabolism in ovarian cancer has been studied extensively, however, certain mechanisms are not fully elucidated. For example, hyperglycaemia drives ovarian tumour growth independently of insulin status (20). Of note, this heightened state of glucose metabolism is thought to accelerate tumour growth through increased aerobic glycolysis in what is known as the 'Warburg effect', and leads to a worse prognosis in cancer, including ovarian cancer (21). Increased expression of the glucose transporter GLUT-1 in ovarian cancer is also linked to a decrease in overall survival, suggesting that glucose abundance is a rate limiting factor of glucose metabolism (22). In this context, investigating the expression of both *FBN1* and the novel glucogenic hormone asprosin in human ovarian tissues will enhance our understanding of the underlying molecular mechanisms implicated in ovarian cancer, as well as the regulation of its tumour microenvironment (20).

In this study -apart from the *in silico FBN1* pan-cancer expression- we provide novel evidence of the protein expression of asprosin in ovarian cancer patients and healthy controls. We also demonstrate -to the best of our knowledge- for the first time expression of the olfactory receptor OR4M1 in the same tissues, raising the prospect of an auto/paracrine regulation at the ovarian level. Finally, we mapped the cellular distribution of asprosin in human ovarian cell lines, as well as the expression of the cognate receptor OR4M1.

Materials and methods

Bioinformatics analysis. A Pancancer set of TCGA data was downloaded through cBioPortal (www.cbioportal.org) and Shiny Methylation Analysis Tool (SMART) (www.bioinfo-zs.com/smartapp/). Expression was validated through GEPIA (gepia.cancer-pku.cn/) and GTeX (gtexportal.org/home/). Survival plots were obtained using Kaplan-Meier Plotter [www.kmplot.com; (23)]. TCGA data sets are described under abbreviations.

Cell culture. SKOV-3 (ECAAC 91091004), PEO1 (ECAAC 10032308), PEO4 (ECAAC 10032309) and MDAH-2774 (ATCC CRL-10303) ovarian cancer cells were cultured using aseptic technique and incubated at 37˚C in humidified conditions at 5% CO_2. Cells were regularly sub-cultured at 80% confluency in T75 filter head flasks (Thermo Fisher Scientific, Inc.). SKOV-3 and MDAH-2774 were cultured in Dulbecco's modified Eagle's medium (DMEM) (Thermo Fisher Scientific, Inc.). PEO1 and PEO4 were cultured in Roswell Park Memorial Institute (RPMI) (Thermo Fisher Scientific, Inc.). Media were supplemented with 10% foetal bovine serum (FBS) and 1% penicillin-streptomycin (Thermo Fisher Scientific, Inc.). Normal ovarian epithelial cells, HOSEpiC (cat. no. 7310) were cultured in Poly-L-Lysine coated flasks (5 μg/ml) according to the protocol provided by the supplier (ScienCell), with Ovarian Epithelial Cell Medium (OEpICM) supplemented with 1% Ovarian Cell Growth Supplement and 1% penicillin-streptomycin (ScienCell) and 10% FBS (Thermo Fisher Scientific, Inc.). For disassociation of adherent

cells, TrypLE express (Thermo Fisher Scientific, Inc.) was used. Cell count and viability were detected manually using a Neubauer Counting chamber with trypan blue (Invitrogen; Thermo Fisher Scientific, Inc.) exclusion method. SKOV-3 were derived from a human epithelial ovarian cancer patient and are haplo-diploid adherent cells that carry a P53 mutation. PEO1 are derived from human ovarian adenocarcinoma. PEO4 were derived from the same patient as PEO1 although were harvested following treatment with platinum-based chemotherapeutics and are cisplatin resistant. MDAH-2774 were derived from a patient with ovarian endometroid adenocarcinoma. The primary cell line, Human Ovarian Surface Epithelial cells (HOSEpiC), referred to as ovarian surface epithelial cells (OSE), were obtained commercially at passage 1 and are classified as normal ovarian epithelial cells.

Clinical ovarian samples. Clinical ovarian cancer samples (n=12, Table I) and samples from healthy volunteers (n=6, Table II) were obtained from patients at the First Department of Obstetrics and Gynaecology, 'Papageorgiou' General Hospital, Medical School, Aristotle University, Thessaloniki, Greece. Specimens from the 12 (average, 61.8 years; range, 48-75) patients with ovarian cancer were taken during laparotomy for debunking surgery. Furthermore, in 6 reproductive-age women (average, 41.7 years; range, 39-45) without any ovarian pathology who had completed their reproductive cycle and underwent laparoscopic myomectomy for leiomyomas during the follicular phase of the cycle, an ovarian sample was taken. Institutional ethical approval was provided, and informed consent was obtained from each patient before the collection of samples (Reference: 14/11/STF/06).

Immunofluorescence. Cells were washed in phosphate buffered saline (PBS) solution (Thermo Fisher Scientific, Inc.), fixed with ice cold methanol, and washed three times with PBS. Samples were blocked with 5% bovine serum albumin (BSA) buffer (Thermo Fisher Scientific, Inc.), covered with parafilm, and left to incubate for 40 min at 37˚C. Asprosin (BioLegend) and OR4M1 (Novus Biologicals) primary antibodies (1:200/1:100 in 5% BSA) were added before incubation at 37˚C for 1 h (asprosin) or room temperature overnight (OR4M1). The coverslips were washed three times with PBS before the addition of secondary Alexa Flour 488 antibody (Merck Millipore) at a concentration of 1:200. The samples were covered with parafilm and placed in a humidified chamber for 30 min at room temperature, before being washed three times with PBS. Coverslips were transferred to a glass slide and sealed with a drop of Molecular ProbesProLong Diamond Antifade Mountant with DAPI (Thermo Fisher Scientific, Inc.) and clear nail varnish. The slides were then analysed, and images captured using a DM4000 microscope (Leica) lens at x100 magnification.

Immunohistochemistry of tissue microarray. Paraffin-embedded ovarian tissue microarray slides were purchased from US Biomax Inc. (cat. no. BC11115c). All tissue samples were collected under Health Insurance Portability and Accountability Act (HIPAA) approved protocols, following the appropriate ethical standards with the donors being fully informed and with their consent. Slides comprised of 100 biopsy cores of ovarian tissue: malignant and adjacent (Table SI). Slides were deparaffinised and rehydrated, followed by antigen retrieval using sodium citrate solution (10 mM Sodium citrate in dH_2O, 0.05% Tween-20, pH 6.0). They were then washed in 0.025% Triton-X in PBS (Thermo Fisher Scientific, Inc.) before a 15-min incubation in 3% H_2O_2 followed by additional washes in 0.025% Triton-X in PBS. The slides were blocked with 5% BSA in PBS, followed by incubation with Asprosin/OR4M1 Antibody (1:200/1:100) overnight in a humidity chamber at 4˚C.

Slides were then washed three times in 0.025% Triton-X in PBS and incubated with a secondary antibody in 1% rabbit serum (ZytoChem Plus HRP-DAB Kit, Zytomed Systems GmbH) for 1 h. The slides were then washed with 0.025% Triton-X in PBS to ensure the removal of unbound secondary antibody. Then streptavidin-HRP conjugate was added to the bound secondary antibody and the slide incubated for a further 30 min within the humidity chamber. Slides were washed with PBS before the addition of DAB stain. These were then counterstained with haematoxylin and washed with 0.1% sodium bicarbonate. Finally, slides were dehydrated before the addition of DPX and coverslips, then left to dry overnight. Immunoreactivity was analysed using a light microscope (Zeiss GmbH). Results were calculated by

Table I. Clinical details of patients with ovarian cancer.

Patient	Histology	Grade	Stage	Age, years
1	Serous	3	IIIC	64
2	Serous	3	IIIC	48
3	Serous	3	IIIC	61
4	Serous	2	IIIC	54
5	Serous	3	IIIC	69
6	Serous	3	IV	65
7	Serous	3	IIIC	75
8	Serous	3	IIIC	65
9	Serous	3	IIIC	56
10	Serous	3	IIIC	64
11	Serous	3	IIIC	64
12	Serous	2	IIIC	56

Table II. Clinical details of the control group.

Patient	Number of fibroids/ patient	Mean diameter of fibroids/ patient, cm	Age, years
1	1	8.9	39
2	4	3.2	42
3	2	6.5	40
4	6	3.7	43
5	2	6.0	45
6	1	10.0	41

Table III. Bio-Rad thermal cycling protocol for use with iTaq™ Universal SYBR‘ Green Supermix (Bio-Rad Laboratories, Inc.).

Step	Temperature, ˚C	Time, sec	Cycle
Activation	95	30	1
Denaturation	95	5	38
Amplification	60	30	
Melt curve analysis	60	Increments of 5	Infinite

two independent reviewers using a percentage score of positive tumour cells, as described previously (24).

RNA isolation, cDNA synthesis and reverse transcription-quantitative PCR (RT-qPCR). Total RNA was extracted from cell lysates using the RNeasy Mini Kit (Qiagen, Inc.), before being reverse transcribed using a cDNA reverse transcription Kit (Applied Biosystems; Thermo Fisher Scientific, Inc.). Sample purity was assessed using Nano-Drop 2000C (Thermo Fisher Scientific, Inc.) and relative gene expression measured using SYBR Green PCR Master Mix (Bio-Rad) and qPCR with a Bio-Rad CFX96 system according to the following conditions (Table III).

FBN1 primers were designed according to the Harvard Primer bank, whereas *OR4M1* were generated according to a 2013 study (15). Additional primers include the housekeeping gene *YWHAZ* (Table IV). RQ values were calculated as previously described (24), according to the comparative $2^{-\Delta\Delta Cq}$ analysis method (25).

Statistical analysis. Statistical analyses were performed using GraphPad prism9® software (GraphPad Software, Inc.). Error bars in graphs are presented as standard error of the mean (SEM). Mann Whitney U test and a one-way ANOVA (Analysis of variance) with Tukey's multiple comparison post hoc statistical tests were applied to the observed measurements from the data. Variances in survival were generated using Kaplan-Meier curves with log-rank test. Beta values were calculated using the SMART methylation tool (SMART). The method for differential analysis conducted by GEPIA is listed as a one-way ANOVA, where disease state (Tumour or Normal) is used as a variable for calculating differential expression: Gene expression against disease state. The expression data are first log2(TPM+1) transformed for differential analysis and the log2FC is defined as median (Tumour) - median (Normal). Genes with higher |log2FC| values and lower q values than pre-set thresholds are considered differentially expressed genes. More information can be accessed at http://gepia.cancer-pku.cn/help.html. Unless stated otherwise, significance was set at P-value <0.05.

Results

Expression of FBN1 in normal tissues. Initial analyses of *FBN1* expression were conducted using publicly available data from The Genotype Tissue Expression (GTEX) project (Fig. 1). Fibroblasts, arteries, adipose tissue (subcutaneous and visceral) and the ovaries are amongst the tissues that express relatively high levels of *FBN1*, as do the studied female reproductive tissues. Brain and whole blood express the lowest *FBN1* levels, along with the liver and pancreas (Fig. 1A). In the same dataset, we further analysed the co-expression of *FBN1* with the proteolytic enzyme *furin*, which may provide an oversight of potential furin-mediated cleavage release of asprosin in these tissues (Fig. 1B). *Furin* is shown to exhibit ubiquitous expression throughout the human body with high levels detected across all tissues, including those with high *FBN1* expression (e.g., normal human reproductive tissues, such as testis, vagina, uterus and ovaries).

Table IV. List of primers utilized in the present study.

Gene	Primer sequences (5'-3')
YWHAZ	Forward: AGACGGAAGGTGCTGAGAAA
	Reverse: GAAGCATTGGGGATCAAGAA
FBN1	Forward: TTTAGCGTCCTACACGAGCC
	Reverse: CCATCCAGGGCAACAGTAAGC
OR4M1	Forward: TCTGTTAATGTCCTATGCCTTCC
	Reverse: AATGTGGGAATAGCAGGTGG

FBN1, fibrillin-1; OR4M1, olfactory receptor 4M1; YWHAZ, tyrosine 3-monooxygenase/tryptophan 5-monooxygenase activation protein ζ.

Pancancer mapping of FBN1. We expanded our observations by assessing the expression of *FBN1* across 33 different cancer types using TCGA datasets through GEPIA. As presented in Fig. 2, significant differential regulation of FBN1 is noted for the following cancer types: bladder urothelial carcinoma (BLCA), cervical squamous cell carcinoma and endocervical adenocarcinoma (CESC), cholangiocarcinoma (CHOL), lymphoid neoplasm diffuse large B-cell lymphoma (DLBC), head neck and squamous cell carcinoma (HNSC), lung adenocarcinoma (LUAD), lung squamous cell carcinoma (LUSC), ovarian serous cystadenocarcinoma (OV), pancreatic adenocarcinoma (PAAD), stomach adenocarcinoma (STAD), thyroid carcinoma (THCA), thymoma (THYM), uterine corpus endometrial carcinoma (UCEC), and uterine carcinosarcoma (UCS). Of the presented cancers, the female reproductive tissues: uterine, cervical, and ovarian exhibit lower *FBN1* expression compared to corresponding normal tissues.

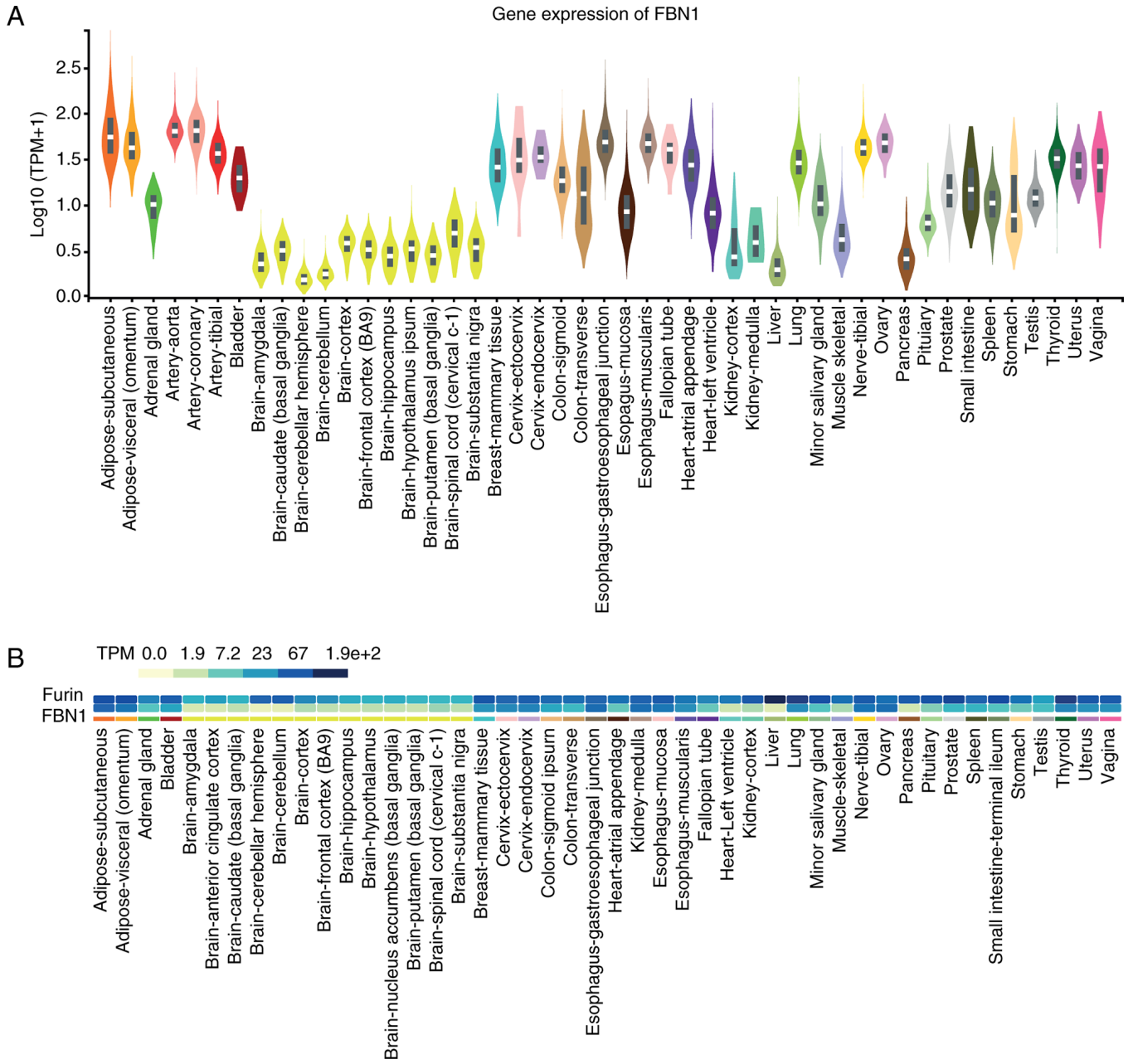

Figure 1. Gene expression of FBN1 in normal tissues. (A) Expression levels of FBN1 in normal human tissues based on available data from The Genotype Tissue Expression project. (B) Co-expression of FBN1 and furin, the enzyme which proteolytically cleaves profibrillin-1 to fibrillin-1 and asprosin, in normal human tissues. The different colours adjacent to furin and FBN1 denote the expression levels of both genes in (B). The darker the colour (dark blue) the higher the expression and the lighter (yellow) the lower the expression (indicated as TPM). The fine different coloured lines underneath the co-expression data in (B) are used for identification purposes and relate to the different coloured violin plots in A. FBN1, fibrillin-1; TPM, transcripts per million.

Given that the methylation status of *FBN1* is of known biomarker potential (26), the FBN1 methylation status for the above cancers was assessed in the same dataset using SMART (Fig. S1). FBN1 methylation in colon adenocarcinoma (COAD) is significantly higher than healthy colon. Similar results are noted for breast (BRCA) and uterine endometrial carcinoma (UCEC). The methylation status of FBN1 within the ovarian cancer data set appears to be highly variable compared to other cancers, as indicated by the beta value of ~0.5; however, there is a lack of comparable normal data for ovarian cancer from TCGA.

Additional insight was sought through the analysis of *FBN1* using cBioPortal. Mutations of FBN1 within the pancancer cohort of TCGA cancers appear to be most frequent in melanoma, uterine, stomach and colorectal cancer (Fig. 3A). A relatively lower frequency of alterations were detected in ovarian cancer samples compared to the other types of cancer, however, the high percentage of deep deletion within the cases presented must be noted.

Gain of function, shallow deletion and diploid appear to show the highest frequency of copy number variation within the samples (Fig. 3B). Six mutations on the *FBN1* gene were identified in cases of serous ovarian cancer (Fig. 3C). Nonsense and splice-site mutations (black and orange lollipops) give rise to a truncated FBN1-encoded protein, whereas the four missense mutations (green lollipops) cause an amino acid substitution. Of note, one mutation has been

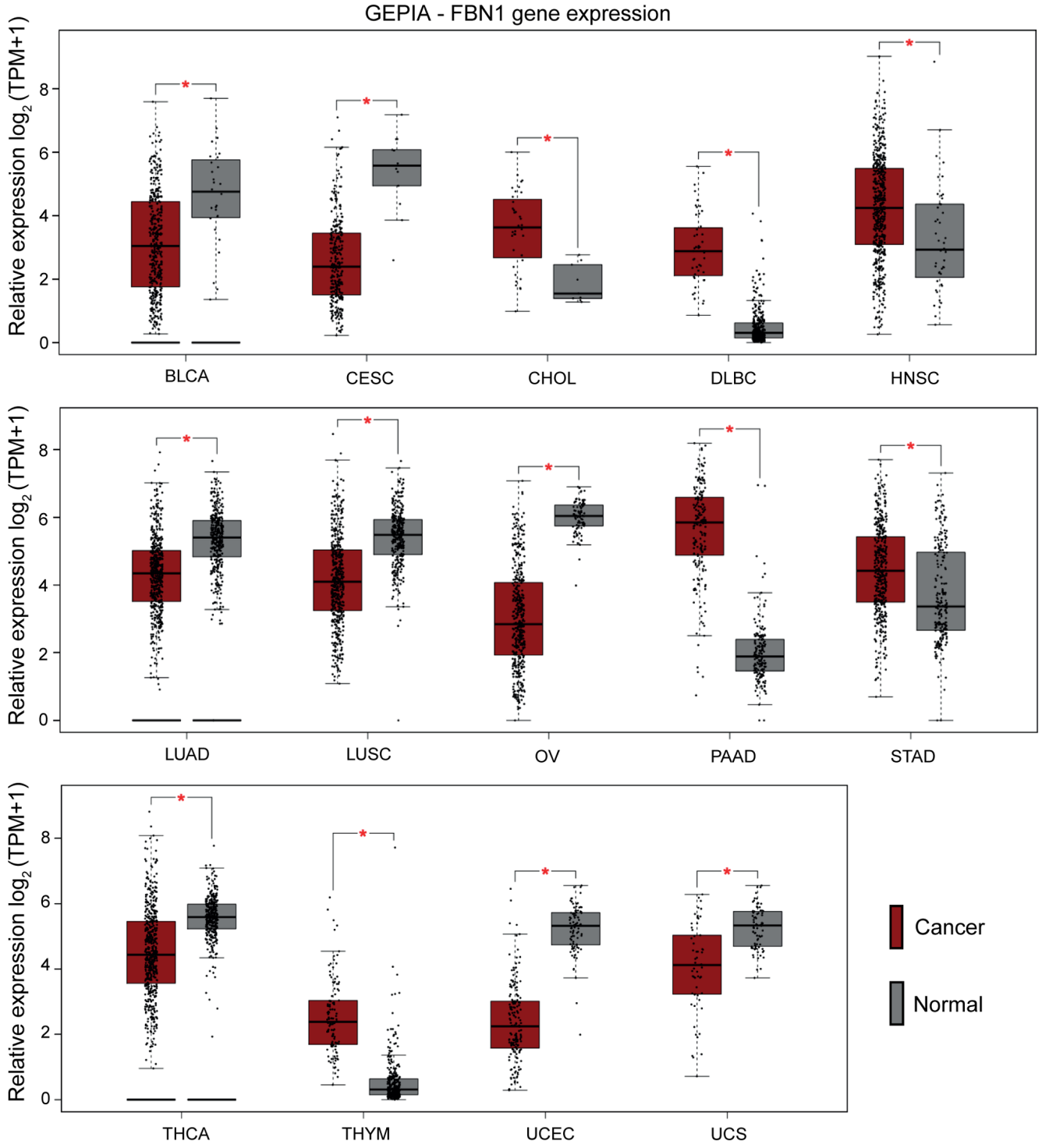

Figure 2. Pancancer profiling of FBN1 expression. Cancer types with significant differences compared with normal tissues (*P<0.01) are presented in the graphs [cancer (red) and normal (grey)]. Cancers with lower expression levels of FBN1 compared with normal samples included UCS, UCEC, THCA, OV, LUSC, LUAD, CESC and BLCA. Those with higher FBN1 expression levels included THYM, STAD, PAAD, HNSC, DLBC and CHOL. BLCA, bladder urothelial carcinoma; CESC, cervical squamous cell carcinoma and endocervical adenocarcinoma; CHOL, cholangiocarcinoma; DLBC, lymphoid neoplasm diffuse large b-cell lymphoma; FBN1, fibrillin-1; GEPIA, Gene Expression Profiling Interactive Analysis; HNSC, head and neck squamous cell carcinoma; LUAD, lung adenocarcinoma; LUSC, lung squamous cell carcinoma; OV, ovarian serous cystadenocarcinoma; PAAD, pancreatic adenocarcinoma; STAD, stomach adenocarcinoma; THCA, thyroid carcinoma; THYM, thymoma; TPM, transcripts per million; UCEC, uterine corpus endometrial carcinoma; UCS, uterine carcinosarcoma.

identified in the asprosin coding region leading to a lysine to arginine (K2840R) substitution.

Expression of FBN1, asprosin and OR4M1 in ovarian cancer. We have validated the in-silico data from TCGA and GTEX (Fig. 4A), using a smaller cohort of patients with ovarian cancer (n=12; stage III and IV). Our data corroborates the previous findings, as it demonstrates that the mRNA expression of *FBN1* was significantly lower in patients with ovarian cancer compared to healthy volunteers (n=6; Fig. 4B). In

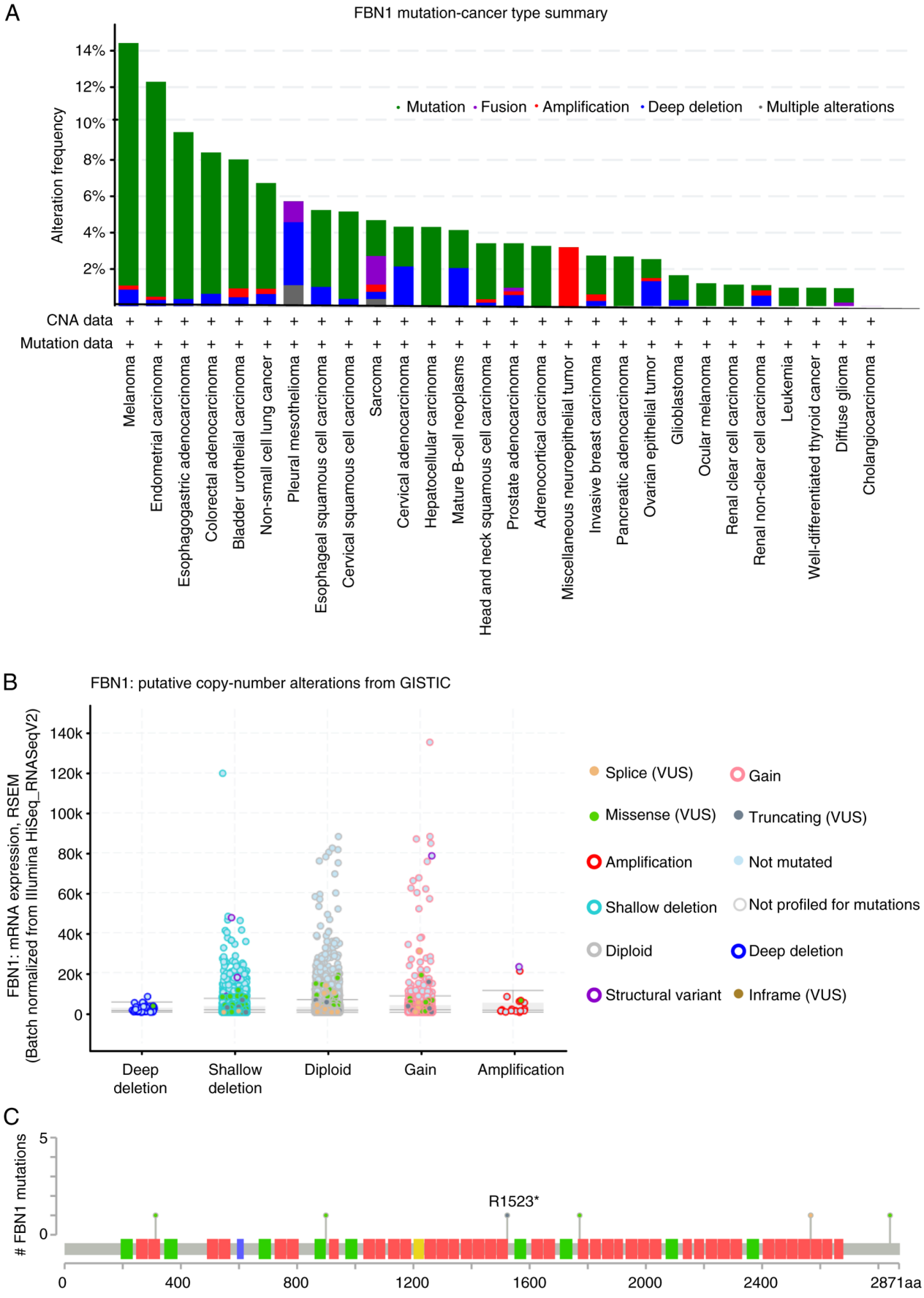

Figure 3. Mutational profile of FBN1. (A) Pancancer overview of the frequency of FBN1 mutations. (B) Copy number of FBN1 alterations across all cancer types (as in Fig. 1A). (C) Location of FBN1 mutations, each lollipop represents an ovarian cancer patient and the corresponding location of the mutation within the gene (Ch15q21.1). Missense mutations are presented as green lollipops, nonsense mutations as black lollipops and splice as orange (source, cBioPortal). CNA, copy number alteration; GISTIC, Genomic Identification of Significant Targets in Cancer; FBN1, fibrillin-1; VUS, variants of unknown significance; RSEM, RNA sequencing by expectation-maximization.

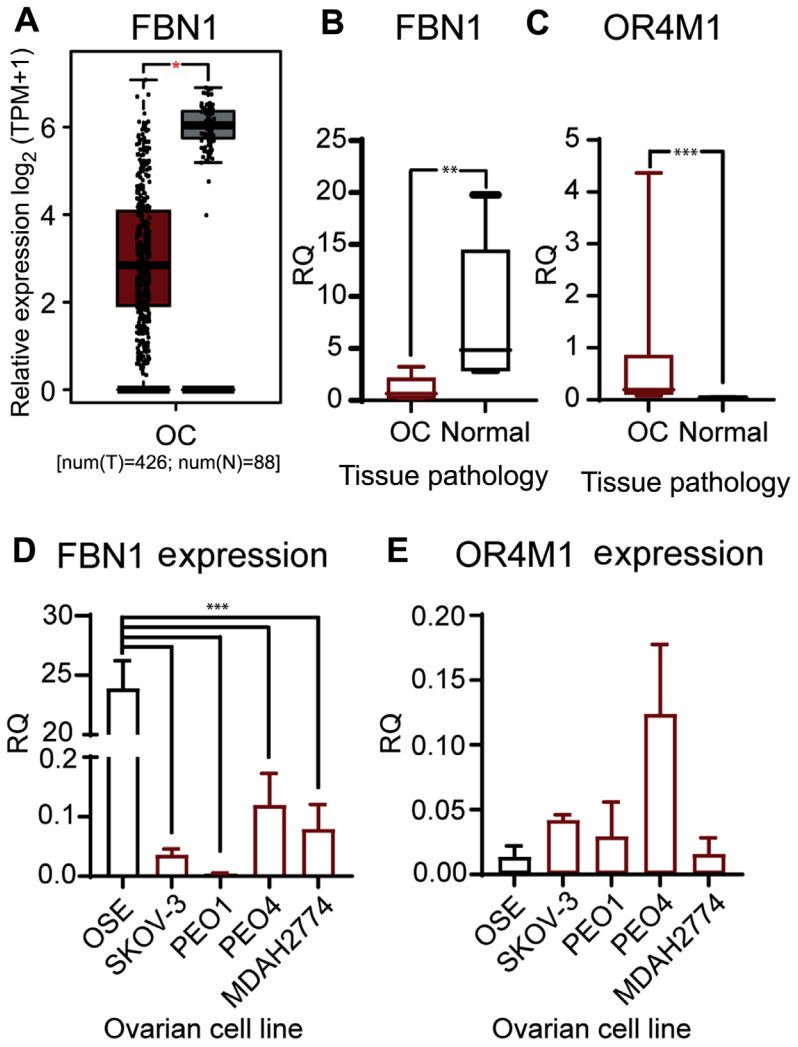

Figure 4. Gene expression of FBN1 and OR4M1 at the ovarian level. (A) Expression data of FBN1 in OC from GEPIA for use as comparison. *P<0.05. Relative expression levels of FBN1 and OR4M1 in OC (red) and normal ovarian tissues (grey) were determined using reverse transcription-quantitative PCR. (B) Significantly lower expression levels of FBN1 in OC samples (OC, n=12; stage III and IV) compared with FBN1 expression in normal ovarian tissue samples from healthy volunteers (n=6). **P<0.001 (samples obtained for the present study; different from the GEPIA cohort in A). (C) Significantly higher expression levels of OR4M1 in OC samples (OC, n=12; stage III and IV) compared with OR4M1 expression in normal ovarian tissue samples from healthy volunteers (n=6). ***P<0.0001. (D) Higher relative expression levels of FBN1 in normal ovarian surface epithelial cells (OSE), and lower expression levels in the studied human ovarian cancer cell lines (SKOV-3, PEO1, PEO4 and MDAH-2774). ***P<0.0001. (E) Lower relative expression levels of OR4M1 in normal ovarian epithelial cells, as well as in the PEO1 and MDAH-2774 human ovarian cancer cell lines, compared with the relatively higher OR4M1 expression noted in SKOV-3 and PEO4 cells. RQ indicates relative change in fold expression to the calibrator gene YWHAZ. FBN1, fibrillin-1; GEPIA, Gene Expression Profiling Interactive Analysis; OC, ovarian cancer; OR4M1, olfactory receptor 4M1; OSE, HOSEpiC cells; TPM, transcripts per million; num(T), number of patients for tumour group; num(N), number of patients for normal group; RQ, relative quantity.

addition, *OR4M1* expression was significantly up regulated in the same ovarian cancer samples (n=12) compared to the controls (n=6; Fig. 4C). We then measured expression of FBN1 and OR4M1 in five ovarian cell lines: one normal ovarian epithelial cell line (HOSEpiC), and four ovarian cancer cell lines namely, SKOV-3, PEO1, PEO4 and MDAH-2774. FBN1 was significantly over-expressed in HOSEpiC cells compared to all studied ovarian cancer cell lines (Fig. 4D), whereas no apparent change in the expression of OR4M1 was noted across all five cell lines (Fig. 4E).

Since FBN1 is differentially regulated in ovarian cancer, its prognostic value was also assessed using Kaplan-Meier plots for overall survival (OS) and progression free survival (PFS), Fig 5. Higher *FBN1* expression was associated with poor OS and PFS, Fig. 5A and D, respectively. This predictive power of FBN1 appears to be significant for patients with late stage ovarian cancer (i.e., III and IV), rather than early stage (i.e., I and II), Fig. 5B and C and E and F for OS and PFS, respectively.

Immunohistochemical analysis of a tissue microarray containing 90 ovarian cancer cores and 10 normal adjacent tissue (NAT) cores, each representing a different clinical case, was used to measure the protein expression of asprosin and OR4M1 (Figs. 6 and 7). Asprosin was aberrantly expressed across all different histological subtypes (Fig. 6A), with no stage-specific variation when samples were grouped to early (I and II) and late (III and IV) ovarian cancer stages (Fig. 6B). Examination of OR4M1 protein expression revealed similar non-specific expression across different histological subtypes (Fig.7A). However, higher expression was detected in early (I and II) compared to late (III and IV) ovarian cancer stages (Fig. 7B).

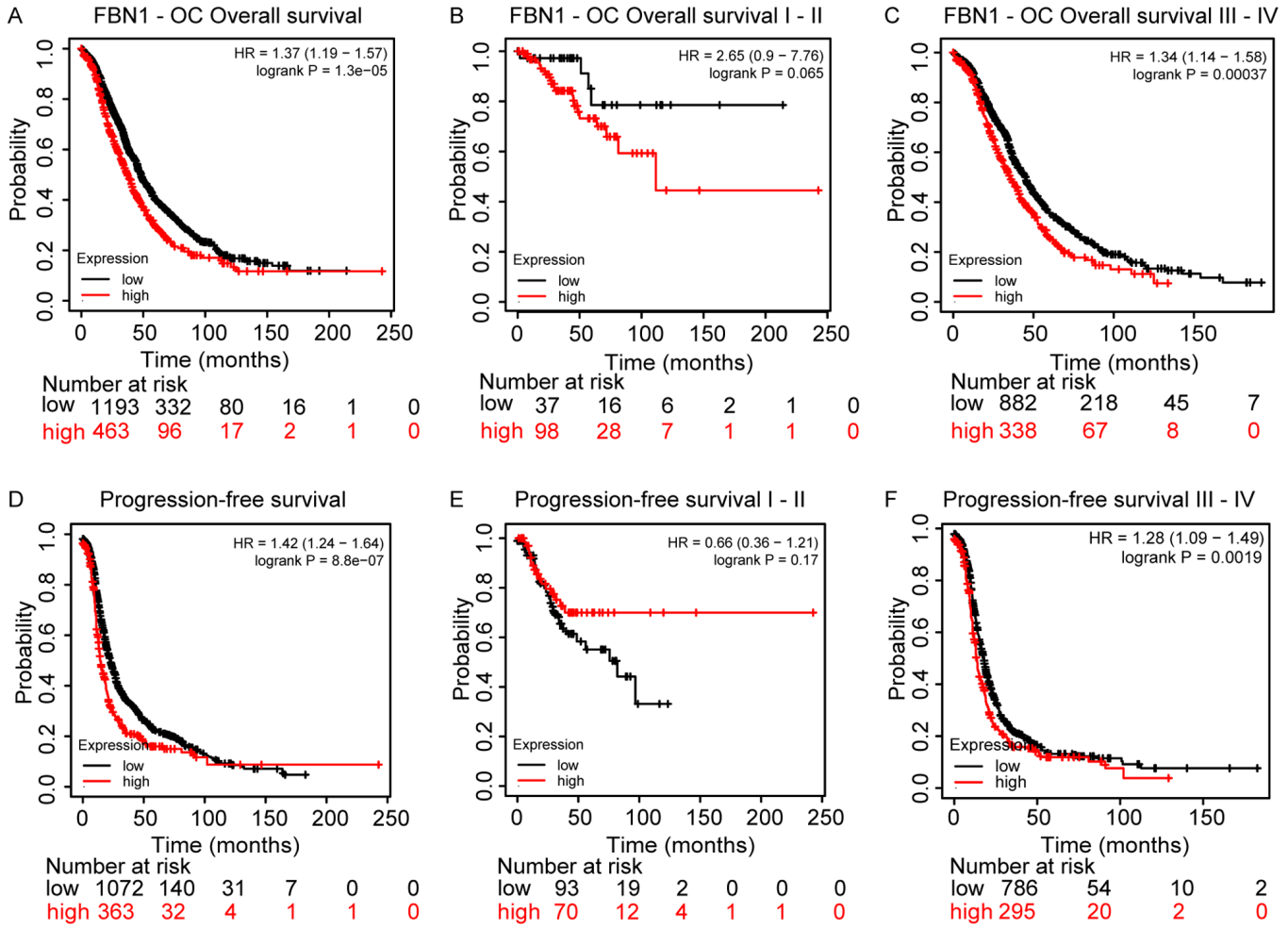

Figure 5. Kaplan-Meier plots revealing the prognostic effects of FBN1 expression in OC. (A) OS in OC. (B) OS in early-stage (I and II) OC. (C) OS in late-stage (III and IV) OC. (D) PFS in OC. (E) PFS in early-stage (I and II) OC. (F) PFS in late-stage (III and IV) OC. FBN1, fibrillin-1; HR, hazard ratio; OC, ovarian cancer; OS, overall survival; PFS, progression-free survival.

Observations on the expression of asprosin and OR4M1 were expanded using the SKOV-3 ovarian cancer cell line, as well as the normal human ovarian epithelial cell line, HOSEpiC (OSE). Similarly, to the tissue sections, asprosin exhibited a cytoplasmic distribution (associated with structures resembling microtubules or cytoskeleton), whereas OR4M1 appears to be expressed on the plasma membrane and cytoplasm in accordance with the expected distribution of a GPCR (Fig. 8).

Discussion

This study presents novel data regarding the expression of *FBN1* (the gene encoding profibrillin-1), asprosin (the novel orexigenic/glucogenic hormone which is cleaved from profibrillin-1), and OR4M1 (the human cognate receptor of asprosin) in cancer, focusing on ovarian cancer. Using an in-silico approach, we demonstrate that FBN1 expression is ubiquitous in normal tissues, with high levels seen in fibrous tissues (e.g. in fibroblast cells) and arteries, in addition to female reproductive tissues, such as the uterus and ovaries. Being the main source for the production of circulating asprosin (9), adipose tissue also exhibited high FBN1 expression. To date, asprosin production is thought to be specific to adipose tissue. However, the noted co-expression of FBN1 with the proteolytic enzyme furin in human tissues is indicative of potential production and release of asprosin from other peripheral tissues, such as the ovaries.

Although multiple studies have shown FBN1 mutations as the cause of Marfan syndrome (MFS), which is further associated with increased risk of tumourigenesis (27), very little is known about the role of FBN1 mutations in cancer. Analysis of over one million cancer cases, including stomach, liver, oesophagus, prostate, gynaecological and other cancers, in a national cohort of patients with MFS in Taiwan showed a higher risk of developing cancer in these patients (27). Of note, the data presented from cBioportal in our study, indicate that six FBN1 mutations were present in patients with ovarian cancer, with one of the missense mutations located in the coding region for asprosin. Future GWAS studies are required to explore the potential involvement of these mutations in ovarian cancer.

The presented data from GEPIA in this study, show differential FBN1 expression in 14 cancers, with higher expression noted in cancers of the stomach (STAD) and pancreas (PAAD). The latter is in line with previous research associating increased FBN1 expression in pancreatic islets with cellular progression from hyperplastic to angiogenic to insulinoma (28). Lower

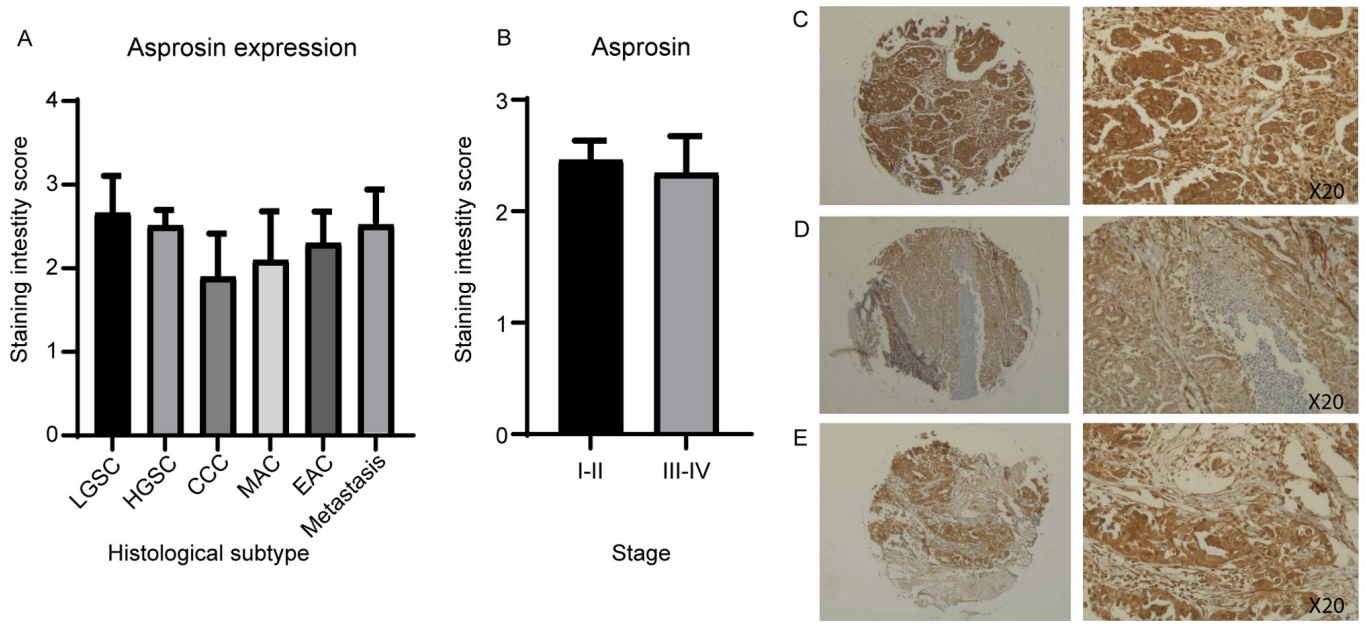

Figure 6. Ovarian tissue microarray, including 90 ovarian cancer cores, stained with asprosin antibody (1:200). Corresponding values for scoring: 0, <10%; 1, 10-25%; 2, 26-50%; 3, 51-75%; and 4, >76% of cells stained. (A) Asprosin staining by histological subtype/grade: LGSC, HGSC, MAC, EAC and CCC. (B) Asprosin staining of early (I and II) and late (III and IV) ovarian cancer stages, revealing no significant difference. (C) HGSC, stage II at x5 (left) and x20 (right) magnification. (D) HGSC, stage I at x5 (left) and x20 (right) magnification. (E) HGSC, stage III at x5 (left) and x20 (right) magnification. CCC, clear cell carcinoma; EAC, endometroid adenocarcinoma; HGSC, high grade serous carcinoma; LGSC, low grade serous carcinoma; MAC, mucinous adenocarcinoma.

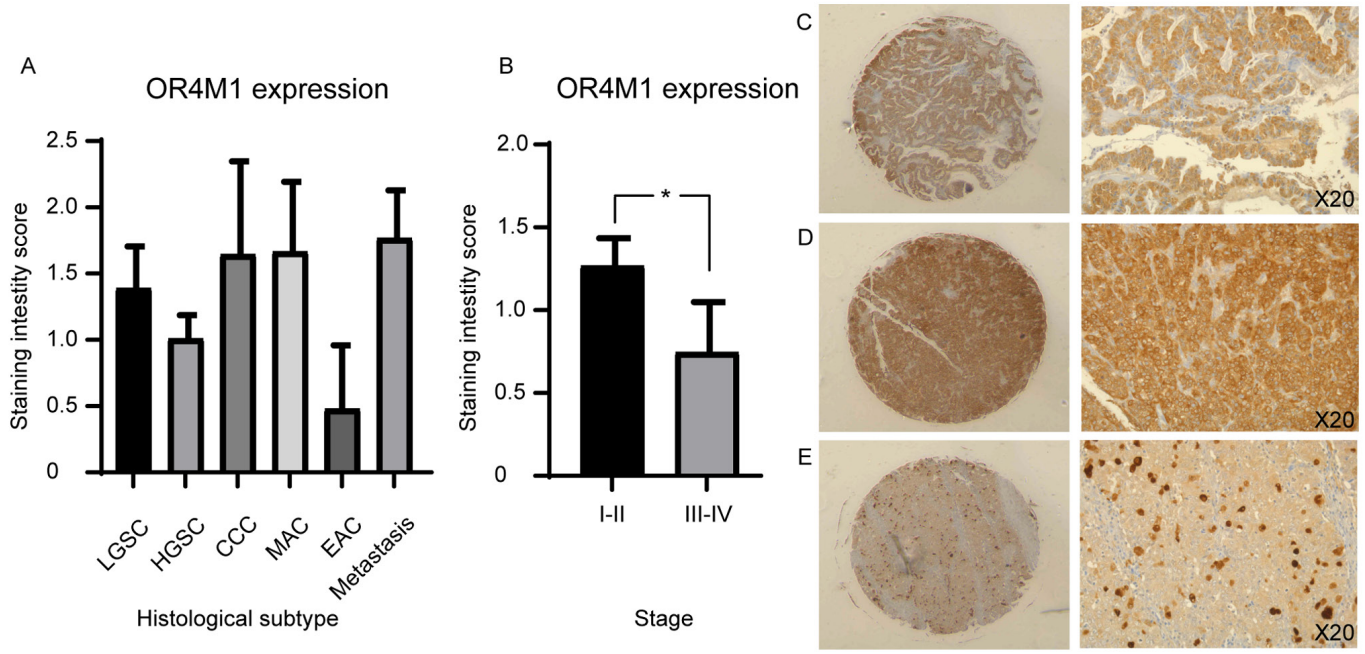

Figure 7. Immunohistochemical staining of an ovarian tissue microarray, including 90 ovarian cancer cores, with OR4M1 antibody (1:100). (A) OR4M1 staining by histological subtype/grade: LGSC, HGSC, MAC, EAC and CCC. (B) Higher OR4M1 staining in early (I and II) compared with late (III and IV) ovarian cancer stages. *P=0.04. (C) HGSC, stage II at x5 (left) and x20 (right) magnification. (D) HGSC, stage I at x5 (left) and x20 (right) magnification. (E) HGSC, stage III at x5 (left) and x20 (right) magnification. CCC, clear cell carcinoma; EAC, endometroid adenocarcinoma; HGSC, high grade serous carcinoma; LGSC, low grade serous carcinoma; MAC, mucinous adenocarcinoma; NAT, normal adjacent tissue; OR4M1, olfactory receptor 4M1.

FBN1 expression, however, was noted in cancers that originate from fibrous tissues, including gynaecological cancers, such as cervical (CESC), endometrial (UCEC), uterine (UCS) and ovarian (OV) cancers. The downregulation of FBN1 in this cohort of cancers may be suggestive of tissue-specific expression compared to up-regulation in other malignancies. Based on a previous study, FBN1 has a single CpG-rich dominant promoter that is highly conserved in mammals (29). Interestingly, a study showed that gene expression and activity of the promoter was significantly higher in MG63 cells (a

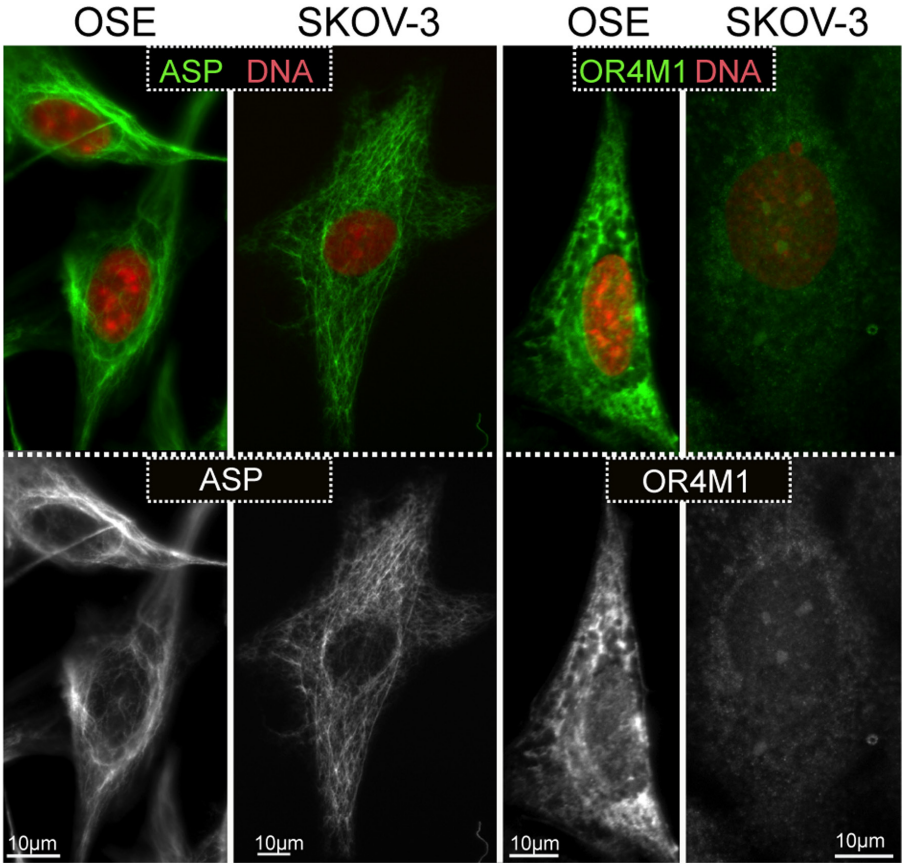

Figure 8. Immunofluorescence imaging of OSE normal human ovarian epithelial cells and SKOV-3 human serous ovarian cancer cells, with DAPI nuclear staining (red) and with ASP and OR4M1 (green). Magnification, x100 using a Leica DM4000 microscope (Scale bar, 10 μm). ASP, asprosin; OR4M1, olfactory receptor 4M1.

human osteosarcoma line) when compared to MDA-MB-231 cells (a breast cancer cell line) (29). This agrees with previous observations that variations in the activity of the promoter region can exert a heritable transcriptional effect (30,31). As such, this might also explain, at least in part, the varying expression of FBN1 among different cancer types. Indeed, transcription factor binding motifs identified in the promoter region of FBN1, subserve tissue-specific functions (29). Of note, furin expression is slightly elevated in ovarian cancer compared to controls (data not shown). Therefore, in terms of the secretion of the cleaved peptide asprosin, the dynamics may be different. Moreover, it is possible that FBN1/asprosin may exert different effects in health and disease. For example, in the normal ovary, it might affect steroidogenesis and in the cancerous tissue may be implicated in the Warburg effect. Especially the later, warrants further investigation given that asprosin is a glucogenic peptide, that stimulates the release of glucose from hepatic cells. It is well known that in cancer cells, there is dramatic increase of the rate of glucose uptake and subsequent lactate production (32). Recently, inhibition of Bcl2 in SKOV3 ovarian cancer cells, appeared to reverse the Warburg effect and promoted oxidative stress-induced apoptosis *in vitro* (33). Further studies are needed to investigate the clinical application of asprosin as a potential mediator of the Warburg effect in ovarian cancer.

Furthermore, changes in the methylation status of FBN1 have shown biomarker value. For example, hypermethylation of Synuclein Alpha (SNCA) and FBN1 in stool samples show excellent sensitivity and specificity for colon cancer (34). Additional data has shown similar potential for colorectal cancer (26). The data presented in our study support these findings as methylation of FBN1 is significantly higher in colon adenocarcinoma (COAD) compared to healthy colon. Similar results are seen for breast (BRCA) and uterine endometrial carcinoma (UCEC). Methylation of FBN1 in normal ovarian tissue requires further investigation, since there is a lack of comparable normal methylation data held through TCGA and SMART for ovarian cancer.

In silico data for ovarian cancer were further validated using clinical ovarian tissue samples from patients with stage III/IV ovarian cancer, as well as both cancer and normal human ovarian epithelial cell lines Our present findings show significantly downregulated FBN1 expression in the ovarian cancer samples compared to those from healthy controls, in accord with the data noted in GEPIA. Moreover, FBN1 expression was detected in the human ovarian cancer cell line SKOV-3, the high-grade serous PEO1 and PEO4 cell lines, and the human endometroid ovarian cancer cell line MDAH-2774, as well as the normal ovarian epithelial cells (OSE). As noted in the clinical ovarian cancer samples, these human ovarian cancer cell lines exhibit relatively lower FBN1 expression compared with the normal ovarian tissue.

The differential - albeit not-significant - expression of FBN1 in the BRCA2 mutant and silent (wild-type) PEO1

and PEO4 cell lines, respectively, is of interest given that the tumour suppressor gene BRCA2 is an inhibitor of FBN1 (18). BRCA2 inhibition of FBN1 is associated with the inhibition of matrix metalloproteases (MMPs), including MMP2, MMP9 and MMP13, as well as the activation of cellular adhesion molecules which protect against metastasis (18). However, it should be noted that database analyses on survival times are often biased because of limited clinical information. These should be validated ideally with prospective cohorts employing sophisticated statistical considerations. Due to the nature of this study, such advanced statistical considerations were not feasible, thus this should be acknowledged as a limitation of the present study. The prognostic value of FBN1 in cancer is continually evolving (19,35,36). In our study, high FBN1 expression predicts lower overall- and progression-free survival of patients with late stages (i.e., III and IV) of ovarian cancer, corroborating previous findings which show promising prognostic potential of FBN1 as part of a panel of genes (19,35). Similarly, elevated FBN1 expression in both colon and bladder cancer are associated with worse overall survival (19,37,38).

Interestingly, previous data suggest that glucose metabolism including hyperglycaemia in ovarian cancer is associated with tumour growth and progression as well as worse survival outcome (20,39). As such, further research is required to elucidate the potential role of the glucogenic hormone and product of FBN1, asprosin, at the level of the ovaries. To that aim and following studies on the expression in normal murine and bovine ovaries (13,14), we provide novel data regarding the expression of both asprosin and its cognate receptor, OR4M1, in normal human ovaries and ovarian cancer.

Using immunohistochemical staining, we show aberrant protein expression of asprosin in ovarian cancer samples and normal adjacent tissue. In routine examination, normal adjacent tissue is often taken from the vicinity (<2 cm) of malignant cells and is frequently used as a control for cancer studies. Of note, recent transcriptome profiling data comparing normal adjacent tissue samples to healthy control tissue - which is removed from a substantial distance away from the primary tumour or from an age matched healthy control - suggest that there is premalignant conditioning of normal adjacent tissue (40). In the present study no apparent differences in asprosin protein expression were observed amongst different histological subtypes or stages of ovarian cancer, with staining representative of high asprosin expression in most cases (cancer and normal adjacent tissue samples). Similar widespread protein expression of asprosin was recently documented in malignant mesothelioma (41).

In our cell lines, this cytoplasmic distribution appeared associated with structures resembling microtubules or cytoskeleton. As this is a secreted protein, one would expect to observe a pattern that resembles the endoplasmic reticulum, or the Golgi, or even a vesicular pattern. One possibility is that asprosin production by furin-mediated cleavage, escapes the conventional secretory route, and follows a non-conventional secretory pathway that may not be dependent on vesicular exocytosis. Future *in vitro* studies using specific markers of cytoplasmic organelles should address this finding. One of the limitations of this study is the inability to measure mRNA expression for asprosin, as this is a cleaved peptide therefore only protein and precursor *FBN1* mRNA expression can be measured. The fact that FBN1 colocalises with furin in the ovary, favours local production of the cleaved product. Future studies should include the measure of asprosin levels from conditioned media of ovarian cell lines and/or ovarian explants to elucidate the secretion rate of asprosin from this tissue.

Moreover, given that asprosin binds to a GPCR, it is expected to have a discrepancy between mRNA and protein levels. It is possible after prolonged exposure to the ligand (i.e. asprosin), OR4M1 might undergo desensitisation, as a mechanism limiting GPCR signalling and subsequent activation of adenylyl cyclase. In doing so, OR4M1 can be detected in the cytoplasm (rather the cytoplasmic membrane) as a process of internalisation, or in lesser amounts if it undergoes lysosomal degradation rather than recycling (42). Future studies should concentrate on activation of second messengers *in vitro*. It is known that GPCRs are capable of activating multiple G proteins (43), therefore it is important to measure release of cAMP, or IP3 and activation of PKA or PKC *in vitro*. It has also been shown that asprosin is capable of binding to Toll-like receptor 4 (TLR4) and activating JNK mediated-pathway in pancreatic β-cells (44). Of note, the role of TLR4 in ovarian cancer is well documented (45), and future studies should also investigate the possibility of asprosin binding to TLR4 as well in ovarian cells.

We acknowledge that there are certain additional limitations in this study. The validation of the *in silico* data is performed on a small number of clinical samples and controls. Moreover, the samples of ovarian cancer where RT-qPCR was performed were all stage III/IV, as such we do not have the data to compare mRNA expression of FBN1 and OR4M1 in early stages of ovarian cancer. *In silico* analysis (Ualcan; http://ualcan.path.uab.edu) indicated that FBN1 is overexpressed across all stages with significantly increased expression when comparing stages II vs. III and II vs IV (data not shown). In addition, we demonstrate protein expression of asprosin in clinical samples and cells, however the study does not examine whether the ovaries are capable of secreting this peptide, since this was beyond the scope of the present paper. Future experiments using conditioned media from ovarian cell lines and/or ovarian explants are planned which will enable us to answer this question.

In conclusion, to the best of our knowledge, this is the first study to demonstrate expression of asprosin and its cognate receptor, OR4M1, in the human ovaries in health and cancer, focusing specifically on ovarian cancer. The presence of the recently identified orexigenic and glucogenic hormone asprosin (the cleaved product of profibrillin-1) in the human ovaries suggests a specific endocrine and/or auto/paracrine role for asprosin in human female reproduction. Indeed, the novel findings of the present study open two distinct lines of investigation: the potential role and effects of asprosin in normal ovaries in terms of fertility and steroidogenesis; as well as the potential involvement of asprosin as a gluconeogenic peptide in cancer. The latter is of particular importance given that hyperglycaemia is a contributing factor to the onset and progression of epithelial ovarian cancer (20). However, it should be noted that the exact role of asprosin and its receptor in the pathogenesis of ovarian cancer and its precise clinical relevance remains to be clarified. Further research is required

to expand on the present findings and elucidate the potential role of asprosin in health and disease using *in vitro* and *in vivo* models, as well as larger cohorts of patients undergoing treatment for ovarian cancer.

Acknowledgements

Not applicable.

Funding

The present study was funded by Cancer Treatment & Research Trust and University Hospitals Coventry and Warwickshire NHS Trust (grant no. 12899).

Availability of data and materials

The datasets used and/or analysed during the current study are available from the corresponding author on reasonable request.

Authors' contributions

MH, HSR, IK, GP and EK conceived the study. RK, JJ, PV and EK developed the methodology. RK, IK, JJ and EK performed data analysis. RK, JJ and EK performed experiments. GP provided resources. GP, MH, HSR, IK and EK collected and prepared clinical samples. RK, EK and IK wrote the original draft. GP, PV, MH, HSR, GP, IK and EK reviewed and edited the manuscript. MH, IK and EK supervised the study. GP, HSR, IK and EK were involved in project administration. GP, HSR and MH acquired funding. EK and IK confirm the authenticity of all the raw data. All authors read and approved the final manuscript.

Ethics approval and consent to participate

The study was conducted according to the guidelines of the Declaration of Helsinki and approved by the Institutional Review Ethics Committee (School of Health Sciences and Social Care; current College of Health, Medicine and Life Sciences) of Brunel University London (Uxbridge, UK) and the Committee for Medical Ethics and Deontology School of Medicine, University of Thessaloniki (reference, 14/11/STF/06; Thessaloniki, Greece). All patients provided oral informed consent for participation to this research study.

Patient consent for publication

Not applicable.

Competing interests

The authors declare that they have no competing interests.

References

1. Lee B, Godfrey M, Vitale E, Hori H, Mattei MG, Sarfarazi M, Tsipouras P, Ramirez F and Hollister DW: Linkage of Marfan syndrome and a phenotypically related disorder to two different fibrillin genes. Nature 352: 330-334, 1991.
2. Klimstra WB, Heidner HW and Johnston RE: The furin protease cleavage recognition sequence of Sindbis virus PE2 can mediate virion attachment to cell surface heparan sulfate. J Virol 73: 6299-6306, 1999.
3. Romere C, Duerrschmid C, Bournat J, Constable P, Jain M, Xia F, Saha PK, Del Solar M, Zhu B, York B, *et al*: Asprosin, a Fasting-Induced Glucogenic Protein Hormone. Cell 165: 566-579, 2016.
4. O'Neill B, Simha V, Kotha V and Garg A: Body fat distribution and metabolic variables in patients with neonatal progeroid syndrome. Am J Med Genet A 143A: 1421-1430, 2007.
5. Wang Y, Qu H, Xiong X, Qiu Y, Liao Y, Chen Y, Zheng Y and Zheng H: Plasma Asprosin Concentrations Are Increased in Individuals with Glucose Dysregulation and Correlated with Insulin Resistance and First-Phase Insulin Secretion. Mediators Inflamm 2018: 9471583, 2018.
6. Li X, Liao M, Shen R, Zhang L, Hu H, Wu J, Wang X, Qu H, Guo S, Long M, *et al*: Plasma Asprosin Levels Are Associated with Glucose Metabolism, Lipid, and Sex Hormone Profiles in Females with Metabolic-Related Diseases. Mediators Inflamm 2018: 7375294, 2018.
7. Wang CY, Lin TA, Liu KH, Liao CH, Liu YY, Wu VCC, Wen MS and Yeh TS: Serum asprosin levels and bariatric surgery outcomes in obese adults. Int J Obes 43: 1019-1025, 2019.
8. Du C, Wang C, Guan X, Li J, Du X, Xu Z, Li B, Liu Y, Fu F, Huo H, *et al*: Asprosin is associated with anorexia and body fat mass in cancer patients. Support Care Cancer 29: 1369-1375, 2021.
9. Duerrschmid C, He Y, Wang C, Li C, Bournat JC, Romere C, Saha PK, Lee ME, Phillips KJ, Jain M, *et al*: Asprosin is a centrally acting orexigenic hormone. Nat Med 23: 1444-1453, 2017.
10. Zhang X, Jiang H, Ma X and Wu H: Increased serum level and impaired response to glucose fluctuation of asprosin is associated with type 2 diabetes mellitus. J Diabetes Investig 11: 349-355, 2020.
11. Li E, Shan H, Chen L, Long A, Zhang Y, Liu Y, Jia L, Wei F, Han J, Li T, *et al*: OLFR734 Mediates Glucose Metabolism as a Receptor of Asprosin. Cell Metab 30: 319-328.e8, 2019.
12. Kerslake R, Hall M, Randeva HS, Spandidos DA, Chatha K, Kyrou I and Karteris E: Co expression of peripheral olfactory receptors with SARS CoV 2 infection mediators: Potential implications beyond loss of smell as a COVID 19 symptom. Int J Mol Med 46: 949-956, 2020.
13. Wei F, Long A and Wang Y: The Asprosin-OLFR734 Hormonal Signaling Axis Modulates Male Fertility. Cell Discov 5: 55, 2019.
14. Maylem ERS, Spicer LJ, Batalha I and Schutz LF: Discovery of a possible role of asprosin in ovarian follicular function. J Mol Endocrinol 66: 35-44, 2021.
15. Zhao W, Ho L, Varghese M, Yemul S, Dams-O'Connor K, Gordon W, Knable L, Freire D, Haroutunian V and Pasinetti GM: Decreased level of olfactory receptors in blood cells following traumatic brain injury and potential association with tauopathy. J Alzheimers Dis 34: 417-429, 2013.
16. Bray F, Ferlay J, Soerjomataram I, Siegel RL, Torre LA and Jemal A: Global cancer statistics 2018: GLOBOCAN estimates of incidence and mortality worldwide for 36 cancers in 185 countries. CA Cancer J Clin 68: 394-424, 2018.
17. Prodoehl MJ, Hatzirodos N, Irving-Rodgers HF, Zhao ZZ, Painter JN, Hickey TE, Gibson MA, Rainey WE, Carr BR, Mason HD, *et al*: Genetic and gene expression analyses of the polycystic ovary syndrome candidate gene fibrillin-3 and other fibrillin family members in human ovaries. Mol Hum Reprod 15: 829-841, 2009.
18. Wang Z, Liu Y, Lu L, Yang L, Yin S, Wang Y, Qi Z, Meng J, Zang R and Yang G: Fibrillin-1, induced by Aurora-A but inhibited by BRCA2, promotes ovarian cancer metastasis. Oncotarget 6: 6670-6683, 2015.
19. Millstein J, Budden T, Goode EL, Anglesio MS, Talhouk A, Intermaggio MP, Leong HS, Chen S, Elatre W, Gilks B, *et al*; AOCS Group: Prognostic gene expression signature for high-grade serous ovarian cancer. Ann Oncol 31: 1240-1250, 2020.
20. Kellenberger LD and Petrik J: Hyperglycemia promotes insulin-independent ovarian tumor growth. Gynecol Oncol 149: 361-370, 2018.
21. Hanahan D and Weinberg R A: Hallmarks of Cancer: The next Generation. Cell 144: 646–674, 2011.

22. Cantuaria G, Fagotti A, Ferrandina G, Magalhaes A, Nadji M, Angioli R, Penalver M, Mancuso S and Scambia G: GLUT-1 expression in ovarian carcinoma: Association with survival and response to chemotherapy. Cancer 92: 1144-1150, 2001.
23. Gyorffy B, Lánczky A and Szállási Z: Implementing an online tool for genome-wide validation of survival-associated biomarkers in ovarian-cancer using microarray data from 1287 patients. Endocr Relat Cancer 19: 197-208, 2012.
24. Saravi S, Katsuta E, Jeyaneethi J, Amin HA, Kaspar M, Takabe K, Pados G, Drenos F, Hall M and Karteris E: H2A Histone Family Member X (H2AX) Is Upregulated in Ovarian Cancer and Demonstrates Utility as a Prognostic Biomarker in Terms of Overall Survival. J Clin Med 9: 2844, 2020.
25. Schmittgen TD and Livak KJ: Analyzing real-time PCR data by the comparative C(T) method. Nat Protoc 3: 1101-1108, 2008.
26. Guo Q, Song Y, Zhang H, Wu X, Xia P and Dang C: Detection of Hypermethylated Fibrillin-1 in the Stool Samples of Colorectal Cancer Patients. Med Oncol 30: 695, 2013.
27. Hsu CW, Wang JC, Liao WI, Chien WC, Chung CH, Tsao CH, Wu YF, Liao MT and Tsai SH: Association between malignancies and Marfan syndrome: A population-based, nested case-control study in Taiwan. BMJ Open 7: e017243, 2017.
28. Naba A, Clauser KR, Mani DR, Carr SA and Hynes RO: Quantitative proteomic profiling of the extracellular matrix of pancreatic islets during the angiogenic switch and insulinoma progression. Sci Rep 7: 40495, 2017.
29. Summers KM, Bokil NJ, Baisden JM, West MJ, Sweet MJ, Raggatt LJ and Hume DA: Experimental and bioinformatic characterisation of the promoter region of the Marfan syndrome gene, FBN1. Genomics 94: 233-240, 2009.
30. De Koning DJ and Haley CS: Genetical Genomics in Humans and Model Organisms. Genetical genomics in humans and model organisms. Trends Genet 21: 377-381, 2005.
31. Hubner N, Wallace CA, Zimdahl H, Petretto E, Schulz H, Maciver F, Mueller M, Hummel O, Monti J, Zidek V, *et al*: Integrated transcriptional profiling and linkage analysis for identification of genes underlying disease. Nat Genet 37: 243-253, 2005.
32. Liberti MV and Locasale JW: The Warburg Effect: How Does It Benefit Cancer Cells? Trends Biochem Sci 41: 211-218, 2016.
33. Dong D, Dong Y, Fu J, Lu S, Yuan C, Xia M and Sun L: Bcl2 inhibitor ABT737 reverses the Warburg effect via the Sirt3-HIF1α axis to promote oxidative stress-induced apoptosis in ovarian cancer cells. Life Sci 255: 117846-117846, 2020.
34. Li WH, Zhang H, Guo Q, Wu XD, Xu ZS, Dang CX, Xia P and Song YC: Detection of SNCA and FBN1 methylation in the stool as a biomarker for colorectal cancer. Dis Markers 2015: 657570, 2015.
35. Chen J, Cai Y, Xu R, Pan J, Zhou J, Mei J, Zhou J and Mei J: Identification of four hub genes as promising biomarkers to evaluate the prognosis of ovarian cancer in silico. Cancer Cell Int 20: 270, 2020.
36. Mo X, Su Z, Yang B, Zeng Z, Lei S and Qiao H: Identification of key genes involved in the development and progression of early-onset colorectal cancer by co-expression network analysis. Oncol Lett 19: 177-186, 2020.
37. Shi S and Tian B: Identification of biomarkers associated with progression and prognosis in bladder cancer via co-expression analysis. Cancer Biomark 24: 183-193, 2019.
38. Zhai X, Xue Q, Liu Q, Guo Y and Chen Z: Colon cancer recurrence associated genes revealed by WGCNA co expression network analysis. Mol Med Rep 16: 6499-6505, 2017.
39. Kellenberger LD, Bruin JE, Greenaway J, Campbell NE, Moorehead RA, Holloway AC and Petrik J: The role of dysregulated glucose metabolism in epithelial ovarian cancer. J Oncol 2010: 514310, 2010.
40. Aran D, Camarda R, Odegaard J, Paik H, Oskotsky B, Krings G, Goga A, Sirota M and Butte AJ: Comprehensive analysis of normal adjacent to tumor transcriptomes. Nat Commun 8: 1077, 2017.
41. Kocaman N and Artaş G: Can novel adipokines, asprosin and meteorin-like, be biomarkers for malignant mesothelioma? Biotech Histochem 95: 171-175, 2020.
42. Rajagopal S and Shenoy SK: GPCR desensitization: Acute and prolonged phases. Cell Signal 41: 9-16, 2018.
43. Karteris E and Randeva HS: Orexin Receptors and G-Protein Coupling: Evidence for Another 'Promiscuous' Seven Transmembrane Domain Receptor. J Pharmacol Sci 93: 126-128, 2003.
44. Lee T, Yun S, Jeong JH and Jung TW: Asprosin impairs insulin secretion in response to glucose and viability through TLR4/JNK-mediated inflammation. Mol Cell Endocrinol 486: 96-104, 2019.
45. Zandi Z, Kashani B, Poursani EM, Bashash D, Kabuli M, Momeny M, Mousavi-Pak SH, Sheikhsaran F, Alimoghaddam K, Mousavi SA, *et al*: TLR4 blockade using TAK-242 suppresses ovarian and breast cancer cells invasion through the inhibition of extracellular matrix degradation and epithelial-mesenchymal transition. Eur J Pharmacol 853: 256-263, 2019.

Figure S1. Methylation analyses of CpG island regions of FBN1 in The Cancer Genome Atlas cancer datasets taken from the Shiny Methylation Analysis Resource Tool. β values for FBN1 are shown for cancer (red) and normal (grey). Significant differences in the FBN1 methylation of BRCA, CESC, CHOL, COAD, KIRP, PRAD, READ, THCA and UCEC. Significant change in methylation indicated as: *P<0.05; **P<0.01; ****P<0.0001. It must be noted that control data are absent for: ACC, DLBC, KICH, LAML, LGG, MESO, OV, TGCT, USC and UVM. ACC, acute myeloid leukaemia; BRCA, Breast invasive carcinoma; CESC, cervical squamous cell carcinoma and endocervical adenocarcinoma; CHOL, cholangiocarcinoma; COAD, colon adenocarcinoma; DLBC, lymphoid neoplasm diffuse large B-cell lymphoma; FBN1, fibrillin-1; KICH, kidney chromophobe; KIRP, kidney renal papillary cell carcinoma; LAML, acute myeloid leukaemia; LGG, brain lower grade glioma; MESO, mesothelioma; ns, not significant; OV, ovarian serous cystadenocarcinoma; PRAD, prostate adenocarcinoma; READ, rectum adenocarcinoma; TGCT, testicular germ cell tumours; THCA, thyroid carcinoma; UCEC, uterine corpus endometrial carcinoma; USC, uterine carcinosarcoma; UVM, uveal melanoma.

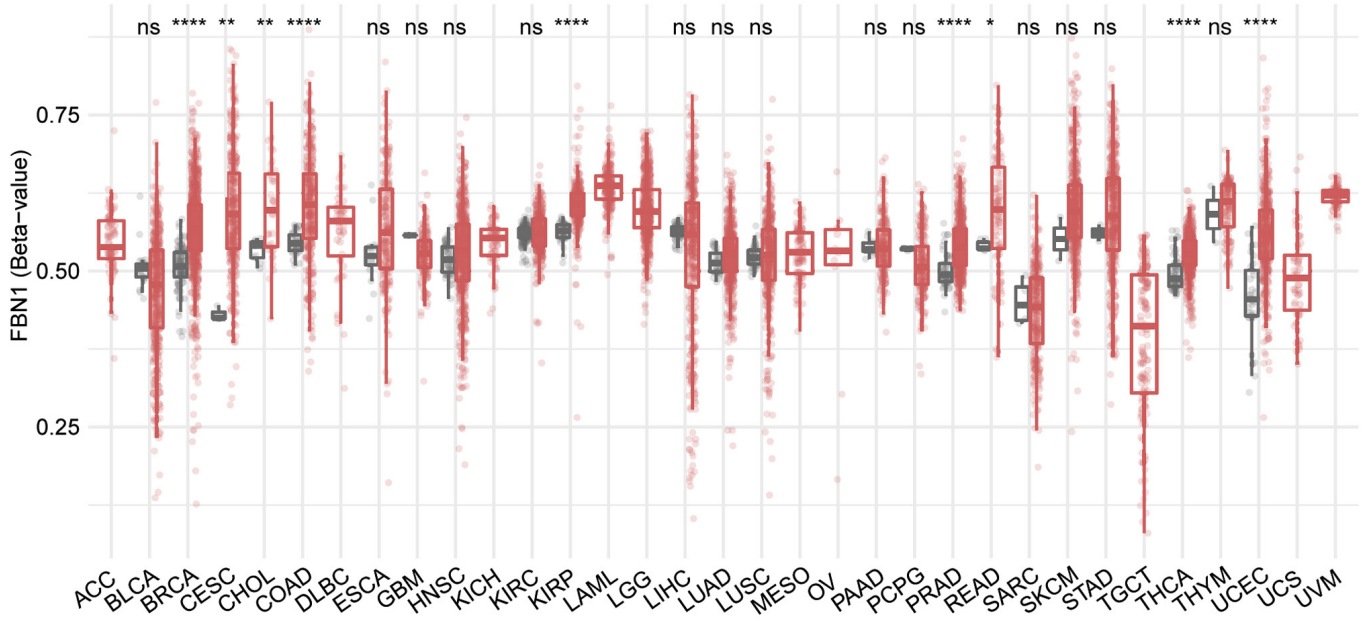

Table SI. List of cores used for the tissue microarray.

Position	Age, years	Organ/ anatomic site	Pathology diagnosis	TNM	Stage	Type	Tissue ID
A1	43	Ovary	Clear cell carcinoma	T1N0M0	I	Malignant	Fov010083
A2	61	Ovary	Clear cell carcinoma	T1aN0M0	IA	Malignant	Fov040482
A3	50	Ovary	Clear cell carcinoma	T1N0M0	I	Malignant	Fov021624
A4	40	Ovary	Clear cell carcinoma	T1N0M0	I	Malignant	Fov010007
A5	48	Ovary	Clear cell carcinoma (necrosis)	T2N0M0	II	Malignant	Fov010015
A6	50	Ovary	Low grade serous carcinoma	T2aN0M0	IIA	Malignant	Fov020291
A7	60	Ovary	Low grade serous carcinoma	T1cN0M0	IC	Malignant	Fov020114
A8	69	Ovary	Endometrioid adenocarcinoma	T1aN0M0	IA	Malignant	Fov010665
A9	41	Ovary	Low grade serous carcinoma	T1N0M0	I	Malignant	Fov050433
A10	37	Ovary	Low grade serous carcinoma	T1aN0M0	IA	Malignant	Fov050422
B1	25	Ovary	Low grade serous carcinoma	T1N0M0	I	Malignant	Fov010772
B2	34	Ovary	Low grade serous carcinoma	T1aN0M0	IA	Malignant	Fov010244
B3	59	Ovary	Low grade serous carcinoma	T1aN0M0	IA	Malignant	Fov020113
B4	34	Ovary	Low grade serous carcinoma	T1bN0M0	IB	Malignant	Fov010243
B5	56	Ovary	High grade serous carcinoma	T2N0M0	II	Malignant	Fov030109

B6	22	Ovary	High grade serous carcinoma	T2bN0M0	IIB	Malignant	Fov010682
B7	33	Ovary	High grade serous carcinoma	T1N0M0	I	Malignant	Fov010873
B8	56	Ovary	High grade serous carcinoma	T1N0M0	I	Malignant	Fov040102
B9	48	Ovary	High grade serous carcinoma	T1N0M0	I	Malignant	Fov010719
B10	43	Ovary	High grade serous carcinoma	T1N0M0	I	Malignant	Fov050462
C1	48	Ovary	High grade serous carcinoma	T2bN0M0	IIB	Malignant	Fov040044
C2	51	Ovary	High grade serous carcinoma	T3cN1M0	IIIC	Malignant	Fov010563
C3	42	Ovary	High grade serous carcinoma	T1N0M0	I	Malignant	Fov020069
C4	47	Ovary	High grade serous carcinoma	T3N0M0	III	Malignant	Fov100004
C5	64	Ovary	High grade serous carcinoma	T1N0M0	I	Malignant	Fov100071
C6	52	Ovary	High grade serous carcinoma	T1aN0M0	IA	Malignant	Fov040095
C7	53	Ovary	High grade serous carcinoma	T2N0M1	IV	Malignant	Fov020111
C8	60	Ovary	High grade serous carcinoma	T1bN0M0	IB	Malignant	Fov020132
C9	54	Ovary	High grade serous carcinoma	T3cN1M0	IIIC	Malignant	Fov010137
C10	53	Ovary	High grade serous carcinoma	T1N0M0	I	Malignant	Fov020262

D1	47	Ovary	High grade serous carcinoma	T1aN0M0	IA	Malignant	Fov020193
D2	48	Ovary	High grade serous carcinoma	T1N0M0	I	Malignant	Fov040164
D3	48	Ovary	High grade serous carcinoma	T3cN0M0	IIIC	Malignant	Fov030120
D4	53	Ovary	High grade serous carcinoma	T1cN0M0	IC	Malignant	Fov031530
D5	26	Ovary	High grade serous carcinoma	T3cN1M0	IIIC	Malignant	Fov010750
D6	35	Ovary	High grade serous carcinoma	T1aN0M0	IA	Malignant	Fov020067
D7	58	Ovary	High grade serous carcinoma	T1N0M0	I	Malignant	Fov020002
D8	60	Ovary	High grade serous carcinoma	T1aN0M0	IA	Malignant	Fov020386
D9	55	Ovary	High grade serous carcinoma	T1N0M0	I	Malignant	Fov010809
D10	67	Ovary	High grade serous carcinoma	T1aN0M0	IA	Malignant	Fov050706
E1	57	Ovary	High grade serous carcinoma	T3cN1M0	IIIC	Malignant	Fov050417
E2	41	Ovary	High grade serous carcinoma	T1N0M0	I	Malignant	Fov020059
E3	63	Ovary	High grade serous carcinoma with necrosis	T1N0M0	I	Malignant	Fov100220
E4	52	Ovary	High grade serous carcinoma	T2N0M0	II	Malignant	Fov010892
E5	66	Ovary	High grade serous carcinoma	T3N1M0	IIIC	Malignant	Fov020106

E6	52	Ovary	High grade serous carcinoma	T1cN0M0	IC	Malignant	Fov020519
E7	64	Ovary	High grade serous carcinoma	T3N1M0	IIIC	Malignant	Fov020776
E8	62	Ovary	High grade serous carcinoma	T2N0M0	II	Malignant	Fov010328
E9	42	Ovary	High grade serous carcinoma	T2N0M0	II	Malignant	Fov010252
E10	49	Ovary	High grade serous carcinoma	T2N0M0	II	Malignant	Fov010181
F1	59	Ovary	High grade serous carcinoma with necrosis	T1cN0M0	IC	Malignant	Fov020486
F2	42	Ovary	High grade serous carcinoma (sparse)	T3cN1M0	IIIC	Malignant	Fov010706
F3	49	Ovary	High grade serous carcinoma	T1aN0M0	IA	Malignant	Fov030970
F4	69	Ovary	High grade serous carcinoma	T2N0M0	II	Malignant	Fov030128
F5	42	Ovary	High grade serous carcinoma	T3N1M0	IIIC	Malignant	Fov110030
F6	53	Ovary	High grade serous carcinoma with necrosis	T1aN0M0	IA	Malignant	Fov020263
F7	47	Ovary	High grade serous carcinoma	T1cN0M0	IC	Malignant	Fov020160
F8	49	Ovary	High grade serous carcinoma	T3N1M0	IIIC	Malignant	Fov010172
F9	52	Ovary	High grade serous carcinoma	T3cN1M0	IIIC	Malignant	Fov021617

F10	55	Ovary	High grade serous carcinoma	T3N1M0	IIIC	Malignant	Fov021215
G1	52	Ovary	High grade serous carcinoma	T2N0M0	II	Malignant	Fov020061
G2	51	Ovary	High grade serous carcinoma	T2N0M0	II	Malignant	Fov010748
G3	41	Ovary	High grade serous carcinoma	T1aN0M0	IA	Malignant	Fov020497
G4	56	Ovary	High grade serous carcinoma	T3N0M0	III	Malignant	Fov100051
G5	55	Ovary	High grade serous carcinoma	T1N0M0	I	Malignant	Fov010903
G6	48	Ovary	High grade serous carcinoma	T3aN0M0	IIIA	Malignant	Fov050734
G7	60	Ovary	High grade serous carcinoma	T2bN0M0	IIB	Malignant	Fov050666
G8	51	Ovary	High grade serous carcinoma	T1aN0M0	IA	Malignant	Fov050388
G9	46	Ovary	Mucinous papillary adenocarcinoma (necrosis)	T1aN0M0	IA	Malignant	Fov020778
G10	49	Ovary	Endometrioid adenocarcinoma	T1N0M0	I	Malignant	Fov020162
H1	34	Ovary	Mucinous adenocarcinoma	T1bN0M0	IB	Malignant	Fov032024
H2	37	Ovary	Mucinous adenocarcinoma	T1aN0M0	IA	Malignant	Fov021635
H3	39	Ovary	Mucinous adenocarcinoma with necrosis	T1aN0M0	IA	Malignant	Fov020599
H4	54	Ovary	Mucinous adenocarcinoma	T2aN0M0	IIA	Malignant	Fov020100
H5	41	Ovary	Mucinous adenocarcinoma with necrosis	T1bN0M0	IB	Malignant	Fov020609

H6	50	Ovary	Mucinous adenocarcinoma	T3cN1M0	IIIC	Malignant	Fov060355
H7	52	Ovary	Mucinous adenocarcinoma	T1bN0M0	IB	Malignant	Fov120131
H8	38	Ovary	Mucinous adenocarcinoma	T1N0M0	I	Malignant	Fov050521
H9	29	Ovary	Mucinous adenocarcinoma	T3N0M0	III	Malignant	Fov020520
H10	58	Ovary	Endometrioid adenocarcinoma	T1aN0M0	IA	Malignant	Fov090031
I1	47	Lymph node	Metastatic serous carcinoma from ovary	-	-	Metastasis	Fov010120
I2	48	Lymph node	Metastatic serous carcinoma from ovary	-	-	Metastasis	Ily020241
I3	46	Lymph node	Metastatic serous carcinoma from ovary		-	Metastasis	Fov010080
I4	54	Lymph node	Metastatic serous carcinoma from ovary	-	-	Metastasis	Fov010094
I5	83	Lymph node	Metastatic serous carcinoma from ovary	-	-	Metastasis	Ily020307
I6	48	Lymph node	Metastatic clear cell carcinoma from ovary	-	-	Metastasis	Ily060045
I7	56	Pelvic cavity	Metastatic serous carcinoma of fibrofatty tissue from ovary of No.64	-	-	Metastasis	Fov100051
I8	57	Greater omentum	Metastatic serous carcinoma from ovary	-	-	Metastasis	Fov010040

I9	50	Lymph node	Metastatic serous carcinoma from ovary	-	-	Metastasis	Ily050024
I10	53	Pelvic cavity	Metastatic serous carcinoma of fibrofatty tissue from ovary	-	-	Metastasis	Fov060929
J1	69	Ovary	Adjacent normal ovary tissue	-	-	NAT	Fov032250
J2	48	Ovary	Adjacent normal ovary tissue	-	-	NAT	Fov120070
J3	53	Ovary	Adjacent normal ovary tissue	-	-	NAT	Fov032237
J4	42	Ovary	Adjacent normal ovary tissue	-	-	NAT	Fov110133
J5	42	Ovary	Adjacent normal ovary tissue	-	-	NAT	Fov120042
J6	40	Ovary	Adjacent normal ovary tissue	-	-	NAT	Fov120139
J7	59	Ovary	Adjacent normal ovary tissue	-	-	NAT	Fov050391
J8	42	Ovary	Adjacent normal ovary tissue	-	-	NAT	Fov120072
J9	35	Ovary	Adjacent normal ovary tissue	-	-	NAT	Fov110136
J10	45	Ovary	Adjacent normal ovary tissue	-	-	NAT	Fov100025

Name, BC11115c; Description, Ovary cancer with adjacent normal tissue array, including pathology grade, TNM and clinical stage, 100 cases.

Chapter 3

Differential regulation of genes by the glucogenic hormone asprosin in ovarian cancer

Statement of Contribution

For the completion of the presented manuscript I contributed towards the following:

- Data curation
- Methodology
- Formal analysis
- Writing—original draft
- Writing—review and editing
- Referencing

Journal of
Clinical Medicine

MDPI

Article

Differential Regulation of Genes by the Glucogenic Hormone Asprosin in Ovarian Cancer

Rachel Kerslake [1], Cristina Sisu [1], Suzana Panfilov [1], Marcia Hall [1,2], Nabeel Khan [1,2], Jeyarooban Jeyaneethi [1], Harpal Randeva [3,4], Ioannis Kyrou [3,4,5,6,7,*,†] and Emmanouil Karteris [1,*,†]

1 Division of Biosciences, College of Health, Medicine and Life Sciences, Brunel University London, Uxbridge UB8 3PH, UK
2 Mount Vernon Cancer Centre, Rickmansworth Road, Northwood HA6 2RN, UK
3 Warwickshire Institute for the Study of Diabetes, Endocrinology and Metabolism (WISDEM), University Hospitals Coventry and Warwickshire NHS Trust, Coventry CV2 2DX, UK
4 Warwick Medical School, University of Warwick, Coventry CV4 7AL, UK
5 Centre for Sport, Exercise and Life Sciences, Research Institute for Health & Wellbeing, Coventry University, Coventry CV1 5FB, UK
6 Aston Medical School, College of Health and Life Sciences, Aston University, Birmingham B4 7ET, UK
7 Laboratory of Dietetics and Quality of Life, Department of Food Science and Human Nutrition, School of Food and Nutritional Sciences, Agricultural University of Athens, 11855 Athens, Greece
* Correspondence: kyrouj@gmail.com (I.K.); emmanouil.karteris@brunel.ac.uk (E.K.)
† These authors contributed equally to this work.

Abstract: Background: Ovarian cancer (OvCa) is one of the most lethal forms of gynaecological malignancy. Altered energy metabolism and increased aerobic glycolysis in OvCa are hallmarks that demand attention. The glucogenic hormone asprosin is often dysregulated in metabolic disorders such as insulin resistance, diabetes (type 2 and gestational), and preeclampsia. Despite association with metabolic disorders, its role in energy metabolism within the tumour microenvironment is yet to be explored. Here, we study the role of asprosin in OvCa using transcriptomics and expand on functional studies with clinical samples. Methods: RNA sequencing, functional gene enrichment analysis, Western blotting and ImageStream. Results: Following treatment with 100 nM of asprosin, the serous OvCa cell line, SKOV-3, displayed 160 and 173 gene regulatory changes, at 4 and 12 h respectively, when compared with control samples ($p < 0.05$ and Log2FC > 1). In addition to energy metabolism and glucose-related pathways, asprosin was shown to alter pathways associated with cell communication, TGF-β signalling, and cell proliferation. Moreover, asprosin was shown to induce phosphorylation of ERK1/2 in the same in vitro model. Using liquid biopsies, we also report for novel expression of asprosin's predicted receptors OR4M1 and TLR4 in cancer-associated circulating cells; with significant reduction seen between pre-chemotherapy and end of first line chemotherapy, in addition to patients under maintenance with bevacizumab +/− olaparib for OR4M1. Conclusions: In relation to OvCa, asprosin appears to regulate numerous signalling pathways in-vitro. The prognostic potential of OR4M1 in liquid biopsies should also be explored further.

Keywords: asprosin; ovarian cancer; OvCa; high grade serous ovarian cancer; HGSC; OR4M1; TLR4; metabolism; RNA sequencing

Citation: Kerslake, R.; Sisu, C.; Panfilov, S.; Hall, M.; Khan, N.; Jeyaneethi, J.; Randeva, H.; Kyrou, I.; Karteris, E. Differential Regulation of Genes by the Glucogenic Hormone Asprosin in Ovarian Cancer. *J. Clin. Med.* **2022**, *11*, 5942. https://doi.org/10.3390/jcm11195942

Academic Editors: Christos R. Iavazzo and Giuseppe Carlo Iorio

Received: 4 August 2022
Accepted: 3 October 2022
Published: 8 October 2022

1. Introduction

Asprosin is an orexigenic hormone involved in the stimulation of appetite as well as the regulation of hepatic glucose. As a c-terminal cleavage product of profibrillin-1, encoded by the gene FBN1, this protein is processed via furin mediated proteolysis [1]. Fasting induces elevated plasma asprosin which stimulates the release of hepatic glucose within the circulation, through G-protein coupled receptor (GPCR) mediated activation [2]. Asprosin is as an adipokine with production primarily localised within white adipose tissue

(WAT),and elevated expression in obesity [3,4]; however, emerging studies also implicate asprosin expression with a growing number of peripheral tissues.

Since its discovery as a glucogenic hormone, asprosin has been implicated in metabolic disorders such as obesity, insulin resistance (IR) and type 2 diabetes mellitus (T2DM) [5,6]. Moreover, asprosin is shown to express a sexually dimorphic profile, with case studies recording higher levels of plasma asprosin in females and showing fluctuations of plasma levels in association with anaerobic exercise for women, yet stable levels in men regardless of exercise [7].

Of note, female metabolic disorders appear to correlate frequently with asprosin dysregulation. Fluctuations of plasma asprosin are seen throughout phases of the menstrual cycle with lower levels reported in women taking progesterone-based oral contraceptives [8]. Asprosin is also associated with pathological pregnancy-related disorders such as preeclampsia and gestational diabetes [9,10]. The role of asprosin has also been studied in relationship to the pathophysiology of polycystic ovarian syndrome (PCOS) [11,12].

The expression profiling of asprosin is incomplete; to date, its expression outside WAT has been shown in normal ovarian stromal and epithelial tissues of heifers and mice [13,14]. Recently, we studied the expression of asprosin and its precursor gene, FBN1, in ovarian cancers (OvCa) of varying grade and subtype; including high grade serous OvCa, which accounts for approximately 80% of OvCa cases [15]. We expanded on these observations in normal human ovarian epithelial and OvCa cell lines as well as normal adjacent tissues (NAT). OvCa affects over 313,000 women globally [16]. Given that >70% patients with OvCa present too late for curative treatment, i.e., Stages III/IV, and that incidence is predicted to increase, efforts to understand the causes including the metabolic drivers of OvCa are vital [17,18].

Aerobic glycolysis, known as the Warburg effect, is an illustrious factor implicated in the progression of many cancers including OvCa [19]. Despite the presence of oxygen, preferential use of the glycolytic pathway, where glucose is used in the rapid production of energy, generating excess lactate, in opposition to aerobic respiration/oxidative phosphorylation, is often favoured utilising excessive glucose [20]. It is well recognized that respiration alone can maintain tumour viability. Aerobic glycolysis is a controllable factor, and aberrant regulation of growth factor signalling is an initiating event in oncogenesis [21]. As a glucogenic hormone, asprosin may prove to have a role in this process and is a promising candidate for investigation within the tumour microenvironment.

Risk factors for OvCa include insulin resistance, diabetes, and obesity [17], factors aligned with the aforementioned disorders associated with dysregulated levels of asprosin. There are reports of asprosin in association with other malignancies, for example, basal cell carcinoma, pancreatic cancer, as well as ductal breast carcinoma [22–24], in addition to our earlier study in OvCa [15]. As such, asprosin provides a promising new candidate for exploration within the OvCa tumour microenvironment, as well as a potential therapeutic target.

In the present study, we investigate changes at transcriptomic level (using RNAseq), in human OvCa cells treated with asprosin in vitro. This research builds upon previous work completed by our group, where we mapped the expression of asprosin within OvCa and presented evidence of the expression of a possible receptor of asprosin within OvCa using clinical samples and cell models [15]. Here, we aim to further elucidate the signalling pathways associated with asprosin using functional enrichment analyses of identified differentially regulated genes (DEGs) and explore its role within the tumour microenvironment.

2. Materials and Methods

2.1. Blood Samples and ImageStream Mark II Analysis

Blood samples from n = 100 OvCa patients were collected from Mount Vernon Cancer Centre, East and North Herts NHS Trust, as part of the CICATRIx study: Sample collection study to explore circulating tumour cells, cell free DNA and leucocytes with ImageStream

analysis in patients with various cancers. The study was approved by the West Midlands–South Birmingham Ethics Committee (reference 16/WM/0196; protocol number RD2016-08). Samples were prepared for imaging as previously described, with the only difference being the substitution of Pan-Cytokeratin (AE1/AE3) antibody with that of OR4M1 or TLR4 [25]. Cell images were captured with the ImageStream® X Mk II and subsequently assessed for the presence of OR4M1 or TLR4 using IDEAS™ software.

Inclusion criteria: Female patients aged 18 y or more, histologically confirmed diagnosis of high-grade serous ovarian cancer (HGSC), availability of formalin-fixed, paraffin-embedded (FFPE) tissue taken at the time of diagnosis of cancer, able to comply with study procedures, life expectancy > 3 months, no contra-indications to blood sampling, biopsy, imaging, etc., and patients willing to anonymously share data and able to provide written informed consent.

Exclusion criteria: Patients with any other form of ovarian cancer, e.g., endometrioid, clear cell, mucinous carcinoma, borderline tumours; lack of written consent; or positive pregnancy test. OvCa staging is defined by the International Federation of Gynecology and Obstetrics (FIGO) staging system. Stage I cancer is confined to the ovaries. Stage II OvCa has metastasized to adjacent locations within the pelvic cavity. Stage III refers to OvCa metastasis outside of the pelvic cavity, and stage IV refers to distant metastases [26].

2.2. Tissue Culture

The SKOV-3 cell line (ECAAC 91091004) was grown in Dulbecco's modified Eagle's medium (DMEM), supplemented with 10% foetal bovine serum and 1% penicillin-streptomycin (Thermo Fisher Scientific, Loughborough, UK). Cells were grown in T75 filter head flasks at 37 °C, in humified conditions at 5% CO_2 and passaged three times at 80–90% confluency before seeding in 6 well plates at a density of 0.3×10^6. Cell count and viability assay were performed using a Neubauer chamber and Trypan blue (Invitrogen; Thermo Fisher Scientific, Loughborough, UK) exclusion method. Cells were treated with 100 nM of asprosin (Biolegend, San Diego, CA, USA) for 4 and 12 h in triplicate with corresponding controls. Duplicate experiments were generated for validation work.

2.3. RNA Extraction and cDNA Synthesis

Treatments were arrested at 4 and 12 h following media removal and washed with PBS (Thermo Fisher Scientific, Loughborough, UK). RNA isolation was achieved using Qiagen RNeasy extraction kit (Qiagen, Manchester, UK), according to the manufacturer's instructions; samples were eluted in 40 ul of deionised water. Purity assessment was performed with NanoDrop 2000C. RNA was stored at −80 °C prior to shipment and sequencing. Duplicate samples were reverse transcribed using Applied Biosystems High-capacity cDNA Reverse Transcription Kit (Thermo Fisher Scientific, Loughborough, UK), for RT-qPCR.

2.4. RT-qPCR Analysis

Relative gene expression of treated vs. control samples for 4 and 12 h were measured using iTaq™ Universal SYBR Green Supermix (Bio-Rad Laboratories, Hercules, CA, USA) with the Bio-Rad CFX96 Touch Real-Time PCR Detection System, according to the provided guidelines. Primers used are listed in Table 1. Primer pairs for TXK were designed through Sigma Aldrich Primer Design with sequences obtained from the Harvard Primer Bank (Primer bank ID-148596973c3) [27]. Primers for MAGI2-AS3, FCGR2A and GAPDH were obtained commercially through Thermo Fisher Scientific.

To quantify expression Ct values were used to calculate the expression fold change conveying the fold change in comparison to a valid calibrator, i.e., control samples. The ΔCt method was applied using the following formulae:

$$\Delta Ct = Ct \text{ gene of interest} - Ct \text{ reference gene}$$

$$\Delta\Delta Ct = \Delta Ct \text{ sample} - \Delta Ct \text{ control average}$$

$$\text{Fold Change Expression} = 2^{-\Delta\Delta Ct}$$

Table 1. Primer sequences used for RNA seq validation.

Gene	Strand F to R
TXK	ACGGAGGCTGCCATAAAACAT
	GGATTGATTGAAAGGCGTGTCT
FCGR2A	CCTGAGAGCGACTCCATTCAG
	GTCTGTAAACAGATTTCATCCGTCCT
MAGI2-AS3	GCTCTCATAGGCCACCTTGC
	CTCCATCCTCATTCTCTCACCAC
GAPDH	GGAGAAGGCTGGGGC
	GATGGCATGGACTGTGG

2.5. RNA Sequencing

Three technical replicates from each cohort (i.e., 3 × no supplement control and 3 × treated) were sent on dry ice for sequencing to Macrogen Seoul, South Korea. Samples underwent a strict quality control assessment (see appendix) before processing and cDNA library construction. Indexed libraries were submitted to an Illumina NovaSeq (Illumina, Inc., San Diego, CA, USA), and the paired-end (2 × 100 bp) sequencing was performed by Macrogen Incorporated using an Illumuna platform. Files were compiled by Macrogen using lllumina package bcl2fastq to convert the base call (BCL) binary results to FASTQ. The average reads of the triplicates for each condition are outlined in Table 2.

Table 2. Total number of reads. For paired-end sequencing values refer to the average sum of read 1 and read 2 in triplicate.

Condition	Average Total Reads
Control (4 h)	70,027,291
100 nM Asprosin (4 h)	69,128,541
Control (12 h)	68,811,451
100 nM Asprosin (12 h)	74,371,331

An RNA seq processing pipeline was designed according to a previous study [28]. Briefly, TopHat2 (v.2.1.1) was used to align reads to the human reference genome, GRCH38 (hg19) with Bowtie2 (v.2.2.6) ultra-high-throughput short read aligner. All experimental replicates were merged using Samtools (v.0.1.19) with selection criteria of high-quality mapped reads set to <30, before transcript assembly and quantification using Cufflinks (v.2.2.1). Cuffdiff (v.2.2.1) was then used to obtain differential expression profiles between time points.

2.6. RNA Sequencing Statistical Analysis

Data processing, modelling, cleaning, visualisation, and statistical analyses were conducted using R (v. 4.1.0, The R Foundation for statistical Computing, Vienna, Austria) with the R Studio desktop application (version 1.4.1717, RStudio, Boston, MA, USA). Calculations include the Pearson correlation coefficient for estimation of gene correlation and expression pattern; student's *t*-test to assess statistical significance between state of expression (e.g., asprosin 100 nM at 4 h vs. no supplement control at 4 h). Threshold for significance was set at a p-value < 0.05. Volcano plots and Venn diagram were generated using R package ggplot2 v.3.3.5. R package pathfindR was used for comprehensive identification of enriched pathways in omics data.

2.7. Functional Annotation

Differentially expressed genes were characterised with FunRich (v.3.1.3), a software used for gene functional classification and annotation [29]. The following characteristics were computed for the associated DEGs: biological pathway, molecular function, biological process, cellular component, and site of expression. We also performed Gene Set Enrichment Analysis (GSEA), comparing controls vs. combined 4 and 12 h treatments, using the GSEA software [30].

2.8. Western Blot

Protein lysate was extracted from treated cells using Laemmli buffer (Sigma Aldrich, Burlington, MA, USA). Samples were separated and transferred using SDS-PAGE gel electrophoresis and a wet transfer process. Membranes were blocked with 5% milk when detecting total proteins and 5% BSA when probing for phosphorylated proteins. Antibodies listed in Table 3 were left to incubate overnight at 4 °C. After washing with TBS Tween 20 (Sigma Aldrich, USA), the secondary antibody in a dilution of 1:2000 was applied for 60 min. Following additional washes, the proteins were exposed to X-ray film using enhanced chemiluminescence (Thermo Fisher Scientific, Loughborough, UK) and developed with Champion RG Universal RTU Developer and Champion RG Universal RTU Fixer solutions using an Agfa Curix 60 machine. Quantification was performed using Image J [31].

Table 3. List of antibodies used in Western blot.

Antibodies	Dilution	Source
GAPDH	1:1000	Cell Signalling
ERK 1/2	1:1000	Thermo Fisher Scientific
P38	1:1000	Cell Signalling
Akt	1:1000	Cell Signalling
Phospho-ERK 1/2	1:1000	Thermo Fisher Scientific
Phospho-P38	1:1000	Cell Signalling
Phospho-Akt	1:1000	Cell Signalling

2.9. Immunohistochemical Staining

An ovarian carcinoma tissue microarray containing 100 unique patient biopsy cores and adjacent tissues was purchased from Biomax Inc., Rockville, MD, USA (BC11115d). The ovarian tissue array contained 90 OvCa cores along with 10 non-adjacent tissue samples; it was not possible to obtain normal ovarian samples due to limited availability commercially, and ethical constraints obtaining extra healthy control tissues. Samples were probed with a 1:50 dilution of TLR4 antibody (Thermo Fisher Scientific, Loughborough, UK) according to our previously published methods [32]. All reagents unless otherwise stated were purchased from Thermo Fisher Scientific (Loughborough, UK). Briefly the FFPE slide was deparaffinized and rehydrated via submersion in histoclear and ethanol, followed by antigen retrieval in sodium citrate at 90 °C. Tissues were blocked with 5% BSA for 60 min (room temperature), before commencing overnight incubation at 4 °C with primary TLR4 antibody. The following day the slide was subjected to a series of washes with PBS 0.025% Triton X-100 prior to secondary antibody incubation (1:200 in 1% rabbit serum; ZytoChem Plus HRP-DAB kit, rabbit, cat. no. HRP008DAB-RB, Zytomed Systems GmbH) for 60 min (room temperature). Next, the slide was treated with streptavidin-HRP conjugate from the same Zytochem kit for 30 min. Final washes were conducted and the tissues were stained with 3,3′-diaminobenzidine (DAB) (Vector Laboratories, Inc., Newark, CA, USA) for 5 min and counterstained with haematoxylin (Merck KGaA, Darmstadt, Germany) for ~10 s before bluing with 0.1% sodium bicarbonate. Immunoreactivity of TLR4 was assessed using a light microscope (Carl Zeiss AG, Oberkochen, Germany). A pheochromocytoma (adrenal gland) core was used as a positive control.

3. Results

3.1. Differentially Expressed Genes (DEGs) upon Treatment with Asprosin

Following treatment with 100 nM of asprosin, the serous OvCa cell line, SKOV-3, displayed 160 and 173 gene changes, at 4 and 12 h, respectively, when compared with control samples extracted at parallel time points, $p < 0.05$ and Log2FC > 1. DEGs were identified using the Cuffdiff multiple-testing module [28]. These changes are mapped in the volcano plots presented in Figure 1.

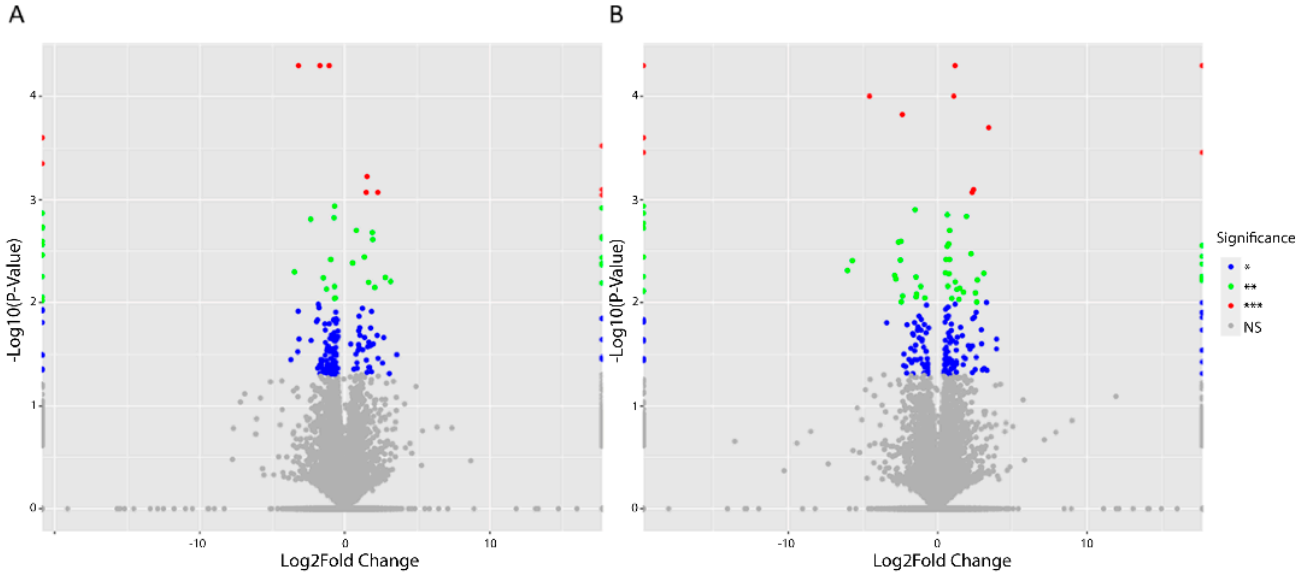

Figure 1. Volcano plots showing differentially regulated genes (DEGs) in SKOV-3 cells treated with 100 nM of asprosin. (**A**) DEGs 4 h post treatment; (**B**) DEGs 12 h following treatment. Significance level is recorded as NS (Non-Significant) = grey; * $p < 0.05$ = blue; ** $p < 0.01$ = green; *** $p < 0.001$ = red.

3.2. Functional Analysis of DEGs

A combination of 321 genes from the SKOV-3 cells were presented as being differentially regulated from the control groups when treated with 100 nM of asprosin compared with control samples extracted at parallel time points. A total of 160 of these DEGs were identified 4 h post treatment and an additional 173 DEGs were detected 12 h following treatment. All genes chosen for functional enrichment analysis were subjected to a threshold of $p < 0.05$ and Log2FC > 1. There were 12 common DEGs between the 4 h and 12 h groups (Figure 2).

Using the Funrich functional annotation data base (version 3.1.4), 58/160 and 64/173 DEGs were recognised for functional annotation from the 4 and 12 h data sets, respectively. Classification of the biological processes, molecular function, biological pathways, sites of expression and cellular components associated with asprosin treatment were identified with fold change expression measured and hypo geometric analysis applied, * $p < 0.05$ (Figure 3).

GSEA analysis showed a number of pathways regulated by asprosin, including apical junction, angiogenesis, TGF-β and notch signalling, reactive oxygen species (ROS) and complement (Figures 4 and 5).

3.3. Validation of Differentially Expressed Genes

Genes that were commonly expressed at both 4 and 12 h were chosen for analysis, in addition to their association with cancer in the literature [33–35]. FCGR2A, MAGI2-AS3 and TXK were up-regulated on initial treatment with asprosin and show a similar increase in expression upon repeat and validation with RT-qPCR, albeit to a lesser effect than seen in RNA sequencing (Figure 6).

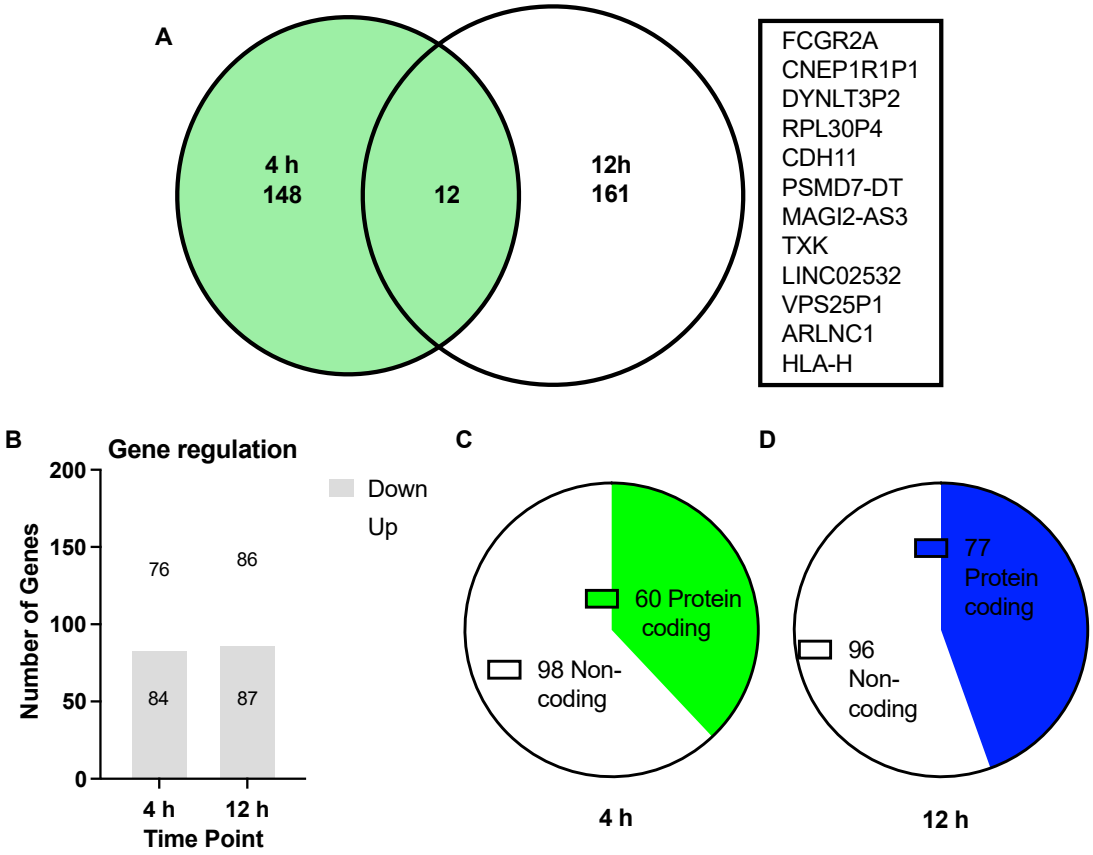

Figure 2. Summary of differentially expressed genes (DEGs) from 4 h (green) and 12 h (blue) data sets, comparing SKOV-3 cells treated with 100 nM of asprosin with non-supplemented controls. (**A**) Venn diagram depicting the number of unique DEGs at 4 h (148) and 12 h (161) with 12 common genes between the overlapping time points annotated to the right of the diagram; (**B**) Bar graph showing the number of up regulated and down regulated DEGs at each time point; (**C**,**D**) Quantification of coding and non-coding genes for each time point: (**C**) 60 protein coding, with 98 non-coding at 4 h; (**D**) 77 protein coding and 96 non-coding at 12 h.

3.4. Asprosin Induces Phosphorylation of ERK1/2

SKOV-3 cells were treated with asprosin (100 nM) for 5 and 15 min and phosphorylation of key kinases was measured using Western blotting. With the exception of ERK1/2, all other kinases (Akt, and p38) did not show an increase in phosphorylation within the times assessed (Figure 7). The increase in ERK1/2 phosphorylation appeared to be significant at 5 min.

3.5. Cancer-Associated Circulating Cells Express Receptors for Asprosin

In our previous study [15], we demonstrated that OvCa tissue expresses OR4M1. Here, we expand on these initial observations, showing that OvCa associated circulating cells express both of the considered receptors for asprosin, OR4M1 and TLR4 (Figure 8).

Moreover, in the case of OR4M1 + ve circulating cells, there is a significant down-regulation as treatment progresses. In this study, 100 patients with high grade serous OvCa, being managed according to standard UK practise, had blood samples taken at various points during their cancer treatment (Figure 9A). The median age was 70 years (range 35–87). All except 7 patients were diagnosed with Stage III or IV high grade serous OvCA. Twenty-eight patients had samples taken at diagnosis prior to starting any treatment at all (pre chemotherapy or PreC). Fourteen patients had samples taken after their primary surgery and prior to any adjuvant chemotherapy treatment. We have grouped these patients together as the pre-chemotherapy cohort (n = 42).

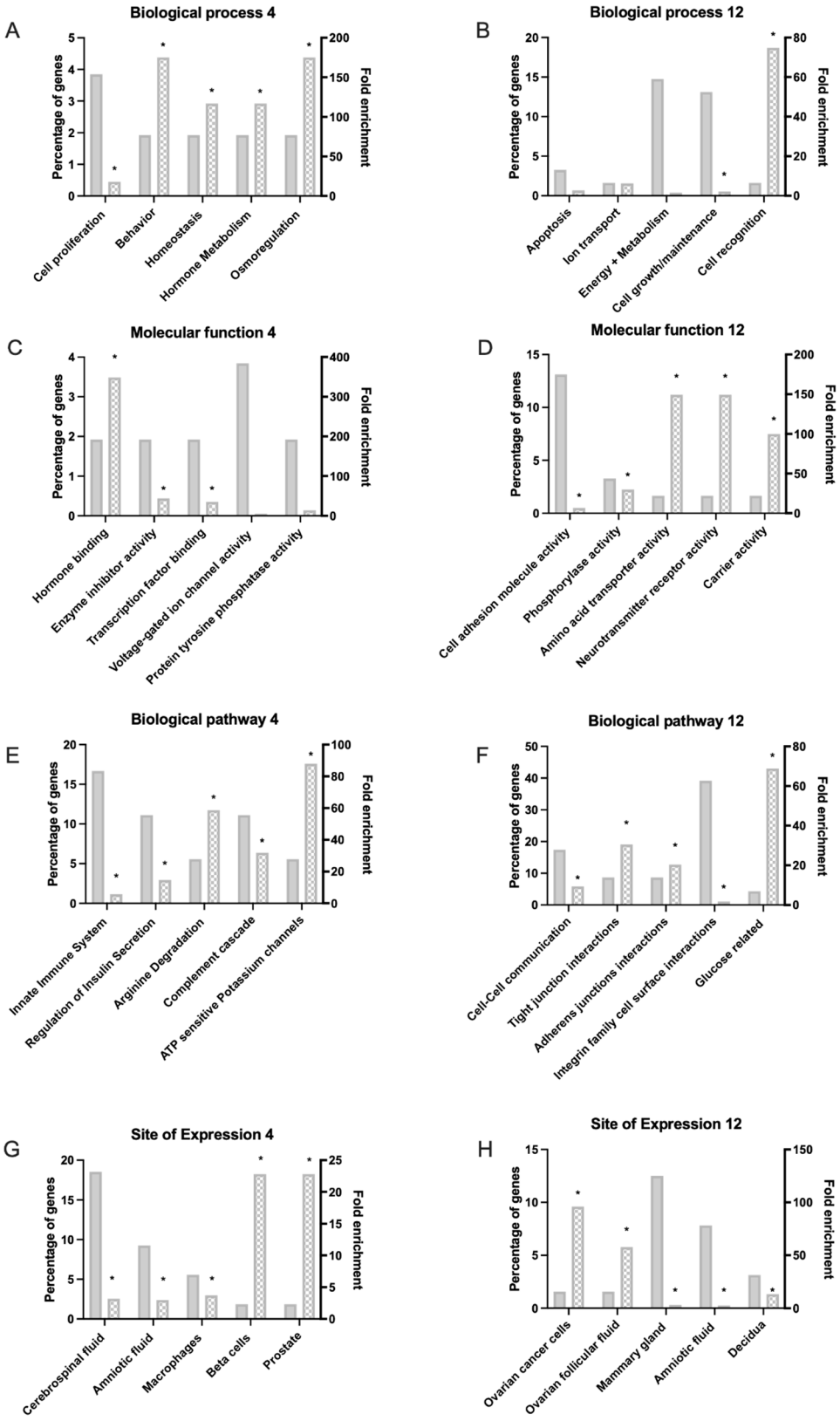

Figure 3. Functional enrichment of differentially expressed genes (DEGs) matched with Funrich data base. (**A**,**C**,**E**,**G**) indicate altered process 4 h after treatment with 100 nM asprosin; (**B**,**D**,**F**,**H**) show processes associated with DEGs 12 h after treatment. (**A**,**B**) Biological process; (**C**,**D**) Molecular function; (**E**,**F**) Biological Pathway; (**G**,**H**) Site of expression. Significant data sets identified using hypo geometric test are indicated by * $p < 0.05$.

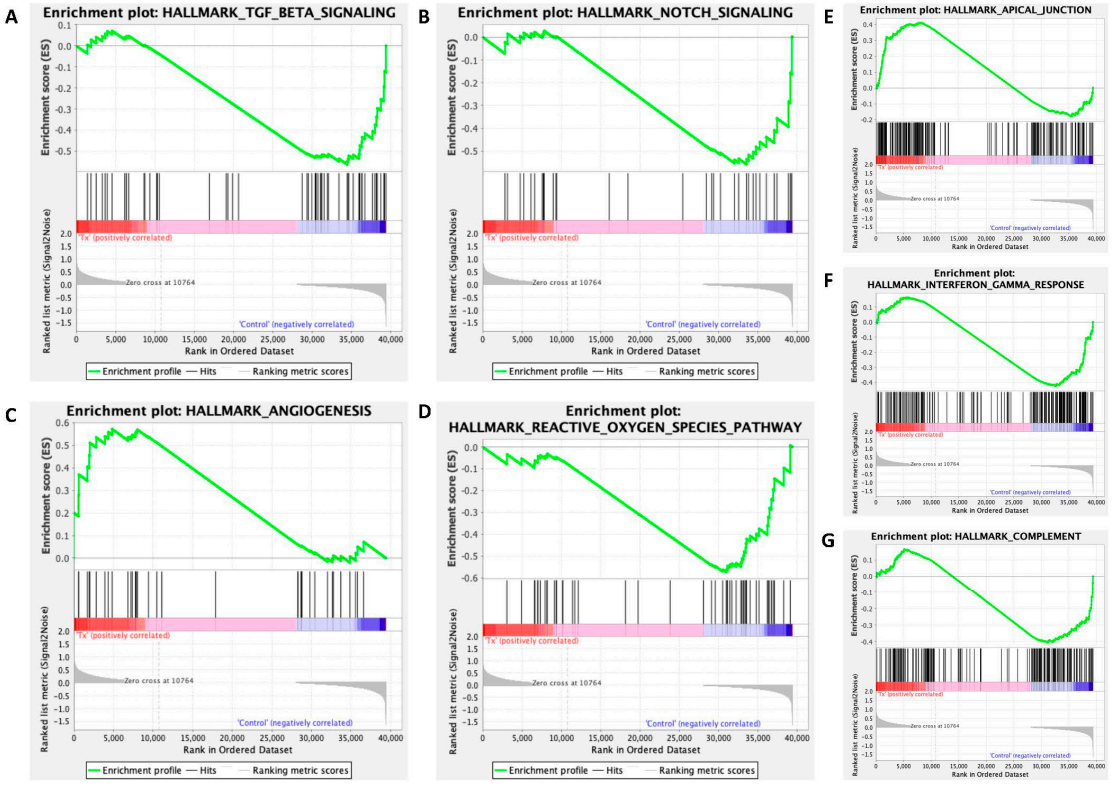

Figure 4. Gene set enrichment analysis (GSEA) of 100 nM asprosin-treated cells at 4 and 12 h combined panel of enrichment score curves: (**A**) TGF Beta Signalling; (**B**) Notch Signalling; (**C**) Angiogenesis; (**D**) Reactive Oxygen Species (ROS); (**E**), Apical Junction; (**F**) Interferon Gamma Response; (**G**) Complement.

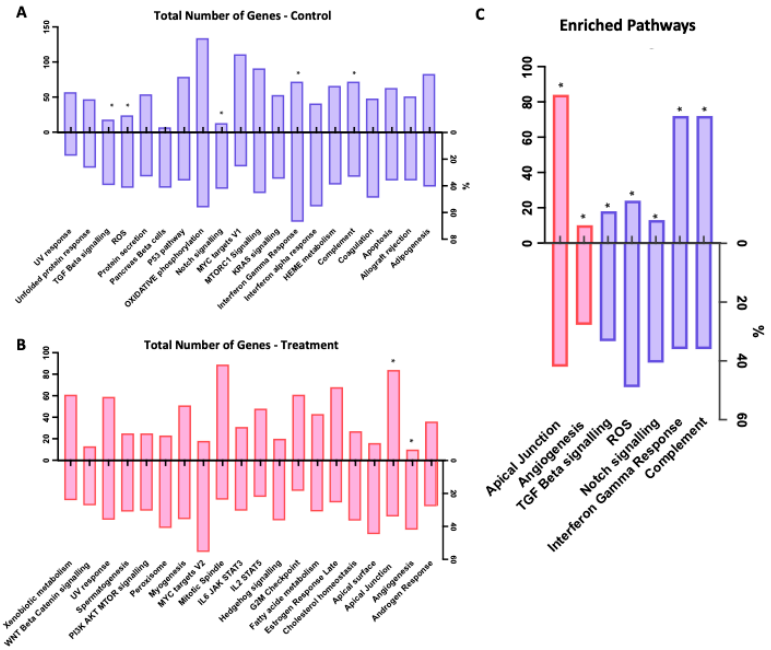

Figure 5. Selection of GSEA identified pathways influenced by asprosin in OvCa treated with 100 nM at 4 and 12 h combined. (**A**) Total pathways influenced by asprosin for control group (down regulated) in blue; (**B**) Total pathways influenced by asprosin for treatment group (up regulated) in red; (**C**) Combined pathways (regulation: up = red, down = blue) with pre-defined GSEA automated nominal p set to * $p = 0.2$.

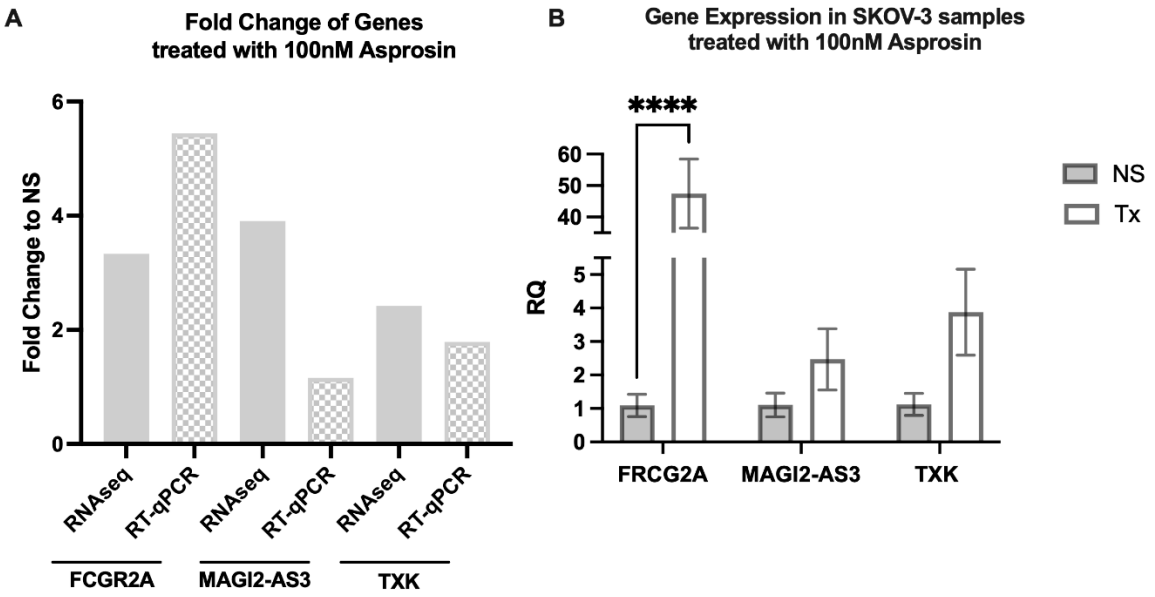

Figure 6. Validation of RNA seq data. Expression of FRCG2A, MAGI2-AS3 and TXK in SKOV-3 cells following treatment (Tx) with 100 nM asprosin at 4 h. (**A**) Gene expression shown as fold change (FC) in gene expression following treatment (100 nM asprosin) at 4 h compared to RNA seq fold increase. (**B**) RT-qPCR analysis of cells treated (Tx) with asprosin (100 nM) versus no supplement (NS) showing an increase in trend for all genes, with a significant change seen for FRCG2A, **** $p < 0.0001$.

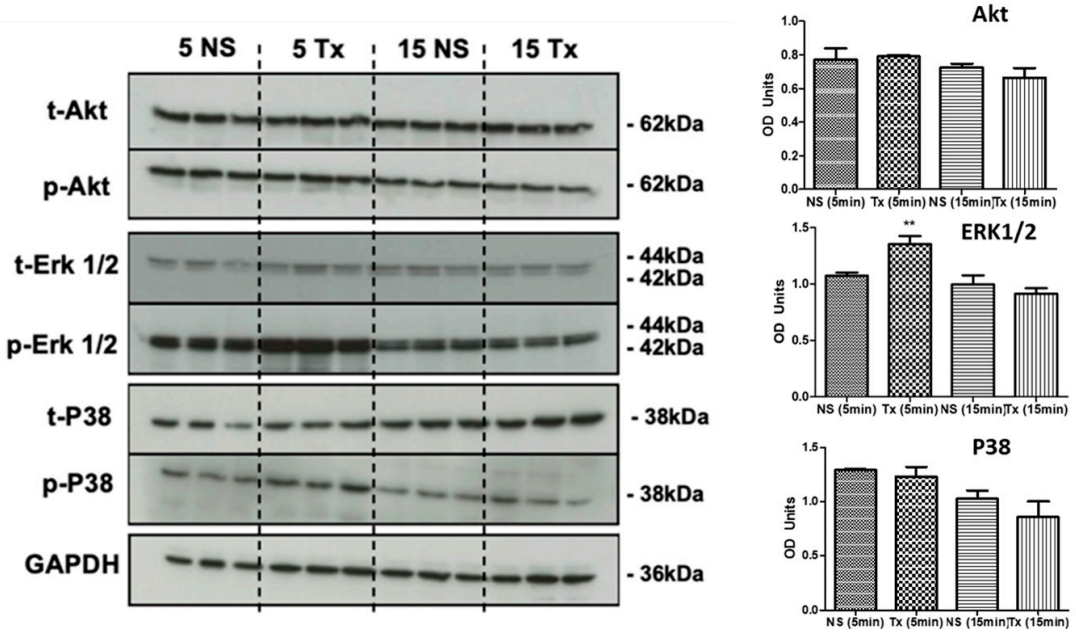

Figure 7. Western blots showing the total and phosphorylated proteins Akt, ERK 1/2, P38, and the loading control GAPDH following treatment with 100 nM of asprosin terminated at 5 and 15 min; followed by densitometric analysis. OD: Optical density, ** $p < 0.01$.

Eight patients had samples taken following completion of their first line chemotherapy treatment (carboplatin/paclitaxel +/− bevacizumab) and any surgery but prior to starting their maintenance bevacizumab (end-of-treatment first line cohort or EOT 1st line). Another 17 patients had samples taken during the maintenance treatment following first line chemotherapy and any surgery (maintenance bevacizumab/+/−olaparib or maintenance bevacizumab /olaparib).

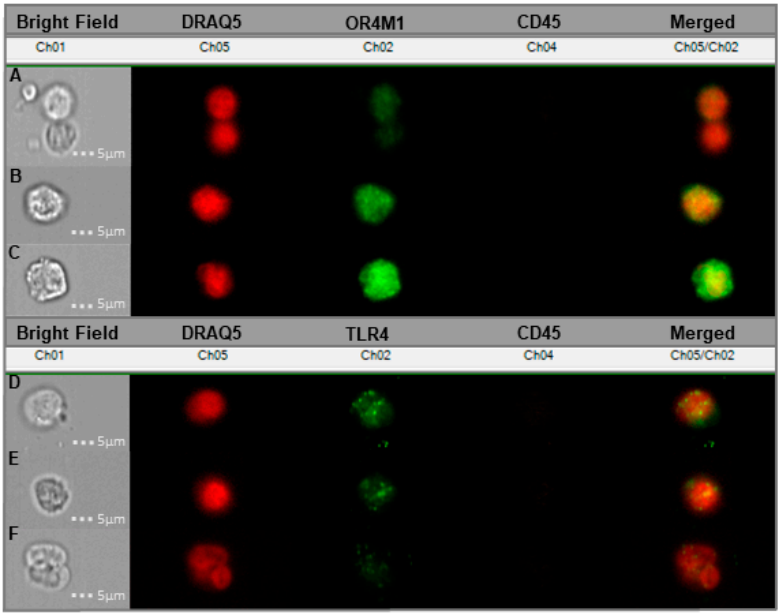

Figure 8. Cancer-associated circulating cells (CCs) from liquid blood biopsies donated by six different serous OvCa patients probed with OR4M1/TLR4. (**A**–**C**) Samples showing the expression of OR4M1 (Ch02—green) in the circulating tumour cells of patients presenting with high grade serous ovarian cancer; (**A**) represents stage IV, (**B**) stage IV and (**C**) stage III; (**D**–**F**) Expression of TLR4 in CCs; here, Ch02 represents TLR4 (green); (**D**) is representative of stage II, (**E**) stage III and (**F**) stage IV. Ch01, Bright Field; Ch02, OR4M1/TLR4 (green); Ch04, CD45—white blood cell exclusion marker (brown); Ch05, DRAQ5—cell nuclear stain (red); Ch02/05, overlay of Ch02 with Ch05. Stages (I–IV) refer to the severity of OvCa metastasis according to the International Federation of Gynaecology and Obstetrics (FIGO) staging system.

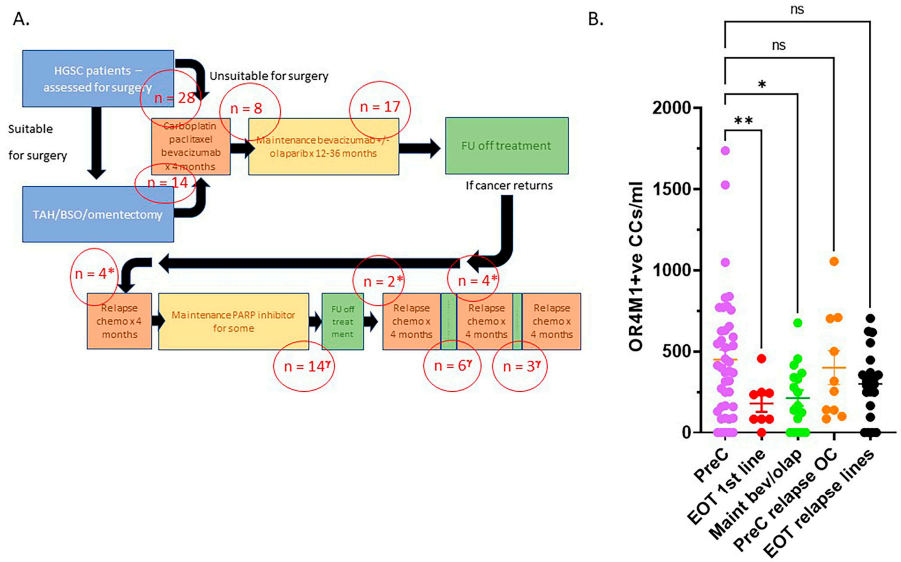

Figure 9. Panel (**A**): Schema of the recruitment of patients. FU: follow up, TAH/BSO: abdominal hysterectomy and bilateral salpingo-oophorectomy. Panel (**B**): OR4M1 + ve circulating cells decrease with chemotherapeutic treatment; 100 patients, representative of patients presenting with high grade serous ovarian cancer (HGSC) stages: I–IV: Pre-chemo (PreC, $n = 42$), end of first line chemotherapy (EOT 1st line, $n = 8$), maintenance bevacizumab +/− olaparib (maint bev/olap, $n = 17$), pre-chemo for relapse OC (PreC relapse OC, $n = 10$), end of chemo for relapse OC (EOT relapse lines, $n = 23$). (Error bars: SEM; significance determined using ANOVA, * $p = 0.012$, ** $p = 0.0069$). CCs: cancer-associated circulating cells.

Ten patients (*) had samples taken prior to commencing chemotherapy treatment for relapse HGSC (PreC for relapse). Four had blood samples taken prior to treatment for first relapse (second line chemotherapy), 2 prior to treatment for second relapse (third line of chemotherapy) and four patients prior to fourth/fifth line of chemotherapy treatment. Finally, 23 patients (γ) had blood taken at the end of chemotherapy treatment for a relapse of their cancer (EOT relapse lines): 14 following treatment for first relapse, most of these were on maintenance PARP inhibitors, 6 following third line chemotherapy (second relapse) and 3 following fourth/fifth line chemotherapy for third/fourth relapse.

Figure 9B demonstrates the numbers of OR4M1 positive CCs/mL per category. There was an average of 450 $\pm$ 60 CCs for the pre-chemotherapy cohort, 179 $\pm$ 51 for the end of first line chemotherapy cohort, 213 $\pm$ 48 for maintenance bevacizumab/+/$-$ olaparib cohort, 400 $\pm$ 104 for PreC relapse OvCa and 300 $\pm$ 43 for EOT-relapse lines. There were no differences in the expression OR4M1 positive CCs in BRCA wt (n = 90, 324 $\pm$ 28) versus BRCAm (n = 10, 419 $\pm$ 117) patients' samples.

4. Discussion

Despite a growing association with metabolic disorders, few forays have yet been made to explore asprosin's role in cancers. Our present work builds upon our previous findings of asprosin expression in OvCa tissue and starts to elucidate the role, if any, that asprosin may elicit over the Warburg effect and the tumour microenvironment [15]. In this study, we provide novel evidence on how asprosin can affect the OvCa transcriptome in vitro. In total, 160 and 173 differentially expressed genes (DEGs) were identified following exposure of SKOV-3 cells to 100 nM of asprosin at 4 and 12 h, respectively. Only 12 of these DEGs were similarly expressed at both time points. These DEGs include: the functionally expressed FCGR2A, CDH11 and TXK; the non-coding RNAs PSMD7-DT, MAGI2-AS3, LINC02532 and ARLNC1; as well as pseudogenes CNEP1R1P1, DYNLT3P2, RPL30P4, VPS25P1 and HLA-H.

Of the functionally expressed genes, many present associations with cancers throughout the literature. FCGR2A, for example, a gene involved in immune response and phagocytosis, is associated with chemotherapeutic and disease response in OvCa [33]. While increased expression, along with diminished CA125, also correlates positively with the survival of patients undergoing relapse, through the provision of enhanced farletuzumab receptor affinity [36]. Increased regulation of FCGR2A in our data following treatment with asprosin (Figure 2), may present a role in therapeutic response that requires future exploration. Furthermore, Cadherin 11 (CDH11), a membrane protein involved in calcium-dependant cell adhesion, essential for bone development and maintenance, is capable of regulating proliferation via ERK 1/2 signalling pathways [37,38]. In OvCa, CDH11 is connected to advanced stage and nodal involvement [39], in addition to migration and metastasis [37], yet displays limited involvement in cancer progression. CDH11 in association with lactic acid, a key metabolite of the Warburg effect, is, however, implicated in the metastatic progression of colorectal cancer [40]. Our research shows an increase in CDH11 expression within OvCa when exposed to asprosin, perhaps indicating association with the Warburg effect. Additional investigation with Kaplan Meier (Km) plotter links an increase of this DEG with poor overall survival (OS) in OvCa, $p < 0.002$ (Supplementary Figure S1). In addition, Yang et al. show that increased expression influences paclitaxel resistance in gastric cancer [41]. The tyrosine kinase, TXK, a signalling molecule involved in T Helper 1 cytokine production, is a predicted inhibitor of proliferation in cancers such as breast and colon [35,42,43]. Asprosin elicits an increase of this gene in our data, perhaps regulating cell growth, while Kaplan Meier analysis correlates high expression positively with OS ($p < 1.5 \times 10^{-6}$).

Non-coding RNAs are increasingly thought to be integral for gene regulation and are emerging targets of cancer biology. For example, the DEG, LINC02532, was recently identified as a marker of radiosensitivity in clear cell renal carcinoma, while ARLNC1, decreased in our data, is associated with maintenance of androgen receptor signalling

in prostate cancer [44,45]. The ncRNA MAGI2-AS3 is ubiquitously expressed in many cancers including OvCa and is another regulator of cell proliferation [46]. Gokulnath et al. show that MAGI2-AS3 can act as a tumour suppressor in high-grade serous carcinoma (HGSC) through the sponging of microRNAs and the suppression of MYC, leading to an inhibition of cell proliferation and migration [34,47]. Asprosin is seen to increase the expression of this gene at both 4 and 12 h. Increased expression, however, is associated with attenuated response to therapeutics such as cisplatin in nasopharyngeal carcinoma as well as lapatinib [48]. Further exploration with a Km plotter also associates increased expression with poor OS $p < 0.018$ (Supplementary Figure S1), perhaps implying biomarker traits. Further research is needed to understand the complex role of this DEG in OvCa.

Moreover, with the exception of HLA-H, which is associated with cervical carcinoma [49], the pseudogenes listed above reveal no hits within the literature (i.e., PubMed circa 20 June 2022). Of note, there were 194 non-coding genes identified following treatment with asprosin consisting of lncRNAs and pseudogenes. The functional classification of many pseudogenes remains to be determined, although there is literature suggesting that pseudogenes are often aberrantly expressed in cancers [50]. Indeed, our group has recently demonstrated a functional role of the lncRNA X-inactive specific transcript (XIST) in lung cancer [51]. Further investigation within the field is required to categorize these genes and the role they play in the ovarian tumour microenvironment.

Functional enrichment presented classifications for 58 of the 160 DEGs from the 4 h data set and 64 of the 173 DEGs from the 12 h data set. Our analysis revealed asprosin mediated dysregulation of key biological processes and hallmarks of cancer such as: apoptosis, cell proliferation and growth, as well as energy and metabolism [52]. The tumour microenvironment is known to be modulated by oncogenes which in turn regulate certain aspects of metabolism, ultimately leading to uncontrolled proliferation and metastasis [53].

Molecular functions dysregulated by asprosin are presented in Figure 3C,D, and include hormone binding, cell adhesion as well as protein tyrosine phosphatase activity; a process recently associated with asprosin mediated appetite stimulation [54]. Additional processes detected indicate that asprosin related DEGs are connected to the regulation of insulin as well as glucose, which align with asprosin's metabolic profile as a glucogenic hormone capable of influencing homeostasis, its role following OR4M1 binding, as well as asprosin's role in insulin resistance [6]. Of note, elevated glucose levels along with increased expression of the glucose transporter, GLUT1, are potential biomarkers for OvCa [55]. The sites of expression with DEGs showing the highest degree of significance at 12 h are highly associated with female reproductive tissues including: OvCa; ovarian follicular fluid; mammary gland and decidua. This expression profile is to be expected of a hormone increasingly implicated with female reproductive disease and further emphasizes the need to assess asprosin's importance in the female metabolic profile.

Gene set enrichment analysis (GSEA) revealed asprosin mediated dysregulation of additional pathways: apical junctions, angiogenesis, transforming growth factor beta (TGF-β), notch signalling, reactive oxygen species (ROS), interferon gamma (IFN-γ) response and complement systems.

Claudins such as CLDN9 and 18 maintain polarity in epithelial/endothelial cells and are integral for the formation of tight cellular junctions known as apical junctions (Figure 4E). These junctions are vital for the polarization of epithelial cells and effective cell communication [56]. CLDN9 and CLDN18 show core enrichment through GSEA analysis in our data sets, Log2FC = 2 and Log2FC = 1.5, respectively. CLDN9 is associated with aerobic glycolysis (Warburg effect) in gastric and endometrial cancers and is associated with poor prognosis in oesophageal cancer [57,58]. CLDN18 has recently been established as a normal gastric tissue marker; however, the presence of a splice variant has been documented in patients with mucinous ovarian cancers, a rare subtype with a poor outlook [59,60]. The over-expression of CLDN18.2 in intestinal type mucinous tissue acts as a potential biomarker of mucinous borderline ovarian tumours, distinguishing Mullerian types, where it is absent, from intestinal sub-types [59,61].

The GSEA-associated pathways, angiogenesis and ROS, are well documented as hallmarks of cancer; OvCa is particularly responsive to anti-angiogenic agents such as bevacizumab [62]. ROS is often dysregulated in cases of hypoxia promoting DNA damage and genomic instability, another key hallmark of high grade serous OvCa [63]. Dysregulation of the Notch pathway in OvCa is indicative of poorer prognosis and increased chemo-resistance [64,65].

TGF-β signalling increases cellular proliferation, epithelial to mesenchymal transition (EMT), and reduces apoptosis. In OvCa, TGF-β regulates cell proliferation through activation of the IGF1R signalling axis, with increased levels associated with poor survival outcome [66]. TGF-β signalling is regulated by Fibrillin-1, the primary product of asprosin's precursor protein profibrillin-1 [67]. Aberration of TGF-β signalling is associated with Marfan's syndrome, an autosomal dominantly inherited connective tissue disorder categorized by skeletal, ocular, and cardiovascular anomalies. Marfan's is associated with mutations in the Fibrillin-1 gene, FBN1; other phenotypic variants such as marfanoid progeroid lipodystrophy syndrome, and neonatal progeroid syndrome form part of this group of 'fibrinillopathies' and are associated with depletion of asprosin, consequently encoded by the final two exons of FBN1 [68,69]. As such, dysregulation of this pathway may indicate an asprosin exerted feedback mechanism in OvCa.

To evaluate the effects of asprosin on common signalling pathways identified in the functional enrichment analysis we explored the phosphorylation status of Akt, ERK 1/2 and P38 using Western blot analysis. Following treatment with 100 nM asprosin, the SKOV-3 model did not demonstrate any change in Akt phosphorylation, 5 or 15 min after asprosin was administered. Nor were there marked changes for p38, an integral molecule involved in cell death which is associated with female cancers [70]. Our data does, however, indicate a short-lived increase in the phosphorylation of ERK 1/2, 5 min after asprosin treatment (Figure 7). The aforementioned, CDH11, which is increased in our data, is an emerging regulator of ERK 1/2. Heightened phosphorylation of ERK 1/2 is associated with increased cell proliferation in cancers including ovarian [71]. This is the first time that changes in ERK 1/2 phosphorylation have been associated with asprosin treatment; as such, its role as a downstream target requires further attention. Despite our study recording no change in Akt phosphorylation for the measured time scales, there are reports of impaired phosphorylation, along with insulin resistance, in mouse skeletal muscle treated with 100 nM of asprosin 24 h after treatment. Therefore, additional longer time points may reveal further post-translational modifications in addition to our short-lived burst of ERK 1/2 phosphorylation; as such, these signalling molecules should not be discounted from future research.

Asprosin appears through the literature to bind promiscuously to three diverse receptors, each responsible for a distinct biological response. Indeed, binding to Olfactory Receptor 4 Member 1 (OR4M1), a G-protein coupled receptor (GPCR), implicates asprosin with glucose regulation; binding to Toll Like Receptor 4 (TLR4), which is aberrantly expressed in OvCa tissues of varying stages, grades and subtypes (Supplementary Figure S2), associates asprosin with insulin resistance in skeletal muscle [2,72]; emerging evidence also implicates stimulation of Protein Tyrosine Phosphatase Receptor delta (PTPRd) by asprosin as a mediator of orexigenic influence [54]. Additional work should seek the use of cross-linked proteins with immunoprecipitation and mass spectrometry to identify which, if not all, receptors asprosin binds to in a cell- or organ-specific manner. However, this falls beyond the scope of the current study as first we sought to explore the expression profile of these receptors.

Here, using liquid biopsies from OvCa patients, we demonstrate novel expression of both OR4M1 and TLR4 in cancer-associated circulating cells (CCs) of patients with high grade serous OvCa, with a significant decline in OR4M1 positive cells seen between pre-chemotherapy and treatments. To the best of our knowledge, this is the first time an olfactory receptor demonstrates a prognostic potential in OvCa. Due to limitations of samples, we could not replicate the study for TLR4, and we acknowledge this limitation.

Interestingly, TLR4 expression has been linked with cellular proliferation and paclitaxel resistance in vitro [73]. The presence of both predicted receptors on the surface of these cells may indicate another potential role of this energy metabolite in cancer-associated circulating cells.

Due to ethical restrictions, we were unable to compare levels of TLR4 and PTPRd. We acknowledge that this is a major limitation of this part of the study, and additional quantification of asprosin-associated receptors TLR4 and PTPRd in liquid biopsies and correlation with progression of treatment will encompass impending studies. Another limitation of the study is the use of a singular OvCa cell line. In the future, other OvCa preclinical models including HEYA8, or OVCAR5 or OVCAR8 should be used to investigate further the effects of asprosin. Future studies should concentrate on performing analysis using a wider repertoire of OvCa in vitro models focussing on metabolic pathways using glycolysis assay and lactate production; in addition, a Seahorse assay should be applied to see how asprosin modulates these functions under normal conditions and following silencing of OR4M1, TLR4 or PTPRd receptors using CRISPR or siRNA. Future studies should also concentrate on assessing changes in the glucose uptake rate and lactate production upon treatment with asprosin in vitro. Finally, further validation of the metabolic pathways from GSEA analyses using a number of in vitro models will be useful. In particular, genes that were highlighted under GSEA analyses and also appeared as significant DEGs such as: ABCC8, that have shown prognostic significance in OvCa, or CLDN18 or 9, given the role of claudins in tumorigenesis require future exploration.

5. Conclusions

This study presents asprosin as a hormone capable of influencing gene regulation within the ovarian tumour microenvironment. 160 and 173 genes were dysregulated following treatment with 100 nM of asprosin in the OvCa cell model SKOV-3, at 4 and 12 h, respectively. Enrichment analysis revealed dysregulated pathways associated with energy metabolism such as oxidative phosphorylation, glucose regulation, ATP channels, glycolysis as well as ROS, in addition to genes such as FCGR2A, CDH11, MAGI2-AS3 as well as CLDN9 and 18. Our annotation accentuates asprosin's role in energy metabolism and presents evidence of possible influence over genes associated with the Warburg effect within the ovarian tumour microenvironment as well as asprosin's potential for further exploration in relation to therapeutic response. The mediation of these pathways by asprosin needs to be explored further to produce a definitive mechanism of action. Our research highlights the importance of asprosin as an emerging regulator of the female-specific metabolic profile.

Supplementary Materials: The following supporting information can be downloaded at: https://www.mdpi.com/article/10.3390/jcm11195942/s1, Figure S1: Kaplan Meier plots showing overall survival (OS) of OvCa patients with dysregulation of the following genes; Figure S2: Immunohistochemical Staining for TLR4 in ovarian cancers and control tissues; Figure S3. Raw data from Western blotting experiments. (**A**), Total and phospho-Akt; (**B**), Total and phos-pho-p38; (**C**), Endo Total and phospho-ERK1/2; (**D**), GAPDH as loading control.

Author Contributions: Conceptualization, I.K., H.R., M.H. and E.K.; methodology, C.S., R.K. and E.K.; software, C.S.; validation, R.K.; formal analysis, R.K., C.S., S.P., J.J., E.K. and N.K.; investigation, R.K., I.K., H.R., M.H., N.K. and E.K.; resources, H.R. and M.H.; writing—original draft preparation, R.K., E.K., C.S. and M.H.; writing—review and editing, R.K., I.K., H.R., M.H., C.S., E.K. and N.K.; visualization, R.K.; supervision, E.K., I.K. and M.H.; project administration, E.K.; funding acquisition; H.R. and M.H.; I.K. and E.K. are joint senior and corresponding co-authors. All authors have read and agreed to the published version of the manuscript.

Funding: The present study was funded by Cancer Treatment & Research Trust (CTRT) and University Hospitals Coventry and Warwickshire NHS Trust (grant no. 12899).

Institutional Review Board Statement: The study was conducted according to the guidelines of the Declaration of Helsinki, Protocol number RD2016-08, and approved by the West Midlands–South Birmingham Ethics Committee (reference 16/WM/0196).

Informed Consent Statement: Informed consent was obtained from all subjects involved in the study.

Data Availability Statement: RNAseq data available upon reasonable request.

Conflicts of Interest: The authors declare no conflict of interest.

References

1. Romere, C.; Duerrschmid, C.; Bournat, J.; Constable, P.; Jain, M.; Xia, F.; Saha, P.K.; Del Solar, M.; Zhu, B.; York, B.; et al. Asprosin, a Fasting-Induced Glucogenic Protein Hormone. *Cell* **2016**, *165*, 566–579. [CrossRef] [PubMed]
2. Li, E.; Shan, H.; Chen, L.; Long, A.; Zhang, Y.; Liu, Y.; Jia, L.; Wei, F.; Han, J.; Li, T.; et al. OLFR734 Mediates Glucose Metabolism as a Receptor of Asprosin. *Cell Metab.* **2019**, *30*, 319–328.e8. [CrossRef] [PubMed]
3. Duerrschmid, C.; He, Y.; Wang, C.; Li, C.; Bournat, J.C.; Romere, C.; Saha, P.K.; Lee, M.E.; Phillips, K.J.; Jain, M.; et al. Asprosin is a centrally acting orexigenic hormone. *Nat. Med.* **2017**, *23*, 1444–1453. [CrossRef]
4. Wang, C.-Y.; Lin, T.-A.; Liu, K.-H.; Liao, C.-H.; Liu, Y.-Y.; Wu, V.C.-C.; Wen, M.-S.; Yeh, T.-S. Serum asprosin levels and bariatric surgery outcomes in obese adults. *Int. J. Obes.* **2018**, *43*, 1019–1025. [CrossRef]
5. Wang, M.; Yin, C.; Wang, L.; Liu, Y.; Li, H.; Li, M.; Yi, X.; Xiao, Y. Serum Asprosin Concentrations Are Increased and Associated with Insulin Resistance in Children with Obesity. *Ann. Nutr. Metab.* **2019**, *75*, 205–212. [CrossRef] [PubMed]
6. Wang, Y.; Qu, H.; Xiong, X.; Qiu, Y.; Liao, Y.; Chen, Y.; Zheng, Y.; Zheng, H. Plasma Asprosin Concentrations Are Increased in Individuals with Glucose Dysregulation and Correlated with Insulin Resistance and First-Phase Insulin Secretion. *Mediat. Inflamm.* **2018**, *2018*, 1–7. [CrossRef] [PubMed]
7. Wiecek, M.; Szymura, J.; Maciejczyk, M.; Kantorowicz, M.; Szygula, Z. Acute Anaerobic Exercise Affects the Secretion of Asprosin, Irisin, and Other Cytokines—A Comparison Between Sexes. *Front. Physiol.* **2018**, *9*, 1782. [CrossRef]
8. Leonard, A.N.; Shill, A.L.; Thackray, A.E.; Stensel, D.J.; Bishop, N.C. Fasted plasma asprosin concentrations are associated with menstrual cycle phase, oral contraceptive use and training status in healthy women. *Eur. J. Appl. Physiol.* **2020**, *121*, 793–801. [CrossRef]
9. Zhong, L.; Long, Y.; Wang, S.; Lian, R.; Deng, L.; Ye, Z.; Wang, Z.; Liu, B. Continuous elevation of plasma asprosin in pregnant women complicated with gestational diabetes mellitus: A nested case-control study. *Placenta* **2020**, *93*, 17–22. [CrossRef]
10. Baykus, Y.; Yavuzkir, S.; Ustebay, S.; Ugur, K.; Deniz, R.; Aydin, S. Asprosin in umbilical cord of newborns and maternal blood of gestational diabetes, preeclampsia, severe preeclampsia, intrauterine growth retardation and macrosemic fetus. *Peptides* **2019**, *120*, 170132. [CrossRef]
11. Chang, C.L.; Huang, S.Y.; Hsu, Y.C.; Chin, T.H.; Soong, Y.K. The serum level of irisin, but not asprosin, is abnormal in polycystic ovary syndrome patients. *Sci. Rep.* **2019**, *9*, 1–11. [CrossRef] [PubMed]
12. Alan, M.; Gürlek, B.; Yilmaz, A.; Aksit, M.; Aslanipour, B.; Gulhan, I.; Mehmet, C.; Taner, C.E. Asprosin: A novel peptide hormone related to insulin resistance in women with polycystic ovary syndrome. *Gynecol. Endocrinol.* **2018**, *35*, 220–223. [CrossRef] [PubMed]
13. Wei, F.; Long, A.; Wang, Y. The Asprosin-OLFR734 hormonal signaling axis modulates male fertility. *Cell Discov.* **2019**, *5*, 55. [CrossRef] [PubMed]
14. Maylem, E.R.S.; Spicer, L.J.; Batalha, I.; Schutz, L.F. Discovery of a possible role of asprosin in ovarian follicular function. *J. Mol. Endocrinol.* **2021**, *66*, 35–44. [CrossRef]
15. Kerslake, R.; Hall, M.; Vagnarelli, P.; Jeyaneethi, J.; Randeva, H.S.; Pados, G.; Kyrou, I.; Karteris, E. A pancancer overview of FBN1, asprosin and its cognate receptor OR4M1 with detailed expression profiling in ovarian cancer. *Oncol. Lett.* **2021**, *22*, 1–14. [CrossRef]
16. Sung, H.; Ferlay, J.; Siegel, R.L.; Laversanne, M.; Soerjomataram, I.; Jemal, A.; Bray, F. Global Cancer Statistics 2020: GLOBOCAN Estimates of Incidence and Mortality Worldwide for 36 Cancers in 185 Countries. *CA Cancer J. Clin.* **2021**, *71*, 209–249. [CrossRef]
17. La Vecchia, C. Ovarian cancer: Epidemiology and risk factors. *Eur. J. Cancer Prev.* **2017**, *26*, 55–62. [CrossRef]
18. Slatnik, C.L.; Duff, E. Ovarian cancer. *Nurse Pr.* **2015**, *40*, 47–54. [CrossRef]
19. Hanahan, D.; Weinberg, R.A. Hallmarks of cancer: The next generation. *Cell* **2011**, *144*, 646–674. [CrossRef]
20. Xie, J.; Wu, H.; Dai, C.; Pan, Q.; Ding, Z.; Hu, D.; Ji, B.; Luo, Y.; Hu, X. Beyond Warburg effect–dual metabolic nature of cancer cells. *Sci. Rep.* **2014**, *4*, 4927. [CrossRef]
21. Liberti, M.V.; Locasale, J.W. The Warburg Effect: How Does it Benefit Cancer Cells? *Trends Biochem. Sci.* **2016**, *41*, 211–218. [CrossRef] [PubMed]
22. Kocaman, N.; Yuksel, E.I.; Demir, B.; Calik, I.; Cicek, D. Two Novel Biomarker Candidates for Differentiating Basal Cell Carcinoma from Trichoblastoma; Asprosin and Meteorine Like Peptide. *Tissue Cell* **2022**, *76*, 101752. [CrossRef] [PubMed]
23. Kang, B. OUP accepted manuscript. *JNCI J. Natl. Cancer Inst.* **2021**. [CrossRef]
24. Akkus, G.; Koyuturk, L.C.; Yilmaz, M.; Hancer, S.; Ozercan, I.H.; Kuloglu, T. Asprosin and meteorin-like protein immunoreactivity in invasive ductal breast carcinoma stages. *Tissue Cell* **2022**, *77*, 1855. [CrossRef]

25. Kumar, J.; Chudasama, D.; Roberts, C.; Kubista, M.; Sjöback, R.; Chatterjee, J.; Anikin, V.; Karteris, E.; Hall, M. Detection of Abundant Non-Haematopoietic Circulating Cancer-Related Cells in Patients with Advanced Epithelial Ovarian Cancer. *Cells* **2019**, *8*, 732. [CrossRef]
26. Mutch, D.G.; Prat, J. 2014 FIGO staging for ovarian, fallopian tube and peritoneal cancer. *Gynecol. Oncol.* **2014**, *133*, 401–404. [CrossRef]
27. Spandidos, A.; Wang, X.; Wang, H.; Seed, B. PrimerBank: A resource of human and mouse PCR primer pairs for gene expression detection and quantification. *Nucleic Acids Res.* **2009**, *38*, D792–D799. [CrossRef]
28. Zahra, A.; Kerslake, R.; Kyrou, I.; Randeva, H.S.; Sisu, C.; Karteris, E. Impact of Environmentally Relevant Concentrations of Bisphenol A (BPA) on the Gene Expression Profile in an In Vitro Model of the Normal Human Ovary. *Int. J. Mol. Sci.* **2022**, *23*, 5334. [CrossRef]
29. Fonseka, P.; Pathan, M.; Chitti, S.V.; Kang, T.; Mathivanan, S. FunRich enables enrichment analysis of OMICs datasets. *J. Mol. Biol.* **2020**, *433*, 166747. [CrossRef]
30. Subramanian, A.; Tamayo, P.; Mootha, V.K.; Mukherjee, S.; Ebert, B.L.; Gillette, M.A.; Paulovich, A.; Pomeroy, S.L.; Golub, T.R.; Lander, E.S.; et al. Gene set enrichment analysis: A knowledge-based approach for interpreting genome-wide expression profiles. *Proc. Natl. Acad. Sci. USA* **2005**, *102*, 15545–15550. [CrossRef]
31. Rogers-Broadway, K.-R.; Chudasama, D.; Pados, G.; Tsolakidis, D.; Goumenou, A.; Hall, M.; Karteris, E. Differential effects of rapalogues, dual kinase inhibitors on human ovarian carcinoma cells in vitro. *Int. J. Oncol.* **2016**, *49*, 133–143. [CrossRef] [PubMed]
32. Kerslake, R.; Randeva, H.S.; Jonigk, D.; Werlein, C.; Robertus, J.L.; Katopodis, P.; Jasker, P.; Spandidos, D.A.; Kyrou, I.; Karteris, E. Protein expression of transmembrane protease serine 4 in the gastrointestinal tract and in healthy, cancer, and SARS-CoV-2 infected lungs. *Mol. Med. Rep.* **2022**, *25*, 1–6. [CrossRef] [PubMed]
33. Wang, W.; Somers, E.B.; Ross, E.N.; Kline, J.B.; O'Shannessy, D.J.; Schweizer, C.; Weil, S.; Grasso, L.; Nicolaides, N.C. FCGR2A and FCGR3A Genotypes Correlate with Farletuzumab Response in Patients with First-Relapsed Ovarian Cancer Exhibiting Low CA125. *Cytogenet. Genome Res.* **2017**, *152*, 169–179. [CrossRef] [PubMed]
34. Gokulnath, P.; de Cristofaro, T.; Manipur, I.; Di Palma, T.; Soriano, A.A.; Guarracino, M.R.; Zannini, M. Long Non-Coding RNA MAGI2-AS3 is a New Player with a Tumor Suppressive Role in High Grade Serous Ovarian Carcinoma. *Cancers* **2019**, *11*, 2008. [CrossRef]
35. Bi, J.; Huang, Y.; Liu, Y. Effect of NOP2 knockdown on colon cancer cell proliferation, migration, and invasion. *Transl Cancer Res.* **2019**, *8*, 6. [CrossRef]
36. Mucaki, E.J.; Zhao, J.Z.L.; Lizotte, D.J.; Rogan, P.K. Predicting responses to platin chemotherapy agents with biochemically-inspired machine learning. *Signal Transduct. Target. Ther.* **2019**, *4*, 1. [CrossRef]
37. Madarampalli, B.; Watts, G.; Panipinto, P.M.; Nguygen, H.N.; Brenner, M.B.; Noss, E.H. Interactions between cadherin-11 and platelet-derived growth factor receptor-alpha signaling link cell adhesion and proliferation. *Biochim. et Biophys. Acta (BBA)-Mol. Basis Dis.* **2019**, *1865*, 1516–1524. [CrossRef]
38. Passanha, F.R.; Divinagracia, M.L.; LaPointe, V.L.S. Cadherin-11 Regulates Cell Proliferation via the PDGFRβ-ERK1/2 Signaling Pathway in Human Mesenchymal Stem Cells. *Stem Cells* **2022**, *40*, 165–174. [CrossRef]
39. Von Bülow, C.; Oliveira-Ferrer, L.; Löning, T.; Trillsch, F.; Mahner, S.; Milde-Langosch, K. Cadherin-11 mRNA and protein expression in ovarian tumors of different malignancy: No evidence of oncogenic or tumor-suppressive function. *Mol. Clin. Oncol.* **2015**, *3*, 1067–1072. [CrossRef]
40. Qian, J.; Gong, Z.-C.; Zhang, Y.-N.; Wu, H.-H.; Zhao, J.; Wang, L.-T.; Ye, L.-J.; Liu, D.; Wang, W.; Kang, X.; et al. Lactic acid promotes metastatic niche formation in bone metastasis of colorectal cancer. *Cell Commun. Signal.* **2021**, *19*, 1–15. [CrossRef]
41. Yang, Z.; Yan, C.; Yu, Z.; He, C.; Li, J.; Li, C.; Yan, M.; Liu, B.; Wu, Y.; Zhu, Z. Downregulation of CDH11 Promotes Metastasis and Resistance to Paclitaxel in Gastric Cancer Cells. *J. Cancer* **2021**, *12*, 65–75. [CrossRef] [PubMed]
42. Maruyama, T.; Nara, K.; Yoshikawa, H.; Suzuki, N. Txk, a member of the non-receptor tyrosine kinase of the Tec family, forms a complex with poly(ADP-ribose) polymerase 1 and elongation factor 1α and regulates interferon-γ gene transcription in Th1 cells. *Clin. Exp. Immunol.* **2006**, *147*, 164–175. [CrossRef] [PubMed]
43. Zhang, Y.; Wester, L.; He, J.; Geiger, T.; Moerkens, M.; Siddappa, R.; Helmijr, J.A.; Timmermans, M.M.; Look, M.P.; Van Deurzen, C.H.M.; et al. IGF1R signaling drives antiestrogen resistance through PAK2/PIX activation in luminal breast cancer. *Oncogene* **2018**, *37*, 1869–1884. [CrossRef] [PubMed]
44. Zhou, X.; Zeng, B.; Li, Y.; Wang, H.; Zhang, X. LINC02532 Contributes to Radiosensitivity in Clear Cell Renal Cell Carcinoma through the miR-654-5p/YY1 Axis. *Molecules* **2021**, *26*, 7040. [CrossRef]
45. Zhang, Y.; Pitchiaya, S.; Cieślik, M.; Niknafs, Y.S.; Tien, J.C.-Y.; Hosono, Y.; Iyer, M.K.; Yazdani, S.; Subramaniam, S.; Shukla, S.; et al. Analysis of the androgen receptor–regulated lncRNA landscape identifies a role for ARLNC1 in prostate cancer progression. *Nat. Genet.* **2018**, *50*, 814–824. [CrossRef]
46. Chai, Y.; Wang, L.; Qu, Y.; Hu, Z. LncRNA MAGI2-As3 Suppresses the Proliferation and Invasion of Cervical Cancer by Sponging MiR-15b. *J. Heal. Eng.* **2022**, *2022*, 1–9. [CrossRef]
47. Chang, H.; Zhang, X.; Li, B.; Meng, X. MAGI2-AS3 suppresses MYC signaling to inhibit cell proliferation and migration in ovarian cancer through targeting miR-525-5p/MXD1 axis. *Cancer Med.* **2020**, *9*, 6377–6386. [CrossRef]

48. Xiang, Z.; Song, S.; Zhu, Z.; Sun, W.; Gifts, J.E.; Sun, S.; Li, Q.S.; Yu, Y.; Li, K.K. LncRNAs GIHCG and SPINT1-AS1 Are Crucial Factors for Pan-Cancer Cells Sensitivity to Lapatinib. *Front. Genet.* **2019**, *10*, 25. [CrossRef]
49. Roychowdhury, A.; Samadder, S.; Das, P.; Mazumder, D.I.; Chatterjee, A.; Addya, S.; Mondal, R.; Roy, A.; Roychoudhury, S.; Panda, C.K. Deregulation of H19 is associated with cervical carcinoma. *Genomics* **2019**, *112*, 961–970. [CrossRef]
50. Xiao-Jie, L.; Ai-Mei, G.; Li-Juan, J.; Jiang, X. Pseudogene in cancer: Real functions and promising signature. *J. Med. Genet.* **2014**, *52*, 17–24. [CrossRef]
51. Katopodis, P.; Dong, Q.; Halai, H.; Fratila, C.I.; Polychronis, A.; Anikin, V.; Sisu, C.; Karteris, E. In Silico and In Vitro Analysis of lncRNA XIST Reveals a Panel of Possible Lung Cancer Regulators and a Five-Gene Diagnostic Signature. *Cancers* **2020**, *12*, 3499. [CrossRef] [PubMed]
52. Hanahan, D. Hallmarks of Cancer: New Dimensions. *Cancer Discov.* **2022**, *12*, 31–46. [CrossRef] [PubMed]
53. Lin, Y.; Liang, X.; Zhang, X.; Ni, Y.; Zhou, X.; Zhao, X. Metabolic cross-talk between ovarian cancer and the tumor microenvironment—Providing potential targets for cancer therapy. *Front. Biosci.* **2022**, *27*, 139. [CrossRef] [PubMed]
54. Mishra, I.; Xie, W.R.; Bournat, J.C.; He, Y.; Wang, C.; Silva, E.S.; Liu, H.; Ku, Z.; Chen, Y.; Erokwu, B.O.; et al. Protein tyrosine phosphatase receptor δ serves as the orexigenic asprosin receptor. *Cell Metab.* **2022**, *34*, 549–563.e8. [CrossRef]
55. Pizzuti, L.; Sergi, D.; Mandoj, C.; Antoniani, B.; Sperati, F.; Chirico, A.; Di Lauro, L.; Valle, M.; Garofalo, A.; Vizza, E.; et al. GLUT 1 receptor expression and circulating levels of fasting glucose in high grade serous ovarian cancer. *J. Cell. Physiol.* **2017**, *233*, 1396–1401. [CrossRef] [PubMed]
56. Rouaud, F.; Sluysmans, S.; Flinois, A.; Shah, J.; Vasileva, E.; Citi, S. Scaffolding proteins of vertebrate apical junctions: Structure, functions and biophysics. *Biochim. et Biophys. Acta (BBA)-Biomembr.* **2020**, *1862*, 183399. [CrossRef] [PubMed]
57. Wang, Z.-H.; Zhang, Y.-Z.; Wang, Y.-S.; Ma, X.-X. Identification of novel cell glycolysis related gene signature predicting survival in patients with endometrial cancer. *Cancer Cell Int.* **2019**, *19*, 1–13. [CrossRef]
58. Kang, H.; Wang, N.; Wang, X.; Zhang, Y.; Lin, S.; Mao, G.; Liu, D.; Dang, C.; Zhou, Z. A glycolysis-related gene signature predicts prognosis of patients with esophageal adenocarcinoma. *Aging* **2020**, *12*, 25828–25844. [CrossRef]
59. Halimi, S.A.; Maeda, D.; Shinozaki-Ushiku, A.; Koso, T.; Matsusaka, K.; Tanaka, M.; Arimoto, T.; Oda, K.; Kawana, K.; Yano, T.; et al. Claudin-18 overexpression in intestinal-type mucinous borderline tumour of the ovary. *Histopathology* **2013**, *63*, 534–544. [CrossRef]
60. Cuylan, Z.F.; Karabuk, E.; Oz, M.; Turan, A.T.; Meydanli, M.M.; Taşkın, S.; Sari, M.E.; Sahin, H.; Ulukent, S.C.; Akbayir, O.; et al. Comparison of stage III mucinous and serous ovarian cancer: A case-control study. *J. Ovarian Res.* **2018**, *11*, 91. [CrossRef]
61. Sahin, U.; Koslowski, M.; Dhaene, K.; Usener, D.; Brandenburg, G.; Seitz, G.; Huber, C.; Türeci, O. Claudin-18 Splice Variant 2 Is a Pan-Cancer Target Suitable for Therapeutic Antibody Development. *Clin. Cancer Res.* **2008**, *14*, 7624–7634. [CrossRef]
62. Hall, M.; Bertelli, G.; Li, L.; Green, C.; Chan, S.; Yeoh, C.C.; Hasan, J.; Jones, R.; Ograbek, A.; Perren, T. Role of front-line bevacizumab in advanced ovarian cancer: The OSCAR study. *Int. J. Gynecol. Cancer* **2019**, *30*, 213–220. [CrossRef]
63. Kim, S.-M.; Hwang, K.-A.; Choi, K.-C. Potential roles of reactive oxygen species derived from chemical substances involved in cancer development in the female reproductive system. *BMB Rep.* **2018**, *51*, 557–562. [CrossRef]
64. Perez-Fidalgo, J.A.; Ortega, B.; Simon, S.; Samartzis, E.P.; Boussios, S. NOTCH signalling in ovarian cancer angiogenesis. *Ann. Transl. Med.* **2020**, *8*, 1705. [CrossRef]
65. Ceccarelli, S.; Megiorni, F.; Bellavia, D.; Marchese, C.; Screpanti, I.; Checquolo, S. Notch3 Targeting: A Novel Weapon against Ovarian Cancer Stem Cells. *Stem Cells Int.* **2019**, *2019*, 1–8. [CrossRef]
66. Alsina-Sanchis, E.; Figueras, A.; Lahiguera, Á.; Vidal, A.; Casanovas, O.; Graupera, M.; Villanueva, A.; Viñals, F. The TGFβ pathway stimulates ovarian cancer cell proliferation by increasing IGF1R levels. *Int. J. Cancer* **2016**, *139*, 1894–1903. [CrossRef]
67. Chaudhry, S.S.; Cain, S.A.; Morgan, A.; Dallas, S.L.; Shuttleworth, C.A.; Kielty, C.M. Fibrillin-1 regulates the bioavailability of TGFβ1. *J. Cell Biol.* **2007**, *176*, 355–367. [CrossRef]
68. Muthu, M.L.; Reinhardt, D.P. Fibrillin-1 and fibrillin-1-derived asprosin in adipose tissue function and metabolic disorders. *J. Cell Commun. Signal.* **2020**, *14*, 159–173. [CrossRef]
69. Davis, M.R.; Summers, K.M. Structure and function of the mammalian fibrillin gene family: Implications for human connective tissue diseases. *Mol. Genet. Metab.* **2012**, *107*, 635–647. [CrossRef]
70. Katopodis, P.; Kerslake, R.; Zikopoulos, A.; Beri, N.; Anikin, V. p38β-MAPK11 and its role in female cancers. *J. Ovarian Res.* **2021**, *14*, 1–12. [CrossRef]
71. Steinmetz, R.; Wagoner, H.A.; Zeng, P.; Hammond, J.R.; Hannon, T.S.; Meyers, J.L.; Pescovitz, O.H. Mechanisms Regulating the Constitutive Activation of the Extracellular Signal-Regulated Kinase (ERK) Signaling Pathway in Ovarian Cancer and the Effect of Ribonucleic Acid Interference for ERK1/2 on Cancer Cell Proliferation. *Mol. Endocrinol.* **2004**, *18*, 2570–2582. [CrossRef]
72. Lee, T.; Yun, S.; Jeong, J.H.; Jung, T.W. Asprosin impairs insulin secretion in response to glucose and viability through TLR4/JNK-mediated inflammation. *Mol. Cell. Endocrinol.* **2019**, *486*, 96–104. [CrossRef]
73. Wang, A.-C.; Ma, Y.-B.; Wu, F.-X.; Ma, Z.-F.; Liu, N.-F.; Gao, R.; Gao, Y.-S.; Sheng, X.-G. TLR4 induces tumor growth and inhibits paclitaxel activity in MyD88-positive human ovarian carcinoma in vitro. *Oncol. Lett.* **2013**, *7*, 871–877. [CrossRef]

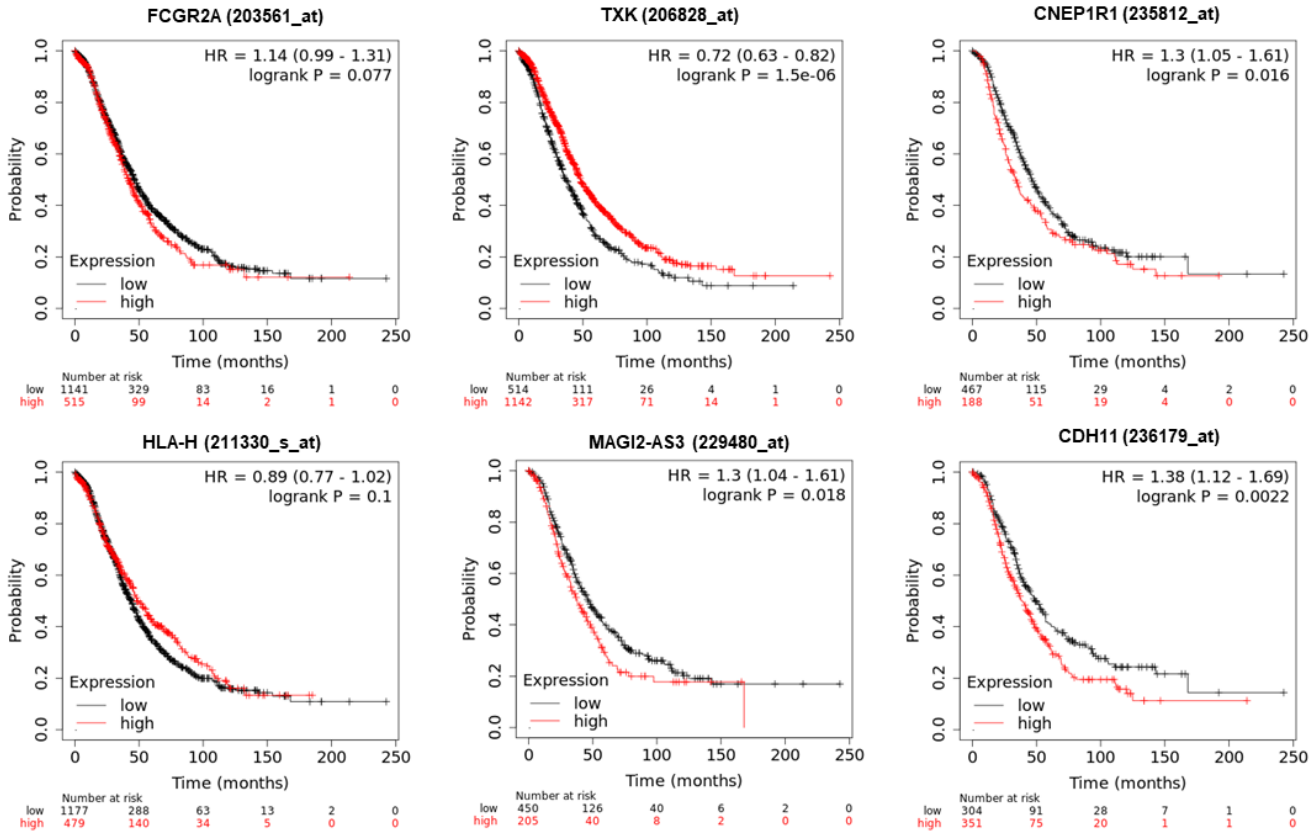

Supplementary Figure S1. Kaplan Meier plots showing overall survival (OS) of OvCa patients with dysregulation of the following genes: A, FCGR2A (p = not significant); B, TXK (*p = 000001.5); C, CNEP1R1 (*p = 0.016); D, HLA-H (p = not significant); E, MAGIC-AS3 (*p = 0.018); F, Alb (*p = 0.0022).

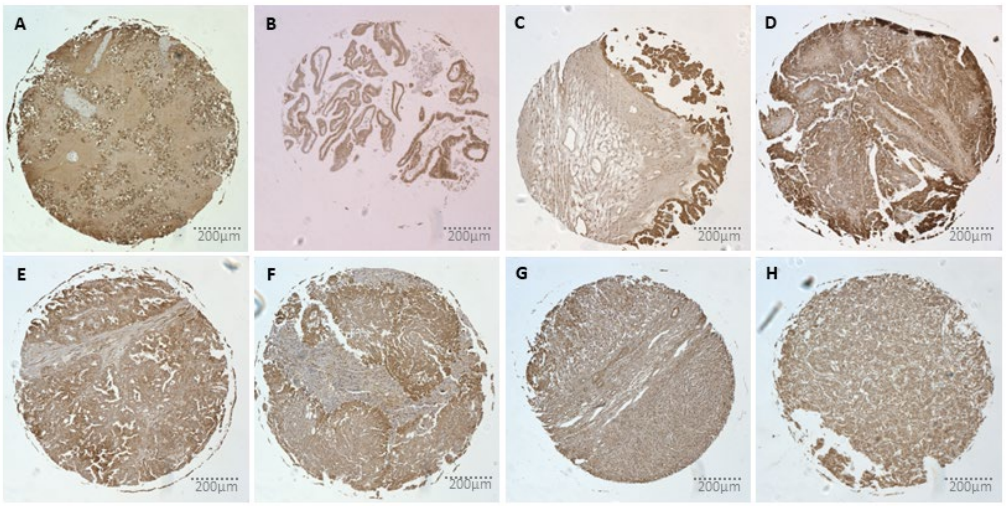

Supplementary Figure S2. Immunohistochemical Staining for TLR4 in ovarian cancers and control tissues at x10 magnification. **A**. Clear Cell Carcinoma, stage II; **B**, Low Grade Serous Carcinoma, stage II; **C**, Endometroid adenocarcinoma, stage I; **D**, High Grade Serous Carcinoma, stage III; **E**, Mucinous Adenocarcinoma, stage III; **F**, Lymph node metastasis from Ovary; **G**, Normal adjacent ovarian tissue; **H,** Control tissue Adrenal Pheochromocytoma.

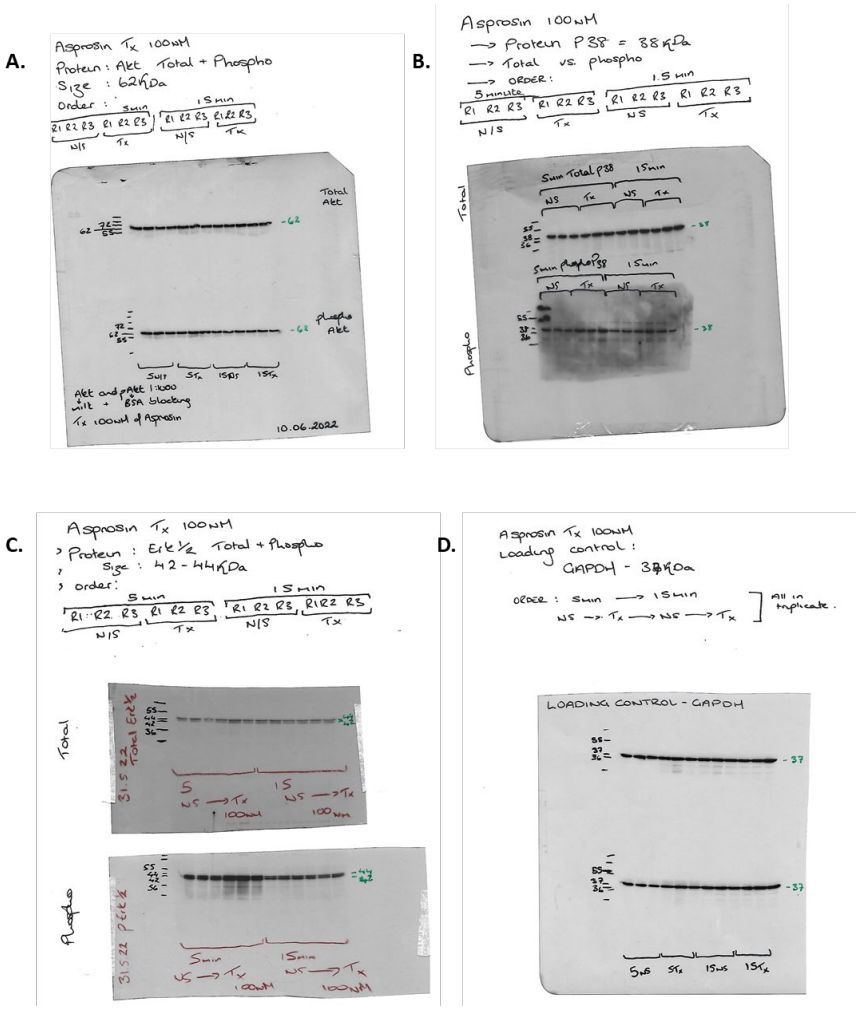

Supplementary Figure S3. Raw data from Western blotting experiments **A**. Total and phospho-Akt; **B**, Total and phospho-p38; **C**, Endo Total and phospho-ERK1/2 **D**, GAPDH as loading control.

Chapter 4

Elevated circulating lactate levels at screening and widespread expression of its cognate receptor, hydroxycarboxylic acid receptor 1 (HCAR1), in ovarian cancer

Statement of Contribution

For the completion of the presented manuscript I contributed towards the following:

- Data curation
- Methodology
- Formal analysis
- Writing—original draft
- Writing—review and editing
- Referencing

Journal of
Clinical Medicine

MDPI

Article

Elevated circulating lactate levels and widespread expression of its cognate receptor, hydroxycarboxylic acid receptor 1 (HCAR1), in ovarian cancer.

Rachel Kerslake[1], Suzana Panfilov[1], Nashrah Mustafa[1], Marcia Hall[1,2], Ioannis Kyrou[3,4,5,6,7], Harpal S. Randeva[3,4], Emmanouil Karteris[1*†], Richard Godfrey[8 *†]

[1] Division of Biosciences, College of Health, Medicine and Life Sciences, Brunel University London, Uxbridge UB8 3PH, UK; Rachel.Kerslake3@brunel.ac.uk, 1914541@brunel.ac.uk, 2129571@brunel.ac.uk, Emmanouil.karteris@brunel.ac.uk
[2] Mount Vernon Cancer Centre, Rickmansworth Road, Northwood, HA6 2RN, UK; Marcia.hall@nhs.net.
[3] Warwickshire Institute for the Study of Diabetes, Endocrinology and Metabolism (WISDEM), University Hospitals Coventry and Warwickshire NHS Trust, Coventry CV2 2DX, UK; harpal.randeva@uhcw.nhs.uk
[4] Warwick Medical School, University of Warwick, Coventry CV4 7AL, UK;
[5] Research Institute for Health & Wellbeing, Coventry University, Coventry CV1 5FB, UK;
[6] Aston Medical School, College of Health and Life Sciences, Aston University, Birmingham, B4 7ET, UK;
[7] Laboratory of Dietetics and Quality of Life, Department of Food Science and Human Nutrition, School of Food and Nutritional Sciences, Agricultural University of Athens, 11855 Athens, Greece, kyrouj@gmail.com
[8] Sport, Health and Exercise Sciences, College of Health, Medicine and Life Sciences, Brunel University London, Uxbridge UB8 3PH, UK; richard.godfrey@brunel.ac.uk
* Correspondence: (RK) richard.godfrey@brunel.ac.uk, (EK) Emmanouil.karteris@brunel.ac.uk
† These authors contributed equally to this work.

Abstract: Background: Augmented glycolysis in cancer cells is a process required for growth and development. The Warburg effect provides evidence of increased glycolysis and lactic acid fermentation in cancer cells. The lactate by-product of glycolysis is receiving growing traction for its role as a cell signalling molecule. Ovarian cancer (OvCa) is also characterised by altered glucose metabolism. We aim to explore circulating lactate levels in patients with high grade serous OvCa (HGSOC) and to elucidate the expression of the lactate receptor hydroxycarboxylic acid receptor 1 (HCAR1) in OvCa. Methods: HCAR1 expression was detected in patient biopsy cores using immunohistochemistry; while lactate was measured from whole blood with a Biosen-C line clinic measuring system. Results: We noted significantly elevated lactate levels in OvCa patients (4.3 ± 1.9 mmol/L) compared with healthy controls (1.4 ± 0.6 mmol/L; $p<0.0001$), with an AUC of 0.96. The gene HCAR1 is overexpressed in OvCa compared to healthy controls ($p<0.001$). Using an OvCa tissue microarray (>75% expression in 100 patients), high protein expression was also recorded across all epithelial OvCa subtypes and ovarian normal adjacent tissue (NAT). Conclusions: Lactate monitoring is a simple, cost-efficient test that can offer point-of-care results. Our data suggest that the potential of circulating lactate as a screening biomarker in OvCa merits further research attention.

Keywords: Lactate, HCAR1, Biomarker, Ovarian Cancer (OvCa), High Grade Serous Ovarian Cancer (HGSOC), Liquid Biopsy, Screening

Citation: To be added by editorial staff during production.

Academic Editor: Firstname Lastname

Received: date
Accepted: date
Published: date

1. Introduction

Lactate is produced when the rate of demand for adenosine triphosphate (ATP) is greater than what can be met through aerobic glycolysis alone. Hence, rather than pyruvate being converted to acetyl CoA and transported into the mitochondrion and to enter the Krebs Cycle, pyruvate is reduced to lactate [1]. This, results in a faster rate of production of nicotinamide adenine dinucleotide (NAD+) and adenosine triphosphate ATP in mammalian cells. The lactate produced here is the L-lactate isomer, whereas bacterial cells typically produce D-Lactate [2]. In humans, blood lactate concentrations are assessed routinely in sports sciences to establish the relative intensity of effort. Circulating lactate levels range from 0.2 to 2.3 mmol/L at rest in healthy individuals, and potentially rise to > 25 mmol/L during maximal exercise [3], [4].

In medical settings, lactate levels are routinely measured in critically ill patients; higher levels represent poorer tissue oxygenation and increased risks of death [5] . Conversely, cancer cells require high levels of energy and consequently have a lower threshold for undertaking glycolysis, even in the presence of adequate oxygen supplies [6]. As such, energy is often produced via the Embden-Meyerhof pathway earlier than in healthy cells under normoxic conditions [7], [8]. This switch leading to lactate production is stimulated through the expression and activation of glycolytic enzymes including glucose transporters (GLUT) 1 and 3 [9]. Of note, GLUT1 is aberrantly expressed in many cancers, including ovarian cancer (OvCa) [10].

Overall, elevated glycolysis in cancer energy flux is relatively well established, while research has variously examined the role of lactate in cancer cell metabolism [6]. This pathway can drive an increase in cellular pH, mRNA expression of monocarboxylic acid transporters (MCTs), MCT1 and MCT4, as well as an increase in the catabolic enzyme, lactate dehydrogenase A (LDH) [11]–[15]. Moreover, lactate transport is also suggested to hold a concurrent role in cancer cell signalling; tumour cells with high glucose and hypoxic environments are thought to produce lactate, which is in turn metabolised by neighbouring tumour cells [16]. LDH is a catalytic enzyme involved in the reversible conversion of pyruvate to lactate during glycolysis. Increased levels of LDH are well documented in many cancer patients including those with melanoma, breast, lung, uterine and colorectal cancers [17], [18]. In this context, LDH are used as part of the risk classifications for metastatic renal cell carcinoma and for non-Hodgkin's lymphoma [17]. As with multiple other malignancies there is evidence that higher levels of LDH are found in patients with more advanced OvCa (FIGO Stage III/IV) and are associated with poor survival [13]. However, testing for LDH is relatively time-consuming, requiring a lab-based cytotoxicity assay (also known as an LDH release assay). In contrast, the measurement of blood lactate concentration is comparatively time-efficient and cost-effective and can be performed with point-of-care testing (e.g. at the outpatient examination room) [4].

To date, an increasing body of evidence associates lactate signalling with multiple roles in the early development and progression of cancer via effects on tumour growth, angiogenesis,metastasis and immunosuppression [19]. In addition, lactate is seen to influence cytokine production through G protein-coupled receptor (GPCR) signalling. [20]. Therefore, lactate's biomarker and prognostic potential are currently under exploration [12]. As such, increased lactate production is now recognised as a pivotal step in early development of malignancy [21]. Further research on its role in the tumour microenvironment is therefore expected to further advance understanding of the underlying cancer biology. Moreover, emerging evidence suggests that lactate production contributes to carcinogenesis, supporting anabolic growth and proliferation in mechanisms outlined by the Warburg effect [6]. There is a plethora of studies on the Warburg effect published over the past decade. The Warburg effect describes how cancer cells alter their metabolism to favor growth and proliferation by increasing glucose uptake and fermenting it to lactate [22]. In line with this, circulating lactate levels 40 times the level of normal resting levels have been observed in head and neck tumours; with altered energy metabolism also being recognised as a hallmark of cancer [6], [23].

Further supporting its potential implication in carcinogenesis is the fact that lactate is not just a by-product of altered metabolic reprogramming but is also implicit in signalling pathways through GPCR activation [6], [24], [25]. So far, it is well-known that the cognate receptor of lactate, hydroxycarboxylic acid receptor 1 (HCAR1; formerly known as GPR81), is a GPCR primarily expressed in adipose tissue; where its activation causes inhibition of lipolysis via a Gi-dependent pathway [26]. However, recently, elevated HCAR1 expression was also implicated in tumour growth and metastasis in cancers, such as breast and pancreatic [25], [27]. Moreover, a study by Wagner et al. suggests that increased HCAR1 expression and activation in cervical cancer cells is capable of modulating cellular DNA repair mechanisms [28]. Additional silencing of HCAR1 may also downregulate levels of BRCA1; a protein involved in DNA repair known for its mutagenic status in breast and ovarian cancer [28], [29].

Although elevated circulating lactate levels have already been documented in certain cancers (e.g., in breast, prostate and colorectal cancer), changes in circulating lactate are yet to be studied in patients with OvCa [30]–[32]; a malignancy characteristically associated with dysregulated energy metabolism and aberrantly expressed glucose [33]. This gynecological malignancy has poor prognosis and usually remains undetected until late stages due to initial non-specific symptoms and the need for invasive examination, such as a transvaginal ultrasound [34]. As such, in the present study, we measured the circulating lactate levels of patients with OvCa, whist we further investigated the expression of its cognate receptor, HCAR1, at both gene and protein level, using in silico tools, tissue microarrays and whole blood lactate analysis techniques.

2. Materials and Methods

2.1. Blood Samples and Lactate Analysis

Blood samples from patients with high grade serous ovarian cancer (HGSOC) (n=53; all diagnosed with Stage III or IV) were collected from the Mount Vernon Cancer Centre, East and North Hertfordshire NHS Trust, as part of the CICATRIx study; 45 healthy adult women were also recruited as study controls.

The median age for patients (n=53) and controls (n=45) studied were 69 years (range 37–84) and 34 years (range 21–59), respectively. Control patients were volunteers who had no significant health concerns and were not receiving treatment. All 53 patients had FIGO Stage III/IV HGSOC, and were being managed according to standard UK practice. This involves primary surgery followed by adjuvant chemotherapy for some and neo-adjuvant chemotherapy with interval or no surgery for others. Following chemotherapy (+/- surgery), patients generally receive maintenance targeted therapy with antiangiogenics (bevacizumab – Bev) and / or PARP inhibitors (PARPi). Blood samples were obtained at various points during treatment. Twenty-five patients had samples taken at diagnosis either prior to starting any treatment at all or after their primary surgery but prior to adjuvant chemotherapy treatment (PreC: n=25). Twelve patients had samples taken when they were in clinical remission, after chemotherapy (maint. Bev./PARPi). Finally, 16 patients had samples taken when they had shown evidence of relapse HGSOC, but prior to starting any further chemotherapy (Relapse OC-PreC). Given the importance of BRCA status in these patients, we further categorized the patients into BRCA wild-type and HRD negative (BRCAwt/HRD-ve, n=40) or BRCA mutant group (germline or somatic) and HRD positive, as demonstrated by the Myriad MyChoice CDx test (BRCAmt/HRD+ve, n=9).

The study was approved by the West Midlands–South Birmingham Ethics Committee (reference 16/WM/0196; protocol number RD2016-08). All participants provided written informed consent. Blood samples were collected either intravenously or via capillary lancet, with the study participants resting, at least 15 minutes prior to donation, to ensure standardized resting conditions. Blood (10 μl) was isolated using Accu-Chek Safe-T-Pro Plus Lancets (Roche, Switzerland), a sterile glass capillary tube (HaB International Ltd.,

Warwickshire), and was mixed with 500 µl of haemolyzing solution (HaB International Ltd., Warwickshire). Samples were inverted to mix before lactate analysis with a Biosen C line Clinic measuring system (EKF Diagnostics, Cardiff, Wales).

2.2. Bioinformatic Analysis

CanSAR (cansar.icr.ac.uk), an integrative translational research and drug discovery knowledge base, was used to present HCAR1 expression across a range of cancers from The Cancer Genome Atlas (TCGA). GTEx (gtexportal.org/home/) was accessed to reveal normal gene expression in female reproductive tissues (cervix, fallopian tube, ovary, uterus, and vagina). GEPIA online tool (gepia.cancer-pku.cn/) allowed gene expression comparison between ovarian epithelial tissue (Genotype-Tissue Expression; GTEx) and OvCa biopsies (TCGA). Therapeutic response and survival rates of patients with OvCa were generated using Kaplan-Meier (KM) survival plots (www.kmplot.com).

2.3. Immunohistochemistry

Protein expression of HCAR1 in OvCa was assessed using immunohistochemical staining, following the methods outlined in our previous work [35]. An OvCa tissue microarray containing 90 OvCa and 10 normal ovarian biopsy samples was purchased from BioMax Inc. cat. No. BC1111d (Supplementary 2.). Tissue samples were collected under Health Insurance Portability and Accountability Act (HIPAA) approved protocols and ethical standards. Unless otherwise stated, reagents were purchased from ThermoFisher Scientific. Briefly, the array was deparaffinised and rehydrated, followed by antigen retrieval using sodium citrate solution (10 mM sodium citrate in dH2O, 0.05% Tween-20, pH 6.0) at 90°C for 10 minutes. Washes in 0.025% Triton-X in PBS preceded 15-minute incubation with 3% H_2O_2. The array, was again washed prior to blocking in 5% BSA in PBS, before overnight incubation at 4°C with HCAR1 primary antibody (1:100). Additional washes preceded an hour incubation with secondary antibody in 1% rabbit serum (ZytoChem Plus HRP-DAB Kit, Zytomed Systems, Germany), before subsequent washes and 30-minute incubation with streptavidin-HRP conjugate of the same brand and further washes. Finally, DAB stain and haematoxylin counterstain were applied followed by bluing with 0.1% sodium bicarbonate. The array was then dehydrated and sealed, before immunoreactivity quantification by the primary investigator and independent reviewers using a Leica light microscope (Zeiss, Oberkochen, Germany).

2.4. Statistical Analysis

Bioinformatic data were generated using open access online analytical tools with preset statistical methodologies with access to TCGA and GTEx data. GEPIA generated differential analysis was calculated using one-way ANOVA, taking gene expression of the normal (GTEx) against disease (TCGA), generating expression as log2(TPM+1). Expression is transformed for differential analysis with log2FC defined as median (Tumour) - median (Normal) with differentially expressed genes (DEGs), characterised as higher |log2FC| and lower q values, compliant with GEPIAs pre-set threshold (http://gepia.cancer-pku.cn/help). Survival variances were generated using Kaplan-Meier plotter (kmplot.com). Statistical analyses for inhouse experiments were performed using GraphPad Prism9® (v.9.4.1 - GraphPad Software, Inc.). Error is represented using the standard error of mean (SEM). An ANOVA or t-test was applied to the data, based on parametric state and variable status. Unless stated otherwise, significance levels were set at $p < 0.05$. Receiver Operating Characteristics (ROC) curves were also generated using GraphPad Prism.

3. Results

3.1. Blood lactate levels are elevated in patients with OvCa

Figure 1A demonstrates lactate levels (mmol/L) in the control (1.4 ± 0.6) versus OvCa groups (4.3 ± 1.9), ****p < 0.0001. There were significantly higher lactate levels seen in all ovarian cancer patient groups when compared with the control group: Pre-Chemo (4.9 ± 1.9), Maintenance Bev/PARPi (3.7 ± 1.9), Relapse-PreChemo (3.8 ± 1.5) ****p < 0.0001. There were no differences between the BRCAwt/HRD negative (4.2 ± 1.8) and BRCAmt/HRD positive (4.9 ± 2.6) groups both of whom had similarly higher levels of lactate than the control group ****p < 0.0001.

Figure 2 presents Receiver Operating Characteristic (ROC) plot depicting lactate concentration comparisons between OvCa patients and healthy controls. Data shows an area under the curve of 0.96, with a high confidence interval (p < 0.0001). The specificity of lactate in OvCa therefore compliments sensitivity with a high level of accuracy.

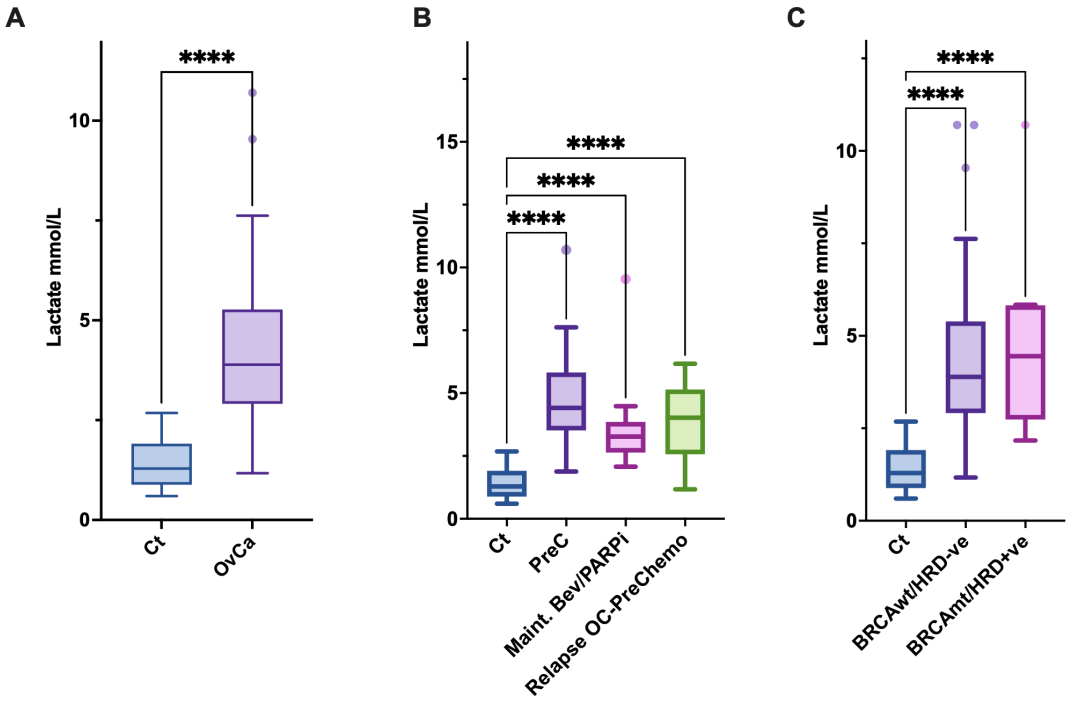

Figure 1. Lactate levels are elevated in OvCa. (**A**): Circulating lactate levels in controls (Ct; n=45), patients with ovarian cancer (OvCa; n=53); ****p<0.0001. (**B**): Controls (Ct) compared to OvCa patients prior to any adjuvant chemotherapy treatment (Prechemotherapy, PreC), patients on maintenance bevacizumab, and or PARP inhibitors (Maint. Bev/PARPi), and those patients with samples taken prior to commencing chemotherapy treatment for HGSOC relapse (Relapse OC-PreChemo); ****p < 0.0001. (**C**): Controls (Ct) compared to OvCa patients with confirmed BRCA wild-type and HRD negative (BRCAwt/HRD-ve) versus patient carrying BRCA mutations or being identified as HRD positive (BRCAmt/HRD+ve); ****p<0.0001.

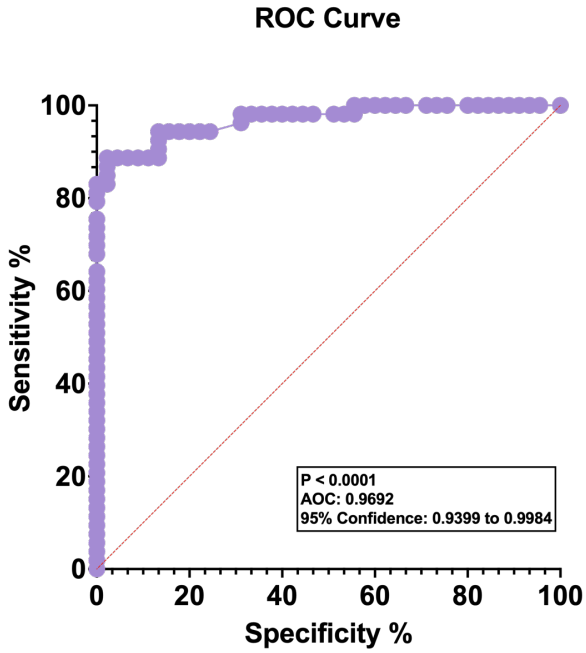

Figure 2. Receiver Operating Characteristic (ROC) plot. Patients with ovarian cancer (OvCa): n=53; healthy female controls: n=45. Area Under the Curve (AUC): 0.9692. 95% confidence measuring between 0.9399 and 0.9984, $p < 0.0001$.

3.2. Elevated gene expression of the lactate receptor HCAR1 in OvCa

A series of in silico and lab-based approaches to map the gene and protein expression of HCAR1 in OvCa, were used. Using data from the public domain, GTEx, widespread expression of HCA1R is seen in numerous cancers and stages (Supplementary Figure 1). Initial analyses of HCAR1 mRNA expression in a range of normal gynaecological tissues indicated that HCAR1 mRNA is present in cervix, fallopian tube, ovary, uterus and vaginal tissues (Figure 3A). Expression of HCAR1 in OvCa tissue (n=426) was significantly upregulated in comparison with normal ovarian epithelial tissue (n=88) (Figure 3B).

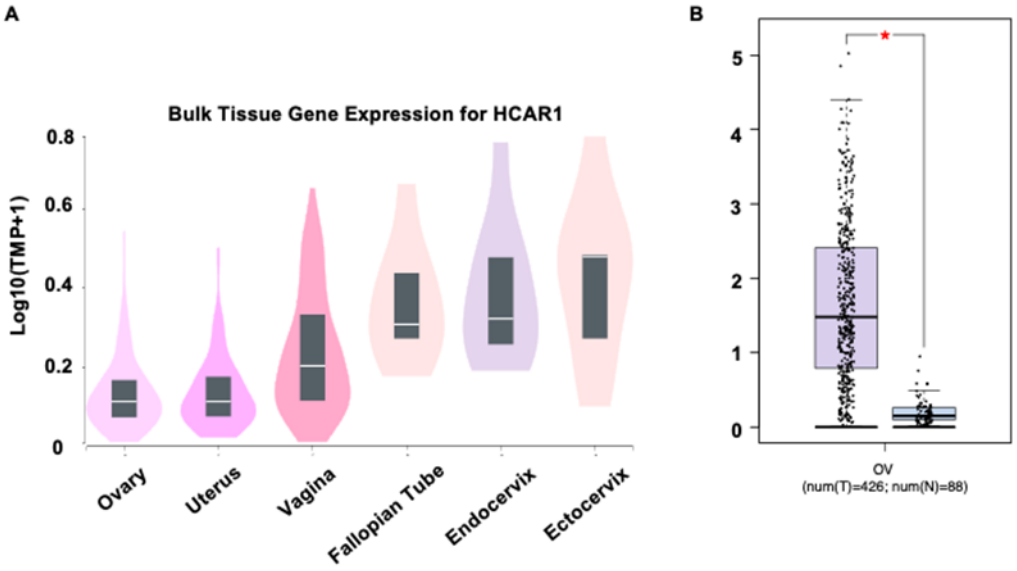

Figure 3. Expression of HCAR1 (hydroxycarboxylic acid receptor 1, HCAR1; formerly known as GPR81) in female reproductive tissues. (A) HCAR1 RNA expression in normal female tissues taken from the Genotype-Tissue Expression project (GETx); (B) HCAR1 expression in ovarian cancer (OvCa) tissue compared with normal ovarian epithelial tissues (OvCa=426; N=88), *p<0.001. TPM: transcripts per million.

3.3. High HCAR1 protein expression across epithelial subtypes of OvCa

A tissue microarray was also used to determine the protein expression of HCAR1 across a panel of different histological subtypes of epithelial OvCa and at different stages (I-IV; Figure 4A-B). Here, HCAR1 expression is widespread throughout the subtypes of OvCa, with varying intensity seen throughout different cell types. Representative images of the different histological subtypes are presented in Figure 4. Based on the staining in HGSOC and Low Grade Serous Ovarian Cancer (LGSOC) (Figure 4C–D), HCAR1 appears localised to the membrane of papillary cells with less intense (light brown) staining seen in the surrounding stroma. In cases of clear cell carcinoma (CCC), clear cytoplasmic regions are surrounded with connective trabeculae and show higher HCAR1 expression within glandular regions (Figure 4E). A similar pattern of high HCAR1 expression is detected in glandular epithelia (Figure 4F), in contrast to central stromal tissue in endometroid adenocarcinoma of the ovary (EAC). Intense (dark brown) staining is also seen amongst mucinous cystic epithelium of mucinous adenocarcinoma (MAC) compared with the surrounding layer of theca cells (Figure 4G). In normal adjacent tissues (NAT), the theca tissue, which encompasses primordial follicles, is surrounded by granulosa cells exhibiting high levels of HCAR1 (Figure 3H). Detailed review of intensity scores is presented in Supplementary Figure 2.

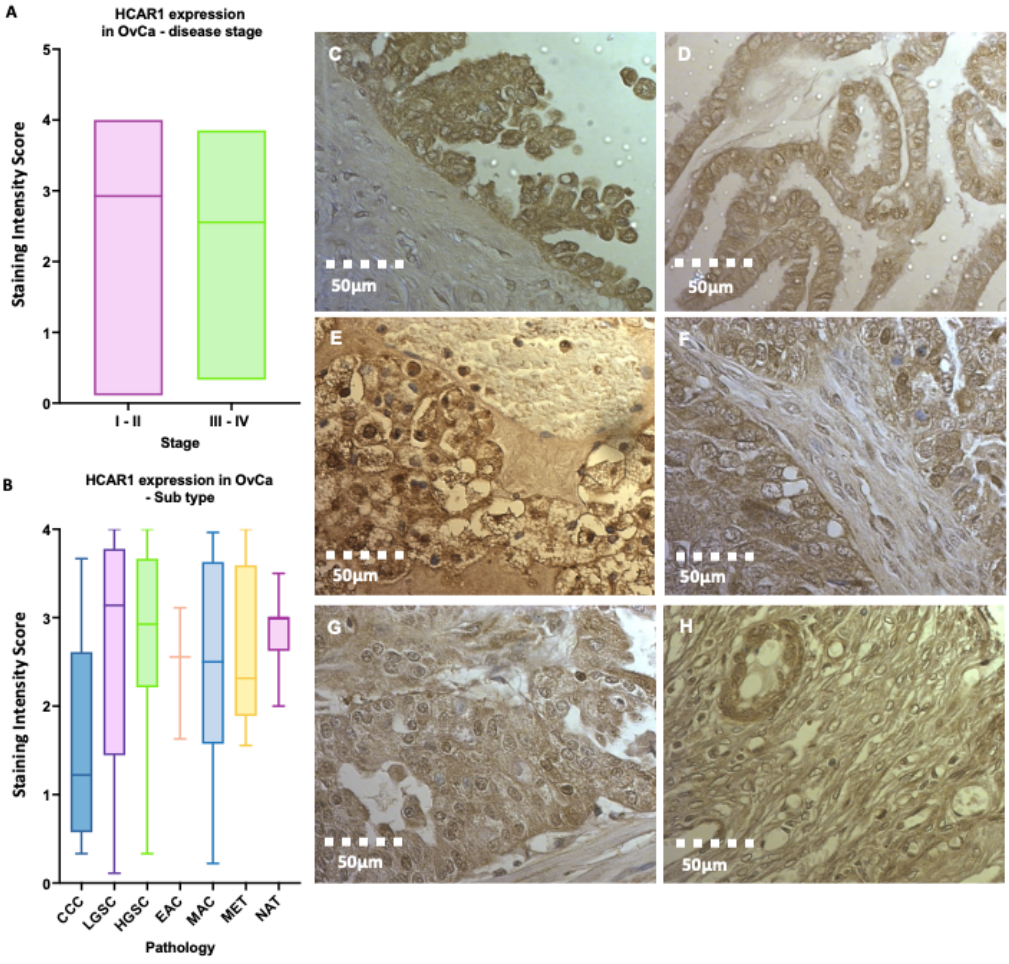

Figure 4. Expression of HCAR1 (hydroxycarboxylic acid receptor 1, HCAR1; formerly known as GPR81) in an ovarian tissue microarray containing biopsies from 90 patients with ovarian cancer (OvCa), in addition to 10 normal adjacent tissue (NAT) samples. (A) Intensity of tissue stained for early (I–II, n=62) and late stage (III–IV, n=18) OvCa, (no significance: ns); (B) Intensity of HCAR1 staining categorised by OvCa subtype: Clear Cell Carcinoma (CCC), High Grade Serous Carcinoma (HGSOC), Low Grade Serous Carcinoma (LGSOC), Endometrioid Adenocarcinoma (EAC), Mucinous Adenocarcinoma (MAC), Lymph node Metastasis (MET), and Normal Adjacent Tissue (NAT). Quantification of cores was conducted by the primary investigator and two unbiased reviewers according to the following visual numeration: 0 = 0–10%; 1 >10–25%; 2 > 2–50%; 3 > 50–75%; 4 > 75–100%, using a DM4000 microscope (Leica). OvCa tissues stained for HCAR1: brown indicating HCAR1 positive cellular components and blue/purple indicating haematoxylin counter stain. (C) HGSOC (stage I); (D) LGSOC (II); (E) CCC (III); (F) EAC (IV); (G) MAC (V); and (H) NAT. Images were captured using an Olympus BX51 light microscope at x40 magnification.

3.4. HCAR1 expression shows little influence on the Overall Survival (OS) or the Progression Free Survival (PFS) of patients with OvCa.

The rates of OS and PFS, in light of HCAR1 expression status (high versus low), were assessed using the Kaplan Meier plotter over a course of 250 months, using data acquired collectively through The Cancer Genome Atlas (TCGA), Gene Expression Omnibus (GEO), and the European Genome-Phenome Archive (EGA). Based on this *in silico* modelling, no overall difference can be noted for OS or PFS, regardless of HCAR1 expression level (Figure 5).

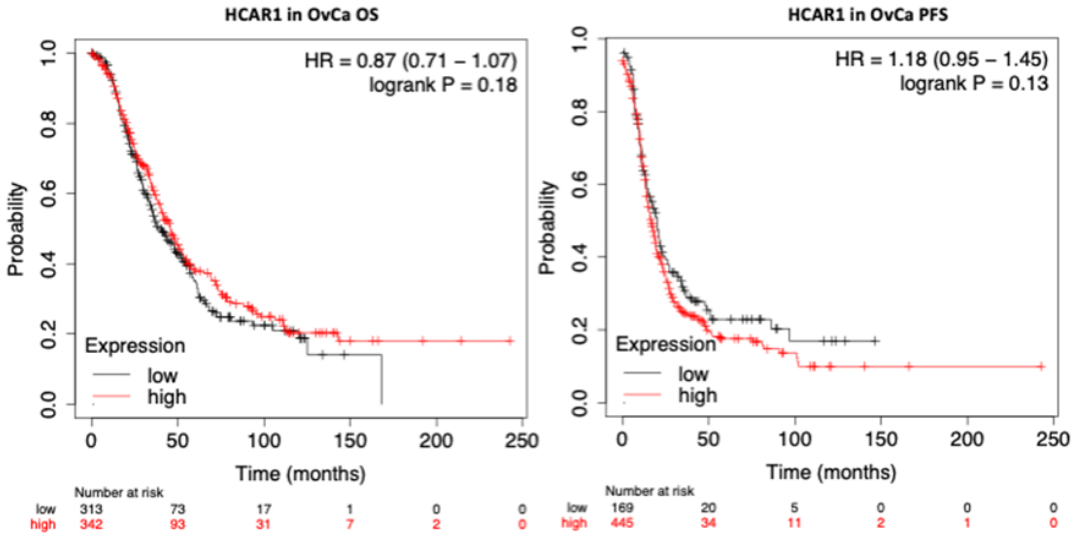

Figure 5. Ovarian Cancer (OvCa) Survival Curve analysis. Kaplan Meier plots revealing the prognostic effects of HCAR1 expression in OvCa; (A) Overall Survival (OS); (B) Progression-Free Survival (PFS). Generated through the Kaplan-Meier plotter (kmplot.com).

4. Discussion

In this study we demonstrate that resting lactate levels from circulating blood are significantly elevated in Stage III/IV OvCa patients compared to healthy controls. The increase noted in our patients, was independent of treatment, current cancer status (remission or recurrence) and BRCA status. Concomitant increased levels of mRNA for the lactate receptor HCA1R in OvCa patients compared to controls were seen as well as widespread protein expression of this GPCR in OvCa patients.

Over the last decade, lactate has increasingly gained traction for its role as a signalling molecule and not just as a by-product of anaerobic cellular processes and glycolysis. The generation of lactate is thought to disrupt natural feedback mechanisms of normal cellular processes and promote metastasis and angiogenesis, thus contributing to poor prognosis in patients with cancer [21], [36]. For example, lactate is thought to promote

tumorigenesis by enhancing TGF-β signalling in regulatory T-cells. It also plays a role in the promotion of inflammation and angiogenesis [29].

Notably, although the normal range of circulating lactate at rest is 0.2 to 2.3 mmol/L, patients with cancer are shown to exhibit markedly higher levels [37]. We substantiate this in our present data, where patients with HGSOC exhibit levels with a median of 4.3 mmol/L, compared to 1.4 mmol/L in the control group. Of note, these patients did not present with typical symptoms of lactic acidosis, a condition characterised by high lactate levels and accompanying symptoms, such as muscle ache, nausea, breathing difficulties or stomach pain. These blood samples were instead taken as part of routine monitoring [38]. Similar results have been recorded in gliomas where interestingly, not only is there a difference between gliomas and normal glial tissue but patients with high grade gliomas have significantly higher levels of resting lactate than those with low grade gliomas, with lactate levels up to 14 mmol/L in the former [25]. Interestingly, emerging data also support the potential of serum lactate as a biomarker of metastasis in brain tumours, while levels have also been studied in relation to bladder cancer using a urine liquid biopsy approach [25]–[27]. Moreover, retrospective data obtained from emergency department visits at a tertiary US hospital (lactate drawn from 1,837 patients with various cancers and 3,603 non-cancer patients) showed that, compared to non-cancer patients, cancer patients with elevated lactate levels exhibited a significantly increased risk of mortality [39]. Future studies are required to prospectively confirm such data and also further explore which bodily fluid encompasses the best liquid biopsy to measure lactate levels from.

This accumulation of resting lactate in patients with cancer, corresponds to an abnormally high metabolic rate and an increase in glycolytic processes within the cancer tissue [7]. Higher lactates may signify both an oxygen deficit within the patients' tissues as well as a preference for the glycolytic pathway, both supporting the Warburg theory [40]. Contrary to the patients without cancer who have high lactate levels of around 9.0 ± 5.3 mmol/L in non-survivors, and around 3.4 ± 1.1 mmol/L in survivors (e.g. those with septic shock, myocardial infarction, respiratory distress etc.), cancer patients are not as obviously sick and are able to undertake most activities of daily living [41], [42].

As aforementioned, the elevated blood levels of lactate in patients with cancer presenting at the emergency department have been noted to negatively impact survival outcomes [39]. In our study, it was not possible to identify a prognostic role for lactate, as we acknowledge the limitation of a small cohort. Larger numbers of HGSOC OvCa patients will therefore provide a better understanding of lactate's clinical utility in prognosis.

To further assess the signalling potential of circulating lactate in the OvCa tumour microenvironment, we explored expression of its cognate receptor, HCAR1, in normal and cancer tissues. Using *in silico* approaches, we confirmed the published widespread HCAR1 expression throughout an array of cancer types, including OvCa (Supplementary 1). It is intriguing to note that normal fallopian tube tissue and cervical tissue have higher HCAR1 expression than tissue from other areas of the female genital tract. Unsurprisingly, HCAR1 protein expression was observed across all histological subtypes of ovarian cancer (Supplementary Figure 2). Interestingly, HCAR1 appears to show localisation around cellular membranes, in accordance with GPCR distribution. Widespread expression with dense staining was also identified in cells that are endocrine active, thus requiring increased energy, such as the granulosa and glandular cells, as well as the papillary type cells of HGSOC and LGSOC. Future studies are required to expand on these present findings, and also explore whether high levels of lactate cause any internalisation of HCAR1. Intense staining of granulosa cells surrounding the primordial follicle was also noted in NAT tissues. Although the over-expression of HCAR1 seen in NAT diverts from the expression trend seen at gene level in the control cohort for normal ovarian tissue, it should be recognised that the proximity of NAT has been shown to bear very similar characteristics to its adjacent malignant tissue, as preconditioning with transcriptional dysregulation may be underway [43].

Of note, lactate holds a complex role within the TME and is also associated with a suppression of innate immunity [44]. Given the rich metabolic state of immune cells, researchers have investigated the expression of HCAR1 in cells of the immune system, detecting HCAR1 expression in macrophages and dendritic cells. In macrophages elevated lactate increases activation of HCAR1 leading to the suppression of NF-kB pathways and subsequent reduction of cytokine production [45]. While in dendritic cells of mice with breast cancer, HCAR1 activation is also shown to reduce the production of IL-6 and IL-12. In addition, HCAR1 stimulation is seen to suppress MHC-II compromising tumour antigen presentation within T-cells preventing tumour recognition [46]. HCAR1 activation in breast cells, also appears to augment the expression of PD-L1 further aiding evasion of the immune system [47].

There are several limitations to this work. Ideally the control group should be a similar size and aged matched, however resting levels of lactate are presented as a standardized range throughout the literature. Furthermore, it will be useful to correlate HCAR1 protein expression from FFPE tissues with resting blood lactate levels in paired clinical samples (i.e. same OvCa patient). Larger cohorts of OvCa patients, with earlier stage, disease would add confidence to the higher resting lactate levels seen in this group and give a better insight as to whether this is related to advanced disease only. Levels of lactate in patients with other histological subtypes of ovarian cancer such as clear cell, mucinous and low grade should also be explored. Correlation of the resting blood lactate levels with HCAR1 protein expression in paired clinical samples (i.e. same OvCa patient) could yield information about the dynamics of lactate and its' effects on patients with advanced OvCa. Finally, further exploration of resting lactate levels and PD-1/PD-L1 expression on cancer cells and assessment of the T cell subsets in OvCa, together with a better understanding of the effect of lactate on macrophages in OvCa may aid understanding of growing cases of OvCa immunotherapy resistance .

5. Conclusions

The novel findings of the present study indicate that circulating lactate levels in patients with OvCa at rest are higher than normal in healthy female controls. This suggests that circulating lactate levels may hold screening potential for earlier detection of OvCa, prompting further diagnostic examinations, as our data indicate with an AUC of 0.96. Circulating lactate levels are already regularly assessed in certain clinical settings, typically to assess the onset of sepsis. Although lactate can be measured routinely in patients, so far this approach has not been utilized to potentially assist cancer diagnosis, management or prognosis [36]. Given that lactate monitoring is a simple, cost efficient, and readily available tool that can offer point-of-care results, the overall findings of the present study suggest that the potential of circulating lactate as a biomarker in OvCa merits further research attention. Thus, prospectively exploring the potential of lactate as an effective screening/prognostic biomarker to aid clinical practice against a common gynaecological cancer that is all too often characterized by late diagnosis and poor overall survival.

6. Patents: N/A

Supplementary Materials: The following supporting information can be downloaded at: www.mdpi.com/xxx/s1, Figure S1: Gene expression of HCAR1 (hydroxycarboxylic acid receptor 1, HCAR1; formerly known as GPR81) from The Cancer Genome Atlas (TCGA) in cancer and normal tissues.; Figure S2: Bland-Altman analysis of immunohistochemistry quantification scores.

Author Contributions: Conceptualisation, E.K., R.G.; Methodology, R.G., R.K., S.P.; Validation, S.P., N.M.; Patient sample collection, M.H., R.K., S.P.; Formal Analysis, R.K., S.P., N.M.; Draft preparation, R.K., R.G., N.M., E.K.; writing—review and editing, R.K., H.S.R., I.K., M.H.; visualization, R.G., H.S.R., I.K., E.K.; supervision, R.G., H.S.R., I.K., M.H., and E.K. R.G. and E.K. are joint senior and corresponding co-authors. All authors have read and agreed to the published version of the manuscript.

Funding: This study was funded through the Cancer Treatment & Research Trust and University Hospitals Coventry and Warwickshire NHS Trust (grant no. 12899).

Institutional Review Board Statement: Institutional Review Board Statement: The study was conducted according to the guidelines of the Declaration of Helsinki, Protocol number RD2016-08, and approved by the West Midlands–South Birmingham Ethics Committee (reference 16/WM/0196).

Informed Consent Statement: Informed consent was obtained from all subjects involved in the study.

Data Availability Statement: Upon request from principal investigator.

Acknowledgments: We would like to extend our heartfelt gratitude to the study patients and volunteers for their sample donations. In addition, we would like to thank Amelia Dingley for her invaluable technical support during lactate analysis and Dr Nabeel Khan for his assistance with clinicopathological data.

Conflicts of Interest: The authors declare no conflict of interest

Reference

[1] B. Alberts *et al.*, *Molecular biology of the cell*, 6th ed., no. 1. Garland Science, Taylor and Francis Group, 2018. Accessed: Jul. 26, 2020. [Online]. Available: http://localhost/site/catalogue/7329

[2] T. Larsen, "Fluorometric determination of d-lactate in biological fluids," *Anal Biochem*, vol. 539, pp. 152–157, Dec. 2017, doi: 10.1016/J.AB.2017.10.026.

[3] P. Wacharasint, T. A. Nakada, J. H. Boyd, J. A. Russell, and K. R. Walley, "Normal-range blood lactate concentration in septic shock is prognostic and predictive," *Shock*, vol. 38, no. 1, pp. 4–10, Jul. 2012, doi: 10.1097/SHK.0B013E318254D41A.

[4] M. L. Goodwin, J. E. Harris, A. Hernández, and L. B. Gladden, "Blood Lactate Measurements and Analysis during Exercise: A Guide for Clinicians," *Journal of diabetes science and technology (Online)*, vol. 1, no. 4, p. 558, 2007, doi: 10.1177/193229680700100414.

[5] J. Bakker, M. W. N. Nijsten, and T. C. Jansen, "Clinical use of lactate monitoring in critically ill patients," *Ann Intensive Care*, vol. 3, no. 1, pp. 1–8, 2013, doi: 10.1186/2110-5820-3-12.

[6] I. San-Millán and G. A. Brooks, "Reexamining cancer metabolism: lactate production for carcinogenesis could be the purpose and explanation of the Warburg Effect," *Carcinogenesis*, vol. 38, no. 2, pp. 119–133, Feb. 2017, doi: 10.1093/CARCIN/BGW127.

[7] D. Hanahan, "Hallmarks of Cancer: New Dimensions," *Cancer Discov*, vol. 12, no. 1, pp. 31–46, Jan. 2022, doi: 10.1158/2159-8290.CD-21-1059.

[8] M. v. Liberti and J. W. Locasale, "The Warburg Effect: How Does it Benefit Cancer Cells?," *Trends in Biochemical Sciences*, vol. 41, no. 3. Elsevier Ltd, pp. 211–218, Mar. 01, 2016. doi: 10.1016/j.tibs.2015.12.001.

[9] L. B. Tanner *et al.*, "Four key steps control glycolytic flux in mammalian cells," *Cell Syst*, vol. 7, no. 1, p. 49, Jul. 2018, doi: 10.1016/J.CELS.2018.06.003.

[10] L. Pizzuti *et al.*, "GLUT 1 receptor expression and circulating levels of fasting glucose in high grade serous ovarian cancer," *J Cell Physiol*, vol. 233, no. 2, pp. 1396–1401, Feb. 2018, doi: 10.1002/jcp.26023.

[11] Y. I. Rattigan *et al.*, "Lactate is a mediator of metabolic cooperation between stromal carcinoma associated fibroblasts and glycolytic tumor cells in the tumor microenvironment," *Exp Cell Res*, vol. 318, no. 4, pp. 326–335, Feb. 2012, doi: 10.1016/J.YEXCR.2011.11.014.

[12] S. Dhup, R. Kumar Dadhich, P. Ettore Porporato, and P. Sonveaux, "Multiple biological activities of lactic acid in cancer: influences on tumor growth, angiogenesis and metastasis," *Curr Pharm Des*, vol. 18, no. 10, pp. 1319–1330, Apr. 2012, doi: 10.2174/138161212799504902.

[13] P. Miao, S. Sheng, X. Sun, J. Liu, and G. Huang, "Lactate dehydrogenase A in cancer: a promising target for diagnosis and therapy," *IUBMB Life*, vol. 65, no. 11, pp. 904–910, Nov. 2013, doi: 10.1002/IUB.1216.

[14] A. di Cello *et al.*, "A more accurate method to interpret lactate dehydrogenase (LDH) isoenzymes' results in patients with uterine masses," *Eur J Obstet Gynecol Reprod Biol*, vol. 236, pp. 143–147, May 2019, doi: 10.1016/J.EJOGRB.2019.03.017.

[15] F. Zhang, Y. Liu, Q. Quan, Y. Meng, and X. Mu, "Diagnostic Value of Preoperative CA125, LDH and HE4 for Leiomyosarcoma of the Female Reproductive System," *Cancer Manag Res*, vol. 13, pp. 4657–4664, 2021, doi: 10.2147/CMAR.S302223.

[16] J. Pérez-Escuredo *et al.*, "Lactate promotes glutamine uptake and metabolism in oxidative cancer cells," *Cell Cycle*, vol. 15, no. 1, pp. 72–83, Jan. 2016, doi: 10.1080/15384101.2015.1120930.

[17] R. Liu *et al.*, "Overall survival of cancer patients with serum lactate dehydrogenase greater than 1000 IU/L," *Tumor Biology*, vol. 37, no. 10, pp. 14083–14088, Oct. 2016, doi: 10.1007/S13277-016-5228-2/TABLES/3.

[18] A. Mollo *et al.*, "Increased LDH5/LDH1 ratio in preoperative diagnosis of uterine sarcoma with inconclusive MRI and LDH total activity but suggestive CT scan: a case report," *BMC Womens Health*, vol. 18, no. 1, Oct. 2018, doi: 10.1186/S12905-018-0662-5.

[19] L. Chen, L. Huang, Y. Gu, W. Cang, P. Sun, and Y. Xiang, "Lactate-Lactylation Hands between Metabolic Reprogramming and Immunosuppression," *Int J Mol Sci*, vol. 23, no. 19, Oct. 2022, doi: 10.3390/IJMS231911943.

[20] E. Pardella, L. Ippolito, E. Giannoni, and P. Chiarugi, "Nutritional and metabolic signalling through GPCRs," *FEBS Lett*, vol. 596, no. 18, Sep. 2022, doi: 10.1002/1873-3468.14441.

[21] F. Hirschhaeuser, U. G. A. Sattler, and W. Mueller-Klieser, "Lactate: a metabolic key player in cancer," *Cancer Res*, vol. 71, no. 22, pp. 6921–6925, Nov. 2011, doi: 10.1158/0008-5472.CAN-11-1457.

[22] M. v. Liberti and J. W. Locasale, "The Warburg Effect: How Does it Benefit Cancer Cells?," *Trends Biochem Sci*, vol. 41, no. 3, pp. 211–218, Mar. 2016, doi: 10.1016/J.TIBS.2015.12.001.

[23] D. M. Brizel *et al.*, "Elevated tumor lactate concentrations predict for an increased risk of metastases in head-and-neck cancer," *International Journal of Radiation Oncology*Biology*Physics*, vol. 51, no. 2, pp. 349–353, Oct. 2001, doi: 10.1016/S0360-3016(01)01630-3.

[24] J. Gu *et al.*, "Tumor metabolite lactate promotes tumorigenesis by modulating MOESIN lactylation and enhancing TGF-β signaling in regulatory T cells," *Cell Rep*, vol. 39, no. 12, Jun. 2022, doi: 10.1016/J.CELREP.2022.110986.

[25] C. L. Roland *et al.*, "Cell surface lactate receptor GPR81 is crucial for cancer cell survival," *Cancer Res*, vol. 74, no. 18, pp. 5301–5310, Jun. 2014, doi: 10.1158/0008-5472.CAN-14-0319.

[26] J. Wellbourne-wood, M. Briquet, M. Alessandri, F. Binda, M. Touya, and J. Y. Chatton, "Evaluation of Hydroxycarboxylic Acid Receptor 1 (HCAR1) as a Building Block for Genetically Encoded Extracellular Lactate Biosensors," *Biosensors (Basel)*, vol. 12, no. 3, Mar. 2022, doi: 10.3390/BIOS12030143.

[27] L. Jin, Y. Guo, J. Chen, Z. Wen, Y. Jiang, and J. Qian, "Lactate receptor HCAR1 regulates cell growth, metastasis and maintenance of cancerspecific energy metabolism in breast cancer cells," *Mol Med Rep*, vol. 26, no. 2, pp. 1–9, Aug. 2022, doi: 10.3892/MMR.2022.12784/HTML.

[28] W. Wagner, K. D. Kania, A. Blauz, and W. M. Ciszewski, "The lactate receptor (HCAR1/GPR81) contributes to doxorubicin chemoresistance via ABCB1 transporter up-regulation in human cervical cancer HeLa cells," *J Physiol Pharmacol*, vol. 68, no. 4, pp. 555–564, Aug. 2017, Accessed: Sep. 18, 2022. [Online]. Available: https://pubmed.ncbi.nlm.nih.gov/29151072/

[29] A. Paul and S. Paul, "The breast cancer susceptibility genes (BRCA) in breast and ovarian cancers," *Front Biosci (Landmark Ed)*, vol. 19, no. 4, pp. 605–618, Jan. 2014, doi: 10.2741/4230.

[30] S. M. Cheung *et al.*, "Lactate concentration in breast cancer using advanced magnetic resonance spectroscopy," *Br J Cancer*, vol. 123, no. 2, pp. 261–267, Jul. 2020, doi: 10.1038/S41416-020-0886-7.

[31] G. D. Luker, "Imaging Hyperpolarized Lactate in Prostate Cancer," *Radiol Imaging Cancer*, vol. 1, no. 2, Nov. 2019, doi: 10.1148/RYCAN.2019194007.

[32] W. Graboń *et al.*, "Lactate Formation in Primary and Metastatic Colon Cancer Cells at Hypoxia and Normoxia," *Cell Biochem Funct*, vol. 34, no. 7, pp. 483–490, Oct. 2016, doi: 10.1002/CBF.3211.

[33] L. D. Kellenberger *et al.*, "The Role of Dysregulated Glucose Metabolism in Epithelial Ovarian Cancer," *J Oncol*, vol. 2010, p. 514310, 2010, doi: 10.1155/2010/514310.

[34] C. Fotopoulou *et al.*, "British Gynaecological Cancer Society (BGCS) epithelial ovarian/fallopian tube/primary peritoneal cancer guidelines: recommendations for practice," *Eur J Obstet Gynecol Reprod Biol*, vol. 213, pp. 123–139, Jun. 2017, doi: 10.1016/J.EJOGRB.2017.04.016.

[35] R. Kerslake *et al.*, "A pancancer overview of FBN1, asprosin and its cognate receptor OR4M1 with detailed expression profiling in ovarian cancer," *Oncol Lett*, vol. 22, no. 3, pp. 1–14, Sep. 2021, doi: 10.3892/OL.2021.12911/HTML.

[36] O. N. Okorie and P. Dellinger, "Lactate: biomarker and potential therapeutic target," *Crit Care Clin*, vol. 27, no. 2, pp. 299–326, Apr. 2011, doi: 10.1016/J.CCC.2010.12.013.

[37] R. Pérez-Tomás and I. Pérez-Guillén, "Lactate in the Tumor Microenvironment: An Essential Molecule in Cancer Progression and Treatment," *Cancers (Basel)*, vol. 12, no. 11, pp. 1–29, Nov. 2020, doi: 10.3390/CANCERS12113244.

[38] P. Heneberg, "Lactic Acidosis in Patients with Solid Cancer," *Antioxid Redox Signal*, Apr. 2022, doi: 10.1089/ARS.2021.0267.

[39] S. A. Maher *et al.*, "Serum Lactate and Mortality in Emergency Department Patients with Cancer," *West J Emerg Med*, vol. 19, no. 5, pp. 827–833, Sep. 2018, doi: 10.5811/WESTJEM.2018.6.37295.

[40] M. G. V. Heiden, L. C. Cantley, and C. B. Thompson, "Understanding the Warburg effect: the metabolic requirements of cell proliferation," *Science*, vol. 324, no. 5930, pp. 1029–1033, May 2009, doi: 10.1126/SCIENCE.1160809.

[41] J. Weinberger, M. Klompas, and C. Rhee, "What Is the Utility of Measuring Lactate Levels in Patients with Sepsis and Septic Shock?," *Semin Respir Crit Care Med*, vol. 42, no. 5, pp. 650–661, Oct. 2021, doi: 10.1055/S-0041-1733915.

[42] N. J. White, S. Looareesuwan, R. E. Phillips, D. A. Warrell, P. Chanthavanich, and P. Pongpaew, "Pathophysiological and prognostic significance of cerebrospinal-fluid lactate in cerebral malaria," *Lancet*, vol. 1, no. 8432, pp. 776–778, Apr. 1985, doi: 10.1016/S0140-6736(85)91445-X.

[43] D. Aran *et al.*, "Comprehensive analysis of normal adjacent to tumor transcriptomes," *Nat Commun*, vol. 8, no. 1, Dec. 2017, doi: 10.1038/S41467-017-01027-Z.

[44] K. Lundø, M. Trauelsen, S. F. Pedersen, and T. W. Schwartz, "Why Warburg Works: Lactate Controls Immune Evasion through GPR81," *Cell Metab*, vol. 31, no. 4, pp. 666–668, Apr. 2020, doi: 10.1016/J.CMET.2020.03.001.

[45] K. Yang *et al.*, "Lactate Suppresses Macrophage Pro-Inflammatory Response to LPS Stimulation by Inhibition of YAP and NF-κB Activation via GPR81-Mediated Signaling," *Front Immunol*, vol. 11, Oct. 2020, doi: 10.3389/FIMMU.2020.587913.

[46] T. P. Brown and V. Ganapathy, "Lactate/GPR81 signaling and proton motive force in cancer: Role in angiogenesis, immune escape, nutrition, and Warburg phenomenon," *Pharmacol Ther*, vol. 206, Feb. 2020, doi: 10.1016/J.PHARMTHERA.2019.107451.

[47] T. P. Brown *et al.*, "The lactate receptor GPR81 promotes breast cancer growth via a paracrine mechanism involving antigen-presenting cells in the tumor microenvironment," *Oncogene*, vol. 39, no. 16, pp. 3292–3304, Apr. 2020, doi: 10.1038/S41388-020-1216-5.

Supplementary Materials

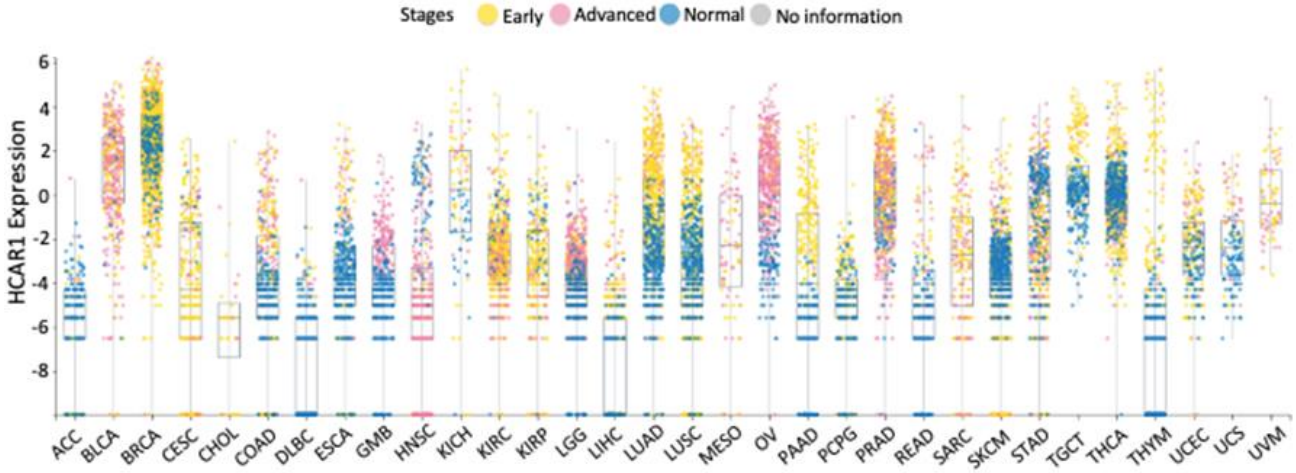

Figure S1. Gene expression of HCAR1 (hydroxycarboxylic acid receptor 1, HCAR1; formerly known as GPR81) from The Cancer Genome Atlas (TCGA) in cancer and normal tissues. Pancancer expression of HCAR1 taken from the canSAR database, showing expression from normal to early, to advanced stages; Abbreviations ACC: Adrenocortical carcinoma; BLCA: Bladder Urothelial Carcinoma; BRCA: Breast invasive carcinoma; CESC: Cervical squamous cell carcinoma and endocervical adenocarcinoma; CHOL: Cholangio carcinoma; COAD: Colon adenocarcinoma; DLBC: Lymphoid Neoplasm Diffuse Large B-cell Lymphoma; ESCA: Oesophageal carcinoma; GBM: Glioblastoma multiforme; HNSC: Head and Neck squamous cell carcinoma; KICH: Kidney Chromophobe; KIRC: Kidney renal clear cell carcinoma; KIRP: Kidney renal papillary cell carcinoma; LAML: Acute Myeloid Leukaemia; LGG: Brain Lower Grade Glioma; LIHC: Liver hepatocellular carcinoma; LUAD: Lung adenocarcinoma; LUSC: Lung squamous cell carcinoma; MESO: Mesothelioma; OV: Ovarian serous cystadenocarcinoma; PAAD: Pancreatic adenocarcinoma; PCPG: Pheochromocytoma and Paraganglioma; PRAD: Prostate adenocarcinoma; READ: Rectal adenocarcinoma; SARC: Sarcoma; SKCM: Skin Cutaneous Melanoma; STAD: Stomach adenocarcinoma; TGCT: Testicular Germ Cell Tumours; THCA: Thyroid carcinoma; THYM: Thymoma; UCEC: Uterine Corpus Endometrial Carcinoma; UCS: Uterine Carcinosarcoma; UVM: Uveal Melanoma. Expression measured as transcripts per million (TPM).

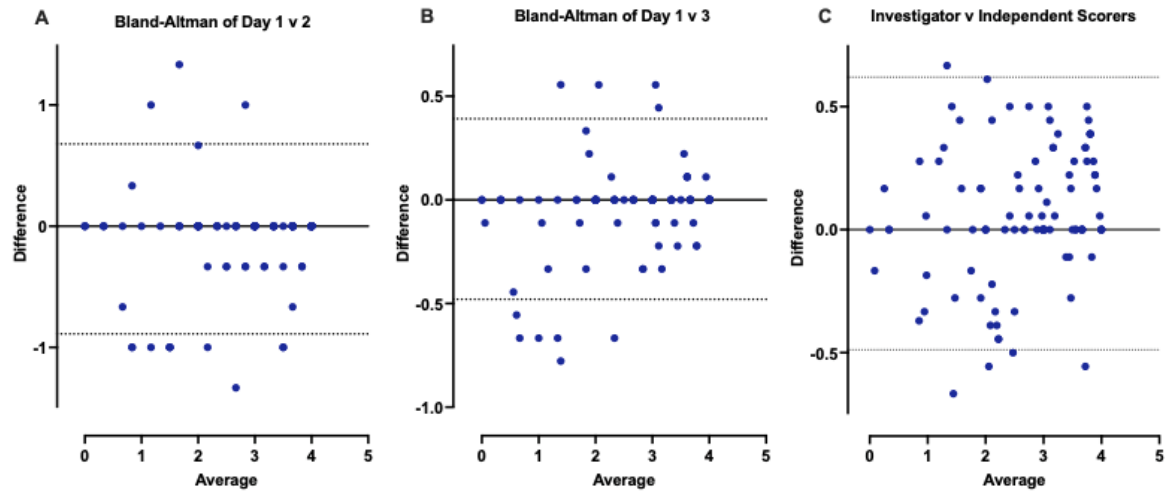

Figure S2. Bland-Altman analysis of immunohistochemistry quantification scores. (**A**) Primary investigator results for day 1 compared with day 2 of numeration, 95% confidence interval represented by the dashed line, each point represents an individual ovarian biopsy; (**B**) Primary

investigator results for day 1 compared to day 3; (**C**) Comparison of quantification scores between primary investigator and independent reviewers for an average of 3 days, an insignificant amount of scores for biopsy cores are seen outside of the 95% confidence limit when data is pooled with independent reviewers.

Chapter 5

A Meta-analysis of 2D vs. 3D Ovarian Cancer Cellular Models

Statement of Contribution

For the completion of the presented manuscript I contributed towards the following:

- Conceptualization
- Data curation
- Methodology
- Formal analysis
- Writing—original draft preparation
- Writing—review and editing
- Referencing

A Meta-analysis of 2D vs. 3D Ovarian Cancer Cellular Models

Rachel Kerslake[1], Birhanu Belay[2], Suzana Panfilov[1], Marcia Hall[1,3], Ioannis Kyrou[4,5,6,7,8], Harpal S. Randeva[4,5], Jari Hyttinen[2], Emmanouil Karteris[1*†] and Cristina Sisu[1*†]

[1]Division of Biosciences, College of Health, Medicine and Life Sciences, Brunel University London, Uxbridge UB8 3PH, UK; Rachel.Kerslake3@brunel.ac.uk, 1914541@brunel.ac.uk, emmanouil.karteris@brunel.ac.uk, cristina.sisu@brunel.ac.uk
[2]Computational Biophysics and Imaging Group, The Faculty of Medicine and Health Technology, Tampere University, Tampere, Finland. jari.hyttinen@tuni.fi, birhanu.belay@tuni.fi
[3]Mount Vernon Cancer Centre, Rickmansworth Road, Northwood, HA6 2RN, UK; Marcia.hall@nhs.net
[4] Warwickshire Institute for the Study of Diabetes, Endocrinology and Metabolism (WISDEM), University Hospitals Coventry and Warwickshire NHS Trust, Coventry CV2 2DX, UK; harpal.randeva@uhcw.nhs.uk
[5] Warwick Medical School, University of Warwick, Coventry CV4 7AL, UK;
[6] Research Institute for Health & Wellbeing, Coventry University, Coventry CV1 5FB, UK;
[7] Aston Medical School, College of Health and Life Sciences, Aston University, Birmingham, B4 7ET, UK;
[8] Laboratory of Dietetics and Quality of Life, Department of Food Science and Human Nutrition, School ofFood and Nutritional Sciences, Agricultural University of Athens, 11855 Athens, Greece, kyrouj@gmail.com
* Correspondence: Correspondence: (CS) cristina.sisu@brunel.ac.uk , (EK) Emmanouil.karteris@brunel.ac.uk

Abstract: Three-dimensional (3D) cancer models are revolutionizing research, allowing for the recapitulation of *in vivo* like response through the use of an *in vitro* system, more complex and physiologically relevant than traditional mono-layer culture. Cancers such as ovarian (OvCa), are prone to developing resistance and are often lethal, and stand to benefit greatly from the enhanced modelling emulated by 3D culture. However current models often fall short of predicted response where reproducibility is limited owing to the lack of standardized methodology and established protocols. This meta-analysis aims to assess the current scope of 3D OvCa models and the differences in genetic profile presented by a vast array of 3D cultures. A meta-analysis of the literature (Pubmed.gov) spanning 2012 – 2022, was used to identify studies with comparable monolayer (2D) counterparts in addition to RNA sequencing and microarray data. From the data 19 cell lines were found to show differential regulation in their gene expression profiles depending on the bio-scaffold (i.e. agarose, collagen or Matrigel) compared to 2D cell cultures. Top genes differentially expressed 2D vs. 3D include C3, CXCL1, 2 and 8, IL1B, SLP1, FN1, IL6, DDIT4, PI3, LAMC2, CCL20, MMP1, IFI27, CFB, and ANGPTL4. Top Enriched Gene sets for 2D vs. 3D include IFN-α and IFN-γ Response, TNF-α signalling, IL-6-JAK-STAT3 signalling, angiogenesis, hedgehog signalling, apoptosis, epithelial mesenchymal transition, hypoxia, and inflammatory response. Our transversal comparison of numerous scaffolds allowed us to highlight the variability that can be induced by these scaffolds in the transcriptional landscape as well as identifying key genes and biological processes that are hallmarks of cancer cells grown in 3D cultures. Future studies are needed to identify which is the most appropriate in vitro/preclinical model to study tumour microenvironment.

Keywords: Ovarian Cancer; High Grade Serous Ovarian Cancer (HGSOC); Monolayer; 2D; 3D; Scaffold; Tumour Microenvironment (TME); Extra cellular matrix (ECM); collagen; Matrigel; agarose

Citation Rachel Kerslake[1], Birhanu Belay[2], Suzana Panfilov[1], Marcia Hall[1,3], Ioannis Kyrou[4,5,6,7,8], Harpal S. Randeva[4,5], Jari Hyttinen[2], Emmanouil Karteris[1*†] and Cristina Sisu[1]. *Cancers* 2022, *volume number*, x.
https://doi.org/10.3390/xxxxx

Academic Editor(s):

Received: date
Accepted: date
Published: date

1. Introduction

Ovarian Cancer

Ovarian cancer (OvCa) is one of the most lethal gynaecological malignancies of the 21st century. Affecting over 313,000 women worldwide, OvCa typically presents at a late stage with non-specific symptoms, causing a detriment to survival outcomes, which fall as low as 20% [2]. The metabolic processes involved in OvCa aetiology however remain poorly understood. There are three main histological types of OvCa. Epithelial OvCa,

accounts for 90% of all cases, with high grade serous ovarian cancer (HGSOC – 70%) being the most prevalent of the five subtypes as well as the most lethal [2]. Other subtypes include low grade serous ovarian cancer (LGSOC – 5%), endometrioid adenocarcinoma of the ovary (EAC – 10%), clear cell carcinoma (CCC – 10%) and mucinous adenocarcinoma (MAC < 3%). The least common are germ line and stromal sex cord tumours which cover 10% of cases [3].

In order gain a better understanding of the events that take place within the tumour microenvironment (TME), a model capable of emulating the *in vivo* milieu is required. The use of conventional monolayer cell culture (two-dimensional; 2D) allows for analysis using a controlled *in vitro* environment to investigate physiological, morphological, and biochemical properties of biological systems [4]. Monolayer culture has served as an integral foundation of biological research since the introduction of immortalised HeLa in 1951 paving the way for thousands of subsequent cell lines [5]. Cell models have since proven invaluable in the modelling of normal physiology and diseases including cancer [6].

Nevertheless, monolayer culture has translational limitations, with differences in gene expression, drug response and cell signalling evident when compared to *in vivo* models [7]. Many processes related to tumorigenesis and metastasis are often over-simplified in monocultures [8]. As a result, monolayer culture often fails to recapitulate the complex microenvironment, diffusion gradients and cellular characteristics associated with *in vivo* systems. Thus, leading to variation from predicted response in animal and computational modelling, as well as clinical testing [7], [9].

As global research efforts strive to answer increasingly complex biological questions, there is a greater need for a representative system capable of physiological emulation. Many studies show that the complexities of tissue organisation, differentiation, and gene expression are demonstrated at higher levels in three-dimensional (3D) cell cultures [10], [11]. This set up allows for cells to be grown in an environment that sustains spatial complexities representative of *in vivo* allowing cells to differentiate and interact in a tissue specific manner [12]. Key differences between monolayer and 3D cultures are summarised in Table 1 [6].

Table 1. Differences between 2D and 3D cell culture systems [13].

2D - Culture	3D - Culture
Cells grown in monolayers – biologically simple	Cells form differentiated aggregates, spheroids, or organoids – biologically complex
Gene and protein expression differ from *in vivo*	Expression closely mimics *in vivo*
Uniform exposure to chemical stimuli; drugs often appear affective	Nonuniform growth results in toxicity profiles and diffusion gradients closely related to *in vivo*
Oxygen diffusion is uniform and higher than many *in vivo* structures; thus, augmenting mitochondrial function and ROS production	Oxygen distribution varies, hypoxic cores are evident; closely mimicking *in vivo* variations of many complexes
Long term culture can result in genetic drift with epigenetic and morphological changes evident	Growth is typically short term, minimizing genetic drift
Can be cheaper and less complex, therefore easily recapitulated in a lab	Requires additional nutrients and biological scaffolds, and can therefore be more expensive and time consuming
Established protocols	Limited established protocols

Further evidence emphasises the importance of the TME for maintained cancer stemness, exerting a significant effect over gene expression [14]. The integration of an extracellular matrix (ECM) i.e., a scaffold, provides the necessary environment for this 3D cellular growth and differentiation [15]. Scaffolds emulate the tissue-tissue interfaces and chemical gradients required within a living system. Recent advancements include 3D organoid systems capable of sustaining a vast array of tumour models including glioblastoma, colon and lung as well as ovarian [16]–[18].

Epithelial OvCa cells grown in 3D, often present with histological features characteristic of the original tumour *in situ* [19]. 3D epithelial OvCa cell lines also present with reduced proliferative rate thought to be enabled by the synthetic ECM [20]. An enhanced response to external stimuli is also evident within OvCa cultures. Thus far 3D OvCa cultures have proven particularly useful as a model of therapeutic resistance; capturing developed resistance to platinum-based therapeutics similar to *in vivo* OvCa response. The OvCa cell line SKOV-3, for example demonstrates a higher degree of chemoresistance to both cisplatin and paclitaxel when cultured in 3D [21]. Moreover, colorectal and pancreatic cancer cells grown in 3D exhibit differential gene expression that is associated with augmented ATP production within 3D cultures. Subsequently, amino acid production and metabolomic activity of glycolytic intermediates are increased when compared with monolayer substrates of the same cell line [22], [23].

A wide array of scaffolds can be used to recapitulate the TME and support differentiation of 3D culture, given that TME is pivotal for the regulation of a diverse array of processes including, migration, proliferation, differentiation, and cell-cell communication [24]. Often interchangeable within the literature, spheroids and organoids differ in complexity. Typically, spheroids are rounded and are comprised of cells grown initially in 2D, and as such retain some simplicity of gene expression. Growth is often achieved using hanging drop method or an ultra-low attachment plate and is ideal for the study of diffusion gradients and core hypoxia [25].

Given the current trajectory of 3D cancer models and their appeal to support the reduction of animal research, it is therefore safe to assume that a complex OvCa on a chip model will soon be achievable. This meta-analysis aims to evaluate the current landscape of OvCa cell models to elucidate differences presented in their genetic profile and associated signalling pathways, when grown in 3D compared to 2D monolayer culture.

2. Materials and Methods

Study Design

The review was designed with the intent to search current literature for studies modelling OvCa using 3D culture techniques and assess the differences in gene regulation between 2D and 3D cultures. The National Centre for Biotechnology Information (NCBI) PubMed data base was searched for studies relevant to the scope of the review between the years 2012 and 2022. No limitations to original language were applied, as long as English translations were available. The filter for human studies was utilised. Search terms applied include: “cancer” AND “ovar*” AND “3d” NOT “sound” NOT “ultra” NOT “imaging” NOT “Ultrasound” NOT “Review”. Literature that was inaccessible via the university institutional access were also removed. Additional searches through NCBI, Sequence Read Archive (SRA) and Gene Expression Omnibus (GEO) accession platforms were also utilised.

Inclusion criteria: Studies were included if they encompassed 3D OvCa models as well as 2D comparisons. In addition, those with associated data from sequencing arrays and RNA sequencing, accessible through GEO or SRA, were also sought.

Exclusion criteria: Studies were discarded if they did not meet the original search criteria. Additional studies that were excluded comprised of those with a lack of comparative 2D culture, no open access and no human samples i.e., the use of animal (usually murine) cell lines. Final exclusion criteria for enrichment encompassed studies with no associated data.

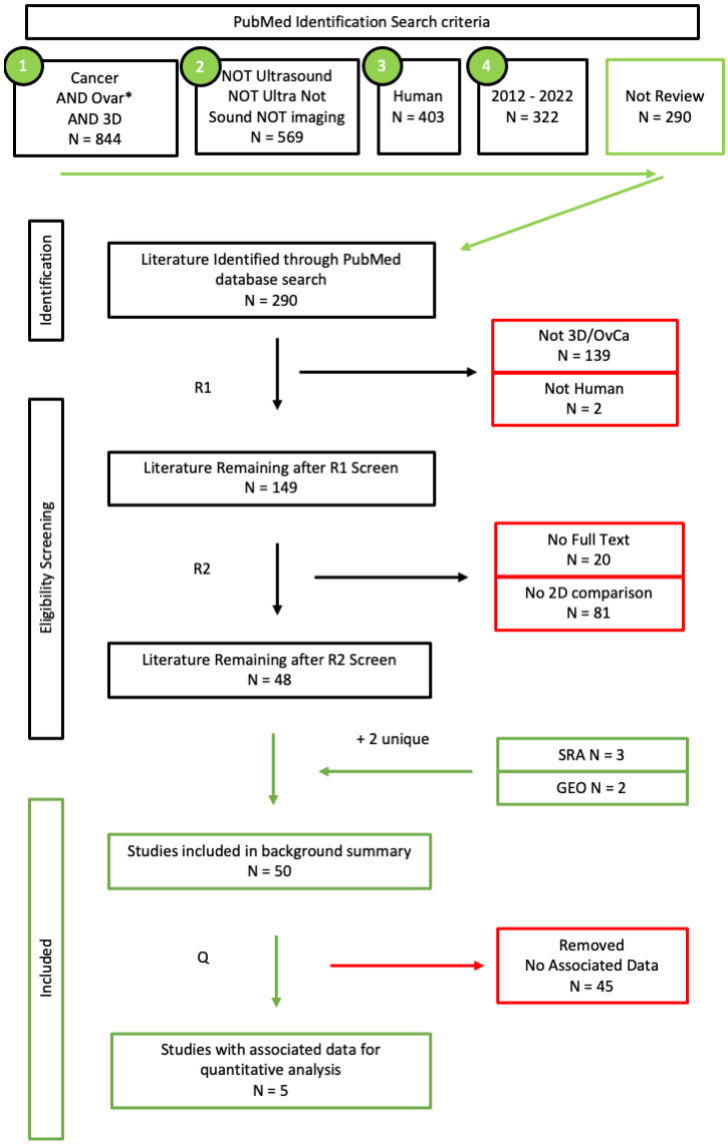

Figure 1. Search Criteria workflow. Studies accessed through Pubmed.gov on the 25/06/2022. Using pre-defined search terms. Articles were subjected to 2 rounds of screening by two independent reviewers. Additional data sought through Sequence Read Archive and Gene Expression Omnibus 07/2022. Studies were split into two groups: those suitable for the background summary (N = 50) and those containing associated data (N = 5). .

Cell Culture and 3D modelling

Unless otherwise stated all reagents were purchased from Thermofisher Scientific. The serous ovarian adenocarcinoma cancer cell line SKOV-3 (ECACC 91091004) were seeded in conventional culture-treated polystyrene T75 flasks. Cells were grown in Dulbecco modified eagle's medium (DMEM), supplemented with 10% foetal bovine serum and 1% penicillin-streptomycin. Media changed every 2 – 3 days with experimental work proceeding after 3 passages. Cell suspension concentrations were calculated using trypan blue exclusion method. For monolayer substrate comparison, cells were seeded in triplicate, at a density of $5x10^6$ in an Ibidi 8-well chamber (Ibidi, Munich, Germany) with complete medium. 3D cultures were generated using a 1:12 ratio of cells suspended in medium mixed with GelTrex™ (batch: 2158356). Each well contained a final concentration of 300µl. The chamber was left to incubate at 37°C for 30 minutes to allow for gelation, 100µl of media was then added to each well. Media changes took place every 2 – 3 days up to day

10. Images were captured each day using a Nikon TS100 Inverted Phase Contrast light microscope (Nikon, Tokyo, Japan).

Certificate of analysis and declaration of mycoplasma free cultures were provided upon receipt of cells from PHE and validated in house with DAPI staining; cells were used following 3 passages from purchase.

Immunofluorescent imaging

On day 10, media was removed. Both 2D and 3D cultures were fixed with 4% paraformaldehyde in PBS for 10 and 30 minutes respectively. Chambers were washed x3 with PBS following incubation with 0.1% triton-x, for 10 minutes. Chambers were again washed prior to blocking with 10% bovine serum albumin (BSA) (Sigma Aldrich, Burlington, MA, USA), for 1 hour at room temperature. BSA was then removed for phalloidin (ATTO-TEC, Siegen, Germany) actin staining, using a 1:1000 dilution in 1% BSA for 30 minutes at room temperature. Chambers were again washed x3 with PBS before the administration of a final DAPI (Invitrogen, Massachusetts, USA) nuclear stain for 10 minutes. Samples were washed to remove residual DAPI and kept hydrated in PBS prior to imaging.

Laser Scanning Confocal Microscopy

Laser scanning confocal microscopy (LSM780, Carl Zeiss, Oberkochen, Germany) was used for 3D imaging of cells cultured in a glass substrate and encapsulated in 3D Geltrex hydrogel. The cell samples were subject to excitation\emission wavelength at 405 nm\410 nm- 495 nm and 488 nm\495 nm – 620 nm, for imaging of nuclei (DAPI) and actin (phalloidin), respectively. The emitted fluorescence signal was recorded using photomultiplier tube (PMT) detectors. The optical Z-stacks were acquired using 63x objective (A plan-Apochromat 63x/1.4 Oil immersion, Carl Zeiss). The laser power, detector gain, and scan speed were optimized to avoid photobleaching. The image size was 2048 pixels x 2048 pixels, with a voxel size of 40 nm x 40 nm in the XY-plane, and 250 nm in the Z-direction. The images were deconvoluted using automatic deconvolution mode with theoretical point spread function using Huygens Essential software (Scientific Volume Imaging, The Netherlands). Avizo software (Thermo Fisher Scientific, Waltham, MA, USA) was used for 3D visualization.

RNA Sequencing – Sequence Read Archive (SRA)

NIH Sequence Read Archive (SRA) data were found using the same search terms outlined in the study design. SRA data in the form of RNA sequencing reads produced with Illumina NextSeq 500 and Illumina HiSeq 2500 were acquired for re-analysis, accession IDs are outlined below in table 2. Briefly, relevant data in the form of FASTQ files were transferred from the SRA data base via Amazon Web Services for in house analysis (Table 2) – full list can be seen in (supplementary Table S1). The corresponding scaffold used within each study are as follows. PRJNA472611, 3D cells were embedded within agarose; PRJNA564843 cells were grown upon a layer of onmental fibroblasts embedded within Collagen; PRJNA530150 3D cells were grown in Matrigel.

Table 2. Accession codes from RNA sequencing of 2D and 3D OvCa cell models.

Accession	Platform	Paired Reads
PRJNA472611	Illumina HiSeq 2500	24
PRJNA530150	Illumina NextSeq 500	32
PRJNA564843	Illumina NextSeq 500	36

The raw RNAseq data was produced using the pipeline previously described to standardise the results for comparison [26]. Briefly, TopHat2 (v.2.1.1) was applied to align reads to the reference human genome, GRCH38 (hg19) using the ultra-high-throughput

short read aligner Bowtie2 (v.2.2.6). Where applicable replicates were merged according to a selection criterion taking only high-quality mapped reads (<30), using Samtools (v.0.1.19). Subsequent transcript assembly and quantification followed using Cufflinks (v.2.2.1). Finally, differential expression profiles were obtained for further analysis using Cuffdiff (v.2.2.1).

RNA Sequencing – Statistical Analysis

The expression data was analysed in R (v. 4.1.0, The R Foundation for statistical Computing, Vienna, Austria) with R studio desktop application (v.2022.07.2, RStudio, Boston, MA, USA) using specific libraries for modelling, visualisation, and statistical analyses for the identification of differentially expressed genes (DEGs). Similar to our previous work, Pearson correlation coefficient was applied for the estimation of gene expression patterns and student's t-test was utilised to assess statistical significance between expression profiles (i.e., 2D vs 3D). Significance thresholds were set for a p-value < 0.05. For identification of enriched pathways in omics data pathfindR was employed. Volcano plots for visualisation were generated using R package ggplot2 (v.3.3.5). DEGs were identified and isolated for subsequent enrichment analysis. Furthermore, we have used the OmicsPlayground online application for exploring the transcriptional landscape of ovarian cancer cells grown in 2D and various 3D systems using as scaffolds agarose, collagen and Matrigel [27].

Gene Expression Omnibus (GEO) Array – Statistical Analysis

Genomic data sets (accession numbers: PRJNA232817 and PRJNA318768) were downloaded from NCBI public repository GEO archive. These OvCa cells were grown using ultra-low attachment and hanging drop techniques. The GEO2R web application was accessed to re-analyse the expression data in line with the research questions within this study (control 2D samples vs. control 3D samples). Thresholds were again set at p-value < 0.05 and LogFC2 > 1 with applied Benjamini & Hochberg (False discovery rate). Volcano plots were generated through GEO2R (https://www.ncbi.nlm.nih.gov/geo/geo2r/).

Functional Enrichment Analysis

Differentially expressed genes (DEGs), identified through GEO2R and SRA analysis, were then subjected to functional enrichment analysis. Funrich (v.3.1.3), was accessed to provide a functional annotation including associated sites of expression, biological processes, and pathways. Enrichment Analysis was performed using Omics Playground for the functional comparison of OvCa genes in 2D vs. 3D [27].

Presentation of Data and Statistical Analysis

Global distribution infographics were generated using R (v.4.1.0) with R studio (v.2022.07.2) along with ggplot2 (v.3.3.6), maps (v.3.4.0) and world map data from natural earth (0.1.0). Subsequent comprehensive background analysis and graphs pertaining to publication data, cell line frequency and associated characteristics were generated using GraphPad Prism9® (v.9.4.1 - GraphPad Software, Inc.). Statistical reliability of Omics Playground data are ensured through the incorporation of Spearman rank correlation, GSVA, ssGSEA, GSEA and Fisher extract test [27].

3. Results

3D Ovarian Cancer models

Literature overview

The geographical spread of the fifty studies selected suggests that the United States of America (USA) are the top publishers of 3D OvCa modelling with over 50% of the research accessed originating within the USA. China, Italy, Korea, and the UK follow, with the majority of the work originating from Europe or North America (Figure 2A, B).

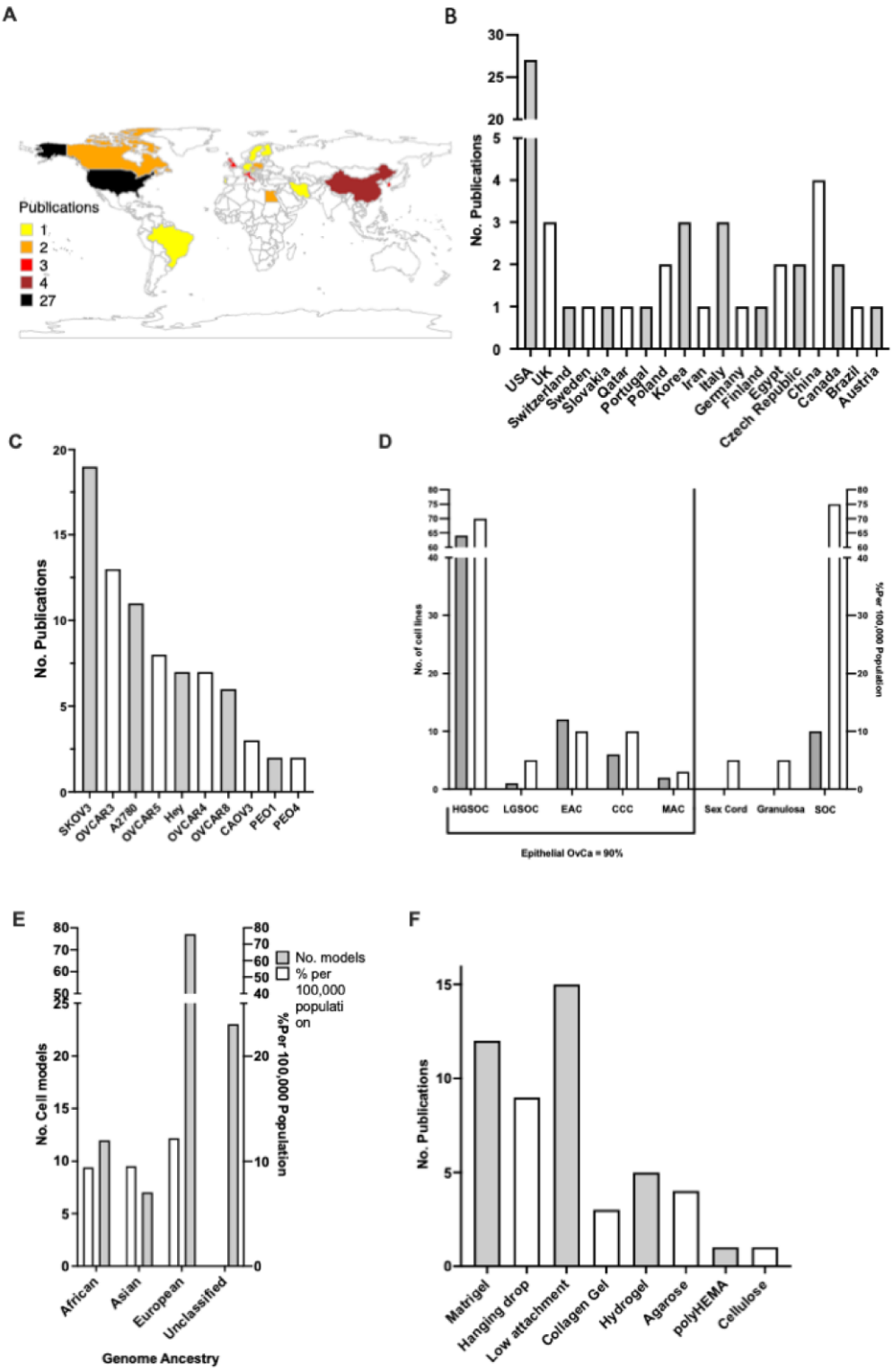

Figure 2. Overview of the published 3D culture experiments in ovarian cancer. **(A)** Gradient map depicting the global spread of publications 2012 – 2022; **(B)** Chart showing no. of publications per country 2012 – 2022; **(C)** Top cell lines used in 3D Ovarian cancer (OvCa) within the literature; **(D),** Trends between the distribution of cell models against actual global rates (white) pertaining to OvCa subtype (grey); **(E),** Genome ancestry of cell lines used (grey), contrasted with actual global OvCa

ethnicity rates (white) (2012 – 2022); **(F)** The ten most frequently used scaffolds for supporting growth of OvCa cells (circa 2012 - 2022) selected from the publication corpus analysed.

To achieve 3D culture, cell lines are grown within a fabricated ECM also known as a scaffold. Within the literature the most commonly used scaffolds for 3D OvCa growth were pre-coated low attachment plates, followed by Matrigel, hanging drop method and plant-based hydrogel (Figure 2C). Over 43 unique OvCa cell lines were utilised throughout the studies. The top 10 represent an array of OvCa subtypes (Figure 2D). The ovarian carcinoma cell line SKOV-3 was the most frequented within the literature, appearing on 19 instances. The trend of studies focusing on OvCa subtypes was compared with the actual global incidence rates. For epithelial OvCa the cell models used followed a similar trend in frequency to actual global incidences, with HGSOC being the most prevalent form of OvCa and also the most studied. Of note sex cord stromal and granulosa OvCa comprises 10% of global cases, however no 3D models were found within the studied literature. The genome ancestry of the cell lines is often overlooked, however given the disparity in care the background of the cell lines used was also sourced (Figure 2E). A disproportionate number of cell lines used are either White (N = 80) in origin or are considered unclassified i.e. no available data (N = 30).

Differentially Expressed Genes

Data accessed through SRA and GEO were screened for OvCa cells grown in 2D and 3D under similar conditions. Three separate studies were chosen encompassing 19 cellular models grown under normal conditions in agarose, Matrigel and collagen-based scaffolds. All cell lines grown in 3D showed differential gene expression when contrasted with the same cell lines under the same conditions but grown in 2D (Figure 3). The number of statistically significant differentially expressed genes (DEGs) with $p < 0.05$, between the 2D and 3D cultures ranged between 234 in PEO1, to 1429 in OVCAR5 cell line.

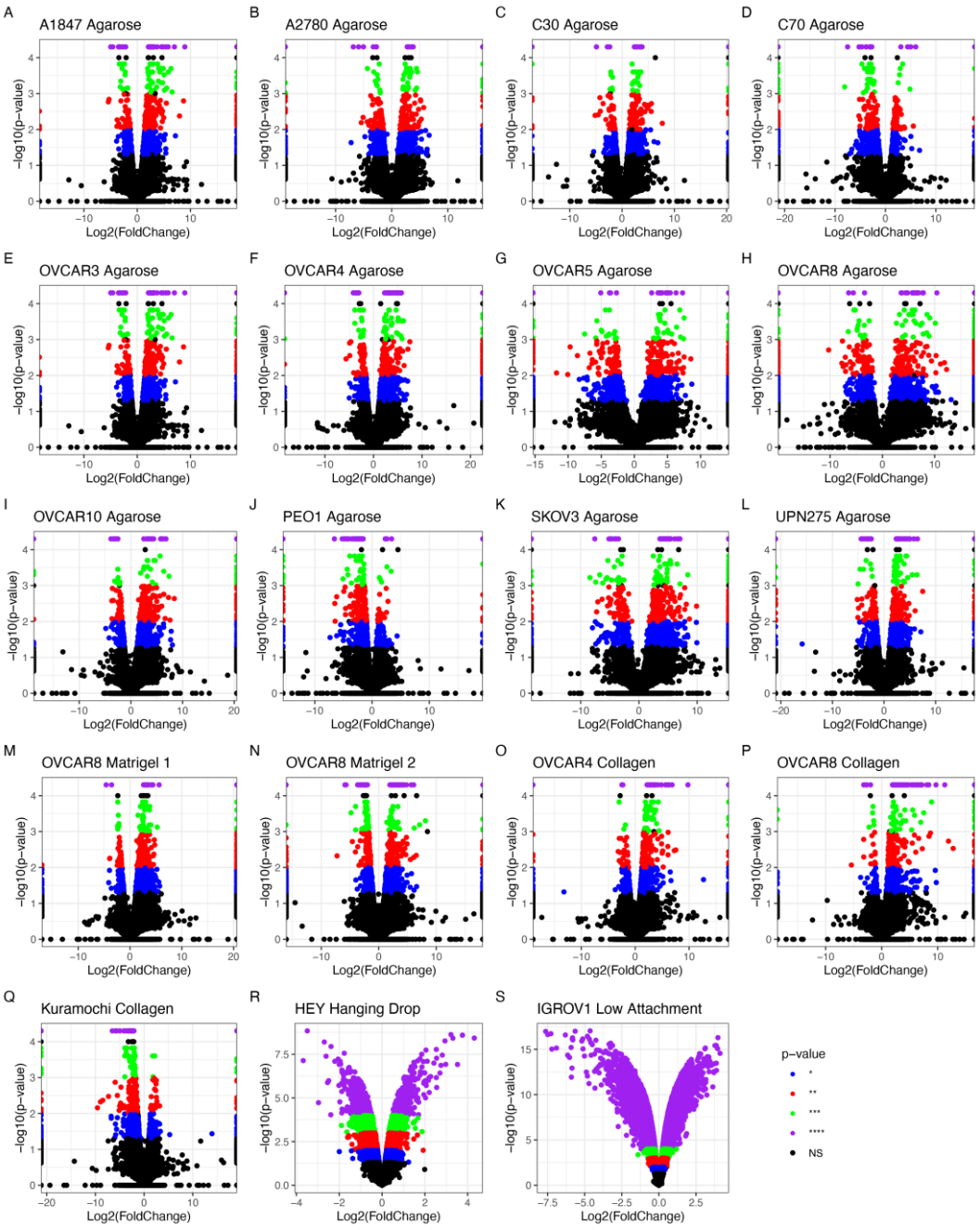

Figure 3. Differentially expressed genes (DEGs) detected by RNA sequencing analysis of OvCa cell lines grown in 2D contrasted with 3D. **(A)–(Q)** show data extracted from RNAseq experiments **(R)–(S)** show data extracted from microarrays. Significance thresholds for **(A)–(Q)** are set at NS > 0.05 = grey/black, *p < 0.05 = blue, **p < 0.01 = red, ***p < 0.001 = green and ****p < 0.0001 = purple. **(R)–(S)** p-value threshold = 0.05, NS data is shown in black. **(A)** – **(L)** have agarose as scaffold, **(M)** – **(N)** are Matrigel, **(O)** – **(Q)** are collagen, **(R)** is hanging drop and **(S)** is low attachment. **(A)** A1847 - Endometrioid Carcinoma of the Ovary (EAC); **(B)** A2780 - EAC; **(C)** C30 - carcinoma; **(D)** C70 - carcinoma; **(E)** OVCAR3 - HGSOC; **(F)** OVCAR4 – HGSOC; **(G)** OVCAR5 - HGSOC; **(H)** OVCAR8 - HGSOC; **(I)** OVCAR10 - HGSOC; **(J)** PEO1 - HGSOC; **(K)** SKOV-3 - Carcinoma; **(L)** UPN275 - Mucinous adenocarcinoma (MAC); **(M)** Kuramochi - HGSOC; **(N)** OVCAR4 Collagen - HGSOC; **(O)** OVCAR8 Matrigel 1 - HGSOC; **(P)** OVCAR8 Matrigel 2 - HGSOC; **(Q)** OVCAR8 Collagen - HGSOC. **(R)** HEY – HGSOC; **(S)** IGROV1 – EAC.

The HGSOC OVCAR8 appeared in all three studies with different accompanying scaffolds: Matrigel, agarose and collagen. Therefore, additional analysis explored the effects of different scaffolds on the genetic profile of these cells (Figure 4). All conditions influenced differential regulation of OVCAR8's transcriptional profile. 13 DEGs were

identified (Table 3) based on their common dysregulation between scaffolds when grown in 3D. Similarly, these genes were seen to feature highly throughout the other 3D models i.e., dysregulation of ANGPTL4 appeared in 12/19 of the studies. When comparing DEGs identified between OVCAR8 cells grown in 2D and 3D, eight were found to be common regardless of their scaffold type (Figure 4 and Table 3).

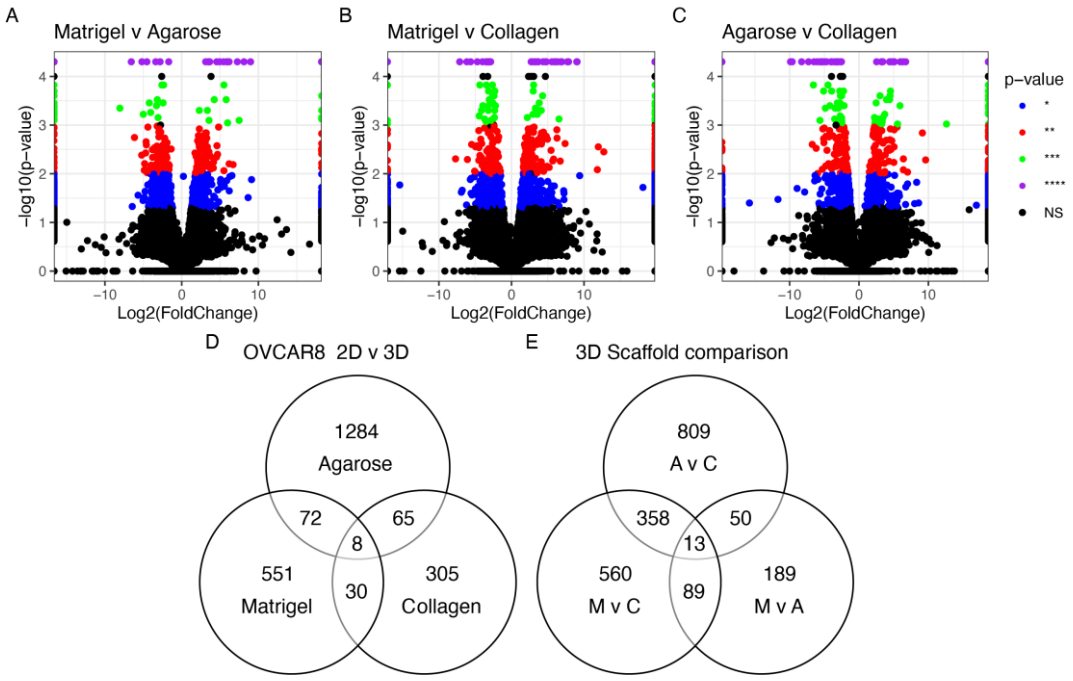

Figure 4. Differentially expressed genes seen in OVCAR8 grown in 3D**. (A)** Agarose vs. Collagen; **(B)** Matrigel vs. Agarose; **(C)** Matrigel vs. Collagen. Threshold set at $p < 0.05$. **(D)** Common genes differentially expressed between OVCAR8 grown in 3D vs. 2D. **(E)** Common genes between **(A - C);** M: Matrigel, C: Collagen, A: Agarose.

Table 3. OVCAR8 genes commonly differentially regulated in 3D conditions grown on agarose, collagen and Matrigel compared to 2D cultures.

Common 3D vs. 2D	Data sets	Scaffold Specific	Data sets
DDIT4	12	RP11-13K12.2	0
ANGPTL4	15	EEF1A1P9	0
SELENBP1	7	EEF1A1P12	0
SULF1	6	TENM2	5
GAL3ST1	7	RP11-297P16.4	3
TNFAIP3	9	GGT1	1
LLNLR-263F3.1	4	IFI44	5
MUC12	4	CXCL2	3
		KIF1A	2
		AC003092.1	3
		INHBA	6
		RP13-143G15.4	7
		GREM1	3

The impact of scaffold and 3D set up as compared to 2D culture on the genetic profile of OvCa cells

We explored the transcriptional landscape in 2D and 3D cultures in 3 different scaffolds (agarose, collagen and Matrigel) for the OVCAR8 cell lines.

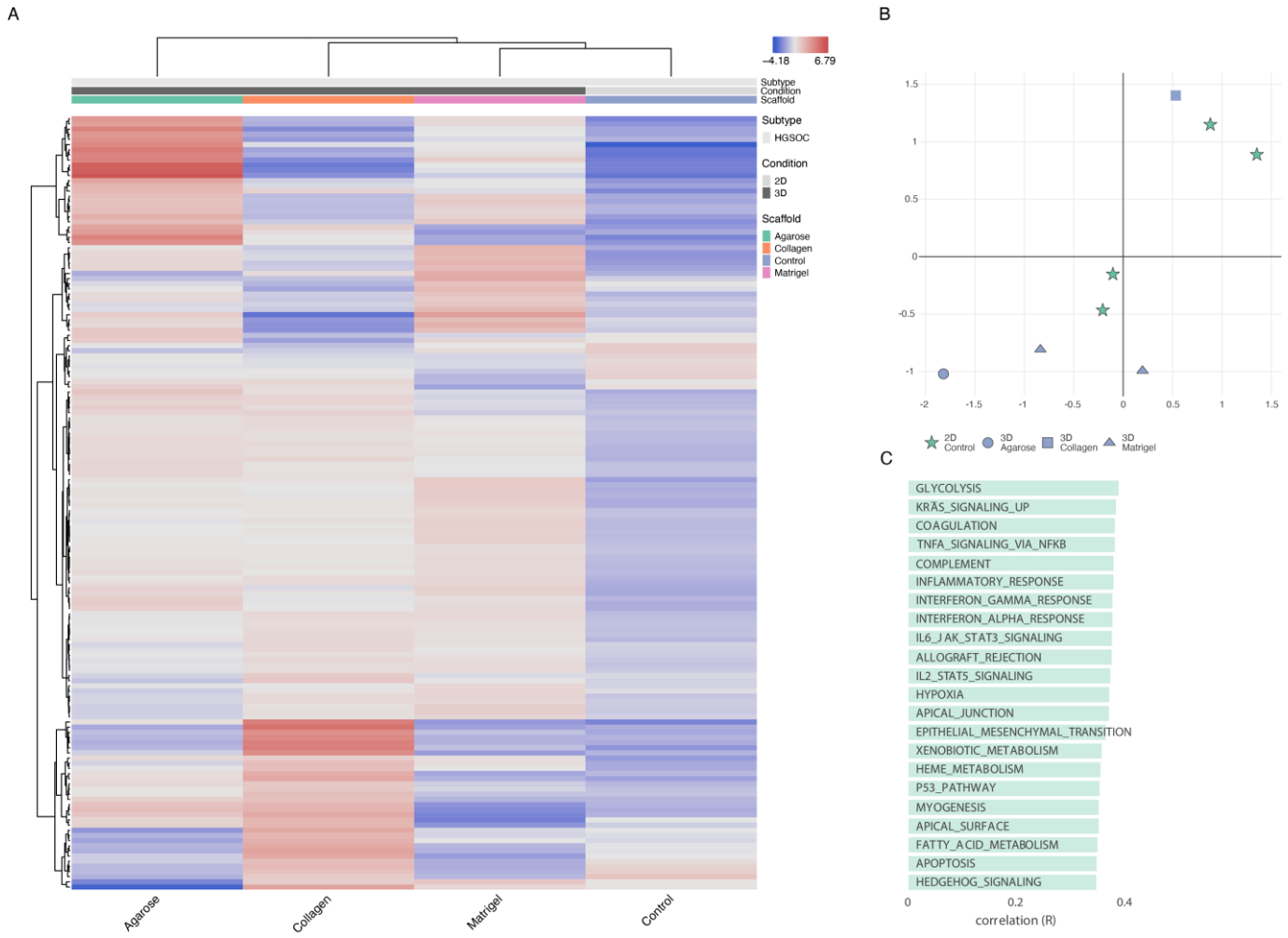

Figure 5. OVCAR8 transcriptional profile in 2D v 3D. **(A)** Top 150 differentially regulated genes from OVCAR8 grown under 2D and 3D conditions. Data originating from 3 unique studies, encompassing 4 growth conditions. 3D cells grown in Matrigel, Collagen and Agarose. 2D cells grown under standard lab conditions as matched controls to each 3D experiment. The gene name list is available in supplementary Table S2; **(B)** T-distributed stochastic neighbor embedding (T-SNE) plot of the genetic profiles of the HGSOC OVCAR8 grown in Matrigel (at 7 and 14 days – triangle), Collagen (square), Agarose (circle) and Monolayer (stars); **(C)** Functional analysis of the top 150 differentially regulated genes between 2D and 3D growth conditions showing key biological pathways associated with them. .

The cells grown in 3D on Matrigel, agarose and those grown on a basement layer of normal omental fibroblasts embedded within collagen, were compared with standard 2D monolayer cultures (Figure 5). The expression profiles of the top 150 DEGs with respect to growth conditions are shown in Figure 5A (supplementary Table S2). This gene set shows a large variability across the four growth conditions. Initial observations reveal a high degree of similarity in gene expression between samples grown in agarose and Matrigel. Collagen samples however show an expression profile that diverges from the 2D expression profile to a lesser extent than OVCAR8 grown on other scaffolds. T-SNE analysis (Figure 5B) recapitulates these observations showing a partial clustering of the 3D profiles, with the collagen 3D culture standing out and showing the highest level of similarity with the 2D culture experiments. The top functional groups of the differentially regulated genes included key metabolic pathways such as glycolysis (Figure 5C).

Next, we explored the genes' transcriptional signatures in the three scaffolds and in the 2D control experiments. We clustered the genes based on pairwise co-expression scores and visualised them using a uniform manifold approximation and projection dimensionality reduction technique (UMAP) (see Figure 6A). We found localised phenotypic clustering patterns in OvCa embedded in collagen and agarose with less variance in

phenotypic expression recorded for samples grown in Matrigel, when compared with 2D. Moreover, Matrigel culture showed an inverted gene expression signature compared to 2D control experiments. Similarly, we analysed cancer hallmark sets with the DEGs of OVCAR8 grown in 2D compared to 3D data (see Figure 6B). Processes with high covariance include: K-Ras signalling, angiogenesis, interferon alpha and gamma response, TNF alpha signalling as well as epithelial to mesenchymal signalling.

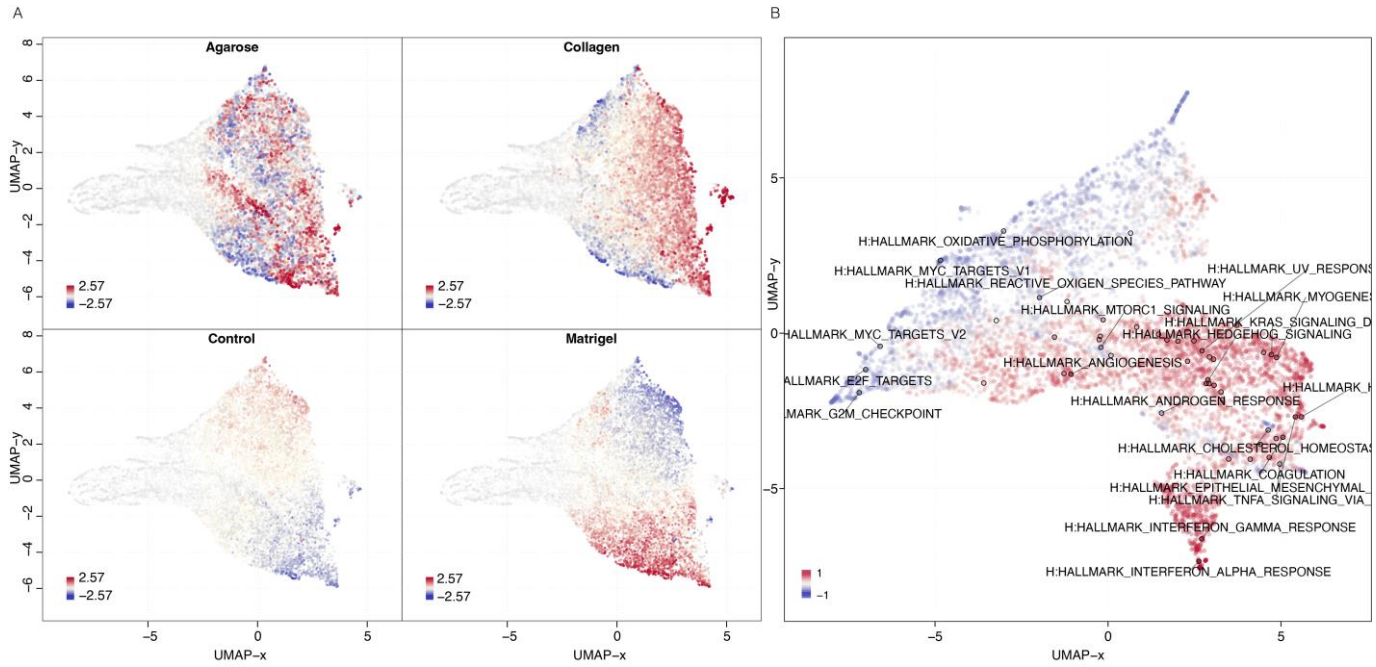

Figure 6. Gene and phenotypic hallmark signature profiles. **(A)** UMAP clustering of genes coloured by relative log-expression in four growth conditions: agarose, collagen, Matrigel and 2D controls. The distance metric is covariance. Genes that are clustered nearby have high covariance. **(B)** UMAP hallmark covariance using OVCAR8 grown in 2D and combined 3D data. Clustering of associated hallmarks. Processes upregulated in 3D are indicated in red. Downregulated are indicated in blue.

Functional Enrichment – 2D vs. 3D

A panel of genes were identified as commonly dysregulated in 3D cultures compared to 2D growth conditions. The cumulative 3D data encompasses OVCAR8 grown on Matrigel, agarose and collagen, while the control data is composed of the experiments using 2D growth conditions. The following genes showed statistically significant differential expression ($p < 0.05$): C3, CXCL1, CXCL8, IL1B, SLPI, FN1, IL6, DDIT4, PI3, LAMC2, CCL20, MMP1, IFI27, CFB, ANGPTL4 and CXCL2 (Figure 7). Furthermore, gene set enrichment analysis revealed that when grown in 3D many processes associated with hallmarks of cancer were also differentially regulated (supplementary Figure S1). Key processes that often show enhanced presentation in 3D growth such as angiogenesis, apoptosis and hypoxia all exhibited enrichment as well.

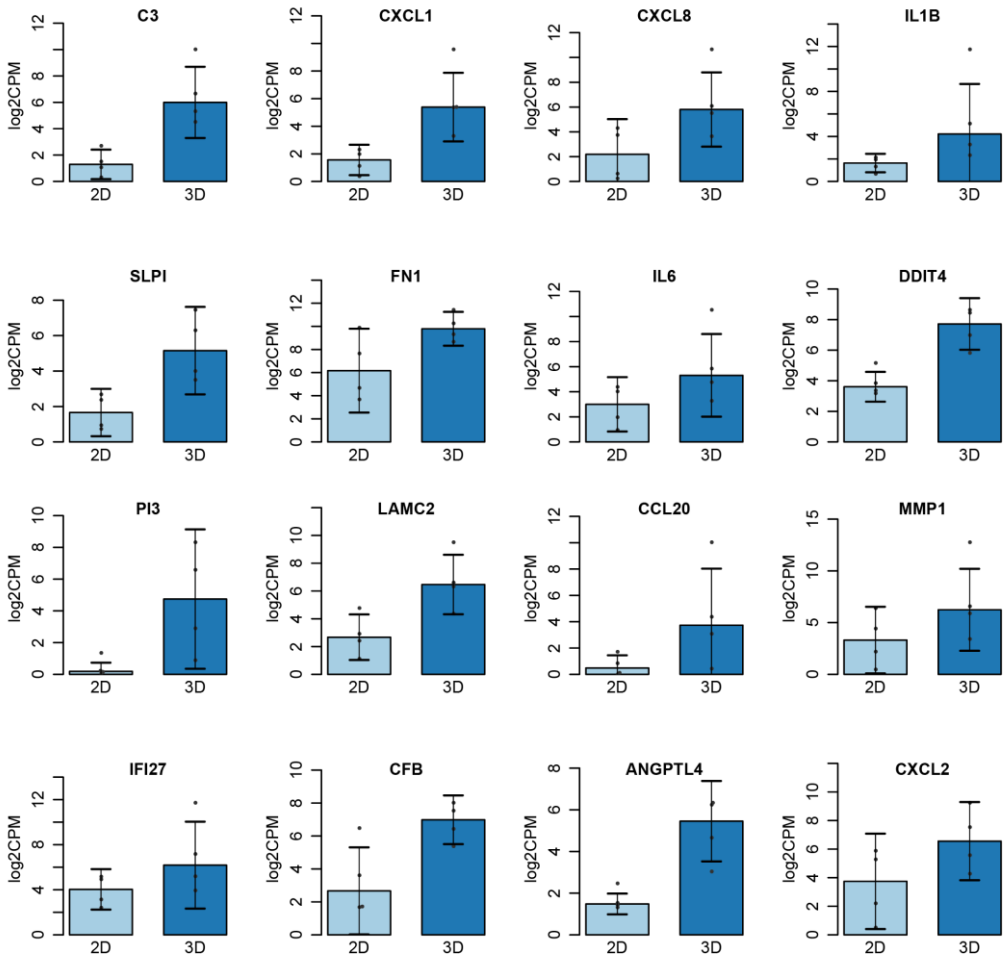

Figure 7. Top Genes Differentially Expressed 2D vs. 3D. Cumulative data for 3D taken from OVCAR8 embedded within Matrigel, Agarose and Collagen. Significance threshold *P < 0.05.

Scaffold Specific Biomarkers – 2D vs. 3D

Next, we examined the transcriptional landscape to identify potential biomarkers of growth conditions (Figure 8). For this we have used a variety of machine learning algorithms as implemented in the OmicsPlayground v2.8.10 to compute a cumulative importance score for all DEGs. The results highlighted 8 key genes that can be used as predictive scaffold biomarkers (Figure 8A). Specifically, cells grown in agarose show condition specific expression for 4 genes: C3, MMP1, IL1B and CCL20. Three potential markers of cells grown in collagen were identified namely: the interferons IFI44L and IFI27 as well as COL3A1. Matrigel was represented with only one significant growth marker: DDIT4. While these 8 biomarker candidates show the highest importance scores, a variety of other genes show scaffold specific expression as well (Figure 8H), suggesting that a number of gene panels can be created to evaluate the impact of growth conditions on the genome biology.

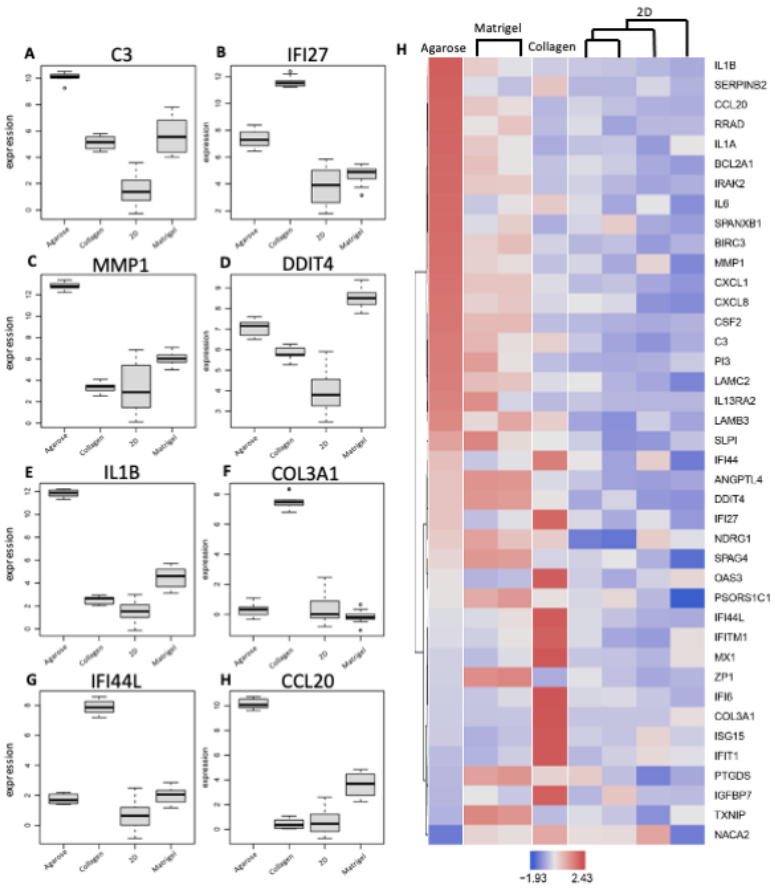

Figure 8. Scaffold specific biomarker identification. **(A - H),** The top 8 genes implicated with expression specific profiling for each condition; **(I)**, Biomarker Heatmap: expression heatmap of top gene features according to their variable importance score. Importance scores are calculated based on multiple machine learning algorithms including LASSO, elastic nets, random forests, and extreme gradient boosting.

Cell line specificity impact on scaffold selection

Following the analysis of the impact of scaffold and the 3D v 2D environment on the transcriptional landscape of the ovarian cancer cell line we looked at differential expression patterns between various cells lines grown on agarose and collagen scaffolds. As expected, we found a good separation of the cell line gene expression characteristics on both scaffolds (Figure 9A,B) using the top 150 differentially expressed genes. Most cell lines have also shown a fair discrimination between the 2D and 3D cultures on agarose, and also a good segregation between cancer subtypes (Figure 9C). However, A1847, OVCAR3, OVCAR4 and SKOV3, on agarose and all cells on collagen (Kuramochi, OVCAR4, and OVCAR8) show poor differentiation between the growth conditions suggesting that these scaffolds are potentially not optimal for recapitulating the tumour environment more accurately than classical 2D cultures in these cell lines.

Functional analysis reflects the diversity of the cell lines grown on each scaffold (Figure 9D). With sex hormones specific pathways characterizing the agarose cultures while cell growth and development pathways, as well as fatty acids metabolism being the dominant features of the collagen grown cell lines. The scaffold impact on cell line specificity was explored by comparing the differentially expressed genes between OVCAR4 and OVCAR8 in agarose and collagen (Figure 9E). We found that there is a good level of correlation between gene expression fold change in the two cell lines for agarose and collagen. Of the top differentially expressed genes, three, SLC34A2, LY6K, BMP7, show the same level of dysregulation between OVCAR8 and OVCAR4 in both growth conditions. However, we also identified 13 genes that show a scaffold specific differential expression pattern between the two cell lines: MMP7, LAMA3, IGFL1, S100A14, ELF3, CYGB, ITGB6,

DKK1, TACSTD2, IL7R, LGALS13, IFI6, FOXD1 being collagen specific, and IL1B, MMP1, CP, UBB, NUPR1, SCGB2A1, GPNMB, IGFBP2, GDF15, CCL20, CYP1A1, VTCN1, KRT19 agarose specific.

Finally, the differential expression patterns identified a set of genes that show both a cell, tumour subtype, and scaffold specific behaviour, and can be used as growth environment biomarkers (Figure 9F-H).

Figure 9. Cell line specific transcription in agarose and collagen. **(A)** and **(B)**, T-SNE plot of the genetic profiles of cell lines grown in agarose and collagen respectively against a 2D control. **(C)** Umap plot of the transcriptional profile of cancer subtypes in agarose vs 2D control, **(D)** Functional analysis of the top 150 differentially regulated genes between 2D and 3D growth conditions showing key biological pathways associated with them for agarose and collagen; the list of genes is shown in supplementary Table S2, **(E)** Similarity of gene differential expression in OVCAR4 vs. OVCAR8

in collagen vs. agarose, **(F) – (H)** The top 8 environment biomarkers for cell lines grown in agarose **(F)** and **(H)**, and collagen **(G)**. .

Recapitulation of 3D OvCa using GelTrex

Leveraging the lessons learned from the study of the transcriptional landscape of OvCa cell lines in different conditions, we attempted to capture the phenotypic changes in vitro between the 2D and 3D cultures. For this we have grown SKOV-3 cells in 3D using the hydrogel-based scaffold GelTrex™. Hydrogel was chosen as it encompasses one of the most common scaffolds within the literature and is not animal derived. In addition, this work sought to assess the ease of using non-established methodology for in house recapitulation. As such hanging drop and ultra-low attachment plates were not included as their use with OvCa is well established within the literature.

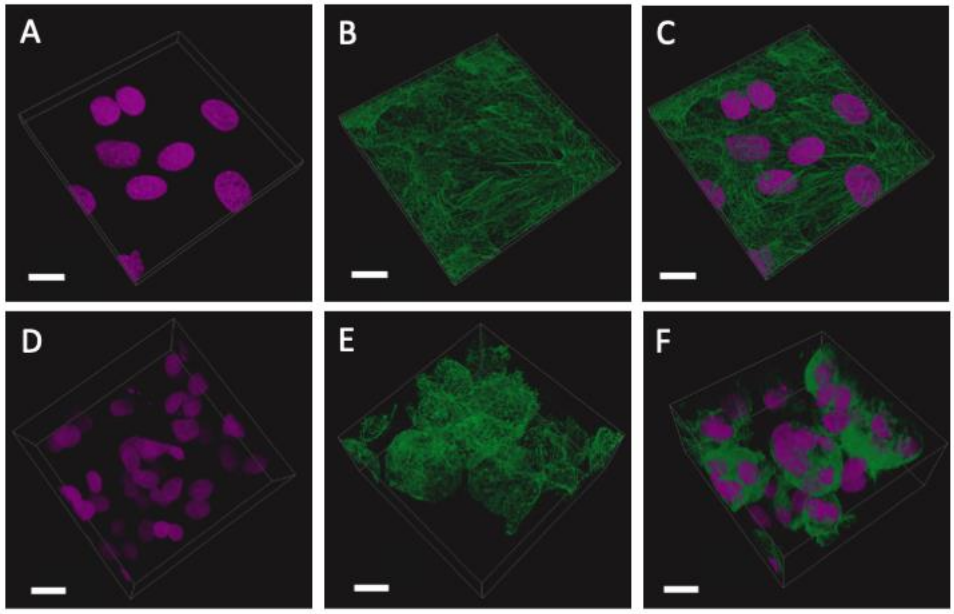

Figure 10. SKOV-3 cells grown for 9 days in conventional monolayer formation compared with those embedded in GelTrex™. **(A – C)** Monolayer cells: nuclei (pink), phalloidin (green) and overlay, showing a single plane of cells across a flat glass substrate; **(D – F)** 3D cells: nuclei (pink), phalloidin (green) and overlay, showing aggregated spheroids with multiple nuclei. The scale bar is 20 μm. .

Figure 10 shows the growth of cells over the course of a 9-day period. Here we adopted a simplistic approach and used a previously tried and tested gel known as GelTrex™. Following the embedding process cells began to aggregate and form spheroid like structures [28]. These structures-maintained circularity and continued to expand in volume as time progressed. The results suggest that the changes at genomic level have a direct impact on the 3D aggregation of cells.

4. Discussion

As OvCa is one of the most lethal gynaecological malignancies, there is a clear need for robust models that will help uncover the molecular mechanisms underpinning the disease development, growth, metastasis, and even potential therapeutic responses. Cancer modelling over the decades has progressed from crude anatomy to *in vitro* cultures, *in vivo* animal models and now to *in vitro* 3D cultures capable of recapitulating *in vivo* systems and associated TME. In this meta-analysis, we have examined the impact of various

scaffolds on the transcriptomic landscape of ovarian cancer cell lines as well as the differences arising from the 3D culture as compared to classical 2D approaches.

Initial literature survey has pointed out USA as the spearhead of 3D culture research in cancer, covering over 50% of published output in the field. Similar to what is observed in 2D cultures, immortalised cell lines take the forefront with SKOV-3 as the most frequently used option, while primary patient samples are used at a reduced rate. Additional cell lines used are OVCAR3, A2780, PEO1 and OVCAR8. The cell line distribution highlights a strong bias towards White European Ancestry. The percentage of East Asian 3D models in the literature are even lower despite associations with early disease onset in Asian women [29], recapitulating the need for engaging ethnic population in cancer research.

Further analysis shows that the associated subtypes of the cell lines used, align closely with the trend seen in actual global incidence rates of OvCa subtypes. HGSOC is the most frequent of epithelial OvCa subtypes encapsulating 70% of global cases [30], making this subtype a prime dataset to study in this work assessing the variability in 3D culture with respect to classic 2D experiments. It must be noted though, that *in vitro* work requires long-time investment, with relevant models, especially in OvCa, a commodity. With the advance of tissue culture techniques towards more physiological relevant systems however, researchers must strive to use validated and up to date cell lines or note their limitations in disease modelling to maintain reliable and repeatable data.

In this study, we also demonstrate how scaffolds recapitulate the ECM necessary for cell differentiation and the growth of 3D structures [24]. In OvCa modelling, where a 2D counterpart has been used for comparison the most frequent scaffolds utilised by researchers are Matrigel, hanging drop, low attachment plates and hydrogel.

Hanging drop is particularly useful for assessing diffusion gradients in an accessible format [31]. In terms of OvCa this method has been utilised in toxicity screening assays for monitoring chemoresistance in drugs such as cisplatin and Niraparib [18], [32]. Grown in ultra-low attachment plates, OvCa cells show altered mitochondrial function through augmented extracellular acidification rates [33]. Re-sensitisation to treatments in cell lines previously thought resistant are also evident using this method, with a number of BRCA wildtype epithelial OvCa cell lines responding to platinum-based therapeutics and showing an increased rate in apoptosis [34]. Cultures, such as those arising from ovarian malignancies, grown in Matrigel often maintain histological features, genetic profiles, and intra-tumoral heterogeneity, similar to the *in vivo* tumour [35]. Matrigel has also proven an effective model of early-stage angiogenesis in an array of cancers including HGSOC [17]. It must be noted that 3D cultures are often chosen to support the principles of the 3Rs (Replacement, Reduction and Refinement) towards more ethical use of animals [36], [37]. Interestingly, OvCa cell migration, cell communication, and chemotherapeutic response have all been successfully modelled using hydrogel, a plant-based alternative to animal-derivative scaffolds. Here cultures show greater similarity to *in vivo* mouse models and clinical data than that of 2D cultures [37].

Leveraging the data from the Gene Expression Omnibus (GEO) and the Sequence Read Achieve allowed us to create a detailed picture of the genomic landscape of ovarian cancer cell lines in 3D cultures using three distinct scaffolds: Matrigel, agarose and collagen. All OvCa cell lines showed a high level of differential regulation with an average of 551 DEGs per data set ranging from 234 DEGs as the minimum and 1429 DEGs as the maximum. The HGSOC cell line OVCAR8 used across multiple studies allowed us to identify key genes and biological process that are hallmarks of 3D culture as well as potential biomarkers of growth environment for the examined scaffolds. Specifically, our analyses highlight a set of 8 genes, namely DDIT4, ANGPTLA, SELENBP1, SULF1, GAL3ST1, TNFAIP3, LLNLR-263F3.1, MUC12 that show statistically significant differential expression patterns in 3D systems as compared to 2D irrespective of the scaffold used. Furthermore, 13 genes have shown an environment specific expression pattern. The top 16 DEGs between 3D and 2D OVCAR8 were also identified. Of note many of the genes identified are key regulators of inflammation and immune response such as C3, CXCL8

(IL-8), SLPI, CXCL1, CXCL2, ILI beta, IL6, CCL20, IFI27 and CFB [38]–[40]. Furthermore, many of the top genes also show structural importance within the ECM i.e. LAMC2, PI3, FN1, and MMP1. Dysregulation of the matrix metalloproteinase, MMP1, is associated with basement membrane degradation and subsequent peritoneal dissemination in OvCa and is correlated with poor patient prognosis [41]. The remaining DEGs, DDIT4 and ANGPTL4, were recently identified as candidate genes for prediction of survival out comes in lung cancer and OvCa patients [42], [43]. Elevated levels of these glycolysis related genes were also seen to negatively affect progression free survival in patients with OvCa [43].

The functional enrichment scores of OVCAR8 cells grown in Matrigel, agarose and collagen, compared with standard 2D mono-layer controls presented a unique expression profile with close relation seen between the 2D samples. However, the 3D collagen OVCAR8 cells expressed a higher degree in variability compared with the other 3D OVCAR8's which show comparatively similar profiles. Earlier studies have suggested that this model is more similar to the *in vivo* environment as it captures 3D growth alongside omental fibroblasts [44].

The top biological processes associated with the DEGs identified between the 2D and 3D include glycolysis, KRAS signalling, coagulation, TNF alpha signalling via NF-κB, complement and inflammatory response. These processes are frequently altered in cancer and are often difficult to model in 2D systems [45]. Glycolysis in particular is often augmented in cancer cells with increased utilisation of this pathway indicative of the Warburg effect [46]. Similar metabolic changes are also evident in 3D colorectal cancer cells when compared to 2D [47]. The inclusion of these processes in the data verifies numerous studies where 3D cells are shown to express more biological relevance to *in vivo* systems than 2D cell cultures, through the expression of pathways typically associated with *in vivo* environments [45], [47]–[51].

Furthermore, some cancer related hallmarks were also highlighted as differentially regulated in the 3D OvCa cells when compared with the 2D samples. Hallmarks of particular interest include apoptosis, oxidative phosphorylation, MYC pathways, ROS, EMT, KRAS signalling, angiogenesis and hypoxia. Numerous studies show that the 3D environment influences these key cancer pathways [45], [47]; here we show that regardless of scaffold the processes are still heavily influenced when grown in 3D. Apoptosis, EMT, KRAS signalling and hypoxia as well as angiogenesis were some of the key cancer associated processes enhanced in 3D growth. Additional processes included complement and inflammatory response pathways which are important factors of tumour immune evasion. Another pathway often seen in cancers was IL6-JAK-STAT3, which is a proliferative driver often implicit with OvCa angiogenesis and tumour metastasis [52].

Moreover, based on the expression profile of OVCAR8 cells grown in 3D vs. 2D, we identified a panel of genes specific to OVCAR8 when grown in different gel-based scaffolds using Omics Playground importance score ranking [27]. The expression profile of these genes was unique to the specific scaffold when compared with the 2D OVCAR8. Biomarkers specific to OvCa cells grown in agarose compared with 2D include: C3, MMP1, ILIB and CCL20. The three biomarkers identified for collagen include: IFI27, COL3A1 and IFI27. Matrigel however only showed one unique marker, DDIT4 a stress included regulator of mTOR previously mentioned for its association with progression free survival in OvCa [43]. Future work should explore the relevance of these markers and the influence they hold within the OvCa TME.

Next, we explored the impact of cell line on various scaffolds and showed that there is a close relationship between the two suggesting that in order to recover the tissue specific behaviour in a model 3D culture, a lot of care must be given to the choice of cell line and scaffold, in order to remove potential experimental biases. Furthermore, the condition specific gene expression patterns suggested that a number of genes can be used as environment biomarkers.

Finally, we explored the impact of transcriptional changes in real time by looking at phenotypic changes of cells grown in 3D vs 2D cultures. Our experiments have shown

that SKOV-3 cells grown in hydrogel are clustering to form simple spheroids, precursors of higher order organoid formations.

In summary this meta-analysis assessed the current landscape of 3D OvCa models within the literature and provided a complex expression profile of OvCa cells grown in 3D. Our transversal comparison of various scaffolds allowed us to highlight the variability that can be induced by various scaffolds in the transcriptional landscape as well as identifying key genes and biological processes that are hallmarks of cancer cells grown in 3D cultures. Moreover, the identification of transcriptional signatures that show genes' specificity in cell line, tumour subtype, and scaffold, and defined as growth environment biomarkers, will allow us to monitor in the future the suitability of 3D culture to recapitulate tissue complexity.

Supplementary Materials: The following supporting information is available: Figure S1: Top Enriched Gene sets for 2D vs. 3D OVCAR8; Table S1: Cell line information and associated accession codes. Table S2: Top 150 differentially expressed genes in OVCAR8 grown on agarose, collagen, Matrigel vs. 2D controls; multiple cell lines (A1847, A2780, C30, C70, OVCAR3, OVCAR4, OVCAR5, OVCAR8, OVCAR10, PEO1, SKOV-3, UPN275) grown on agarose vs. 2D controls; and Kuramochi, OVCAR4, and OVCAR8, grown on collagen vs. 2D controls.

Author Contributions: For research articles with several authors, a short paragraph specifying their individual contributions must be provided. The following statements should be used "Conceptualization, C.S and R.K.; methodology, C.S., R.K., S.P., EK and B.B.; software, C.S. and B.B.; validation, R.K., S.P. and C.S.; formal analysis, R.K., BB; investigation, R.K., E.K., C.S.; resources, C.S., I.K., H.R., J.H., and M.H.; data curation, R.K. and C.S.; writing—original draft preparation, R.K.; writing—review and editing, R.K., C.S., and E.K.; visualization, C.S.; supervision, E.K., I.K., M.H.; project administration, E.K., H.R., J.H., funding acquisition, I.K., H.R., M.H. All authors have read and agreed to the published version of the manuscript

Funding: This study was funded through the Cancer Treatment & Research Trust and University Hospitals Coventry and Warwickshire NHS Trust (grant no. 12899).

Data Availability Statement: RNAseq and Array data can be found via the following NCBI accession codes: PRJNA472611, PRJNA530150, PRJNA564843, PRJNA564843, PRJNA232817, and PRJNA318768. A full list of samples can be viewed in supplementary Table S1.

Acknowledgments: The authors acknowledge the Biocenter Finland (BF) and Tampere Imaging Facility (TIF) for the service.

Conflicts of Interest: The authors declare no conflict of interest.

References

[1] R. L. Siegel, K. D. Miller, and A. Jemal, "Cancer statistics, 2019," *CA Cancer J Clin*, vol. 69, no. 1, pp. 7–34, Jan. 2019, doi: 10.3322/CAAC.21551.

[2] U. A. Matulonis, A. K. Sood, L. Fallowfield, B. E. Howitt, J. Sehouli, and B. Y. Karlan, "Ovarian cancer," *Nat Rev Dis Primers*, vol. 2, pp. 1–22, Aug. 2016, doi: 10.1038/nrdp.2016.61.

[3] T. Kolenda *et al.*, "Tumor microenvironment - Unknown niche with powerful therapeutic potential," *Rep Pract Oncol Radiother*, vol. 23, no. 3, pp. 143–153, May 2018, doi: 10.1016/J.RPOR.2018.01.004.

[4] B. Jordan, "[The legacy of Henrietta Lacks]," *Med Sci (Paris)*, vol. 37, no. 12, pp. 1189–1193, Dec. 2021, doi: 10.1051/MEDSCI/2021181.

[5] M. Kapałczyńska *et al.*, "2D and 3D cell cultures – a comparison of different types of cancer cell cultures," *Archives of Medical Science*, vol. 14, no. 4, pp. 910–919, 2018, doi: 10.5114/aoms.2016.63743.

[6] K. Duval *et al.*, “Modeling physiological events in 2D vs. 3D cell culture,” *Physiology*, vol. 32, no. 4. American Physiological Society, pp. 266–277, Jun. 14, 2017. doi: 10.1152/physiol.00036.2016.

[7] A. Riedl *et al.*, “Comparison of cancer cells in 2D vs 3D culture reveals differences in AKT-mTOR-S6K signaling and drug responses,” *J Cell Sci*, vol. 130, no. 1, pp. 203–218, Jan. 2017, doi: 10.1242/JCS.188102/259005/AM/COMPARISON-OF-CANCER-CELLS-CULTURED-IN-2D-VS-3D.

[8] M. Cekanova and K. Rathore, “Animal models and therapeutic molecular targets of cancer: utility and limitations,” *Drug Des Devel Ther*, vol. 8, pp. 1911–1922, Oct. 2014, doi: 10.2147/DDDT.S49584.

[9] B. Zhang, A. Korolj, B. F. L. Lai, and M. Radisic, “Advances in organ-on-a-chip engineering,” *Nature Reviews Materials*, vol. 3, no. 8. Nature Publishing Group, pp. 257–278, Aug. 01, 2018. doi: 10.1038/s41578-018-0034-7.

[10] A. C. Luca *et al.*, “Impact of the 3D microenvironment on phenotype, gene expression, and EGFR inhibition of colorectal cancer cell lines,” *PLoS One*, vol. 8, no. 3, Mar. 2013, doi: 10.1371/JOURNAL.PONE.0059689.

[11] V. van Duinen, S. J. Trietsch, J. Joore, P. Vulto, and T. Hankemeier, “Microfluidic 3D cell culture: From tools to tissue models,” *Current Opinion in Biotechnology*, vol. 35. Elsevier Ltd, pp. 118–126, Dec. 01, 2015. doi: 10.1016/j.copbio.2015.05.002.

[12] R. Edmondson, J. J. Broglie, A. F. Adcock, and L. Yang, “Three-dimensional cell culture systems and their applications in drug discovery and cell-based biosensors,” *Assay and Drug Development Technologies*, vol. 12, no. 4. Mary Ann Liebert Inc., pp. 207–218, May 01, 2014. doi: 10.1089/adt.2014.573.

[13] H. A. Kenny, T. Krausz, S. D. Yamada, and E. Lengyel, “Use of a novel 3D culture model to elucidate the role of mesothelial cells, fibroblasts and extra-cellular matrices on adhesion and invasion of ovarian cancer cells to the omentum,” *Int J Cancer*, vol. 121, no. 7, pp. 1463–1472, Oct. 2007, doi: 10.1002/ijc.22874.

[14] L. A. Osório, E. Silva, and R. E. Mackay, “A Review of Biomaterials and Scaffold Fabrication for Organ-on-a-Chip (OOAC) Systems,” *Bioengineering (Basel)*, vol. 8, no. 8, Aug. 2021, doi: 10.3390/BIOENGINEERING8080113.

[15] S. Kawai *et al.*, “Three-dimensional culture models mimic colon cancer heterogeneity induced by different microenvironments,” *Sci Rep*, vol. 10, no. 1, p. 3156, Feb. 2020, doi: 10.1038/S41598-020-60145-9.

[16] Y. M. Salinas-Vera *et al.*, “A Three-Dimensional Culture-Based Assay to Detect Early Stages of Vasculogenic Mimicry in Ovarian Cancer Cells,” *Methods Mol Biol*, vol. 2514, pp. 53–60, 2022, doi: 10.1007/978-1-0716-2403-6_6.

[17] M. R. Ward Rashidi *et al.*, “Engineered 3D Model of Cancer Stem Cell Enrichment and Chemoresistance,” *Neoplasia*, vol. 21, no. 8, pp. 822–836, Aug. 2019, doi: 10.1016/J.NEO.2019.06.005.

[18] M. Zietarska *et al.*, “Molecular description of a 3D in vitro model for the study of epithelial ovarian cancer (EOC),” *Mol Carcinog*, vol. 46, no. 10, pp. 872–885, Oct. 2007, doi: 10.1002/mc.20315.

[19] A. Lin *et al.*, “3D cell culture models and organ-on-a-chip: Meet separation science and mass spectrometry,” *Electrophoresis*, vol. 41, no. 1–2. Wiley-VCH Verlag, pp. 56–64, Jan. 01, 2020. doi: 10.1002/elps.201900170.

[20] S. L'Espérance, M. Bachvarova, B. Tetu, A. M. Mes-Masson, and D. Bachvarov, "Global gene expression analysis of early response to chemotherapy treatment in ovarian cancer spheroids," *BMC Genomics*, vol. 9, no. 1, pp. 1–21, Feb. 2008, doi: 10.1186/1471-2164-9-99.

[21] T. R. Tidwell, G. v. Røsland, K. J. Tronstad, K. Søreide, and H. R. Hagland, "Metabolic flux analysis of 3D spheroids reveals significant differences in glucose metabolism from matched 2D cultures of colorectal cancer and pancreatic ductal adenocarcinoma cell lines," *Cancer Metab*, vol. 10, no. 1, Dec. 2022, doi: 10.1186/S40170-022-00285-W.

[22] R. Ikari *et al.*, "Differences in the Central Energy Metabolism of Cancer Cells between Conventional 2D and Novel 3D Culture Systems," *Int J Mol Sci*, vol. 22, no. 4, pp. 1–13, Feb. 2021, doi: 10.3390/IJMS22041805.

[23] K. J. Ornell, K. S. Mistretta, E. Newman, C. Q. Ralston, and J. M. Coburn, "Three-Dimensional, Scaffolded Tumor Model to Study Cell-Driven Microenvironment Effects and Therapeutic Responses," *ACS Biomater Sci Eng*, vol. 5, no. 12, pp. 6742–6754, Dec. 2019, doi: 10.1021/ACSBIOMATERIALS.9B01267.

[24] C. Jensen and Y. Teng, "Is It Time to Start Transitioning From 2D to 3D Cell Culture?," *Front Mol Biosci*, vol. 7, Mar. 2020, doi: 10.3389/FMOLB.2020.00033.

[25] R. Kerslake *et al.*, "Differential Regulation of Genes by the Glucogenic Hormone Asprosin in Ovarian Cancer," *J Clin Med*, vol. 11, no. 19, Oct. 2022, doi: 10.3390/JCM11195942.

[26] M. Akhmedov, A. Martinelli, R. Geiger, and I. Kwee, "Omics Playground: a comprehensive self-service platform for visualization, analytics and exploration of Big Omics Data," *NAR Genom Bioinform*, vol. 2, no. 1, Mar. 2020, doi: 10.1093/NARGAB/LQZ019.

[27] A. Kletzmayr, F. Clement Frey, M. Zimmermann, D. Eberli, and C. Millan, "An Automatable Hydrogel Culture Platform for Evaluating Efficacy of Antibody-Based Therapeutics in Overcoming Chemoresistance," *Biotechnol J*, vol. 15, no. 5, May 2020, doi: 10.1002/BIOT.201900439.

[28] F. Shen, S. Chen, Y. Gao, X. Dai, and Q. Chen, "The prevalence of malignant and borderline ovarian cancer in pre- and post-menopausal Chinese women," *Oncotarget*, vol. 8, no. 46, pp. 80589–80594, 2017, doi: 10.18632/ONCOTARGET.20384.

[29] R. Vang, I. M. Shih, and R. J. Kurman, "OVARIAN LOW-GRADE AND HIGH-GRADE SEROUS CARCINOMA: Pathogenesis, Clinicopathologic and Molecular Biologic Features, and Diagnostic Problems," *Adv Anat Pathol*, vol. 16, no. 5, p. 267, Sep. 2009, doi: 10.1097/PAP.0B013E3181B4FFFA.

[30] S. C. Lesher-Pérez *et al.*, "Dispersible oxygen microsensors map oxygen gradients in three-dimensional cell cultures," *Biomater Sci*, vol. 5, no. 10, pp. 2106–2113, Oct. 2017, doi: 10.1039/C7BM00119C.

[31] E. Bahar, J. Y. Kim, D. C. Kim, H. S. Kim, and H. Yoon, "Combination of Niraparib, Cisplatin and Twist Knockdown in Cisplatin-Resistant Ovarian Cancer Cells Potentially Enhances Synthetic Lethality through ER-Stress Mediated Mitochondrial Apoptosis Pathway," *Int J Mol Sci*, vol. 22, no. 8, Apr. 2021, doi: 10.3390/IJMS22083916.

[32] Z. Javed *et al.*, "Optimization of Extracellular Flux Assay to Measure Respiration of Anchorage-independent Tumor Cell Spheroids," *Bio Protoc*, vol. 12, no. 4, Feb. 2022, doi: 10.21769/BIOPROTOC.4321.

[33] B. Patra *et al.*, “Carboplatin sensitivity in epithelial ovarian cancer cell lines: The impact of model systems,” *PLoS One*, vol. 15, no. 12, Dec. 2020, doi: 10.1371/JOURNAL.PONE.0244549.

[34] Y. Maru, N. Tanaka, M. Itami, and Y. Hippo, “Efficient use of patient-derived organoids as a preclinical model for gynecologic tumors,” *Gynecol Oncol*, vol. 154, no. 1, pp. 189–198, Jul. 2019, doi: 10.1016/J.YGYNO.2019.05.005.

[35] M. T. Kozlowski, C. J. Crook, and H. T. Ku, “Towards organoid culture without Matrigel,” *Commun Biol*, vol. 4, no. 1, Dec. 2021, doi: 10.1038/S42003-021-02910-8.

[36] P. McGonigle and B. Ruggeri, “Animal models of human disease: challenges in enabling translation,” *Biochem Pharmacol*, vol. 87, no. 1, pp. 162–171, Jan. 2014, doi: 10.1016/J.BCP.2013.08.006.

[37] S. Lagies *et al.*, “Cells grown in three-dimensional spheroids mirror in vivo metabolic response of epithelial cells,” *Communications Biology 2020 3:1*, vol. 3, no. 1, pp. 1–10, May 2020, doi: 10.1038/s42003-020-0973-6.

[38] B. M. Tang *et al.*, “A novel immune biomarker IFI27 discriminates between influenza and bacteria in patients with suspected respiratory infection,” *European Respiratory Journal*, vol. 49, no. 6, p. 20, Jun. 2017, doi: 10.1183/13993003.02098-2016.

[39] K. Taniguchi and M. Karin, “IL-6 and related cytokines as the critical lynchpins between inflammation and cancer,” *Semin Immunol*, vol. 26, no. 1, pp. 54–74, 2014, doi: 10.1016/J.SMIM.2014.01.001.

[40] C. A. Feghali and T. M. Wright, “Cytokines in acute and chronic inflammation,” *Front Biosci*, vol. 2, 1997, doi: 10.2741/A171.

[41] A. Yokoi *et al.*, “Malignant extracellular vesicles carrying MMP1 mRNA facilitate peritoneal dissemination in ovarian cancer,” *Nature Communications 2017 8:1*, vol. 8, no. 1, pp. 1–15, Mar. 2017, doi: 10.1038/ncomms14470.

[42] C. Liu, Y. Li, M. Wei, L. Zhao, Y. Yu, and G. Li, “Identification of a novel glycolysis-related gene signature that can predict the survival of patients with lung adenocarcinoma,” *Cell Cycle*, vol. 18, no. 5, pp. 568–579, Mar. 2019, doi: 10.1080/15384101.2019.1578146.

[43] D. Zhang *et al.*, “Identification of a glycolysis-related gene signature for survival prediction of ovarian cancer patients,” *Cancer Med*, vol. 10, no. 22, p. 8222, Nov. 2021, doi: 10.1002/CAM4.4317.

[44] S. Mitra *et al.*, “Transcriptome Profiling Reveals Matrisome Alteration as a Key Feature of Ovarian Cancer Progression,” *Cancers (Basel)*, vol. 11, no. 10, Oct. 2019, doi: 10.3390/CANCERS11101513.

[45] R. Ikari *et al.*, “Differences in the Central Energy Metabolism of Cancer Cells between Conventional 2D and Novel 3D Culture Systems,” *Int J Mol Sci*, vol. 22, no. 4, pp. 1–13, Feb. 2021, doi: 10.3390/IJMS22041805.

[46] J. Xie *et al.*, “Beyond Warburg effect - Dual metabolic nature of cancer cells,” *Sci Rep*, vol. 4, May 2014, doi: 10.1038/srep04927.

[47] T. R. Tidwell, G. v. Røsland, K. J. Tronstad, K. Søreide, and H. R. Hagland, “Metabolic flux analysis of 3D spheroids reveals significant differences in glucose metabolism from matched 2D cultures of colorectal

cancer and pancreatic ductal adenocarcinoma cell lines," *Cancer & Metabolism 2022 10:1*, vol. 10, no. 1, pp. 1–16, May 2022, doi: 10.1186/S40170-022-00285-W.

[48] Y. D. Vasilets, K. v. Dergilev, Z. I. Tsokolaeva, and E. v. Parfenova, "Culturing of Cardiac Cells in 3D Spheroids Modulates Their Expression Profile and Increases Secretion of Proangiogenic Growth Factors," *Bull Exp Biol Med*, vol. 173, no. 2, pp. 235–239, Jun. 2022, doi: 10.1007/S10517-022-05525-Z.

[49] A. B. di Stefano *et al.*, "Cell quality evaluation with gene expression analysis of spheroids (3D) and adherent (2D) adipose stem cells," *Gene*, vol. 768, Feb. 2021, doi: 10.1016/J.GENE.2020.145269.

[50] A. Spitz *et al.*, "Global gene expression profile of periodontal ligament cells submitted to mechanical loading: A systematic review," *Arch Oral Biol*, vol. 118, Oct. 2020, doi: 10.1016/J.ARCHORAL-BIO.2020.104884.

[51] K. Duval *et al.*, "Modeling Physiological Events in 2D vs. 3D Cell Culture," *Physiology (Bethesda)*, vol. 32, no. 4, pp. 266–277, Jun. 2017, doi: 10.1152/PHYSIOL.00036.2016.

[52] R. Liang *et al.*, "STAT3 signaling in ovarian cancer: a potential therapeutic target," *J Cancer*, vol. 11, no. 4, p. 837, 2020, doi: 10.7150/JCA.35011.

A Meta-analysis of 2D vs. 3D Ovarian Cancer Cellular Models

Rachel Kerslake[1], Birhanu Belay[2], Suzana Panfilov[1], Marcia Hall[1,3], Ioannis Kyrou[4,5,6,7,8], Harpal S. Randeva[4,5], Jari Hyttinen[2], Emmanouil Karteris[1*†] and Cristina Sisu[1*†]

Supplementary Materials

Table S1. Cell line information and associated accession codes.

Accession Number	SRA code	Cell line	Subtype	Condition	Scaffold
PRJNA472611	SRR7204219	A1847	Carcinoma	3D	Agarose
	SRR7204220	A1847	Carcinoma	2D	/
	SRR7204221	A2780	HGSOC	3D	Agarose
	SRR7204222	A2780	HGSOC	2D	/
	SRR7204223	OVCAR3	HGSOC	3D	Agarose
	SRR7204224	OVCAR3	HGSOC	2D	/
	SRR7204225	OVCAR4	HGSOC	3D	Agarose
	SRR7204226	OVCAR4	HGSOC	2D	/
	SRR7204227	OVCAR5	HGSOC	3D	Agarose
	SRR7204228	OVCAR5	HGSOC	2D	/
	SRR7204231	OVCAR10	HGSOC	3D	Agarose
	SRR7204232	OVCAR10	HGSOC	2D	/
	SRR7204233	OVCAR8	HGSOC	3D	Agarose
	SRR7204234	OVCAR8	HGSOC	2D	/
	SRR7204235	SKOV-3	HGSOC	3D	Agarose
	SRR7204236	SKOV-3	HGSOC	2D	/
	SRR7204237	PEO1	HGSOC	3D	Agarose
	SRR7204238	PEO1	HGSOC	2D	/
	SRR7204229	C30	Carcinoma	3D	Agarose
	SRR7204230	C30	Carcinoma	2D	/
	SRR7204242	C70	Carcinoma	3D	Agarose
	SRR7204241	C70	Carcinoma	2D	/
	SRR7204240	UPN275	MAC	3D	Agarose
	SRR7204239	UPN275	MAC	2D	/
PRJNA530150	SRR8823257	OVCAR8	HGSOC	2D	/
	SRR8823258	OVCAR8	HGSOC	2D	/
	SRR8823259	OVCAR8	HGSOC	2D	/
	SRR8823260	OVCAR8	HGSOC	2D	/
	SRR8823265	OVCAR8	HGSOC	3D	Matrigel

	SRR8823266	OVCAR8	HGSOC	3D	Matrigel
	SRR8823267	OVCAR8	HGSOC	3D	Matrigel
	SRR8823268	OVCAR8	HGSOC	3D	Matrigel
	SRR8823273	OVCAR8	HGSOC	2D	/
	SRR8823273	OVCAR8	HGSOC	2D	/
	SRR8823273	OVCAR8	HGSOC	2D	/
	SRR8823273	OVCAR8	HGSOC	2D	/
	SRR8823280	OVCAR8	HGSOC	3D	Matrigel
	SRR8823281	OVCAR8	HGSOC	3D	Matrigel
	SRR8823282	OVCAR8	HGSOC	3D	Matrigel
	SRR8823283	OVCAR8	HGSOC	3D	Matrigel
PRJNA564843	SRR10096845	OVCAR8	HGSOC	2D	/
	SRR10096844	OVCAR8	HGSOC	2D	/
	SRR10096843	OVCAR8	HGSOC	2D	/
	SRR10096841	OVCAR8	HGSOC	3D	Collagen
	SRR10096842	OVCAR8	HGSOC	3D	Collagen
	SRR10096840	OVCAR8	HGSOC	3D	Collagen
	SRR10096839	OVCAR4	HGSOC	2D	/
	SRR10096838	OVCAR4	HGSOC	2D	/
	SRR10096837	OVCAR4	HGSOC	2D	/
	SRR10096836	OVCAR4	HGSOC	3D	Collagen
	SRR10096835	OVCAR4	HGSOC	3D	Collagen
	SRR10096834	OVCAR4	HGSOC	3D	Collagen
	SRR10096828	Kuramochi	HGSOC	3D	Collagen
	SRR10096829	Kuramochi	HGSOC	3D	Collagen
	SRR10096830	Kuramochi	HGSOC	3D	Collagen
	SRR10096831	Kuramochi	HGSOC	2D	/
	SRR10096832	Kuramochi	HGSOC	2D	/
	SRR10096833	Kuramochi	HGSOC	2D	/
PRJNA232817	GSM1300206	IGROV-1	EAC	2D	/
	GSM1300207	IGROV-1	EAC	2D	/
	GSM1300208	IGROV-1	EAC	2D	/
	GSM1300209	IGROV-1	EAC	3D	Low Attachment
	GSM1300210	IGROV-1	EAC	3D	Low Attachment
	GSM1300211	IGROV-1	EAC	3D	Low Attachment
PRJNA318768	GSM2125384	HEY	HGSOC	2D	/
	GSM2125385	HEY	HGSOC	2D	/
	GSM2125386	HEY	HGSOC	2D	/
	GSM2125387	HEY	HGSOC	2D	/

	GSM2125388	HEY	HGSOC	3D	Hanging drop
	GSM2125389	HEY	HGSOC	3D	Hanging drop
	GSM2125390	HEY	HGSOC	3D	Hanging drop
	GSM2125391	HEY	HGSOC	3D	Hanging drop

Table S2: Top 150 differentially expressed genes in **OVCAR8** grown on agarose, collagen, Matrigel vs. 2D controls; multiple cell lines (A1847, A2780, C30, C70, OVCAR3, OVCAR4, OVCAR5, OVCAR8, OVCAR10, PEO1, SKOV-3, UPN275) grown on **agarose** vs. 2D controls; and Kuramochi, OVCAR4, and OVCAR8, grown on **collagen** vs. 2D controls.

OVCAR8	OVCAR8	OVCAR8	Agarose	Agarose	Agarose	Collagen	Collagen	Collagen
ACTB	EVL	PAX8	ADAMTS1	FOXD1	NUPR1	A2M	GNGT2	OXTR
ADAMTS1	FAM83A	PDCD10	ADAMTS6	GALNT3	PAX8	ABI3	GOLIM4	PDCD10
ADAMTS6	FBN2	PDE1C	ADGRG6	GBP1	PDCD10	ADGRG1	ID4	PKP3
AEBP1	FGFBP1	PDPN	AKT3	GBP2	PLAT	AFAP1L2	IFI27	PLPP2
AJAP1	FN1	PHYHD1	ANPEP	GDF15	PLIN2	AKT3	IFI44	PRSS22
ALDOC	GFRA1	PI3	ATP2B2	GJB2	PLTP	APOE	IFI44L	PTGS1
ANGPTL4	GGT1	PLIN2	AXL	GLDC	PPP1R14A	ARID4A	IFI6	RAB25
ANPEP	GREM1	PLTP	BEX1	GLUL	PRAME	BAALC	IFITM1	RAPGEF3
ANXA8L1	GSTM3	PPP1R14A	BMP7	GPNMB	PROM1	BHLHE41	IGF2	REC8
ARMCX2	HBQ1	PRAME	BST2	GSTM3	PRSS22	BMP7	IGFBP2	RHOD
B4GALNT4	HCLS1	PTGDS	C3	HGD	PTGS1	BOC	IGFBP5	RNF212
BCAT1	HLA-DRB1	PTK7	CALB2	IDO1	RAB25	C3	IGFBP7	S100A1
BCL2A1	HSPB2	PTPRS	CBLC	IGFBP2	S100A14	CBLC	IGFL1	S100A14
BEX1	IFI27	RFTN1	CCL2	IGFBP3	S100A9	CCDC146	IL18	S100A4
BEX4	IFI44	RPL7	CCL20	IGFBP5	SCGB2A1	CCL2	IL1R2	S100A9
BGN	IFI44L	RSPO4	CD70	IGFBP7	SCOC	CDA	IL7R	SC5D
BHLHE40	IFI6	SAA1	CD74	IL1B	SDC2	CDH1	ITGB3	SCGB2A1
BNIP3	IFITM1	SCOC	CDH1	IL1R1	SGIP1	CDH6	ITGB6	SELENBP1
BST2	IGFBP2	SDC2	CDH6	IL1R2	SLC17A9	CFI	KCNC3	SFN
C3	IGFBP3	SEMA3C	CDKN2A	IL6	SLC34A2	CLDN16	KISS1	SFTA2
C3orf14	IGFN1	SERPINB2	CHI3L1	IL7R	SLC38A5	CLDN4	KLK8	SLC17A9
CALB1	IL1A	SLC38A5	CLDN11	ITGB6	SLC39A4	CLDN7	KRT19	SLC34A2
CALB2	IL1B	SLC39A4	CLDN4	KCNC3	SLPI	CNTN1	KRT7	SLC38A5
CCL2	IL6	SLC6A15	COL18A1	KISS1	SNRPN	COL1A2	KRTCAP3	SLPI
CCL20	LAMC2	SLFN11	COL23A1	KLK10	SOX17	COL26A1	LAD1	SMIM22
CD70	LAPTM5	SLPI	COL26A1	KLK8	SPANXB1	COL3A1	LAMA3	SOX17
CDH13	LAYN	SNCA	CP	KRT19	SPARC	CP	LCN2	SPARC
CDH2	LDHB	SNRPN	CRB3	KRT23	SPINT2	CRB3	LEMD1	SPON1
CDKN2A	MAP1B	SPAG4	CXCL1	KRTCAP3	SPON1	CTCFL	LGALS13	SPP1
CFB	MFSD2B	SPANXB1	CXCL2	LAD1	SPP1	CYGB	LGR5	ST14
CLGN	MGMT	SPINT2	CXCL8	LAMA3	ST14	DAPL1	LGR6	ST6GALNAC1
CLMP	MMP1	SRGN	CYGB	LAMC2	ST6GALNAC1	DCDC2	LIPG	STRA6
COL3A1	MSLN	ST20-MTHFS	CYP1A1	LCN2	TACSTD2	DKK 1.00	LRRN2	SULF1
COL7A1	MT1M	STMN3	DKK 1.00	LCP1	TAGLN	DPEP3	LY6K	SYNE4
CRIP1	MTAP	SUN3	ECM1	LDHB	TFPI2	EDN2	LYPD1	TACSTD2
CTCFL	MX1	TENM2	EDN2	LGALS13	TGFBI	ELF3	MAL2	TFPI2
CTSF	MYEF2	TFPI2	EHD2	LGR5	TMC4	EMX2	MECOM	TGFBI

CXCL1	NACA2	TGFBI	ELF3	LY6K	TMPRSS4	EPB41L3	MLPH	THY1
CXCL2	NDN	THBS1	EMX2	MACROD2	TNFRSF6B	EPCAM	MMP7	TMC4
CXCL5	NDRG1	TRIM58	EPS8L1	MAL2	TRIML2	EPS8L1	MPZL2	TNC
CXCL8	NEFH	TSPAN1	ERP27	MECOM	TSPAN1	ESRP1	MUC16	TNFRSF6B
DDIT4	NETO2	TSPYL5	ESRP1	MMP1	TSTD1	FABP3	MX1	TRIM58
DKK 1.00	NEURL1	TUSC3	EYA2	MMP7	TUSC3	FBXO2	MX2	TSPYL5
DUSP23	NMRAL1	TYMP	FABP6	MPZL2	UBB	FKBP10	MYH7B	TSTD1
DZIP1	NNMT	UBB	FAM83A	MUC16	UCHL1	FLNC	NDN	TUSC3
EDARADD	NPPB	UCHL1	FAT2	NCAM1	UQCRH	FN1	NEFH	UBB
EFEMP2	NPW	UCP2	FKBP10	NETO2	UQCRHL	FOXD1	NKAIN4	UQCRH
EGR1	NRG1	ZNF699	FLNC	NPPB	VTCN1	FXYD6	NPTX2	UQCRHL
ELOVL2	OAS3	ZNF83	FN1	NPTX2	WFDC2	GDF15	NRCAM	WFDC2
ESM1	P3H2	ZSCAN18	FOSL1	NRCAM	WNT7A	GLUL	NXPH2	WNT7A

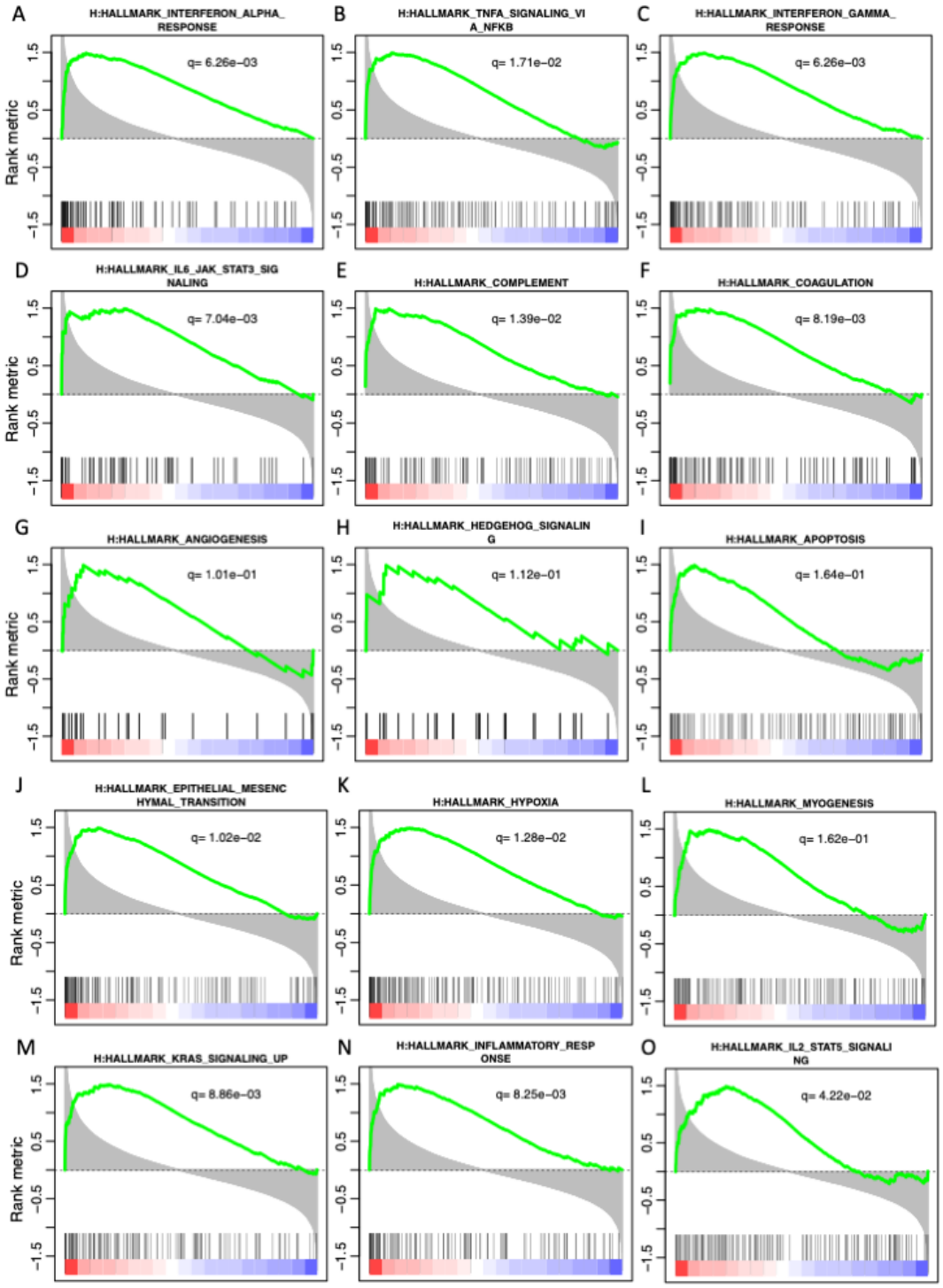

Figure S1. Top Enriched Gene sets for 2D vs. 3D OVCAR8. Combined panel of enrichment curves showing processes associated with cancer hallmarks. **(A)**, Interferon Alpha Response; **(B)**, TNF-a signalling; **(C)**, Interferon Gamma Response; **(D),** IL-6-JAK-STAT3 signalling; **(E)**, Complement; **(F)**, Coagulation; **(G)**, Angiogenesis; **(H)**, Hedgehog signalling; **(I)**, Apoptosis; **(J),** Epithelial Mesenchymal Transition; **(K)**, Hypoxia; **(L)**, Myogenesis; **(M)**, KRAS signalling; **(N)**, Inflammatory Response; **(O)**, IL-2 STAT3 signalling and. Black

vertical bars represent gene rank using shorted list metric. Green curve corresponds to “running statistics” of the enrichment score (ES).

Chapter 6

Co-expression of peripheral olfactory receptors with SARS-CoV-2 infection mediators: Potential implications beyond loss of smell as a COVID-19 symptom

Statement of Contribution

For the completion of the presented manuscript I contributed towards the following:

- Conceptualization
- Data curation
- Methodology
- Formal analysis
- Writing—original draft
- Writing—review and editing
- Referencing

Co-expression of peripheral olfactory receptors with SARS-CoV-2 infection mediators: Potential implications beyond loss of smell as a COVID-19 symptom

RACHEL KERSLAKE[1], MARCIA HALL[1,2], HARPAL S. RANDEVA[3-5], DEMETRIOS A. SPANDIDOS[6], KAMALJIT CHATHA[5,7], IOANNIS KYROU[3-5*] and EMMANOUIL KARTERIS[1*]

[1]Biosciences, College of Health and Life Sciences, Brunel University London, Uxbridge UB8 3PH; [2]Mount Vernon Cancer Centre, Northwood HA6 2RN; [3]Warwickshire Institute for the Study of Diabetes, Endocrinology and Metabolism (WISDEM), University Hospitals Coventry and Warwickshire NHS Trust, Coventry CV2 2DX; [4]Aston Medical Research Institute, Aston Medical School, Aston University, Birmingham B4 7ET; [5]Warwick Medical School, University of Warwick, Coventry CV4 7AL, UK; [6]Laboratory of Clinical Virology, Medical School, University of Crete, 71409 Heraklion, Greece; [7]Department of Biochemistry and Immunology, University Hospitals Coventry and Warwickshire NHS Trust, Coventry CV2 2DX, UK

Received May 29, 2020; Accepted June 17, 2020

DOI: 10.3892/ijmm.2020.4646

Abstract. Severe acute respiratory syndrome (SARS) coronavirus-2 (SARS-CoV-2) enters into human host cells via mechanisms facilitated mostly by angiotensin-converting enzyme 2 (ACE2) and transmembrane protease serine 2 (TMPRSS2). New loss of smell (anosmia/hyposmia) is now recognized as a COVID-19 related symptom, which may be caused by SARS-CoV-2 infection and damage of the olfactory receptor (OR) cells in the nasal neuro-epithelium and/or central involvement of the olfactory bulb. ORs are also expressed peripherally (e.g., in tissues of the gastrointestinal and respiratory systems) and it is possible that their local functions could also be impaired by SARS-CoV-2 infection of these tissues. Using Gene Expression Profiling Interactive Analysis, The Cancer Genome Atlas, Genotype-Tissue Expression, cBioPortal and Shiny Methylation Analysis Resource Tool, we highlight the expression of peripheral ORs in both healthy and malignant tissues, and describe their co-expression with key mediators of SARS-CoV-2 infection, such as ACE2 and TMPRSS2, as well as cathepsin L (CTSL; another cellular protease mediating SARS-CoV-2 infection of host cells). A wide expression profile of peripheral ORs was noted, particularly in tissues such as the prostate, testis, thyroid, brain, liver, kidney and bladder, as well as tissues with known involvement in cardio-metabolic disease (e.g., the adipose tissue, pancreas and heart). Among these, OR51E2, in particular, was significantly upregulated in prostate adenocarcinoma (PRAD) and co-expressed primarily with TMPRSS2. Functional networks of this OR were further analysed using the GeneMANIA interactive tool, showing that OR51E2 interacts with a plethora of genes related to the prostate. Further *in vitro* and clinical studies are clearly required to elucidate the role of ORs, both at the olfactory level and the periphery, in the context of COVID-19.

Correspondence to: Dr Emmanouil Karteris, Biosciences, College of Health and Life Sciences, Brunel University London, Kingston Lane, Uxbridge UB8 3PH, UK
E-mail: emmanouil.karteris@brunel.ac.uk

*Contributed equally

Key words: olfactory receptors, pan-cancer, DNA methylation, COVID-19, angiotensin-converting enzyme 2, transmembrane protease serine 2, cathepsin L, prostate cancer, anosmia, SARS-CoV-2

Introduction

The ongoing COVID-19 pandemic caused by the severe acute respiratory syndrome (SARS) coronavirus-2 (SARS-CoV-2) infection has affected over 6.5 million people thus far, resulting in the death of over four hundred thousand individuals worldwide (1). Recently, new loss of the sense of smell, either total (anosmia) or partial (hyposmia), has been recognised as a symptom of COVID-19 by the World Health Organisation (WHO) and the US Centres for Disease Control and Prevention (CDC) (www.cdc.gov/coronavirus/2019-ncov/symptoms-testing/symptoms.html).

Accordingly, additional research focus has now been placed on exploring anosmia and the involvement of olfactory receptors (ORs) in COVID-19 (2). Although poorly defined, more than 400 functional ORs are expressed in the human body, with corresponding ligands which remain mostly unclassified (3). Thought to be located primarily in

the olfactory epithelium of the nasal cavity, these G-Protein Coupled Receptors (GPCRs) are also known to be expressed in peripheral tissues (4). As such, in humans, ORs are involved in additional processes/pathways other than those for smell perception, which have been identified to mediate physiological functions in the cardiovascular, gastrointestinal and respiratory system (5,6). For example, ORs appear to be involved in widespread chemosensory systems, with OR51E2 expressed in the airway smooth muscle acting on processes which lead to increased airway smooth muscle mass that is a hallmark of asthma (4). Of note, the severity of COVID-19 shows a positive association with certain comorbidities which affect these tissues/systems, including asthma, obesity, diabetes and cancer (7).

Fusion of the SARS-CoV-2 spike proteins with the host transmembrane receptor angiotensin-converting enzyme 2 (ACE2) is shown to instigate spike protein cleavage through interaction with cellular proteases, such as transmembrane protease serine 2 (TMPRSS2), consequently allowing viral entry into the host cell (8,9). Additional intracellular proteases, such as cathepsin L (CTSL), might also mediate host cell infection by SARS-CoV-2 (8,9). Upon entry, the virus is then able to cause cellular damage and instigate a response which may result in a spectrum of clinical sequelae, ranging from anosmia to pneumonia, respiratory failure, cardiovascular distress and death (10).

Given the negligible expression of ACE2 and TMPRSS2 in olfactory neuronal cells and substantial expression in the olfactory epithelium, it has been postulated that sustentacular cells (supporting cells) are also involved in local viral entry and anosmia (11). Additional evidence including the expression of ACE2 and TMPRSS2 by the olfactory mucosa supports the notion that SARS-CoV-2 is capable of infecting non-neuronal cell types and, thus, subsequently disrupt odour perception (12).

The present study aimed to identify, both in normal and cancer tissues, the co-expression profile of a number of ORs which are known to be expressed in peripheral tissues in relationship to key mediators of the SARS-CoV-2 infection, namely ACE2, TMPRSS2 and CTSL. As such, concentrating on non-neuronal (peripheral) expression of ORs, here we provide a comprehensive analysis of the expression profile of ORs in peripheral tissues, several of which co-express ACE2, TMPRSS2 and CTSL and are correspondingly associated with comorbidities predisposing to severe COVID-19 (Fig. 1).

Data collection methods

Bioinformatic analysis. Expression analysis of ACE2, CTSL, TMPRSS2, OR51E2, OR10Q1, OR2A1, OR2W3, OR1J4, OR2A7, OR1Q1, OR6A2, OR1J1 and OR4M1 were validated through the Genotype-Tissue Expression (GTEx), The Cancer Genome Atlas (TCGA) and GEPIA (http://gepia.cancer). Information regarding TCGA cohort pan-cancer data and methylation data acquired through cBioPortal (http://www.cbioportal.org/) and Shiny Methylation Analysis Resource Tool (SMART) (http://www.bioinfo-zs.com/smartapp). Network localisation data were acquired through GeneMANIA software (http://genemania.org). Data sets accessed for pan-cancer analysis: ACC, adrenocortical carcinoma; BLCA, bladder urothelial carcinoma; BRCA, breast invasive carcinoma; CESC, cervical squamous cell carcinoma and endocervical adenocarcinoma; CHOL, cholangiocarcinoma; COAD, colon adenocarcinoma; DLBC, lymphoid neoplasm diffuse large B cell lymphoma; ESCA, oesophageal carcinoma; GBM, glioblastoma multiforme; HNSC, head and neck squamous cell carcinoma; KICH, kidney chromophobe; KIRC, kidney renal clear cell carcinoma; KIRP, kidney renal papillary cell carcinoma; LAML, acute myeloid leukaemia; LGG, brain lower grade glioma; LIHC, liver hepatocellular carcinoma; LUAD, lung adenocarcinoma; LUSC, lung squamous cell carcinoma; MESO, mesothelioma; OV, ovarian serous cystadenocarcinoma; PAAD, pancreatic adenocarcinoma; PCPG, pheochromocytoma and paraganglioma; PRAD, prostate adenocarcinoma; READ, rectum adenocarcinoma; SARC, sarcoma; SKCM, skin cutaneous melanoma; STAD, stomach adenocarcinoma; TGCT, testicular germ cell tumours; THCA, thyroid carcinoma; THYM, thymoma; UCEC, uterine corpus endometrial carcinoma; UCS, uterine carcinosarcoma and UVM, uveal melanoma.

Results

Using GTEx Multi Gene Query expression, data was obtained for the assessment of ten ORs in normal tissues (Fig. 2). These data show that: OR51E2 is primarily expressed in the prostate, arteries and colon; OR10Q1 is expressed in adipose tissue, breast, salivary gland, pancreas and testis; OR2A1 exhibited a much wider distribution in adipose tissue, arteries, breast, fibroblasts, cervix, lung, tibial nerve, ovary, skin, thyroid, uterus and vagina; OR2W3 is primarily expressed in tibial nerve, brain, thyroid and whole blood; OR1J4 is primarily expressed in the bladder, fibroblasts, cervix, lung, salivary gland, and testis; OR2A7 is highly expressed in the bladder, breast, colon, oesophagus, skin, small intestine, thyroid, lung and vagina; OR1Q1 is primarily expressed in the bladder and fibroblasts; OR6A2 exhibited high expression in the bladder, testis, thyroid, uterus and vagina; OR1J1 is primarily expressed in the bladder, fibroblasts, and testis. Information regarding the expression of OR4M1 in healthy tissues is limited (expression in testis only) with mapping and classification being an ongoing process.

Fig. 3 presents the GTEx gene expression data regarding the co-expression of ORs with ACE2, TMPRSS2 and CTSL in multiple normal tissues, including the lungs, oesophagus, salivary gland, colon, testis, thyroid and kidney, as well as tissues with established involvement in cardio-metabolic syndrome (e.g., the heart, pancreas and adipose tissue). These data corroborate recent findings showing relatively high expression of ACE2 and CTSL in the majority of tissues assessed, with varying levels of TMPRSS2 recorded (13,14).

Given that cancer is concidered as a comorbididity which predisposes to severe COVID-19, we also investigated the pan-cancer expression of ORs, including data regarding methylation and mutational profiles. Using the TCGA datasets for all cancers, only four ORs appeared to be significantly differentially regulated (Fig. 4). OR2A1 was down-regulated in OV and THCA; OR2W3 was down-regulated in THYM; OR2A7 was down-regulated in SKCM and THCA; whereas OR51E2 was down-regulated in COAD and READ but up-regulated in PRAD.

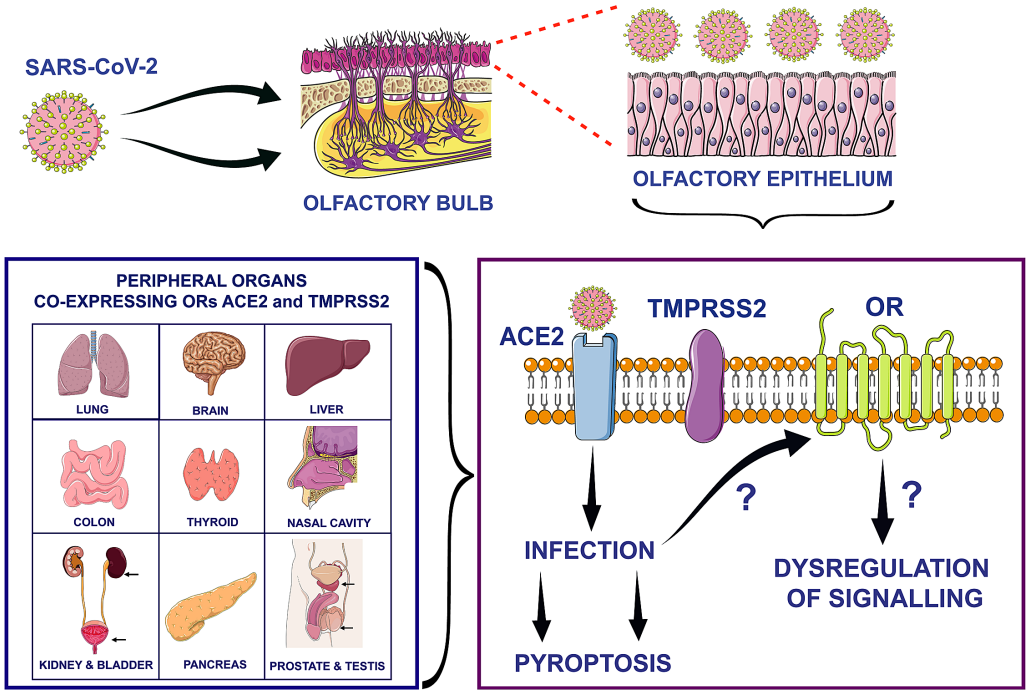

Figure 1. Following entry of SARS-CoV-2 into host cells which is facilitated by ACE2 and TMPRSS2, the function of ORs could be potentially impaired (in part or completely) in infected olfactory and peripheral tissues where ORs are also expressed. The present research highlights the expression of peripheral ORs in both healthy and malignant tissues and identifies their co-expression with key mediators of SARS-CoV-2 infection, such as ACE2 and TMPRSS2. Further research is required to explore whether this co-expression could potentially have additional COVID-19 related consequences due to damage of infected cells expressing ORs and/or impaired OR function in these peripheral tissues, in a similar way to SARS-CoV-2 infection causing loss of smell (anosmia) which is now recognized as a COVID-19 related symptom. ACE2, angiotensin-converting enzyme 2; TMPRSS2, transmembrane protease serine 2; ORs, olfactory receptors.

Subsequently, using the SMART tool, the promoter methylation status of these ORs in comparison to ACE2, TMPRSS2 and CTSL was also investigated (Fig. 5). Data sets without comparable normal tissue have been removed (all OR methylation data can be viewed in Fig. S1). Lower promoter methylation often indicates higher protein gene expression due to reduced inhibition of the promoter region. However, despite the extensive data regarding decreased methylation status within an array of data sets, when compared with GEPIA expression data, changes in methylation status of nine ORs did not significantly correlate with changes in gene expression. Of the differentially methylated genes, only OR51E2 exhibits both lower tumour methylation and significant increase in gene expression in PRAD (Fig. 4).

Finally, the data from cBioPortal revealed that the highest level of alterations in the data set for these ORs relates to gene amplification or mutation across the cancer panel (Fig. 6). Supplementary Fig. S2 presents further breakdown of this mutational profile. Of note, melanoma appears to have a high frequency of OR alterations compared to the other cancer types, while the only OR to present with an alteration in the form of a fusion is OR51E2 in PRAD.

Discussion

In this *in silico* study, we present novel evidence regarding the peripheral tissue distribution of ORs and their co-expression pattern in relationship to key mediators of SARS-CoV-2 infection. The potential involvement of ORs in the loss of smell as one of the COVID-19 presenting symptoms has been hypothesized since the first clinical cases of COVID-19 patients with anosmia (15). Based on our present findings, it is plausible that SARS-CoV-2 infection may exert damage and impair the function of ORs, not only in the nasal epithelium, but also peripherally with wider implications.

Indeed, given the known expression and involvement of the airway smooth muscle ORs in bronchodilation and airway relaxation (5); such peripheral expression of ORs may have additional implications relating to COVID-19. As such, damage and potential interference with signalling pathways associated with OR functions, as noted for nasal epithelial ORs, may contribute to underlying mechanisms predisposing to adverse COVID-19 related clinical outcomes in patients with certain comorbidities (e.g., asthma or cancer) (16). In addition, our findings suggest potential links which should be explored in the context of male preponderance for severe COVID-19, given that a number of ORs were overexpressed in testes. Indeed, the latter is an organ prone to infections by other viruses, including HIV, hepatitis or papilloma among other, which can cause viral orchitis or even lead to testicular cancer (17). Therefore, the possibility that the testes represents an additional target organ for SARS-CoV-2 merits further investigation.

The notion that SARS-CoV-2 infection might induce transcriptional changes of ORs is also supported by available data regarding effects of SARS-CoV infection on gene expression profiles. For example, a study by Reghunathan *et al* (18) in patients with SARS showed that this viral infection can alter the expression of immune response genes. SARS-CoV transfected monocytes have been shown to exhibit changes

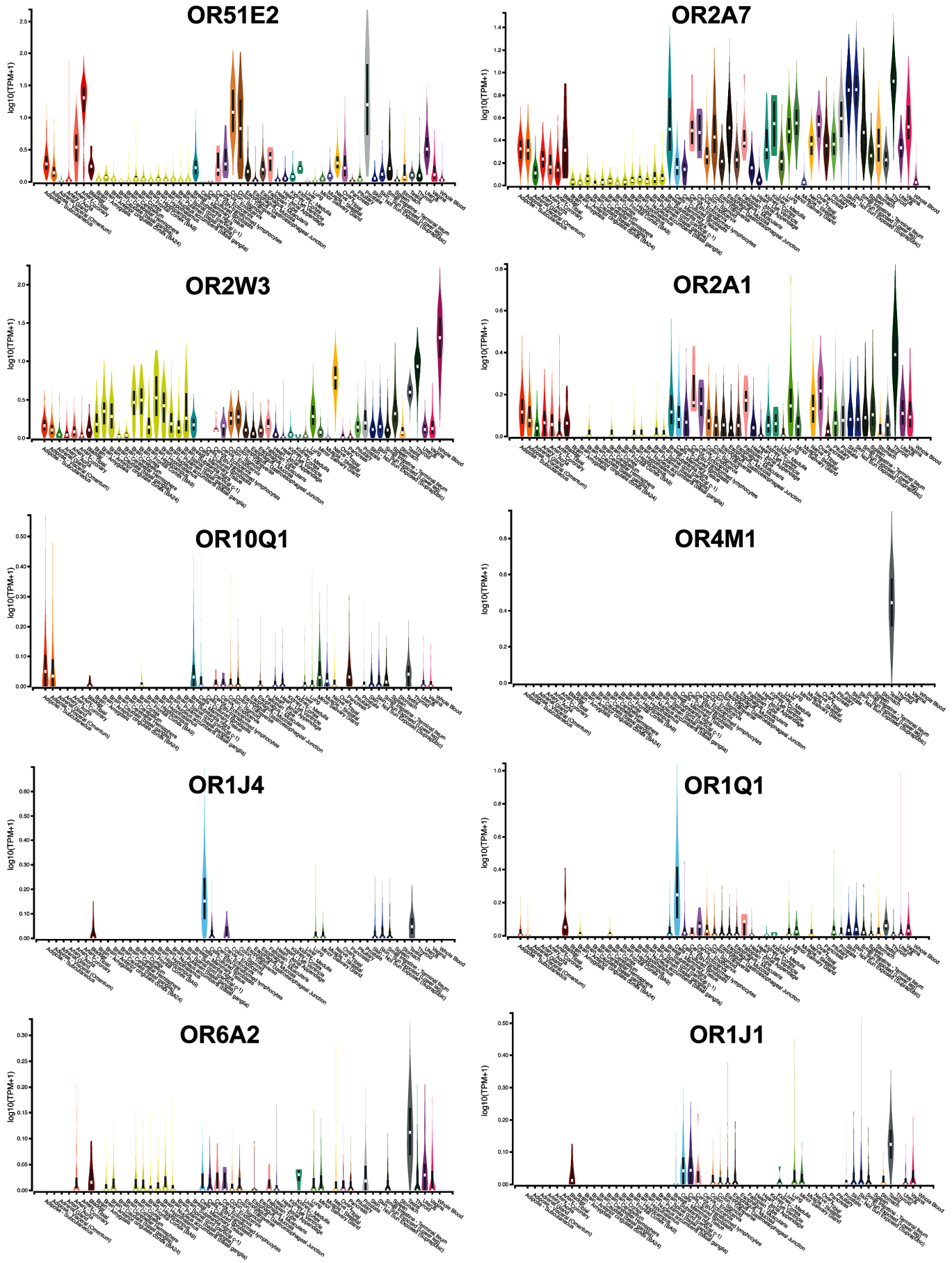

Figure 2. Expression of ORs in normal peripheral tissues using the GTEx database. Wide range of expression was noted for OR51E2, OR2A7, OR10Q1, OR1Q1, OR2A1, OR6A2 and OR2W3. OR2W3 shows the highest level of tissue specific expression, whilst OR1J1 and OR1J4 show minimal levels of protein expression. ORs, olfactory receptors.

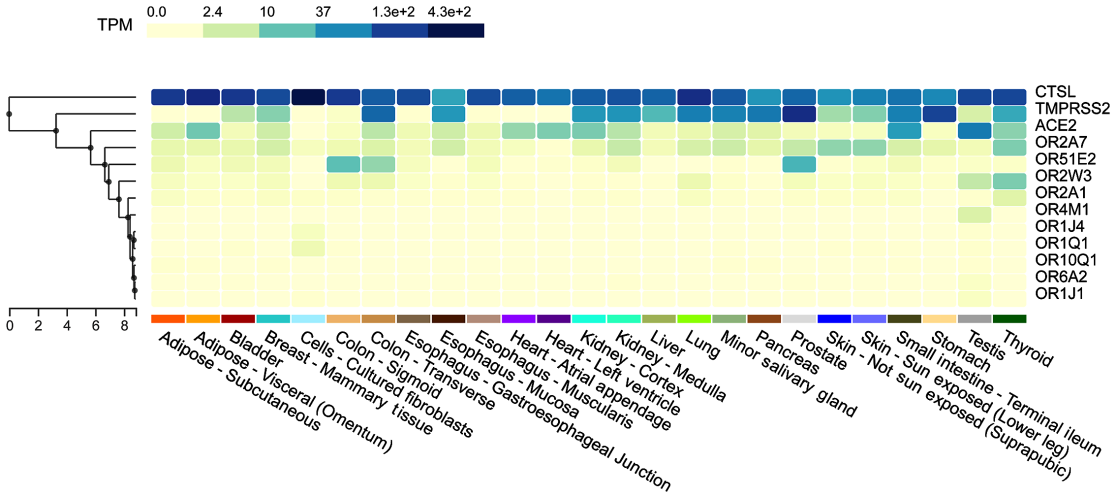

Figure 3. GTEx Multi Gene Query Map showing the co-expression of of ACE2, TMPRSS2, CTSL and peripheral ORs in normal tissues. Relitively high co-expression of ORs in relation to ACE2, TMPRSS2 and CTSL is documented in the colon, testis and thyroid. CTSL is vastly expressed throughout the full range of these tissues. ACE2, angiotensin-converting enzyme 2; TMPRSS2, transmembrane protease serine 2; CTSL, cathepsin L; ORs, olfactory receptors.

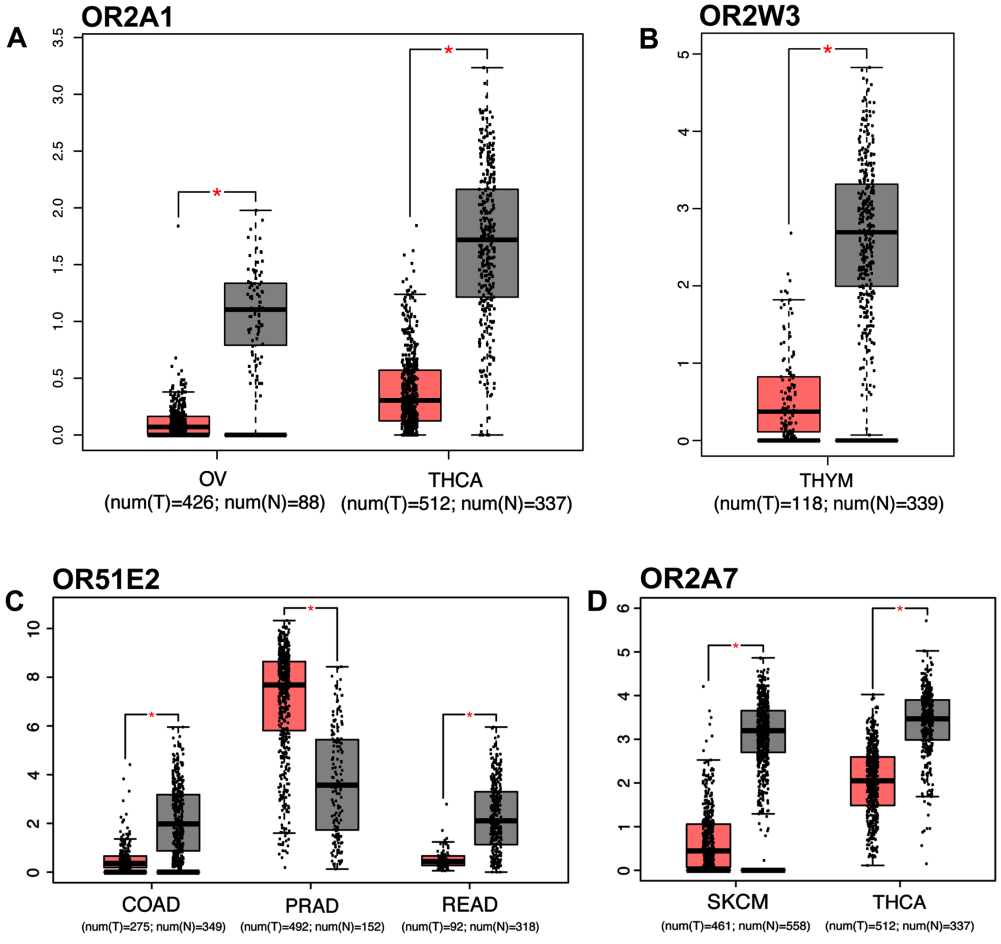

Figure 4. Pan-cancer expression of ORs. (A) Significant decrease in the expression of OR2A1 in OV and THCA tumours (Red) compared to normal (Grey). (B) Significant decrease in tumour expression of OR2W3 for THYM. (C) Significant increase in expression of OR51E2 in PRAD and decrease in COAD and READ tumour data set. (D) Significant decrease of OR2A7 in both SKCM and THCA. ORs, olfactory receptors; OV, ovarian serous cystadenocarcinoma; THCA, thyroid carcinoma; THYM, thymoma; PRAD, prostate adenocarcinoma; COAD, colon adenocarcinoma; READ, rectum adenocarcinoma; SKCM, skin cutaneous melanoma.

in immune-related genes, such as interferons, cathepsin and cytokine-related signalling genes (19). Of note, murine lung epithelial cells infected by another coronavirus (MHV-1) have been shown to exhibit certain gene expression changes, including downregulation of an OR (OLFR291), and changes in other components downstream of GPCR signalling (20).

In the present study, a comprehensive map of differential methylation of ORs across a wide repertoire of cancers is

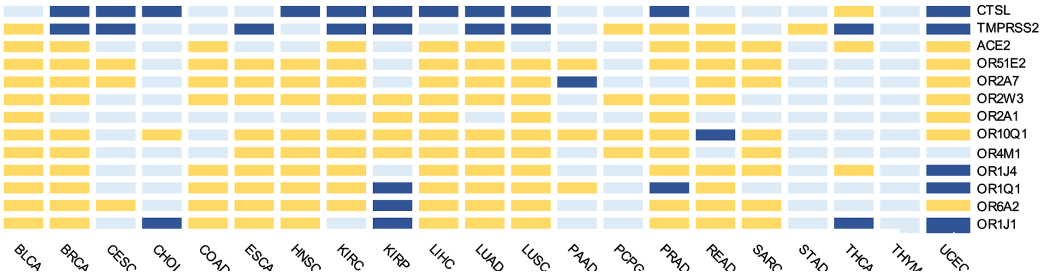

Figure 5. Pan-cancer methylation analysis of OR genes co-expressed with ACE2, TMPRSS2 and CTSL. CTSL: higher expression across a number of tumour sets (blue). ORs: the majority of data sets indicate lower methylation within tumour samples (yellow). High percentage of differentially methylated ORs across 14 cancers within the panel. No statistically significant difference detected (light blue). Data sets with an absence of control were omitted from this graph. ORs, olfactory receptors, ACE2, angiotensin-converting enzyme 2; TMPRSS2, transmembrane protease serine 2; CTSL, cathepsin L.

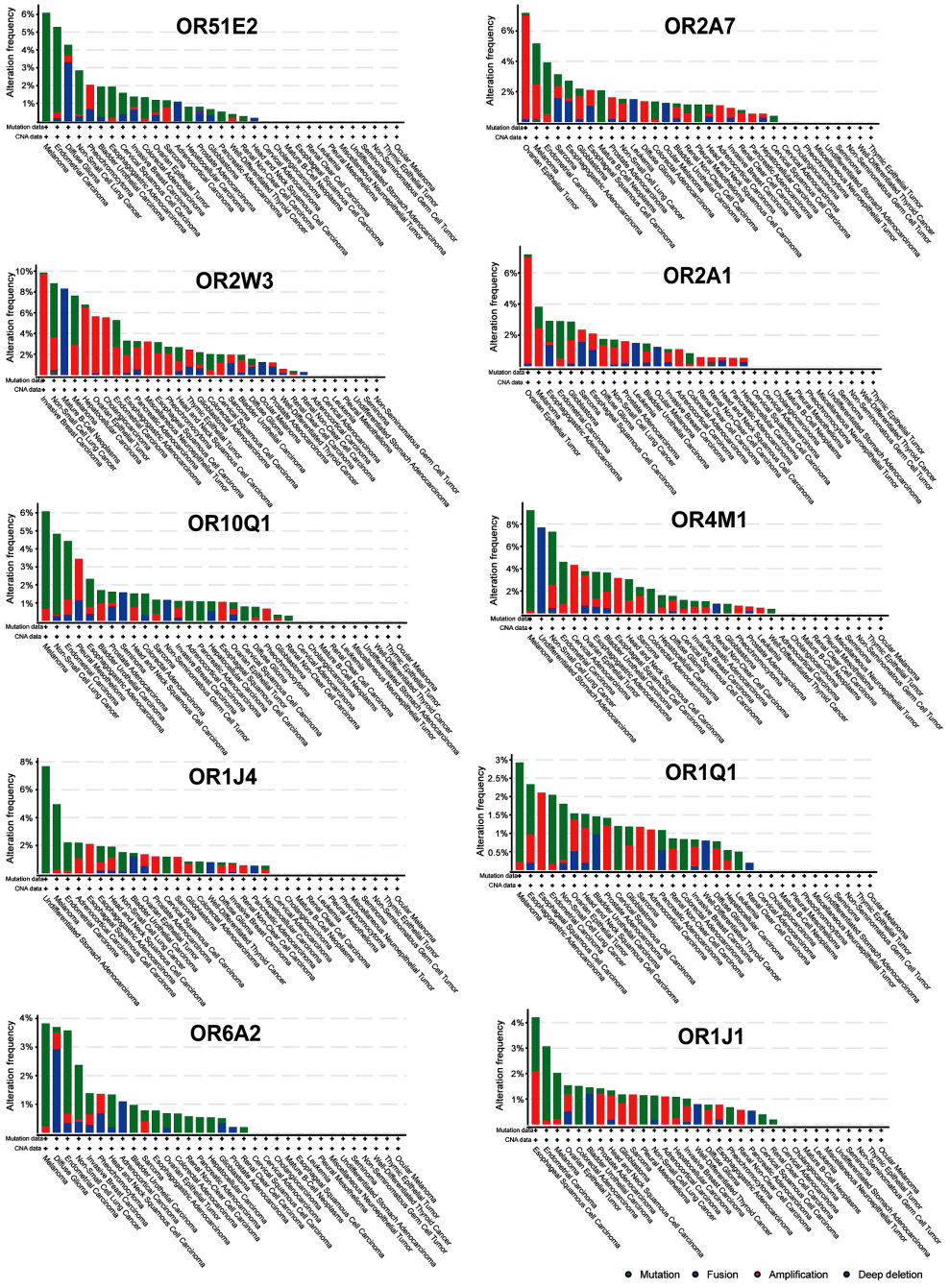

Figure 6. Pan-cancer view of OR gene alterations (cBioPortal). OR51E2, expressed a high number of mutations and a fusion in the prostate; OR2A7-OR2A1, alterations are primarily amplification; OR10Q1, range of amplifications, most frequent level of mutations recorded in melanoma and non-small cell lung cancer; OR4M1, high frequency of mutation in melanoma and notable frequency of deep deletions in stomach adenocarcinoma; OR1J4-OR1J1, range of mutations, amplifications and deletions. OR, olfactory receptor.

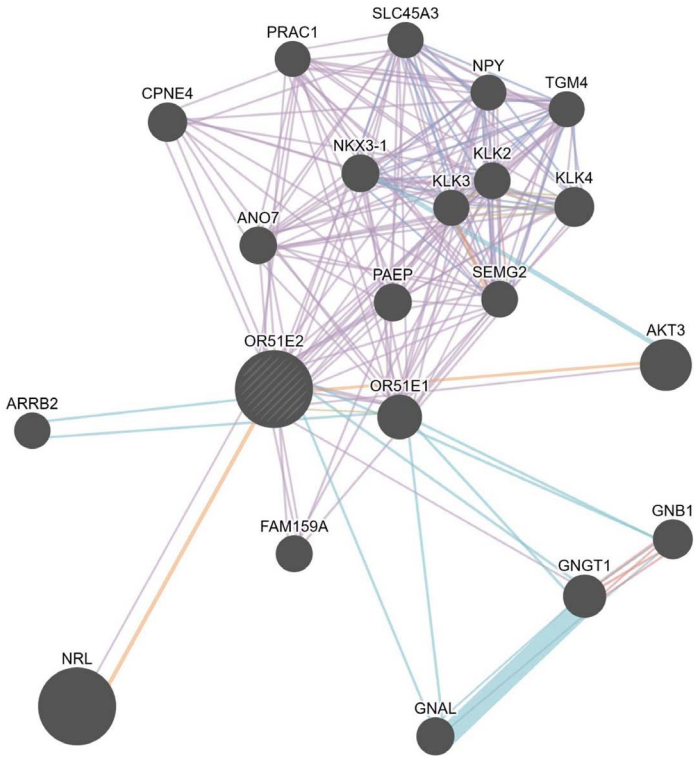

Figure 7. Network annotation of genes interacting with olfactory receptor OR51E2 (GeneMANIA). Visual representation of prostate specific genes and prostate specific biomarkers, such as KLK2 and KLK4, co-expressed (purple), have physical interactions (pink) and co-localised (blue) with OR51E2.

provided. Changes in DNA methylation can be one of the many steps towards malignant transformation (21). It is noteworthy that, among the studied ORs, OR51E2 was significantly overexpressed in PRAD with no apparent difference in the expression between Caucasian and African American groups. Notably, previous studies have implicated this OR in prostate cancer (6,22), whilst 19-hydroxyandrostenedione (a testosterone metabolite) is endogenously produced upon OR51E2 activation (23). Interestingly, it has been suggested that androgen sensitivity can be a determinant of the severity COVID-19 manifests (24). Moreover, increased TMPRSS2 expression has also been recorded for the prostate (14,25). The noted high levels of TMPRSS2 and CTSL expression, coupled with the presented data regarding OR expression (e.g., OR51E2) in malignant and healthy tissues suggest additional implications which merit further research; for example, regarding increased expression in the prostate and predisposition to severe COVID-19 documented in male patients (14,25).

Interestingly, using the GeneMANIA software to gain better insight into the network of genes interacting with OR51E2, co-expression was noted with a plethora of genes related to prostate cancer (Fig. 7). One of the suggested interactions of this receptor is with KLK3 (kallikrein 3 or prostate specific antigen; PSA). KLK2 and KLK4 are also amongst the genes interacting with OR51E2 and are considered potential biomarkers for screening and monitoring of prostate cancer (26). Similarly, OR51E2 interactions were also noted with anoctamin 7 (ANO7), a prostate specific gene associated with aggressive disease; NKX3.1, a prostatic tumour suppressor gene; as well as prostate cancer susceptibility candidate 1 (PRAC1) (27,28). Knockdown of PRAC1 in human prostate epithelial stem cells has been shown to compromise their sphere formation *in vitro* (29). Furthermore, as a GPCR, OR51E2 interacts with arrestin β2 (ARRβ2) which has been shown to be involved in β-2 adrenergic receptor signalling, inducing prostate cancer cell progression (30). Finally, OR51E2 also appears to interact with serine/threonine kinase 3 (AKT3), a well characterised kinase that has been shown to promote prostate cancer cell proliferation (31).

In conclusion, the present study offers new data regarding the expression of ORs in peripheral tissues and their co-expression pattern with key mediators of SARS-CoV-2 cell entry and infection (i.e., ACE2, TMPRSS2, and CTSL). Involvement of impaired OR signalling/function due to SARS-CoV-2 infection leading, not only in anosmia, but also in sequelae from other peripheral tissues (e.g., from the respiratory system or the prostate) is an intriguing hypothesis which merits further investigation in order to clarify the complete spectrum of OR functions that may be impaired in COVID-19. We acknowledge the limitations of our *in silico* approach, thus further *in vitro*, *in vivo* and clinical studies are clearly required to elucidate the role of ORs, both at the olfactory level and the periphery, in the context of COVID-19.

Acknowledgements

Not applicable.

Funding

No funding was received.

Availability of data and materials

All data generated or analysed during this study are included in this published article (and its supplementary information files).

Authors' contributions

RK consulted the literature, analysed the data, produced the figures and contributed towards the manuscript. RK, MH, KC, HSR and DAS have contributed to the conception and design of the study, writing of the manuscript, providing revision and contributing towards final edits. IK and EK contributed equally to the conception of the work, data and literature analysis as well as interpretation. All authors read and approved the final manuscript.

Ethics approval and consent to participate

Not applicable.

Patient consent for publication

Not applicable.

Competing interests

DAS is the Editor-in-Chief for the journal, but had no personal involvement in the reviewing process, or any influence in terms of adjudicating on the final decision, for this article. The other authors declare that they have no competing interests.

References

1. World Health Organization (WHO): Coronavirus disease 2019 (COVID-19): situation report, 139. WHO, Geneva, 2020. https://www.who.int/emergencies/diseases/novel-coronavirus-2019/situation-reports. Accessed June 8, 2020.
2. Pellegrino R, Cooper KW, Di Pizio A, Joseph PV, Bhutani S and Parma V: Corona Viruses and the Chemical Senses: Past, Present, and Future. Chem Senses bjaa031, 2020.
3. Mainland JD, Keller A, Li YR, Zhou T, Trimmer C, Snyder LL, Moberly AH, Adipietro KA, Liu WL, Zhuang H, *et al*: The missense of smell: Functional variability in the human odorant receptor repertoire. Nat Neurosci 17: 114-120, 2014.
4. Maßberg D and Hatt H: Human olfactory receptors: Novel cellular functions outside of the nose. Physiol Rev 98: 1739-1763, 2018.
5. An SS and Liggett SB: Taste and smell GPCRs in the lung: Evidence for a previously unrecognized widespread chemosensory system. Cell Signal 41: 82-88, 2018.
6. Neuhaus EM, Zhang W, Gelis L, Deng Y, Noldus J and Hatt H: Activation of an olfactory receptor inhibits proliferation of prostate cancer cells. J Biol Chem 284: 16218-16225, 2009.
7. Gosain R, Abdou Y, Singh A, Rana N, Puzanov I and Ernstoff MS: COVID-19 and cancer: a comprehensive review. Curr Oncol Rep 22, 53, 2020.
8. Hoffmann M, Kleine-Weber H, Schroeder S, Krüger N, Herrler T, Erichsen S, Schiergens TS, Herrler G, Wu NH, Nitsche A, *et al*: SARS-CoV-2 cell entry depends on ACE2 and TMPRSS2 and is blocked by a clinically proven protease inhibitor. Cell 181: 271-280.e8, 2020.
9. Walls AC, Park YJ, Tortorici MA, Wall A, McGuire AT and Veesler D: Structure, function, and antigenicity of the SARS-CoV-2 spike glycoprotein. Cell 181: 281-292.e6, 2020.
10. Yuki K, Fujiogi M and Koutsogiannaki S: COVID-19 pathophysiology: A review. Clin Immunol 215: 108427, 2020.
11. Butowt R and Bilinska K: SARS-CoV-2: olfaction, brain infection, and the urgent need for clinical samples allowing earlier virus detection. ACS Chem Neurosci 11: 1200-1203, 2020.
12. Brann DH, Tsukahara T, Weinreb C, Lipovsek M, Van den Berge K, Gong B, Chance R, Macaulay IC, Chou H, Fletcher R, *et al*. Non-neuronal expression of SARS-CoV-2 entry genes in the olfactory system suggests mechanisms underlying COVID-19-associated anosmia. bioRxiv: 10.1101/2020.03.25.009084.
13. Chai P, Yu J, Ge S, Jia R and Fan X: Genetic alteration, RNA expression, and DNA methylation profiling of coronavirus disease 2019 (COVID-19) receptor ACE2 in malignancies: A pan-cancer analysis. J Hematol Oncol 13: 43, 2020.
14. Katopodis P, Anikin V, Randeva HS, Spandidos DA, Chatha K, Kyrou I and Karteris E: Pan-cancer analysis of transmembrane protease serine 2 and cathepsin L that mediate cellular SARS-CoV-2 infection leading to COVID-19. Int J Oncol 57: 533-539, 2020.
15. Eliezer M, Hautefort C, Hamel AL, Verillaud B, Herman P, Houdart E and Eloit C: Sudden and complete olfactory loss function as a possible symptom of COVID-19. JAMA Otolaryngol Head Neck Surg: April 8, 2020 (Epub ahead of print).
16. Bilinska K, Jakubowska P, Von Bartheld CS and Butowt R: Von Bartheld CS and Butowt R: Expression of the SARS-CoV-2 entry proteins, ACE2 and TMPRSS2, in cells of the olfactory epithelium: identification of cell types and trends with age. ACS Chem Neurosci 11: 1555-1562, 2020.
17. Wang S, Zhou X, Zhang T and Wang Z: The need for urogenital tract monitoring in COVID-19. Nat Rev Urol 17: 314-315, 2020.
18. Reghunathan R, Jayapal M, Hsu LY, Chng HH, Tai D, Leung BP and Melendez AJ: Expression profile of immune response genes in patients with Severe Acute Respiratory Syndrome. BMC Immunol 6: 2, 2005.
19. Hu W, Yen YT, Singh S, Kao CL and Ba WH: SARS-CoV regulates immune function-related gene expression in human monocytic cells. Viral Immunol 25: 277-288, 2012.
20. VanLeuven JT, Ridenhour BJ, Gonzalez AJ, Miller CR and Miura TA: Lung epithelial cells have virus-specific and shared gene expression responses to infection by diverse respiratory viruses. PLoS One 12: e0178408, 2017.
21. Wajed SA, Laird PW and DeMeester TR: DNA methylation: An alternative pathway to cancer. Ann Surg 234: 10-20, 2001.
22. Xia C, Ma W, Wang F, Hua SB and Liu M: Identification of a prostate-specific G-protein coupled receptor in prostate cancer. Oncogene 20: 5903-5907, 2001.
23. Abaffy T, Bain JR, Muehlbauer MJ, Spasojevic I, Lodha S, Bruguera E, O'Neal SK, Kim SY and Matsunami H: A testosterone metabolite 19-hydroxyandrostenedione induces neuroendocrine trans-differentiation of prostate cancer cells via an ectopic olfactory receptor. Front Oncol 8: 162, 2018.
24. Wambier CG, Goren A, Vaño-Galván S, Ramos PM, Ossimetha A, Nau G, Herrera S and McCoy J: Androgen sensitivity gateway to COVID-19 disease severity. Drug Dev Res: May 15, 2020 (Epub ahead of print).
25. Stopsack KH, Mucci LA, Antonarakis ES, Nelson PS and Kantoff PW: TMPRSS2 and COVID-19: Serendipity or opportunity for intervention? Cancer Discov 10: 779-782, 2020.
26. Hong SK: Kallikreins as biomarkers for prostate cancer. BioMed Res Int 2014: 526341, 2014.
27. Kaikkonen E, Rantapero T, Zhang Q, Taimen P, Laitinen V, Kallajoki M, Jambulingam D, Ettala O, Knaapila J, Boström PJ, *et al*; PRACTICAL Consortium: ANO7 is associated with aggressive prostate cancer. Int J Cancer 143: 2479-2487, 2018.
28. Gurel B, Ali TZ, Montgomery EA, Begum S, Hicks J, Goggins M, Eberhart CG, Clark DP, Bieberich CJ, Epstein JI, *et al*: NKX3.1 as a marker of prostatic origin in metastatic tumors. Am J Surg Pathol 34: 1097-1105, 2010.
29. Hu WY, Hu DP, Xie L, Li Y, Majumdar S, Nonn L, Hu H, Shioda T and Prins GS: Isolation and functional interrogation of adult human prostate epithelial stem cells at single cell resolution. Stem Cell Res (Amst) 23: 1-12, 2017.
30. Zhang P, He X, Tan J, Zhou X and Zou L: β-arrestin2 mediates β-2 adrenergic receptor signaling inducing prostate cancer cell progression. Oncol Rep 26: 1471-1477, 2011.
31. Lin HP, Lin CY, Huo C, Jan YJ, Tseng JC, Jiang SS, Kuo YY, Chen SC, Wang CT, Chan TM, *et al*: AKT3 promotes prostate cancer proliferation cells through regulation of Akt, B-Raf, and TSC1/TSC2. Oncotarget 6: 27097-27112, 2015.

Figure S1. Detailed methylation analyses of the pan-cancer methylation status of data sets from The Cancer Genome Atlas (TCGA) using the Shiny Methylation Analysis Resource Tool (SMART). β-values for olfactory receptors (ORs) show median, cancer (red) and normal (grey), data sets between 0.5-0.9. A high range (0.1-0.9) of β-values between individual samples, represented by the scatter; OR1J4 stands out as having β-values lower than 0.5; OR2A1, OR10Q1 and OR4M1 exhibit the highest level (median β-value 0.75) of tumour and normal methylation. Significant change in methylation indicated as: *P<0.05; **P<0.01; ***P<0.001; ****P<0.0001, while non-significant change as: N/S: P>0.05. It must be noted that control data are absent for: AAC, DLBC, KICH, OV, MESO, USC and UVM.

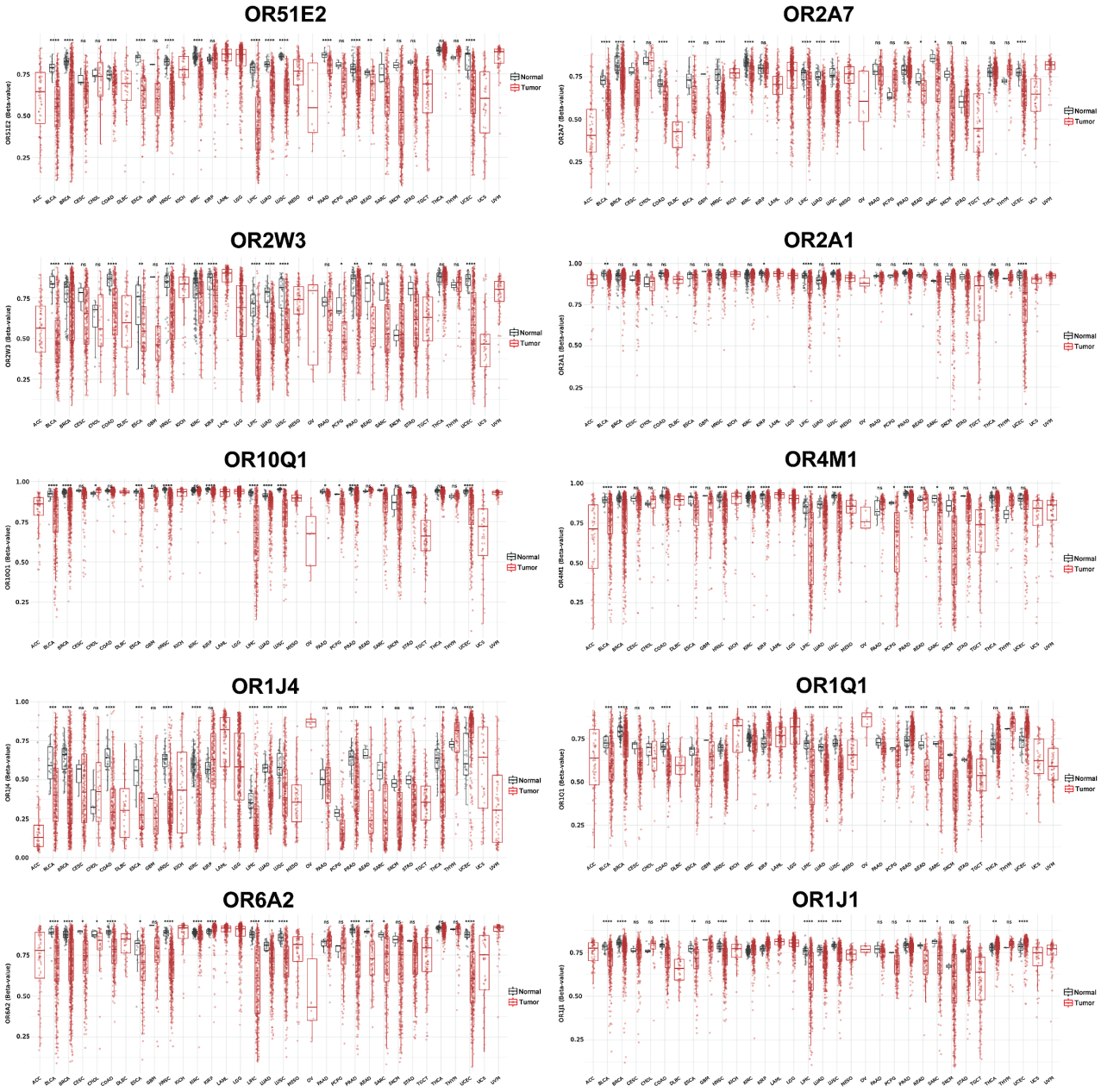

Figure S2. Pan-cancer distribution of olfactory receptor (OR) mutation types from RNAseq data (cBioportal). OR2A7, OR2W3 and OR2A1 exhibit a high distribution of amplification/gain of function throughout the range of tumour groups (red); OR51E2, OR10Q1, OR1J4, OR1Q1, OR6A2 and OR1J1 primarily exhibit mutations in the form of shallow deletions (blue) across the range of tumours; OR4M1 presents with limited sample size, expressing a range of shallow deletions and amplification across the data set.

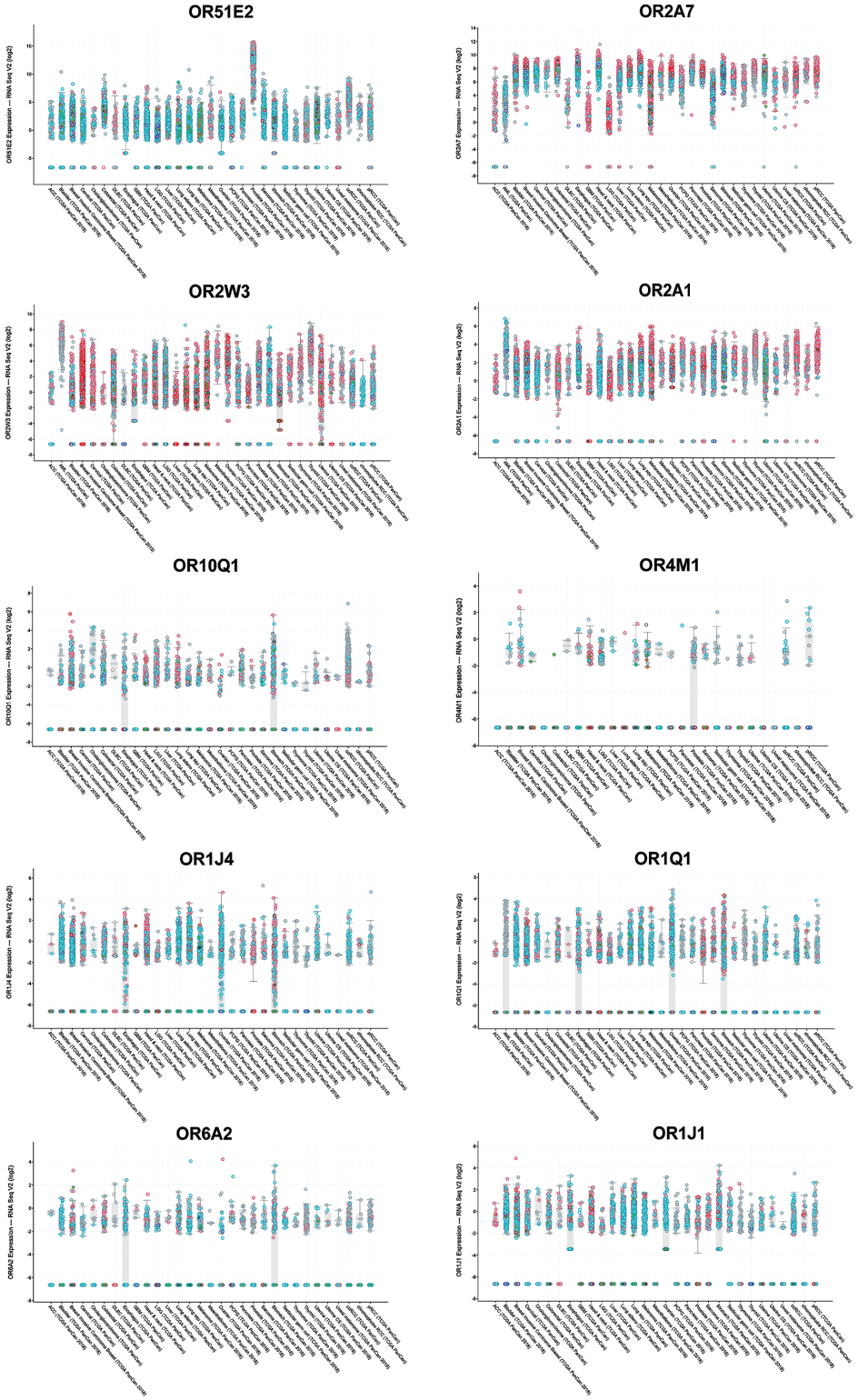

Chapter 7

Discussion

7.1 Summary of Findings

In this thesis I have explored the potential of asprosin and glycolytic molecules as biomarkers of OvCa. The visual summary is shown in Figure 7.1. The green line indicates asprosin investigation, showing widespread expression in OvCa, as well as elevated expression of the predicted receptor OR4M1 in early stages. Additional functional enrichment analysis following treatment with 100nM of asprosin showed dysregulated signalling associated with known hallmarks of cancer. OR4M1 also showed promise as a biomarker of OvCa using Liquid biopsy. Red line shows elevated blood lactate seen in OvCa patients compared to controls; while the blue line depicts the investigation of OvCa cellular models showing augmentation of pathways known as cancer hallmarks in 3D cells, with scaffold specific biomarkers also detected. Finally, the purple line summarises SARS-CoV-2 as a comorbidity of cancer with dysregulation of olfaction. Entry mediator and OR expression were explored peripherally indicating potential for elevated OR dysfunction in a plethora of cancers.

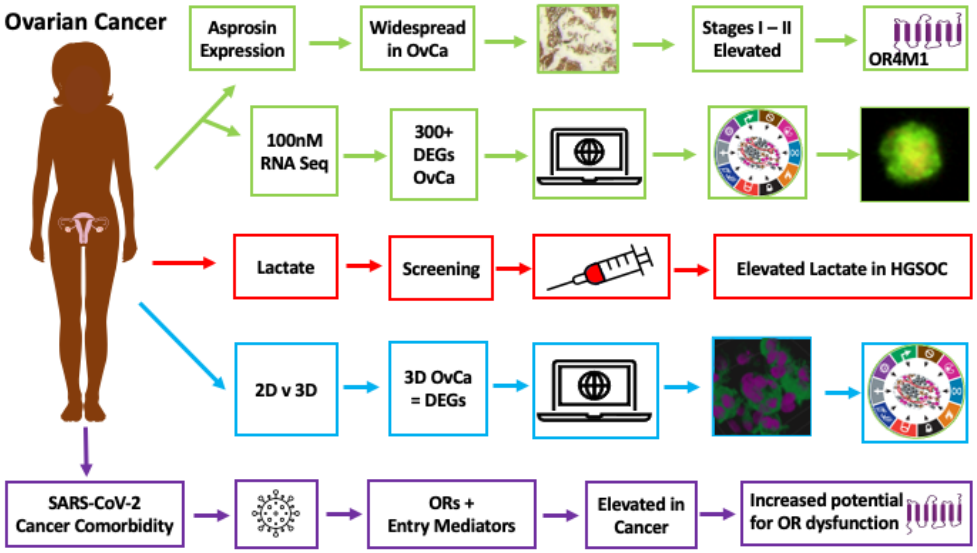

FIGURE 7.1: Thesis Summary
Summary of asprosin and glycolytic molecules as biomarkers of OvCa. Each colour coded box denotes a different line of investigation.

7.1.1 General Remarks - Ovarian Cancer

Clinicians and researchers have remained consistent over the decades in their description of OvCa as the most lethal form of gynaecological malignancy. Despite advancements in histological characterisation, treatment approaches and molecular understanding, mortality rates continue to rise (Sung et al., 2021). When detected at a late stage, which is often the case, survival rates for OvCa present as low as 29% (Elias, Guo, and Bast, 2018). Despite the low mortality, OvCa detection is often delayed owing to the non-specific nature of symptoms (Fotopoulou et al., 2017). Research would therefore benefit from an increased arsenal of molecular/metabolic and biochemical understanding and screening approaches.

It is well known that a high glucose environment fuels metabolic disease, where OvCa's affinity for glucose comes at a detriment to survival (Xintaropoulou et al., 2018; Kellenberger and Petrik, 2018). High glucose in epithelial OvCa for example is often associated with worsening of OS and a decline in PFS (Kellenberger and Petrik, 2018; Lamkin et al., 2009). Advancements in research underpin aerobic glycolysis as a hallmark of cancer, requiring attention with many avenues for exploitation (Hanahan, 2022). Nevertheless, efforts to target glucose and glycolytic pathways in

OvCa often present with challenges in the form of detriment to surrounding tissues and are therefore under constant refinement with novel glucogenic hormones and downstream metabolites presenting new avenues for screening technologies and therapeutics (Xintaropoulou et al., 2018).

7.1.2 Asprosin in the Ovary

Discovered in 2016, asprosin is a novel glucogenic hormone, involved in hepatic glucose release and the stimulation of appetite in mammals (Romere et al., 2016). Over the last few years plasma asprosin has become increasingly associated with the female metabolic profile in both health and disease (Baykus et al., 2019). Despite asprosin's associated role in female metabolism, expression in humans peripherally to white adipose tissue however remained elusive (Romere et al., 2016). Emerging studies have also implicated elevated expression of asprosin with breast cancer (Akkus et al., 2022b) However, the role of asprosin within the TME remains unclear. Given the additional association between elevated asprosin and metabolic disorders characterised as risk factors of OvCa i.e. dysregulated glucose, IR, DM, obesity, PCOS and pregnancy, the role of apsrosin in cancers warranted further investigation (Kellenberger et al., 2010).

Widespread tissue expression of the encoding gene for asprosin, FBN1, was already established within the literature; however expression in cancer was unclear (Wang et al., 2015). This work presents ubiquitous expression of the gene FBN1 throughout human tissues, with significant dysregulation in 10 cancer types, including OvCa (Kerslake et al., 2021). However as a cleavage product of FBN1, production of asprosin in these tissues remained elusive. Normal ovarian and OvCa samples were therefore used to explore expression (Chapter 2). RT-qPCR and IHC analysis of patient biopsies and cell lines revealed widespread expression of asprosin throughout an array of epithelial OvCa subtypes, in addition to adjacent normal samples. Thus corroborating results seen in normal animal tissues, where asprosin expression in the testis and ovaries of mice was recently mapped (Maylem et al., 2021). In the ovary of mice and heifers, asprosin is thought to increase androstenedione production and deplete IGF1-induced proliferation; while in the testes of mice, asprosin is shown to support sperm motility and improve fertility (Maylem et al., 2021; Maurya and Singh, 2022). The presence of apsrosin in reproductive tissues, therefore implies an intrinsic role in reproduction, fertility and steroidogenesis.

Receptor availability is often a limitation of ligand binding action; therefore with the primary receptor of asprosin under debate the expression profile of OR4M1 and TLR4 in cancer was also sought. Using over 100 matched ovarian biopsy samples expression was verified in normal ovarian tissues as well as OvCa. Both receptors displayed widespread expression with no variation between epithelial OvCa subtpes; despite reports of lower TLR4 expression in CCC (Block et al., 2018). Apart from an association with tauopathy in traumatic brain injury the expression of OR4M1 in human tissues is relatively unexplored with animal studies taking the forefront, as such there was no comparison within the literature to draw (Zhao et al., 2013). Work presented in Chapter 2, is therefore the first to map expression of OR4M1 within the human ovary. Here, OR4M1 showed elevated protein expression compared to NAT during early OvCa staging (I - II) followed by a marked decline in later stages (III - IV). Given the growing associations between ORs and their potential as cancer biomarkers, OR4M1's elevated expression in OvCa, especially in the early often undetectable stages, requires further exploration. Future work will therefore assess the expression of OR4M1 in a larger cohort, encompassing a higher volume of samples per OvCa stage. Normal ovarian biopsy samples are difficult to obtain, owing to the risk unnecessary biopsy poses to fertility, however a larger control cohort must also be sought to confirm findings (Donnez et al., 2003).

It must be noted that since the writing of this thesis an additional receptor, with orexigenic properties, has also been suggested: PTPRD (Mishra et al., 2022). However expression beyond *in silico*, which implies elevation in OvCa, is yet to be explored (Wang, Li, and Li, 2021). The elevated expression of predicted receptors in OvCa may therefore support elevated asprosin binding and associated signalling.

Given the presence of asprosin and associated receptor expression within OvCa, asprosin's role was sought using the serous ovarian cancer cell line, SKOV-3; one of the most widely studied cellular models of OvCa (Beaufort et al., 2014). Given that asprosin is produced under periods of glucose starvation, all cellular assays took place under normal conditions using cellular medium supplemented with glucose, to avoid additional production of asprosin that may influence results (Romere et al., 2016). Future work will assess the effects of glucose starvation on asprosin production in OvCa. Data obtained using cell treatment assays, RNA sequencing analysis and an array of molecular techniques, suggested activation of signalling pathways

associated with all three of asprosin's predicted receptors. Western blot analysis revealed short lived phosphorylation of the kinase ERK 1/2, five minutes after treatment with asprosin. Activation of which is instigated by a number of receptors including PTPRD and TLR4; and is associated with proliferation, differentiation and cell survival in addition to progression of cancers, including OvCa (Block et al., 2018; Wang, Li, and Li, 2021). Asprosin-TLR4-ERK 1/2 signalling is also shown to influence IR in pancreatic beta cells, a process in OvCa that was also dysregulated following treatment with asprosin (Nam et al., 2022). Additional investigation revealed asprosin related GPCR activation and related signalling, in addition to pathways associated with augmented glucose regulation and ATP+ potassium channel activation; processes common to OR4M1-asprosin mediated signalling (Li, Ge, and Lu, 2019).

Although rare, receptor promiscuity is possible, and evidence presented in this work may be indicative of an implied affinity by asprosin for all three receptors. Future work should therefore seek fluorescent ligand binding assays, as well as gene editing techniques such as CRISPR-cas9 and small interfering RNA (siRNA) to uncover the binding potential of asprosin with each receptor. These techniques can be applied to silence and/or over express each receptor within OvCa cell models (with possible translation to *in vivo* models), allowing for the observational study of downstream action following asprosin treatments. Unfortunately time, finance and resource prevented these methods from being accessed.

Beyond receptor exploration, over 300 differentially regulated genes (DEGs) were detected in OvCa following treatment with asprosin. Many of the identified genes are common to OvCa, in addition to mammary tissues and amniotic fluid; further stressing a role for asprosin as a key regulator of female metabolism. GSEA and functional assessment of asprosin associated DEGs in the TME was also sought revealing the activation of many pathways including TGF-β signalling, ROS and angiogenesis; pathways categorically known as hallmarks of cancer (Hanahan, 2022).

TGF-β signalling is known to modulate epithelial to mesenchymal (EMT) signalling in OvCa while supporting invasion and metastasis through decreased cell adhesion and elevated mobility (Vergara et al., 2010). While dysregulation of ROS associated pathways in OvCa cells including SKOV-3, is seen to prevent apoptosis through ERK1/2, AKT-NF-κB-dependant signaling pathways (Saunders et al., 2010). Further

research by Zhang et al., goes on to associate asprosin with the inhibition of apoptosis through the suppression of ROS in mesenchymal stromal cells, again through ERK1/2-SOD2 signalling (Zhang et al., 2019c). However conflicting studies suggest that ROS in cancer may also trigger pyroptosis (inflammatory cell death through autophagy) when elevated in OvCa (Zhang et al., 2020). Future research should therefore seek a cell migration and wound healing assay in addition to an annexin IV assay to provide further insight over asprosin's role in ERK1/2 - ROS mediated proliferation and/or apoptosis (Aggarwal et al., 2019). Unfortunately limitations in the way of lab access due to a global pandemic and shortages in reagents, such as Matrigel, stalled further *in vitro* analyses.

A large portion of DEGs instigated by asprosin were non-protein coding i.e. pseudogenes and long non-coding RNAs. Pseudogenes often remain untranslated, however 10% are processed (Pink and Carter, 2013). These transcribed pseudogenes are thought to have superfluous functional significance. However, an increasing number are implicated in the transcriptional regulation of other genes as well as post transcriptional regulation of mRNA, particularly in cancer (Stasiak et al., 2021). Of the pseudogenes dysregulated by asprosin the following showed sustained dysregulation from four to twelve hours post treatment: CNEP1R1P1, DYNLT3P2, RPL30P4, VPS25P1 and HLA-H. Unfortunately many of the pseudogenes identified in this study remain unclassified. Kaplan meier analysis did however reveal worsening OS in OvCa patients with elevated CNEP1R1P1 expression ($p < 0.016$). Additional non-coding RNAs such as MAGI2-AS3 (elevated by asprosin) were also seen to correlate with poor OS ($p < 0.018$). The role of MAGI2-AS3 in OvCa is unclear. However emerging evidence shows a potential role for MAGI2-AS3 as a tumour suppressor involved in the sponging of micro-RNAs and sequestering of downstream signalling associated with cell growth (Gokulnath et al., 2019).

Increasing evidence supports a role for asprosin in female metabolism and disease. This work supports that notion, through identification of asprosin within OvCa; with functional enrichment showing the potential for a complex role within the TME with much to be explored. It must be noted as a limitation however that OvCa often presents in menopausal women, with oestrogen exposure having a profound effect on OvCa development (Liang and Shang, 2013). Oestrogen also correlates positively with asprosin; it was not possible however to obtain the menopausal status and the past use of HRT in patients or the cell lines used throughout this thesis (Leonard

et al., 2021b). As such future research would benefit from this information as well as the combined study of asprosin with key female reproductive hormones, including the measurement of oestrogen following OvCa treatment with asprosin.

This work does however outline a solid framework for further investigation of asprosin within the ovarian TME, and association with processes such as ROS, TGF-β and angiogenesis; all primary hallmarks of OvCa growth (Hanahan, 2022). Future work will therefore seek to assess the functional significance of asprosin and related GSEA enriched pathways in OvCa.

7.1.3 Liquid Biopsy and Ovarian Cancer Biomarkers

Over 80% of patients with OvCa receive their diagnosis at a late stage i.e. stages III-IV, where survival rates are as low as 29% (Elias, Guo, and Bast, 2018). This is often due to the unspecific nature of symptoms and lack of current screening techniques offered in healthcare settings (Fotopoulou et al., 2017). If detected early, the chance of survival raises to 92%. Therefore patients with OvCa would benefit greatly from routine screening. However, there are currently no screening frameworks for OvCa. Instead diagnosis is often only achieved after symptoms reach severity due to lack of sensitivity of current diagnostic tools such as CA125 and need for invasive procedure (Fotopoulou et al., 2017). Emerging evidence however supports the use of liquid biopsy as an effective tool in cancer diagnosis.

Liquid biopsy is a rapidly evolving field of research used for the screening of numerous diseases in clinical settings, including cancer (Andree, Dalum, and Terstappen, 2016). Unlike surgical biopsies, liquid biopsies such as blood, allow for sequential disease monitoring, throughout diagnosis, treatment and beyond using a series of cell specific biomarkers (Chudasama et al., 2019b). With CellSearch receiving FDA approval for use in breast, colorectal and prostate cancer, the potential for CC analysis in additional cancers looks promising (Andree, Dalum, and Terstappen, 2016). However, owing to the heterogenicity of OvCa CC's and loss of cellular adhesion (and associated molecules) during EMT, the use of epithelial cellular biomarkers such as EpCAM in OvCa CC detection is often problematic. As such current biomarkers often provide inconsistent and non-comparable results (Hulstaert et al., 2022; Andree, Dalum, and Terstappen, 2016). Novel biomarkers, unique to OvCa CCs may therefore aid clinical detection and prognosis.

This work sought to investigate the expression of asprosin's receptors, OR4M1 and TLR4, in CCs given their novel expression profile in OvCa (Kerslake et al., 2021). Using affinity based ImageStream Flowcytometry with accompanying haematopoietic exclusion markers CD45 and DRAQ5, both receptors were detected in the CCs of HGSOC patients. Regardless of OR4M1 binding potential with asprosin, ORs increasingly show biomarker potential in their own right. Breast, prostate and colon cancer for example all show elevated expression of ORs such as OR2W3, OR51E2 and OR51B4 (Masjedi, Zwiebel, and Giorgio, 2019; Pronin and Slepak, 2021; Weber et al., 2017). Therefore elevated levels of OR4M1 in the blood, as seen in Chapter 3, may act as a biomarker for disease progression and treatment efficacy in OvCa. OR4M1 also exhibits declining expression in CCs throughout clinical treatment cycles. Initial high levels were recorded in patients prior to treatment and at initial screening appointments. OR4M1 positive CCs were then seen to drop as treatment progressed. Throughout analysis patients received an array of therapeutics including platinum based cisplatin, monoclonal antibodies such as bevicuzimab as well as the PARP inhibitor olaparib (Tao et al., 2009; Qu et al., 2022; Fotopoulou et al., 2017). As OvCa progresses drug resistance is often increasingly evident as such future work should seek larger sample sizes and follow individual patients (in place of grouped samples), throughout the treatment course to assess the potential of OR4M1 in personalised medicine approaches.

Whether OR4M1 expression is unique to OvCa and associated CCs however remains unclear, work in the final chapter of this thesis provides gene expression profiles of OR4M1 in a plethora of cancers, indicating potential for protein expression within additional tissues (Kerslake et al., 2020). Future work will therefore explore similar protein expression of OR4M1 in an array of cancers. Seeing as asprosin activated signalling of OR4M1 influences GPCR signalling and consequent hepatic glucose regulation, the role of asprosin activated OR4M1 signalling in CCs also warrants further investigation. Elevated circulating asprosin in OvCa patients, and its ability to exert effects over ROS and angiogenesis, may influence tumour progression and metastasis within this population of non-adherent OvCa cells (Ikari et al., 2021; Kerslake et al., 2022a). Therefore OR4M1 could also be further explored as a potential therapeutic target.

As previously mentioned TLR4 expression in OvCa is well established (Block et al., 2018). The expression of TLR4 within OvCa CCs however is novel to this work.

Unfortunately the cohort of patients within this section of research fell short of the intended. Delays in patient appointments and processing of blood samples due to the Covid-19 pandemic greatly hindered blood sample collection. As such the detection of TLR4 expression in CCs was limited to a small population of patients, all at varying points of disease management. As such the quantity of TLR4 CCs analysed for each category i.e. screening (initial detection), treatment, end of treatment and relapse were not sufficient for the application of statistical analysis. TLR4 CC analysis would therefore benefit from longitudinal analysis over an extended time period. Additional work may also incorporate PTPRD analysis, the most recently annotated asprosin receptor, thus allowing for complex patient profiles to be built.

7.1.4 Lactate a Novel Screening Molecule in OvCa

Early detection and sequential monitoring of OvCa, continues to prove difficult (Hulstaert et al., 2022). Therefore Chapter 4 sought a metabolic specific approach, looking instead at one of the most abundant molecules associated with elevated energy production in cancer, lactate (Liberti and Locasale, 2016). Until recently lactate was assumed to be a secondary product of glycolysis either requiring clearance or conversion to pyruvate for subsequent ATP production through the Krebs cycle and OXPHOS (Alberts et al., 2018). Emerging data however implies a role for lactate as a signalling molecule within the TME, exerting its effect via the GPCR HCAR1 (Jin et al., 2022).

Studies suggest that elevated levels of HCAR1 in cervical and breast cancer, modulate cellular repair through inhibition of BRCA1; an integral protein of DNA repair known for its mutagenic status in breast and ovarian cancer (Jin et al., 2022; Wagner et al., 2017). Investigation showed widespread expression of HCAR1 in OvCa of varying sub types and grade, with no difference seen between OvCa patient BRCA status (Chapter 3).

HCAR1 activation in cancer is also associated with tumour growth and the instigation of angiogenic factors such as AREG (Roland et al., 2014; Lee et al., 2016). In breast cancer particularly, HCAR1 is seen to regulate growth and metastasis through the activation of PI3K/Akt-dependent pathways (Roland et al., 2014). Jin et al., also show augmented energy metabolism in breast cancer cells, with high expression driving reactivation of OXPHOS (Jin et al., 2022).

Understanding of the complex role of HCAR1-lactate in cancer barely scratches the surface; yet growing data continues to note elevated levels of lactate in solid tumours of various tissues of origin. A US based study for example found that regardless of tumour type, elevated lactate correlated poorly with the survival of cancer patients admitted via the emergency room (Maher et al., 2018).

Work presented in Chapter 4 shows significant elevation of lactate in OvCa patients, with levels reaching as high as 10 mmol/L corroborating data seen in other solid tumours such as breast which also record elevated levels as high as 20 mmol/L in cancer patients (Cheung et al., 2020). ROC plotter data generated shows an AUC of 0.9692; with a high confidence interval, thus indicating the diagnostic potential of this test in determining diseased state.

In comparison to tissue biopsies and other blood based tests, blood lactate sample collection is simple, non-invasive, cost efficient, and unlike many metabolites, remains viable for testing following whole blood storage at -20° (McCaughan, McRae, and Smith, 2000). Lactate presents with a fixed normal resting level of 0.2 - 2.3 mmol/L in healthy individuals; making results outside the normal range easy to detect in clinical settings (Birkó et al., 2020). As such this screening technique may benefit OvCa patients given the initial dismissal of unspecific symptoms and often late stage of detection.

The incorporation of additional markers such as lactate may overcome limitations posed by current methods such as non-cancer related elevation of CA125 in PCOS, endometriosis and smoking (Lycke et al., 2021). Therefore lactate shows potential to strengthen existing diagnostic frameworks for earlier OvCa detection (Dochez et al., 2019). Given that blood lactate concentration can be easily measured at routine appointments using just a drop of blood, lactate could prove highly efficient for timely referrals. In theory this could act in a similar manner to existing mammogram and cervical smear assessments i.e. positive results may not always indicate cancer, however they can prompt further life saving investigation (Sachan et al., 2018; Goetz et al., 2019). Going forward early screening and detection of OvCa is imperative given the high rate of mortality associated with late stage detection in OvCa (Elias, Guo, and Bast, 2018).

7.1.5 3D Models of Ovarian Cancer

Models of disease often fail to recapitulate the complex microenvironment that is necessary for tumour development and growth (Duval et al., 2017). In addition, pharmocokinetics are not always accurate within *in vivo* systems, leading to undesired off-target responses in clinical settings. In lung cancer for example, only 5% of therapies assessed in mice make their way to phase III clinical trials (Rybinski et al., 2020). Therefore advanced pre-animal assessments are vital to minimise the use of animals, a common goal sought by many researchers and supported by research councils (Marrella et al., 2021). As such 3D tissue culture has emerged over the last few decades as a more complex model capable of recapitulating *in vivo* characteristics, such as TME interface, diffusion gradients and cellular differentiation, while residing as an *in vitro* system (Loessner et al., 2010).

The current application of OvCa 3D models however is non-standardised and often requires in-house validation and protocol optimisation, making the access of 3D OvCa modelling challenging. Research presented in Chapter 5 assesses the published landscape of OvCa 3D modelling within the last decade.

Over 50% of 3D OvCa research is currently produced by the USA with models often capturing the growth of HGSOC, the most persistent and lethal form of OvCa (Matulonis et al., 2016). Scaffolds varied throughout all studies, with the most used being hanging drop, low adhesive plates, matrigel and hydrogels. Plant based hydrogel presented as an easily accessible common scaffold and as such was used to test the ease of SKOV-3 organoid generation. Adapting methodologies presented in Kletzmayr et al., a 3D culture was generated, proving relatively simplistic in approach (Kletzmayr et al., 2020).

The most frequently used cell line was SKOV-3; which incidentally was also the chosen model throughout this thesis. Despite recent demotion of characterisation from HGSOC to serous adenocarcinoma, SKOV-3 is one of the most abundantly studied and well characterised epithelial OvCa cell lines (Beaufort et al., 2014). SKOV-3 therefore presents with a plethora of literature and associated genomic and functional data for use in comparison and validation of epithelial OvCa studies.

Prior to 2022, over 290 studies had presented data regarding OvCa cells grown in 3D alongside conventional monolayer cultures. Enrichment indicates that cells grown

in 3D show enhanced modelling of tumour core hypoxia, angiogenesis, drug response and cell to cell signalling (Kletzmayr et al., 2020; Loessner et al., 2010). In addition, 3D tissue culture has proven particularly useful in the modelling of therapeutic response; showing developed resistance to platinum based therapeutics over time in a similar manner to response seen during progression and/or relapse of *in vivo* serous OvCa (L'Espérance et al., 2008). Moreover, 3D OvCa cultures were also shown to retain histological features often associated with *in vivo* tumours (Maru et al., 2019). Enhanced gene expression and signalling within the TME of 3D OvCa cultures compared to monolayer culture was also detected indicating elevated adhesion and angiogenic signalling in addition to graduated cell proliferation, apoptosis and differentiation (Tofani et al., 2021). Finally a panel of growth environment specific OVCAR8 biomarkers were identified encompassing genes commonly dysregulated in OvCa. Future work should therefore explore the relevance of these markers and their influence within the OvCa TME.

Given the importance of the TME in OvCa growth and progression, future research should consider the superiority of 3D OvCa modelling in addressing research questions. Enhanced understanding of the OvCa TME and associated augmentation of glycolytic pathways will improve molecular understanding of a disorder characterised by elevated glucose and consequently poor OS (Kellenberger and Petrik, 2018; Alsina-Sanchís et al., 2017). Moreover, adoption of 3D cultures instead of *in vivo* models, will contribute towards the principles of the 3Rs (Replacement, Reduction and Refinement).

7.1.6 Olfactory Receptors in Cancer and Covid-19

While working towards this thesis a global pandemic struck, derailing the lives of millions and causing detrimental effects to healthcare and research (Bhagat et al., 2022). Cancer care in particular saw delays in diagnosis, treatment (inc. surgery) and monitoring (Maringe et al., 2020). As OvCa is often detected in late stages requiring invasive examination and surgical treatment, early detection methods are of increasing importance (Fotopoulou et al., 2017). Taking into account the risk Covid-19 posed to those with cancer, and the potential burden future pandemics may pose to global healthcare, novel biomarkers and screening technologies that are quick, effective and easy to use are increasingly vital (Maßberg and Hatt, 2018; Cucinotta and Vanelli, 2020). Therefore during lab closures and the initial stages of this research

project, research efforts were adapted to support advancements in the understanding of an unknown disease that posed an increased risk to cancer patients.

Following the facilitated entry of SARS-CoV-2 by ACE2 and TMPRSS2, the function of ORs showed potential impairment (anosmia) in infected olfactory epithelium (Butowt and Bartheld, 2021). Additional research shows that infection extends to peripheral tissues such as the lung and GI, where the expression of entry mediators as well as peripheral ORs are evident. As mentioned ORs also show increasing relevance as cancer biomarkers with noted elevation in many cancers (Maßberg and Hatt, 2018). Therefore the impairment of ORs by SARS-CoV-2 infection beyond the nasal epithelium could also be a possibility. Open access *in silico* data bases were used to gain a better understanding of the role of SARS-CoV-2 in peripheral tissues and cancer.

The present research detected OR gene expression in both healthy and malignant tissues peripherally to the nasal epithelium and correlates co-expression with high expression of key SARS-CoV-2 infection entry mediators, such as ACE2 and TMPRSS2. In addition prostate, colon and lung cancer all exhibited significantly elevated OR expression, in conjunction with high levels of SARS-CoV-2 entry mediators such as ACE2 and TMPRSS2. Further research is required to explore the functional consequences of these co-expression patterns in cancer patients with SARS-CoV-2 infection; and whether SARS-CoV-2 impairs receptor function in peripheral tissues in a similar manner to the impairment of ORs within the nasal epithelium (anosmia).

Therefore, in addition to biomarkers of cancer, elevated ORs may also indicate increased susceptibility to SARS-CoV-2 infection in cancer patients. This work further highlights the need for a greater understanding of ORs in the periphery (Kerslake et al., 2020).

7.1.7 Concluding Remarks

This work presents evidence of asprosin's role in OvCa, an often lethal gynaecological malignancy that is associated with elevated glucose metabolism. Enrichment analysis implicates asprosin with cancer related processes such as angiogenesis, ROS and TGF-β signalling. Widespread expression of asprosin's predicted receptors TLR4 and OR4M1, was noted at ovarian level; with elevated OR4M1, detected in early stages (I - II), showing potential as a novel biomarker in both tissue and

liquid biopsies. Additional investigation of peripheral OR expression revealed co-localisation with cell entry mediators of SARS-CoV-2 showing potential to disrupt processes beyond the nasal epithelium.

Moreover, this study, provides evidence of the potential for glycolytic metabolites in OvCa screening. Here it is seen that resting levels of lactate, a signalling molecule and glycolytic product, are significantly elevated in OvCa when compared with normal control subjects; corroborating trends seen in other solid tumours. High lactate levels were recorded regardless of treatment, age or BRCA status in OvCa patients, and therefore prove promising as a screening method. Future work should also explore the use of more sophisticated *in vitro* models and clinical samples, to model the complex OvCa tumour microenvironment and asprosin associated signalling. These future studies will provide a better insight of the role of asprosin as a glucogenic hormone in cancer, and how it might be involved with the Warburg effect.

Further research in the form of a meta-analysis provides an overview of *in vitro* 3D OvCa modelling; showing differential regulation of genes between 2D and 3D OvCa state for a panel of 19 cell lines. Scaffold specific markers were also identified alongside enrichment of *in vivo* processes that are often difficult to capture in 2D such as glycolysis, angiogenesis and hypoxia. Future use of 3D scaffolds and/or OOC approaches, should enhance the understanding of glycolytic processes and the effects of newly-discovered hormones, to further the molecular understanding of a gynaecological disease that has far too long been classified as the "most lethal".

Chapter 8

Appendix A

8.1 Chapter Amendments

Appendix A.

1. **Amendments to Chapter 2, "A pancancer overview of FBN1, asprosin and its cognate receptor OR4M1 with detailed expression profiling in ovarian cancer" – Figure 8.**

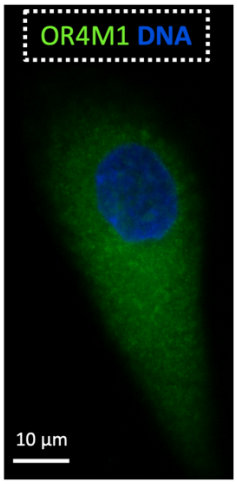

Figure S2 (Panel 4 top right of Figure 8). Immunofluorescence image of SKOV-3 human serous ovarian cancer cell, with DAPI nuclear staining (blue) and OR4M1 (green). Magnification, x100 using a Leica DM4000 microscope (Scale bar, 10 µm). OR4M1, olfactory receptor 4M1.

2. **Amendments to Chapter 3, "Differential regulation of genes by the glucogenic hormone asprosin in ovarian cancer" – Methodology.**

Section: 2.5. RNA Sequencing.

“Briefly, TopHat2 (v.2.1.1) was used to align reads to the human reference genome, GRCH38 with Bowtie2 (v.2.2.6) ultra-high-throughput short read aligner.”

3. **Amendments to Chapter 3, "Differential regulation of genes by the glucogenic hormone asprosin in ovarian cancer" – Figure 3 (Legend).**

Figure 3. Functional enrichment of differentially expressed genes (DEGs) matched with Funrich data base. (A,C,E,G) indicate altered process 4 h after treatment with 100nM asprosin; (B,D,F,H) show processes associated with DEGs 12 h after treatment. (A,B) Biological process; (C,D) Molecular function; (E,F) Biological Pathway; (G,H) Site of expression. Significant data sets identified using hypo geometric test are indicated by * $p < 0.05$. Percentage of genes = grey bars; Fold enrichment = checked bars.

Bibliography

Aggarwal, V. et al. (2019). "Role of Reactive Oxygen Species in Cancer Progression: Molecular Mechanisms and Recent Advancements". In: *Biomolecules* 9.11. DOI: 10.3390/biom9110735.

Ahmed, A., H. P. Redmond, and J. H. Wang (2013). "Links between Toll-like receptor 4 and breast cancer". In: *Oncoimmunology* 2.2, e22945. DOI: 10.4161/onci.22945.

Ahmed, A. A. et al. (2010). "Driver mutations in TP53 are ubiquitous in high grade serous carcinoma of the ovary". In: *Journal of Pathology* 221.1, pp. 49–56. ISSN: 00223417. DOI: 10.1002/path.2696.

Aisenberg, W. H. et al. (2016). "Defining an olfactory receptor function in airway smooth muscle cells". In: *Sci Rep* 6, p. 38231. DOI: 10.1038/srep38231.

Akkus, G. et al. (2022a). "Asprosin and meteorin-like protein immunoreactivity in invasive ductal breast carcinoma stages". In: *Tissue and Cell* 77, p. 101855. ISSN: 0040-8166. DOI: 10.1016/J.TICE.2022.101855.

– (2022b). "Asprosin and meteorin-like protein immunoreactivity in invasive ductal breast carcinoma stages". In: *Tissue Cell* 77, p. 101855. DOI: 10.1016/j.tice.2022.101855.

Alberts, B. et al. (2018). *Molecular biology of the cell*. 6th ed. 1. Garland Science, Taylor and Francis Group, 1–1 volume (various pagings) : ISBN: 9780815344322 (hardcover).

Alix-Panabières, C. and K. Pantel (2021). "Liquid Biopsy: From Discovery to Clinical Application". In: *Cancer Discov* 11.4, pp. 858–873.

Alsaif, M. et al. (2022). "Serum Asprosin Concentrations in Children with Prader-Willi Syndrome: Correlations with Metabolic Parameters". In: *J Clin Med* 11.8. DOI: 10.3390/jcm11082268.

Alsina-Sanchís, E. et al. (2017). "TGFbeta Controls Ovarian Cancer Cell Proliferation". In: *International Journal of Molecular Sciences 2017, Vol. 18, Page 1658* 18.8, p. 1658. ISSN: 1422-0067. DOI: 10.3390/IJMS18081658.

Anderson, N. M. and M. C. Simon (2020). "The tumor microenvironment". In: *Curr Biol* 30.16, R921–R925. DOI: 10.1016/j.cub.2020.06.081.

Andree, K. C., G. van Dalum, and L. W. M. M. Terstappen (2016). "Challenges in circulating tumor cell detection by the CellSearch system". In: *Mol Oncol* 10.3, pp. 395–407. DOI: 10.1016/j.molonc.2015.12.002.

Andrews, L. and D. G. Mutch (2017). *Hereditary Ovarian Cancer and Risk Reduction*. DOI: 10.1016/j.bpobgyn.2016.10.017.

Baczewska, M. et al. (2022). "Energy Substrate Transporters in High-Grade Ovarian Cancer: Gene Expression and Clinical Implications". In: *Int J Mol Sci* 23.16. DOI: 10.3390/ijms23168968.

Bae, W. J. et al. (2019). "PTPRD-inactivation-induced CXCL8 promotes angiogenesis and metastasis in gastric cancer and is inhibited by metformin". In: *J Exp Clin Cancer Res* 38.1, p. 484. DOI: 10.1186/s13046-019-1469-4.

Balani, S., L. V. Nguyen, and C. J. Eaves (2017). *Modeling the process of human tumorigenesis*.

Bär, S. I., B. Biersack, and R. Schobert (2022). "3D cell cultures, as a surrogate for animal models, enhance the diagnostic value of preclinical in vitro investigations by adding information on the tumour microenvironment: a comparative study of new dual-mode HDAC inhibitors". In: *Invest New Drugs* 40.5, pp. 953–961. DOI: 10.1007/s10637-022-01280-0.

Batchu, R. B. et al. (2021). "IL-10 Signaling in the Tumor Microenvironment of Ovarian Cancer". In: *Adv Exp Med Biol* 1290, pp. 51–65.

Baykus, Y. et al. (2019). "Asprosin in umbilical cord of newborns and maternal blood of gestational diabetes, preeclampsia, severe preeclampsia, intrauterine growth retardation and macrosemic fetus". In: *Peptides* 120. ISSN: 18735169. DOI: 10.1016/j.peptides.2019.170132.

Beaufort, C. M. et al. (2014). "Ovarian cancer cell line panel (OCCP): clinical importance of in vitro morphological subtypes". In: *PLoS One* 9.9, e103988. DOI: 10.1371/journal.pone.0103988.

Bell, D. et al. (2011). "Integrated genomic analyses of ovarian carcinoma". In: *Nature* 474.7353, pp. 609–615. ISSN: 14764687. DOI: 10.1038/nature10166.

Beral, V. (2007). "Ovarian cancer and hormone replacement therapy in the Million Women Study". In: *Lancet* 369.9574, pp. 1703–1710. ISSN: 01406736. DOI: 10.1016/S0140-6736(07)60534-0.

Berek, J. S. et al. (2021). "Cancer of the ovary, fallopian tube, and peritoneum: 2021 update". In: *Int J Gynaecol Obstet* 155 Suppl 1, pp. 61–85. DOI: 10.1002/ijgo.13878.

Bhagat, S. et al. (2022). "Novel corona virus (COVID-19) pandemic: current status and possible strategies for detection and treatment of the disease". In: *Expert Rev Anti Infect Ther* 20.10, pp. 1275–1298. DOI: 10.1080/14787210.2021.1835469.

Bharadwaj, S. et al. (2015). "Serum lactate as a potential biomarker of non-glial brain tumors". In: *Journal of clinical neuroscience : official journal of the Neurosurgical Society of Australasia* 22.10, pp. 1625–1627. ISSN: 1532-2653. DOI: 10.1016/J.JOCN.2015.05.009.

Birkó, Z. et al. (2020). "Novel Molecular Markers in Glioblastoma-Benefits of Liquid Biopsy". In: *Int J Mol Sci* 21.20. DOI: 10.3390/ijms21207522.

Block, M. S. et al. (2018). "MyD88 and TLR4 Expression in Epithelial Ovarian Cancer". In: *Mayo Clin Proc* 93.3, pp. 307–320. DOI: 10.1016/j.mayocp.2017.10.023.

Botteri, E. et al. (2010). "Modeling the relationship between circulating tumour cells number and prognosis of metastatic breast cancer". In: *Breast Cancer Res Treat* 122.1, pp. 211–7. DOI: 10.1007/s10549-009-0668-7.

Brann, D. H. et al. (2020). "Non-neuronal expression of SARS-CoV-2 entry genes in the olfactory system suggests mechanisms underlying COVID-19-associated anosmia". In: *bioRxiv*, p. 2020.03.25.009084. DOI: 10.1101/2020.03.25.009084.

Bryant, H. E. et al. (2005). "Specific killing of BRCA2-deficient tumours with inhibitors of poly(ADP-ribose) polymerase". In: *Nature* 434.7035, pp. 913–7. DOI: 10.1038/nature03443.

Bryant, H. E. et al. (2009). "PARP is activated at stalled forks to mediate Mre11-dependent replication restart and recombination". In: *EMBO J* 28.17, pp. 2601–15. DOI: 10.1038/emboj.2009.206.

Budhwani, K. I. et al. (2022). "A hitchhiker's guide to cancer models". In: *Trends in biotechnology* 40.11. ISSN: 1879-3096. DOI: 10.1016/J.TIBTECH.2022.04.003.

Butowt, R. and C. S. von Bartheld (2021). "Anosmia in COVID-19: Underlying Mechanisms and Assessment of an Olfactory Route to Brain Infection". In: *Neuroscientist* 27.6, pp. 582–603.

Cadagan, D., R. Khan, and S. Amer (2016). "Thecal cell sensitivity to luteinizing hormone and insulin in polycystic ovarian syndrome". In: *Reprod Biol* 16.1, pp. 53–60. DOI: 10.1016/j.repbio.2015.12.006.

Cekanova, M. and K. Rathore (2014). "Animal models and therapeutic molecular targets of cancer: utility and limitations". In: *Drug Des Devel Ther* 8, pp. 1911–21.

Cengiz, A. et al. (2019). "The Role of 18F-FDG PET/CT in Detecting Ovarian Cancer Recurrence in Patients with Elevated CA-125 Levels". In: *Mol Imaging Radionucl Ther* 28.1, pp. 8–14.

Chaudhry, S. S. et al. (2007). "Fibrillin-1 regulates the bioavailability of TGFbeta1". In: 176.3. ISSN: 00219525.

Chen, J., S. C. Almo, and Y. Wu (2017). "General principles of binding between cell surface receptors and multi-specific ligands: A computational study". In: *PLoS Comput Biol* 13.10, e1005805. DOI: 10.1371/journal.pcbi.1005805.

Cheung, S. M. et al. (2020). "Lactate concentration in breast cancer using advanced magnetic resonance spectroscopy". In: *British journal of cancer* 123.2, pp. 261–267. ISSN: 1532-1827. DOI: 10.1038/S41416-020-0886-7.

Chudasama, D. et al. (2019a). "Liquid Biopsies in Lung Cancer: Four Emerging Technologies and Potential Clinical Applications". In: *Cancers (Basel)* 11.3. DOI: 10.3390/cancers11030331.

– (2019b). "Liquid biopsies in lung cancer: Four emerging technologies and potential clinical applications". In: *Cancers* 11.3, p. 331. ISSN: 20726694. DOI: 10.3390/cancers11030331.

Chung, C. et al. (2022). "Odorant receptors in cancer". In: *BMB reports* 55 (2), pp. 72–80. ISSN: 1976-670X. DOI: 10.5483/BMBREP.2022.55.2.010.

Corica, D. et al. (June 2021a). "Asprosin serum levels and glucose homeostasis in children with obesity". In: *Cytokine* 142, p. 155477.

Corica, D. et al. (2021b). "Meal-Related Asprosin Serum Levels Are Affected by Insulin Resistance and Impaired Fasting Glucose in Children With Obesity". In: *Front Endocrinol (Lausanne)* 12, p. 805700. DOI: 10.3389/fendo.2021.805700.

Craig, E. R. et al. (2016). "Metabolic risk factors and mechanisms of disease in epithelial ovarian cancer: A review". In: *Gynecol Oncol* 143.3, pp. 674–683. DOI: 10.1016/j.ygyno.2016.10.005.

Cucinotta, D. and M. Vanelli (2020). "WHO Declares COVID-19 a Pandemic". In: *Acta Biomed* 91, pp. 157–160.

Dasari, S. and P. B. Tchounwou (2014). "Cisplatin in cancer therapy: molecular mechanisms of action". In: *Eur J Pharmacol* 740, pp. 364–78.

Davern, M. et al. (2022). "Acidosis significantly alters immune checkpoint expression profiles of T cells from oesophageal adenocarcinoma patients". In: *Cancer immunology, immunotherapy:CII*. ISSN: 1432-0851. DOI: 10.1007/S00262-022-03228-Y.

Dejanovic, D., N. L. Hansen, and A. Loft (2021). "PET/CT Variants and Pitfalls in Gynecological Cancers". In: *Semin Nucl Med* 51.6, pp. 593–610.

Dimitrov, D. S. (2004). "Virus entry: molecular mechanisms and biomedical applications". In: *Nat Rev Microbiol* 2.2, pp. 109–22. DOI: 10.1038/nrmicro817.

Ding, D. C. et al. (2018). "Association between polycystic ovarian syndrome and endometrial, ovarian, and breast cancer: A population-based cohort study in Taiwan". In: *Medicine (United States)* 97.39. ISSN: 15365964. DOI: 10.1097/MD.0000000000012608.

Dochez, V. et al. (2019). "Biomarkers and algorithms for diagnosis of ovarian cancer: CA125, HE4, RMI and ROMA, a review". In: *Journal of Ovarian Research 2019 12:1* 12.1, pp. 1–9. ISSN: 1757-2215. DOI: 10.1186/S13048-019-0503-7.

Donnez, J. et al. (2003). "Safety of conservative management and fertility outcome in women with borderline tumors of the ovary". In: *Fertil Steril* 79.5, pp. 1216–21.

Du, C. et al. (2021). "Asprosin is associated with anorexia and body fat mass in cancer patients". In: *Support Care Cancer* 29.3, pp. 1369–1375. DOI: 10.1007/s00520-020-05621-8.

Duerrschmid, C. et al. (2017). "Asprosin is a centrally acting orexigenic hormone". In: *Nature Medicine* 23.12, pp. 1444–1453. ISSN: 1546170X. DOI: 10.1038/nm.4432.

Dunneram, Y., D. C. Greenwood, and J. E. Cade (2019). "Diet, menopause and the risk of ovarian, endometrial and breast cancer". In: *Proc Nutr Soc* 78.3, pp. 438–448.

Duval, K. et al. (2017). *Modeling physiological events in 2D vs. 3D cell culture*. DOI: 10.1152/physiol.00036.2016.

Ebell, M. H., M. B. Culp, and T. J. Radke (2016). "A Systematic Review of Symptoms for the Diagnosis of Ovarian Cancer". In: *American Journal of Preventive Medicine* 50.3, pp. 384–394. ISSN: 18732607. DOI: 10.1016/j.amepre.2015.09.023.

Elias, K. M., J. Guo, and R. C. Bast (2018). *Early Detection of Ovarian Cancer*. DOI: 10.1016/j.hoc.2018.07.003.

Engbersen, M. P. et al. (2021). "The role of CT, PET-CT, and MRI in ovarian cancer". In: *Br J Radiol* 94.1125, p. 20210117.

Ferris, J. S. et al. (2014). "Oral contraceptive and reproductive risk factors for ovarian cancer within sisters in the breast cancer family registry". In: *British Journal of Cancer* 110.4, pp. 1074–1080. ISSN: 00070920. DOI: 10.1038/bjc.2013.803.

Filipe, A. et al. (2022). "Differential Expression of RAD51AP1 in Ovarian Cancer: Effects of siRNA In Vitro". In: *J Pers Med* 12.2.

Flaum, N. et al. (2020). "Epithelial ovarian cancer risk: A review of the current genetic landscape". In: *Clinical Genetics* 97.1, pp. 54–63. ISSN: 13990004. DOI: 10.1111/cge.13566.

Flisikowska, T. et al. (2022). "A humanized minipig model for the toxicological testing of therapeutic recombinant antibodies". In: *Nat Biomed Eng*. DOI: 10.1038/s41551-022-00921-2.

Fotopoulou, C. et al. (2017). "British Gynaecological Cancer Society (BGCS) epithelial ovarian/fallopian tube/primary peritoneal cancer guidelines: recommendations for practice". In: *Eur J Obstet Gynecol Reprod Biol* 213, pp. 123–139.

Franco, N. H. (2013). "Animal Experiments in Biomedical Research: A Historical Perspective". In: *Animals (Basel)* 3.1, pp. 238–73. DOI: 10.3390/ani3010238.

Goetz, M. P. et al. (2019). "NCCN Guidelines Insights: Breast Cancer, Version 3.2018". In: *J Natl Compr Canc Netw* 17.2, pp. 118–126. DOI: 10.6004/jnccn.2019.0009.

Gokulnath, P. et al. (2019). "Long Non-Coding RNA MAGI2-AS3 is a New Player with a Tumor Suppressive Role in High Grade Serous Ovarian Carcinoma". In: 11.12, p. 2008. ISSN: 2072-6694. DOI: 10.3390/CANCERS11122008.

Gonzalez, V. D. et al. (2021). "High-grade serous ovarian tumor cells modulate NK cell function to create an immune-tolerant microenvironment". In: *Cell Rep* 36.9, p. 109632.

González-Martín, A. et al. (2019). "Niraparib in Patients with Newly Diagnosed Advanced Ovarian Cancer". In: *N Engl J Med* 381.25, pp. 2391–2402. DOI: 10.1056/NEJMoa1910962.

Groener, J. B. et al. (2019). "Asprosin response in hypoglycemia is not related to hypoglycemia unawareness but rather to insulin resistance in type 1 diabetes". In: *PLoS ONE* 14.9. ISSN: 19326203. DOI: 10.1371/journal.pone.0222771.

Gu, J. et al. (2022). "Tumor metabolite lactate promotes tumorigenesis by modulating MOESIN lactylation and enhancing TGF-beta signaling in regulatory T cells". In: *Cell reports* 39.12. ISSN: 2211-1247. DOI: 10.1016/J.CELREP.2022.110986.

Gupta, K. et al. (2021). "Cancer patients and COVID-19: Mortality, serious complications, biomarkers, and ways forward". In: *Cancer Treat Res Commun* 26, p. 100285. DOI: 10.1016/j.ctarc.2020.100285.

Güven, C. and H. Kafadar (2022). "Evaluation of Plasma Asprosin Concentration in Patients with Coronary Artery Disease". In: *Braz J Cardiovasc Surg* 37.4, pp. 493–500. DOI: 10.21470/1678-9741-2021-0003.

Hall, J. E. (2015). "Endocrinology of the Menopause". In: *Endocrinol Metab Clin North Am* 44.3, pp. 485–96.

Hall, M. et al. (2020). "Role of front-line bevacizumab in advanced ovarian cancer: the OSCAR study". In: *International journal of gynecological cancer : official journal of the International Gynecological Cancer Society* 30.2, pp. 213–220. ISSN: 1525-1438. DOI: 10.1136/IJGC-2019-000512.

Hanahan, D. (2022). "Hallmarks of Cancer: New Dimensions". In: *Cancer Discovery* 12.1, pp. 31–46. ISSN: 2159-8274. DOI: 10.1158/2159-8290.CD-21-1059.

Hanahan, D. and R. A. Weinberg (2011). *Hallmarks of cancer: The next generation*. DOI: 10.1016/j.cell.2011.02.013.

Hao, Y., D. Baker, and P. T. Dijke (2019). *TGF-beta-mediated epithelial-mesenchymal transition and cancer metastasis*. DOI: 10.3390/ijms20112767.

Harmon, C. et al. (2019). "Lactate-Mediated Acidification of Tumor Microenvironment Induces Apoptosis of Liver-Resident NK Cells in Colorectal Liver Metastasis". In: *Cancer Immunol Res* 7.2, pp. 335–346. DOI: 10.1158/2326-6066.CIR-18-0481.

Hoffmann, J. G., W. Xie, and A. R. Chopra (2020). "Energy Regulation Mechanism and Therapeutic Potential of Asprosin". In: *Diabetes* 69.4, pp. 559–566. DOI: 10.2337/dbi19-0009.

Hoffmann, T. et al. (2022). "Correlation of metabolic characteristics with maternal, fetal and placental asprosin in human pregnancy". In: *Endocr Connect* 11.3. DOI: 10.1530/EC-22-0069.

Hong, T. et al. (2021). "PARP inhibition promotes ferroptosis via repressing SLC7A11 and synergizes with ferroptosis inducers in BRCA-proficient ovarian cancer". In: *Redox Biol* 42, p. 101928. DOI: 10.1016/j.redox.2021.101928.

Hong, Y., F. Fang, and Q. Zhang (2016). "Circulating tumor cell clusters: What we know and what we expect (Review)". In: *Int J Oncol* 49.6, pp. 2206–2216. DOI: 10.3892/ijo.2016.3747.

Huang, S. L. et al. (2020). "Role of the TLR4-androgen receptor axis and genistein in taxol-resistant ovarian cancer cells". In: *Biochemical pharmacology* 177. ISSN: 1873-2968. DOI: 10.1016/J.BCP.2020.113965.

Huang, S.-L. et al. (2021). "TLR4/IL-6/IRF1 signaling regulates androgen receptor expression: A potential therapeutic target to overcome taxol resistance in ovarian cancer". In: *Biochem Pharmacol* 186, p. 114456. DOI: 10.1016/j.bcp.2021.114456.

Hulstaert, E. et al. (2022). "RNA biomarkers from proximal liquid biopsy for diagnosis of ovarian cancer". In: *Neoplasia* 24.2, pp. 155–164.

Husain, B. et al. (2022). "Cell-based receptor discovery identifies host factors specifically targeted by the SARS CoV-2 spike". In: *Communications biology* 5 (1). ISSN: 2399-3642. DOI: 10.1038/S42003-022-03695-0.

Ikari, R. et al. (2021). "Differences in the Central Energy Metabolism of Cancer Cells between Conventional 2D and Novel 3D Culture Systems". In: *Int J Mol Sci* 22.4.

Jeong, T. B. et al. (2019). "Comparison of toxic responses to acetaminophen challenge in ICR mice originating from different sources". In: *Lab Anim Res* 35, p. 16. DOI: 10.1186/s42826-019-0017-x.

Jessmon, P. et al. (2017). "Epidemiology and treatment patterns of epithelial ovarian cancer". In: *Expert Review of Anticancer Therapy* 17.5, pp. 427–437. ISSN: 17448328. DOI: 10.1080/14737140.2017.1299575.

Jiang, Z. et al. (2019). "Increased glycolysis correlates with elevated immune activity in tumor immune microenvironment". In: *EBioMedicine* 42, pp. 431–442. ISSN: 23523964. DOI: 10.1016/j.ebiom.2019.03.068.

Jin, L. et al. (2022). "Lactate receptor HCAR1 regulates cell growth, metastasis and maintenance of cancer-specific energy metabolism in breast cancer cells". In: *Mol Med Rep* 26.2. DOI: 10.3892/mmr.2022.12784.

Jordan, B. (2021). "[The legacy of Henrietta Lacks]". In: *Med Sci (Paris)* 37.12, pp. 1189–1193. DOI: 10.1051/medsci/2021181.

Kaku, T. et al. (2003). "Histological classification of ovarian cancer". In: *Medical Electron Microscopy*. Vol. 36. 1. Springer, pp. 9–17. DOI: 10.1007/s007950300002.

Kalluri, R. and R. A. Weinberg (2009). "The basics of epithelial-mesenchymal transition". In: *J Clin Invest* 119.6, pp. 1420–8. DOI: 10.1172/JCI39104.

Kamani, M., U. Akgor, and M. Gültekin (2022). "Review of the literature on combined oral contraceptives and cancer". In: *Ecancermedicalscience* 16, p. 1416. DOI: 10.3332/ecancer.2022.1416.

Kamb, A. (2005). "What's wrong with our cancer models?" In: *Nature Reviews Drug Discovery* 4.2, pp. 161–165. ISSN: 14741776. DOI: 10.1038/nrd1635.

Kanzler, H. et al. (2007). "Therapeutic targeting of innate immunity with Toll-like receptor agonists and antagonists". In: *Nat Med* 13.5, pp. 552–9. DOI: 10.1038/nm1589.

Kapałczyńska, M. et al. (2018). "2D and 3D cell cultures – a comparison of different types of cancer cell cultures". In: *Archives of Medical Science* 14.4, pp. 910–919. ISSN: 18969151. DOI: 10.5114/aoms.2016.63743.

Kashani, B. et al. (2021). "The role of toll-like receptor 4 (TLR4) in cancer progression: A possible therapeutic target?" In: *J Cell Physiol* 236.6, pp. 4121–4137. DOI: 10.1002/jcp.30166.

Katopodis, P. et al. (2020). "Pan-cancer analysis of transmembrane protease serine 2 and cathepsin L that mediate cellular SARS-CoV-2 infection leading to COVID-19". In: *Int J Oncol* 57.2, pp. 533–539. DOI: 10.3892/ijo.2020.5071.

Katopodis, P. et al. (2021). "COVID-19 and SARS-CoV-2 host cell entry mediators: Expression profiling of TMRSS4 in health and disease". In: *Int J Mol Med* 47.4. DOI: 10.3892/ijmm.2021.4897.

Kaur, G. and J. M. Dufour (2012). "Cell lines: Valuable tools or useless artifacts". In: *Spermatogenesis* 2.1, pp. 1–5. DOI: 10.4161/spmg.19885.

Ke, F. et al. (2020a). "Combination of asprosin and adiponectin as a novel marker for diagnosing non-alcoholic fatty liver disease". In: *Cytokine* 134, p. 155184. DOI: 10.1016/j.cyto.2020.155184.

Ke, X. et al. (2020b). "Serum Levels of Asprosin, a Novel Adipokine, Are Significantly Lowered in Patients with Acromegaly". In: *International journal of endocrinology* 2020. ISSN: 1687-8337. DOI: 10.1155/2020/8855996.

Keddem, S. et al. (2022). "Gonorrhea and Chlamydia Testing and Case Rates Among Women Veterans in the Veterans Health Administration". In: *Journal of general internal medicine* 37.Suppl 3, pp. 706–713. ISSN: 1525-1497. DOI: 10.1007/S11606-022-07578-2.

Kellenberger, L. D. et al. (2010). "The Role of Dysregulated Glucose Metabolism in Epithelial Ovarian Cancer". In: *Journal of Oncology* 2010. Ed. by M. M. Markman, p. 514310. ISSN: 1687-8450. DOI: 10.1155/2010/514310.

Kellenberger, L. D. and J. Petrik (2018). "Hyperglycemia promotes insulin-independent ovarian tumor growth". In: *Gynecologic Oncology* 149.2, pp. 361–370. ISSN: 10956859. DOI: 10.1016/j.ygyno.2018.02.003.

Kerslake, R. et al. (2020). "Co-expression of peripheral olfactory receptors with SARS-CoV-2 infection mediators: Potential implications beyond loss of smell as a COVID-19 symptom". In: *International Journal of Molecular Medicine* 46.3, pp. 949–956. ISSN: 1107-3756. DOI: 10.3892/ijmm.2020.4646.

Kerslake, R. et al. (2021). "A pancancer overview of FBN1, asprosin and its cognate receptor OR4M1 with detailed expression profiling in ovarian cancer". In: *Oncology Letters* 22.3, pp. 1–14. ISSN: 17921082. DOI: 10.3892/OL.2021.12911/HTML.

Kerslake, R. et al. (2022a). "Differential Regulation of Genes by the Glucogenic Hormone Asprosin in Ovarian Cancer". In: *J Clin Med* 11.19. DOI: 10.3390/jcm11195942.

Kerslake, R. et al. (2022b). "Protein expression of transmembrane protease serine 4 in the gastrointestinal tract and in healthy, cancer, and SARS-CoV-2 infected lungs". In: *Mol Med Rep* 25.4. DOI: 10.3892/mmr.2022.12654.

Kletzmayr, A. et al. (2020). "An Automatable Hydrogel Culture Platform for Evaluating Efficacy of Antibody-Based Therapeutics in Overcoming Chemoresistance". In: *Biotechnol J* 15.5, e1900439. DOI: 10.1002/biot.201900439.

Kobayashi, H. (2022). "Recent advances in understanding the metabolic plasticity of ovarian cancer: A systematic review". In: *Heliyon* 8.11, e11487.

Kobilka, B. K. (2007). *G protein coupled receptor structure and activation*. DOI: 10.1016/j.bbamem.2006.10.021.

Kompaniyets, L. et al. (2021). "Underlying Medical Conditions and Severe Illness Among 540,667 Adults Hospitalized With COVID-19, March 2020-March 2021". In: *Prev Chronic Dis* 18, E66. DOI: 10.5888/pcd18.210123.

Koushik, A. et al. (2017). "Hormonal and reproductive factors and the risk of ovarian cancer". In: *Cancer Causes and Control* 28.5, pp. 393–403. ISSN: 15737225. DOI: 10.1007/s10552-016-0848-9.

Krebs, M. G. et al. (2010). *Circulating tumour cells: Their utility in cancer management and predicting outcomes*. DOI: 10.1177/1758834010378414.

Kuchenbaecker, K. B. et al. (2017). "Risks of Breast, Ovarian, and Contralateral Breast Cancer for BRCA1 and BRCA2 Mutation Carriers". In: *JAMA* 317.23, pp. 2402–2416. DOI: 10.1001/jama.2017.7112.

Kumar et al. (2019). "Detection of Abundant Non-Haematopoietic Circulating Cancer-Related Cells in Patients with Advanced Epithelial Ovarian Cancer". In: *Cells* 8.7, p. 732. ISSN: 2073-4409. DOI: 10.3390/cells8070732.

Kurman, R. J. and I. M. Shih (2016). *The dualistic model of ovarian carcinogenesis revisited, revised, and expanded*. DOI: 10.1016/j.ajpath.2015.11.011.

La Vecchia, C. (2017). "Ovarian cancer: Epidemiology and risk factors". In: *European Journal of Cancer Prevention* 26.1, pp. 55–62. ISSN: 14735709. DOI: 10.1097/CEJ.0000000000000217.

Lamkin, D. M. et al. (2009). "Glucose as a prognostic factor in ovarian carcinoma". In: *Cancer* 115.5, pp. 1021–1027. ISSN: 0008543X. DOI: 10.1002/cncr.24126.

Larsen, T. (2017). "Fluorometric determination of d-lactate in biological fluids". In: *Analytical biochemistry* 539, pp. 152–157. ISSN: 1096-0309. DOI: 10.1016/J.AB.2017.10.026.

Lee, B. et al. (1991). "Linkage of Marfan syndrome and a phenotypically related disorder to two different fibrillin genes". In: *Nature* 352.6333, pp. 330–334. ISSN: 00280836. DOI: 10.1038/352330a0.

Lee, T. et al. (2019). "Asprosin impairs insulin secretion in response to glucose and viability through TLR4/JNK-mediated inflammation". In: *Molecular and Cellular Endocrinology* 486, pp. 96–104. ISSN: 18728057. DOI: 10.1016/j.mce.2019.03.001.

Lee, Y. J. et al. (2016). "G-protein-coupled receptor 81 promotes a malignant phenotype in breast cancer through angiogenic factor secretion". In: *Oncotarget* 7.43, pp. 70898–70911. DOI: 10.18632/oncotarget.12286.

Lengyel, E. et al. (2014). *Epithelial ovarian cancer experimental models*. DOI: 10.1038/onc.2013.321.

Leonard, A. N. et al. (2021a). "Fasted plasma asprosin concentrations are associated with menstrual cycle phase, oral contraceptive use and training status in healthy women". In: *European journal of applied physiology* 121.3, pp. 793–801. ISSN: 1439-6327. DOI: 10.1007/S00421-020-04570-8.

Leonard, A. N. et al. (2021b). "Fasted plasma asprosin concentrations are associated with menstrual cycle phase, oral contraceptive use and training status in healthy women". In: *Eur J Appl Physiol* 121.3, pp. 793–801. DOI: 10.1007/s00421-020-04570-8.

L'Espérance, S. et al. (2008). "Global gene expression analysis of early response to chemotherapy treatment in ovarian cancer spheroids". In: *BMC Genomics* 9.1, pp. 1–21. ISSN: 14712164. DOI: 10.1186/1471-2164-9-99.

Lheureux, S. et al. (2019). *Epithelial ovarian cancer*. DOI: 10.1016/S0140-6736(18)32552-2.

Li, B. et al. (2022a). "From musk to body odor: Decoding olfaction through genetic variation". In: *PLoS Genet* 18.2, e1009564. DOI: 10.1371/journal.pgen.1009564.

Li, E. et al. (2019). "OLFR734 Mediates Glucose Metabolism as a Receptor of Asprosin". In: *Cell Metab* 30.2, 319–328.e8. DOI: 10.1016/j.cmet.2019.05.022.

Li, M. et al. (2021). "Olfactory receptor 5B21 drives breast cancer metastasis". In: *iScience* 24.12, p. 103519. DOI: 10.1016/j.isci.2021.103519.

Li, W.-h. et al. (2015). "Detection of SNCA and FBN1 methylation in the stool as a biomarker for colorectal cancer". In: *Dis Markers* 2015, p. 657570. DOI: 10.1155/2015/657570.

Li, X. et al. (2022b). "Lactate metabolism in human health and disease". In: *Signal Transduct Target Ther* 7.1, p. 305. DOI: 10.1038/s41392-022-01151-3.

Li, X. et al. (2022c). "Spike protein mediated membrane fusion during SARS-CoV-2 infection". In: *J Med Virol*. DOI: 10.1002/jmv.28212.

Li, Y., D. Ge, and C. Lu (2019). "The SMART App: An interactive web application for comprehensive DNA methylation analysis and visualization". In: *Epigenetics and Chromatin* 12.1, p. 71. ISSN: 17568935. DOI: 10.1186/s13072-019-0316-3.

Liang, J. and Y. Shang (2013). "Estrogen and cancer". In: *Annu Rev Physiol* 75, pp. 225–40.

Lianidou, E. and K. Pantel (2019). "Liquid biopsies". In: *Genes, Chromosomes and Cancer* 58.4, pp. 219–232. ISSN: 10452257. DOI: 10.1002/gcc.22695.

Liberti, M. V. and J. W. Locasale (2016). *The Warburg Effect: How Does it Benefit Cancer Cells?* DOI: 10.1016/j.tibs.2015.12.001.

Lin, M. et al. (2020). "Genetic and molecular mechanism for distinct clinical phenotypes conveyed by allelic truncating mutations implicated in FBN1". In: *Molecular Genetics & Genomic Medicine* 8.1, p. 1023. DOI: 10.1002/MGG3.1023.

Lindheim, S. R. et al. (2018). "Ovulation Induction for the General Gynecologist". In: *Journal of Obstetrics and Gynecology of India* 68.4, pp. 242–252. ISSN: 09756434. DOI: 10.1007/S13224-018-1130-8/TABLES/2.

Lindsay, T. J. and K. R. Vitrikas (2015). "Evaluation and treatment of infertility". In: *Am Fam Physician* 91.5, pp. 308–14.

Liu, J. et al. (2022). "Prevalence of reproductive tract infections among women preparing to conceive in Chongqing, China: trends and risk factors". In: *Reproductive health* 19.1, p. 197. ISSN: 1742-4755. DOI: 10.1186/S12978-022-01502-X.

Liu, Y. et al. (2019). "Menopausal Hormone Replacement Therapy and the Risk of Ovarian Cancer: A Meta-Analysis". In: *Front Endocrinol (Lausanne)* 10, p. 801.

Loessner, D. et al. (2010). "Bioengineered 3D platform to explore cell-ECM interactions and drug resistance of epithelial ovarian cancer cells". In: *Biomaterials* 31.32, pp. 8494–8506. ISSN: 01429612. DOI: 10.1016/j.biomaterials.2010.07.064.

Long, W. et al. (2019). "Decreased Circulating Levels of Asprosin in Obese Children". In: *Hormone Research in Paediatrics* 91.4. ISSN: 16632826. DOI: 10.1159/000500523.

Loosen, S. H. et al. (2022). "Obesity and lipid metabolism disorders determine the risk for development of long COVID syndrome: a cross-sectional study from 50,402 COVID-19 patients". In: *Infection* 50.5, pp. 1165–1170. DOI: 10.1007/s15010-022-01784-0.

Lunt, S. Y. and M. G. Vander Heiden (2011). "Aerobic Glycolysis: Meeting the Metabolic Requirements of Cell Proliferation". In: *Annual Review of Cell and Developmental Biology* 27.1, pp. 441–464. ISSN: 1081-0706. DOI: 10.1146/annurev-cellbio-092910-154237.

Luo, X. et al. (2021). "Shaping Immune Responses in the Tumor Microenvironment of Ovarian Cancer". In: *Front Immunol* 12, p. 692360.

Lycke, M. et al. (2021). "Consideration should be given to smoking, endometriosis, renal function (eGFR) and age when interpreting CA125 and HE4 in ovarian tumor diagnostics". In: *Clinical chemistry and laboratory medicine* 59.12, pp. 1954–1962. ISSN: 1437-4331. DOI: 10.1515/CCLM-2021-0510.

Mackenzie, M. and S. Cohn (2022). "You Can Change a Girl's Life Today: The Truth About Periods and Endometriosis". In: *NASN Sch Nurse*, p. 1942602X221127247. DOI: 10.1177/1942602X221127247.

Macpherson, A. M. et al. (2020). "Epithelial Ovarian Cancer and the Immune System: Biology, Interactions, Challenges and Potential Advances for Immunotherapy". In: *J Clin Med* 9.9.

Maher, S. A. et al. (2018). "Serum Lactate and Mortality in Emergency Department Patients with Cancer". In: *West J Emerg Med* 19.5, pp. 827–833. DOI: 10.5811/westjem.2018.6.37295.

Mainland, J. D. et al. (2014). "The missense of smell: Functional variability in the human odorant receptor repertoire". In: *Nature Neuroscience* 17.1, pp. 114–120. ISSN: 10976256. DOI: 10.1038/nn.3598.

Mandato, V. D. and L. Aguzzoli (2020). "Management of ovarian cancer during the COVID-19 pandemic". In: *Int J Gynaecol Obstet* 149.3, pp. 382–383. DOI: 10.1002/ijgo.13167.

Manosalva, C. et al. (2021). "Role of Lactate in Inflammatory Processes: Friend or Foe". In: *Front Immunol* 12, p. 808799. DOI: 10.3389/fimmu.2021.808799.

Marchese, S. and E. Silva (2012). "Disruption of 3D MCF-12A breast cell cultures by estrogens–an in vitro model for ER-mediated changes indicative of hormonal carcinogenesis". In: *PLoS One* 7.10, e45767. DOI: 10.1371/journal.pone.0045767.

Mari, R. et al. (2019). "Liquid Biopsies for Ovarian Carcinoma: How Blood Tests May Improve the Clinical Management of a Deadly Disease". In: *Cancers (Basel)* 11.6. DOI: 10.3390/cancers11060774.

Maringe, C. et al. (2020). "The impact of the COVID-19 pandemic on cancer deaths due to delays in diagnosis in England, UK: a national, population-based, modelling study". In: *Lancet Oncol* 21.8, pp. 1023–1034. DOI: 10.1016/S1470-2045(20)30388-0.

Marrella, A. et al. (2021). "3D fluid-dynamic ovarian cancer model resembling systemic drug administration for efficacy assay". In: *ALTEX* 38.1, pp. 82–94.

Maru, Y. et al. (2019). "Efficient use of patient-derived organoids as a preclinical model for gynecologic tumors". In: *Gynecol Oncol* 154.1, pp. 189–198.

Masjedi, S., L. J. Zwiebel, and T. D. Giorgio (2019). "Olfactory receptor gene abundance in invasive breast carcinoma". In: *Scientific Reports* 9.1, pp. 1–12. ISSN: 20452322. DOI: 10.1038/s41598-019-50085-4.

Maßberg, D. and H. Hatt (2018). *Human olfactory receptors: Novel cellular functions outside of the nose*. DOI: 10.1152/PHYSREV.00013.2017.

Matulonis, U. A. et al. (2016). "Ovarian cancer". In: *Nature Reviews Disease Primers* 2, pp. 1–22. ISSN: 2056676X. DOI: 10.1038/nrdp.2016.61.

Maurer, T. et al. (2020). "An exercise and nutrition intervention for ovarian cancer patients during and after first-line chemotherapy (BENITA study): A randomized controlled pilot trial". In: *International Journal of Gynecological Cancer* 30.4, pp. 541–545. ISSN: 15251438. DOI: 10.1136/ijgc-2019-000585.

Maurya, S. and A. Singh (2022). "Asprosin modulates testicular functions during ageing in mice". In: *Gen Comp Endocrinol* 323-324, p. 114036. DOI: 10.1016/j.ygcen.2022.114036.

Maylem, E. R. S. et al. (2021). "Discovery of a possible role of asprosin in ovarian follicular function". In: *Journal of Molecular Endocrinology* 66.1, pp. 35–44. ISSN: 14796813. DOI: 10.1530/JME-20-0218.

Maylem, E. R. S. et al. (2022). "A potential role of fibrillin-1 (FBN1) mRNA and asprosin in follicular development in water buffalo". In: *Theriogenology* 178, pp. 67–72. DOI: 10.1016/j.theriogenology.2021.11.004.

Mazur-Bialy, A. I. (2021). "Asprosin-A Fasting-Induced, Glucogenic, and Orexigenic Adipokine as a New Promising Player. Will It Be a New Factor in the Treatment of Obesity, Diabetes, or Infertility? A Review of the Literature". In: *Nutrients* 13.2. DOI: 10.3390/nu13020620.

McCaughan, H. M., R. Z. McRae, and H. K. Smith (2000). "The stability of lactate concentration in preserved blood microsamples". In: *Int J Sports Med* 21.1, pp. 37–40.

McGonigle, P. and B. Ruggeri (2014). *Animal models of human disease: Challenges in enabling translation*. DOI: 10.1016/j.bcp.2013.08.006.

McLean, K. and G. Mehta (2017). "Tumor Microenvironment and Models of Ovarian Cancer: The 11th Biennial Rivkin Center Ovarian Cancer Research Symposium". In: *International journal of gynecological cancer : official journal of the International Gynecological Cancer Society*. Vol. 27. 9S Suppl 5. NLM (Medline), S2–S9. DOI: 10.1097/IGC.0000000000001119.

Medina, M. Á. (2018). *Mathematical modeling of cancer metabolism*. DOI: 10.1016/j.critrevonc.2018.02.004.

Meehan, M. et al. (2012). "Protein tyrosine phosphatase receptor delta acts as a neuroblastoma tumor suppressor by destabilizing the aurora kinase A oncogene". In: *Mol Cancer* 11, p. 6. DOI: 10.1186/1476-4598-11-6.

Messinis, I. E., C. I. Messini, and K. Dafopoulos (2014). *Novel aspects of the endocrinology of the menstrual cycle*. DOI: 10.1016/j.rbmo.2014.02.003.

Milewicz, D. M. et al. (1995). "A mutation in FBN1 disrupts profibrillin processing and results in isolated skeletal features of the Marian syndrome". In: *Journal of Clinical Investigation* 95.5, pp. 2373–2378. ISSN: 00219738. DOI: 10.1172/JCI117930.

Mishra, D. K. et al. (2012). "Human lung cancer cells grown in an ex vivo 3D lung model produce matrix metalloproteinases not produced in 2D culture". In: *PLoS One* 7.9, e45308. DOI: 10.1371/journal.pone.0045308.

Mishra, I. et al. (2022). "Protein tyrosine phosphatase receptor δ serves as the orexigenic asprosin receptor". In: *Cell metabolism* 34.4, 549–563.e8. ISSN: 1932-7420. DOI: 10.1016/J.CMET.2022.02.012.

Monzer, A. et al. (2022). "Novel therapeutic diiminoquinone exhibits anticancer effects on human colorectal cancer cells in two-dimensional and three-dimensional

in vitro models". In: *World J Gastroenterol* 28.33, pp. 4787–4811. DOI: 10.3748/wjg.v28.i33.4787.

Moorman, P. G. et al. (2016). "Reproductive factors and ovarian cancer risk in African-American women". In: *Annals of Epidemiology* 26.9, pp. 654–662. ISSN: 18732585. DOI: 10.1016/j.annepidem.2016.07.004.

Morcos, Y. A. T. et al. (2022). "Sensitive asprosin detection in clinical samples reveals serum/saliva correlation and indicates cartilage as source for serum asprosin". In: *Sci Rep* 12.1, p. 1340. DOI: 10.1038/s41598-022-05060-x.

Morita, R. et al. (2016). "Olfactory receptor family 7 subfamily C member 1 is a novel marker of colon cancer-initiating cells and is a potent target of immunotherapy". In: *Clinical Cancer Research* 22.13, pp. 3298–3309. ISSN: 15573265. DOI: 10.1158/1078-0432.CCR-15-1709.

Muz, B. et al. (2015). "The role of hypoxia in cancer progression, angiogenesis, metastasis, and resistance to therapy". In: *Hypoxia (Auckl)* 3, pp. 83–92. DOI: 10.2147/HP.S93413.

Myungjin Lee, J. et al. (2013). "A three-dimensional microenvironment alters protein expression and chemosensitivity of epithelial ovarian cancer cells in vitro". In: *Laboratory Investigation* 93.5, pp. 528–542. ISSN: 00236837. DOI: 10.1038/labinvest.2013.41.

N, H. et al. (2012). "Menarche, menopause, and breast cancer risk: individual participant meta-analysis, including 118 964 women with breast cancer from 117 epidemiological studies". In: *Lancet Oncol* 13.11, pp. 1141–51.

Nakashima, A. et al. (2013). "XAgonist-independent GPCR activity regulates anterior-posterior targeting of olfactory sensory neurons". In: *Cell* 154.6, pp. 1314–1325. ISSN: 00928674. DOI: 10.1016/j.cell.2013.08.033.

Nalbandian, M., Z. Radak, and M. Takeda (2018). "Evaluation of Blood Lactate and Plasma Insulin During High-intensity Exercise by Antecubital Vein Catheterization". In: *J Vis Exp* 135. DOI: 10.3791/56890.

Nam, H. et al. (2022). "A Serum Marker for Early Pancreatic Cancer With a Possible Link to Diabetes". In: *Journal of the National Cancer Institute* 114.2, pp. 228–234. ISSN: 1460-2105. DOI: 10.1093/JNCI/DJAB191.

Neuhaus, E. M. et al. (2009). "Activation of an olfactory receptor inhibits proliferation of prostate cancer cells". In: *Journal of Biological Chemistry* 284.24, pp. 16218–16225. ISSN: 00219258. DOI: 10.1074/jbc.M109.012096.

Neuhaus, W. et al. (2022). "The Rise of Three Rs Centres and Platforms in Europe". In: *Altern Lab Anim* 50.2, pp. 90–120. DOI: 10.1177/02611929221099165.

O'Neill, B. et al. (2007). "Body fat distribution and metabolic variables in patients with neonatal progeroid syndrome". In: *American Journal of Medical Genetics Part A* 143A.13, pp. 1421–1430. ISSN: 15524825. DOI: 10.1002/ajmg.a.31840.

Ornell, K. J. et al. (2019). "Three-Dimensional, Scaffolded Tumor Model to Study Cell-Driven Microenvironment Effects and Therapeutic Responses". In: *ACS Biomater Sci Eng* 5.12, pp. 6742–6754.

Pache, B. et al. (2022). "[Human Papillomavirus: screening of cervical and anal cancers]". In: *Rev Med Suisse* 18.800, pp. 1950–1955. DOI: 10.53738/REVMED.2022.18.800.1950.

Paterlini-Brechot, P. and N. L. Benali (2007). *Circulating tumor cells (CTC) detection: Clinical impact and future directions*. DOI: 10.1016/j.canlet.2006.12.014.

Paul, A. and S. Paul (2014). "The breast cancer susceptibility genes (BRCA) in breast and ovarian cancers". In: *Frontiers in bioscience (Landmark edition)* 19.4, pp. 605–618. ISSN: 2768-6698. DOI: 10.2741/4230.

Pearce, C. L. et al. (2012). "Association between endometriosis and risk of histological subtypes of ovarian cancer: A pooled analysis of case-control studies". In: *The Lancet Oncology* 13.4, pp. 385–394. ISSN: 14702045. DOI: 10.1016/S1470-2045(11)70404-1.

Pelizzoni, G. and S. Scaglione (2023). "3D Human Tumor Tissues Cultured in Dynamic Conditions as Alternative In Vitro Disease Models". In: *Methods Mol Biol* 2572, pp. 203–210. DOI: 10.1007/978-1-0716-2703-7_16.

Pellegrino, R. et al. (2020). "Coronaviruses and the Chemical Senses: Past, Present, and Future". In: *Chemical Senses*. ISSN: 1464-3553. DOI: 10.1093/chemse/bjaa031.

Peng, R. et al. (2021). "Cell entry by SARS-CoV-2". In: *Trends Biochem Sci* 46.10, pp. 848–860. DOI: 10.1016/j.tibs.2021.06.001.

Pérez-Tomás, R. and I. Pérez-Guillén (2020). "Lactate in the Tumor Microenvironment: An Essential Molecule in Cancer Progression and Treatment". In: *Cancers (Basel)* 12.11. DOI: 10.3390/cancers12113244.

Piekos, J. A. et al. (2022). "Uterine fibroid polygenic risk score (PRS) associates and predicts risk for uterine fibroid". In: *Hum Genet* 141.11, pp. 1739–1748. DOI: 10.1007/s00439-022-02442-z.

Pink, R. C. and D. R. F. Carter (2013). "Pseudogenes as regulators of biological function". In: *Essays Biochem* 54, pp. 103–12.

Pink, R. C. et al. (2022). "Utilising extracellular vesicles for early cancer diagnostics: benefits, challenges and recommendations for the future". In: *Br J Cancer* 126.3, pp. 323–330.

Pizzuti, L. et al. (2018). "GLUT 1 receptor expression and circulating levels of fasting glucose in high grade serous ovarian cancer". In: *Journal of Cellular Physiology* 233.2, pp. 1396–1401. ISSN: 00219541. DOI: 10.1002/jcp.26023.

Pokhriyal, R. et al. (2019). "Chemotherapy Resistance in Advanced Ovarian Cancer Patients". In: *https://doi.org/10.1177/1179299X19860815* 11, p. 1179299X1986081. ISSN: 1179-299X. DOI: 10.1177/1179299X19860815.

Preston, C. C. et al. (2011). "Immunity and immune suppression in human ovarian cancer". In: *Immunotherapy* 3.4, p. 539. ISSN: 1750743X. DOI: 10.2217/IMT.11.20.

Pronin, A. and V. Slepak (2021). "Ectopically expressed olfactory receptors OR51E1 and OR51E2 suppress proliferation and promote cell death in a prostate cancer cell line". In: 296, p. 100475.

Qin, T. et al. (2022). "Harnessing preclinical models for the interrogation of ovarian cancer". In: *J Exp Clin Cancer Res* 41.1, p. 277. DOI: 10.1186/s13046-022-02486-z.

Qiu, W. et al. (2016). "Dietary fat intake and ovarian cancer risk: a meta-analysis of epidemiological studies". In: *Oncotarget* 7.24, pp. 37390–37406.

Qu, N. et al. (2022). "Superior anticancer potential of nano-paclitaxel combined bevacizumab treatment in ovarian cancer". In: *Curr Pharm Biotechnol*. DOI: 10.2174/1389201023666221011115301.

Ray-Coquard, I. et al. (2019). "Olaparib plus Bevacizumab as First-Line Maintenance in Ovarian Cancer". In: *N Engl J Med* 381.25, pp. 2416–2428. DOI: 10.1056/NEJMoa1911361.

Rehli, M. (2002). "Of mice and men: species variations of Toll-like receptor expression". In: *Trends Immunol* 23.8, pp. 375–8. DOI: 10.1016/s1471-4906(02)02259-7.

Reid, B. M., J. B. Permuth, and T. A. Sellers (2017). *Epidemiology of ovarian cancer: a review*. DOI: 10.20892/j.issn.2095-3941.2016.0084.

Ribatti, D. (2022). "Immunosuppressive effects of vascular endothelial growth factor". In: *Oncology letters* 24.4. ISSN: 1792-1082. DOI: 10.3892/OL.2022.13489.

Rimon-Dahari, N. et al. (2016). "Ovarian folliculogenesis". In: *Results and Problems in Cell Differentiation* 58, pp. 167–190. ISSN: 18610412. DOI: 10.1007/978-3-319-31973-5_7.

Robinson, N. B. et al. (2019). "The current state of animal models in research: A review". In: *Int J Surg* 72, pp. 9–13. DOI: 10.1016/j.ijsu.2019.10.015.

Rodríguez-Gutiérrez, R., A. Salcido-Montenegro, and J. G. González-González (2018). "Early Clinical Expressions of Insulin Resistance: The Real Enemy to Look For". In: *Diabetes Ther* 9.1, pp. 435–438. DOI: 10.1007/s13300-017-0348-2.

Roland, C. L. et al. (2014). "Cell surface lactate receptor GPR81 is crucial for cancer cell survival". In: *Cancer Res* 74.18, pp. 5301–10.

Romere, C. et al. (2016). "Asprosin, a Fasting-Induced Glucogenic Protein Hormone". In: *Cell* 165.3, pp. 566–579. ISSN: 10974172. DOI: 10.1016/j.cell.2016.02.063.

Rose, M. et al. (2020). "PARP Inhibitors: Clinical Relevance, Mechanisms of Action and Tumor Resistance". In: *Front Cell Dev Biol* 8, p. 564601. DOI: 10.3389/fcell.2020.564601.

Roth, G. A. et al. (2020). "Global Burden of Cardiovascular Diseases and Risk Factors, 1990–2019: Update From the GBD 2019 Study". In: *Journal of the American College of Cardiology* 76.25, pp. 2982–3021. ISSN: 0735-1097. DOI: 10.1016/J.JACC.2020.11.010.

Roy, R., J. Chun, and S. N. Powell (2011). "BRCA1 and BRCA2: different roles in a common pathway of genome protection". In: *Nat Rev Cancer* 12.1, pp. 68–78. DOI: 10.1038/nrc3181.

Russell, B. et al. (2021). "Risk of COVID-19 death in cancer patients: an analysis from Guy's Cancer Centre and King's College Hospital in London". In: *Br J Cancer* 125.7, pp. 939–947. DOI: 10.1038/s41416-021-01500-z.

Rybinski, B. et al. (2020). "Preclinical Metrics Correlate With Drug Activity in Phase II Trials of Targeted Therapies for Non-Small Cell Lung Cancer". In: *Front Oncol* 10, p. 587377. DOI: 10.3389/fonc.2020.587377.

Sachan, P. L. et al. (2018). "A Study on Cervical Cancer Screening Using Pap Smear Test and Clinical Correlation". In: *Asia Pac J Oncol Nurs* 5.3, pp. 337–341. DOI: 10.4103/apjon.apjon_15_18.

Salas-Benito, D. et al. (2020). "Inflammation and immunity in ovarian cancer". In: *EJC Suppl* 15, pp. 56–66.

Saunders, J. A. et al. (2010). "Reactive oxygen species mediate lysophosphatidic acid induced signaling in ovarian cancer cells". In: *Free Radic Biol Med* 49.12, pp. 2058–67. DOI: 10.1016/j.freeradbiomed.2010.10.663.

Schliep, K. C. et al. (2022). "Endometriosis diagnosis, staging and typology and adverse pregnancy outcome history". In: *Paediatric and perinatal epidemiology* 36.6. ISSN: 1365-3016. DOI: 10.1111/PPE.12887.

Shen, F. et al. (2017). "The prevalence of malignant and borderline ovarian cancer in pre- and post-menopausal Chinese women". In: *Oncotarget* 8.46, pp. 80589–80594. ISSN: 19492553. DOI: 10.18632/oncotarget.20384.

Shestov, A. A. et al. (2014). "Quantitative determinants of aerobic glycolysis identify flux through the enzyme GAPDH as a limiting step". In: *eLife* 3.July2014, pp. 1–18. ISSN: 2050084X. DOI: 10.7554/eLife.03342.

Siegel, R. L., K. D. Miller, and A. Jemal (2019). "Cancer statistics, 2019". In: *CA: A Cancer Journal for Clinicians* 69.1, pp. 7–34. ISSN: 1542-4863. DOI: 10.3322/CAAC.21551.

Silveira, H. S. et al. (2020). "P-MAPA activates TLR2 and TLR4 signaling while its combination with IL-12 stimulates CD4+ and CD8+ effector T cells in ovarian cancer". In: *Life Sci* 254, p. 117786.

Simmons, R. (2005). "Developmental origins of adult metabolic disease: concepts and controversies". In: *Trends Endocrinology Metabolism* 16.8, pp. 390–4. DOI: 10.1016/j.tem.2005.08.004.

Sims, O. T. et al. (2021). "Stigma and Endometriosis: A Brief Overview and Recommendations to Improve Psychosocial Well-Being and Diagnostic Delay". In: *Int J Environ Res Public Health* 18.15. DOI: 10.3390/ijerph18158210.

Singh, N. et al. (2019). "Inflammation and cancer". In: *Ann Afr Med* 18.3, pp. 121–126.

Slatnik, C. L. and E. Duff (2015). "Ovarian cancer: Ensuring early diagnosis". In: *Nurse Practitioner* 40.9, pp. 47–54. ISSN: 15388662. DOI: 10.1097/01.NPR.0000450742.00077.a2.

Sohrabi, C. et al. (2020). "World Health Organization declares global emergency: A review of the 2019 novel coronavirus (COVID-19)". In: *International Journal of Surgery* 76, pp. 71–76. ISSN: 1743-9191. DOI: 10.1016/J.IJSU.2020.02.034.

Spehr, M. and S. D. Munger (2009). *Olfactory receptors: G protein-coupled receptors and beyond*. DOI: 10.1111/j.1471-4159.2009.06085.x.

Stasiak, M. et al. (2021). "The World of Pseudogenes: New Diagnostic and Therapeutic Targets in Cancers or Still Mystery Molecules?" In: *Life (Basel)* 11.12.

Sun, H. et al. (2019). "Global, regional, and national prevalence and disability-adjusted life-years for infertility in 195 countries and territories, 1990-2017: results from a global burden of disease study, 2017". In: *Aging (Albany NY)* 11.23, pp. 10952–10991. DOI: 10.18632/aging.102497.

Sun, W. et al. (2016). "Association of insulin resistance with breast, ovarian, endometrial and cervical cancers in non-diabetic women". In: *American Journal of Cancer Research* 6.10, pp. 2334–2344. ISSN: 21566976.

Sung, H. et al. (2021). "Global Cancer Statistics 2020: GLOBOCAN Estimates of Incidence and Mortality Worldwide for 36 Cancers in 185 Countries". In: *CA: A Cancer Journal for Clinicians* 71.3, pp. 209–249. ISSN: 0007-9235. DOI: 10.3322/CAAC.21660.

Sungnak, W. et al. (2020). "SARS-CoV-2 entry factors are highly expressed in nasal epithelial cells together with innate immune genes". In: *Nat Med* 26.5, pp. 681–687. DOI: 10.1038/s41591-020-0868-6.

Tao, X. et al. (2009). "Anti-angiogenesis therapy with bevacizumab for patients with ovarian granulosa cell tumors". In: *Gynecol Oncol* 114.3, pp. 431–6. DOI: 10.1016/j.ygyno.2009.04.021.

Taylor, L. (2022). "Covid-19: True global death toll from pandemic is almost 15 million, says WHO". In: *BMJ* 377, o1144. DOI: 10.1136/bmj.o1144.

Tchounwou, P. B. et al. (2021). "Advances in Our Understanding of the Molecular Mechanisms of Action of Cisplatin in Cancer Therapy". In: *J Exp Pharmacol* 13, pp. 303–328. DOI: 10.2147/JEP.S267383.

Thériault, B. L. and M. W. Nachtigal (2011). "Human ovarian cancer cell morphology, motility, and proliferation are differentially influenced by autocrine TGFbeta superfamily signalling". In: *Cancer Letters* 313.1, pp. 108–121. ISSN: 03043835. DOI: 10.1016/j.canlet.2011.08.033.

Tidwell, T. R. et al. (2022). "Metabolic flux analysis of 3D spheroids reveals significant differences in glucose metabolism from matched 2D cultures of colorectal cancer and pancreatic ductal adenocarcinoma cell lines". In: *Cancer Metab* 10.1, p. 9.

Tofani, L. B. et al. (2021). "Generation of a Three-Dimensional in Vitro Ovarian Cancer Co-Culture Model for Drug Screening Assays". In: *Journal of Pharmaceutical Sciences* 0.0. ISSN: 00223549. DOI: 10.1016/j.xphs.2021.04.003.

Tomita, H. et al. (2020). "The Protein Tyrosine Phosphatase Receptor Delta Regulates Developmental Neurogenesis". In: *Cell Rep* 30.1, 215–228.e5. DOI: 10.1016/j.celrep.2019.11.033.

Toutain, P.-L., A. Ferran, and A. Bousquet-Mélou (2010). "Species differences in pharmacokinetics and pharmacodynamics". In: *Handb Exp Pharmacol* 199, pp. 19–48. DOI: 10.1007/978-3-642-10324-7_2.

Tratar, U. L., S. Horvat, and M. Cemazar (2018). *Transgenic mouse models in cancer research*. DOI: 10.3389/fonc.2018.00268.

Troisi, R. et al. (2018). "Estrogen Metabolism in Postmenopausal Women Exposed In Utero to Diethylstilbestrol". In: *Cancer Epidemiol Biomarkers Prev* 27.10, pp. 1208–1213. DOI: 10.1158/1055-9965.EPI-18-0135.

Tsang, S. I. et al. (2022). "Experimental models for ovarian cancer research". In: *Exp Cell Res* 416.1, p. 113150. DOI: 10.1016/j.yexcr.2022.113150.

Tu, Q. et al. (2015). "CellSearch technology applied to the detection and quantification of tumor cells in CSF of patients with lung cancer leptomeningeal metastasis". In: *Lung Cancer* 90.2, pp. 352–7. DOI: 10.1016/j.lungcan.2015.09.008.

Ugur, K et al. (2022). "Asprosin, visfatin and subfatin as new biomarkers of obesity and metabolic syndrome". In: *Eur Rev Med Pharmacol Sci* 26.6, pp. 2124–2133. DOI: 10.26355/eurrev_202203_28360.

Van Norman, G. A. (2019). "Limitations of Animal Studies for Predicting Toxicity in Clinical Trials: Is it Time to Rethink Our Current Approach?" In: *JACC Basic Transl Sci* 4.7, pp. 845–854. DOI: 10.1016/j.jacbts.2019.10.008.

Vander Heiden, M. G., L. C. Cantley, and C. B. Thompson (2009). "Understanding the Warburg effect: the metabolic requirements of cell proliferation". In: *Science* 324.5930, pp. 1029–33. DOI: 10.1126/science.1160809.

Vaure, C. and Y. Liu (2014). "A comparative review of toll-like receptor 4 expression and functionality in different animal species". In: *Front Immunol* 5, p. 316. DOI: 10.3389/fimmu.2014.00316.

Veitinger, S. and H. Hatt (2017). "Ectopic Expression of Mammalian Olfactory Receptors". In: *Springer Handbooks*. Springer, pp. 83–84. DOI: 10.1007/978-3-319-26932-0_33.

Vergara, D. et al. (2010). "Epithelial-mesenchymal transition in ovarian cancer". In: *Cancer Lett* 291.1, pp. 59–66. DOI: 10.1016/j.canlet.2009.09.017.

Vigneswaran, K. and H. Hamoda (2022). "Hormone replacement therapy - Current recommendations". In: *Best Pract Res Clin Obstet Gynaecol* 81, pp. 8–21.

Villarreal, I. M. et al. (2021). "Olfactory and taste disorders in healthcare workers with COVID-19 infection". In: *Eur Arch Otorhinolaryngol* 278.6, pp. 2123–2127. DOI: 10.1007/s00405-020-06237-8.

Wacharasint, P. et al. (2012). "Normal-range blood lactate concentration in septic shock is prognostic and predictive". In: *Shock* 38.1, pp. 4–10. ISSN: 10732322. DOI: 10.1097/SHK.0B013E318254D41A.

Wagner, W. et al. (2017). "The lactate receptor (HCAR1/GPR81) contributes to doxorubicin chemoresistance via ABCB1 transporter up-regulation in human cervical cancer HeLa cells". In: *Journal of physiology and pharmacology : an official journal of the Polish Physiological Society* 68.4, pp. 555–564. ISSN: 1899-1505.

Wang, M. et al. (2020). "Serum Asprosin Concentrations Are Increased and Associated with Insulin Resistance in Children with Obesity". In: *Annals of Nutrition and Metabolism* 75.4, pp. 205–212. ISSN: 14219697. DOI: 10.1159/000503808.

Wang, Y., B. X. Li, and X. Li (2021). "Identification and Validation of Angiogenesis-Related Gene Expression for Predicting Prognosis in Patients With Ovarian Cancer". In: *Front Oncol* 11, p. 783666. DOI: 10.3389/fonc.2021.783666.

Wang, Y. et al. (2018). "Plasma Asprosin Concentrations Are Increased in Individuals with Glucose Dysregulation and Correlated with Insulin Resistance and First-Phase Insulin Secretion". In: *Mediators Inflamm* 2018, p. 9471583. DOI: 10.1155/2018/9471583.

Wang, Z. H. et al. (2019). "Identification of novel cell glycolysis related gene signature predicting survival in patients with endometrial cancer". In: *Cancer Cell International* 19.1. ISSN: 14752867. DOI: 10.1186/S12935-019-1001-0.

Wang, Z. et al. (2015). "Fibrillin-1, induced by Aurora-A but inhibited by BRCA2, promotes ovarian cancer metastasis". In: *Oncotarget* 6.9, pp. 6670–6683. ISSN: 19492553. DOI: 10.18632/oncotarget.3118.

Warburg, O., F. Wind, and E. Negelein (1927). "The metabolism of tumors in the body". In: *Journal of General Physiology* 8.6, pp. 519–530. ISSN: 15407748. DOI: 10.1085/jgp.8.6.519.

Webb, P. M. and S. J. Jordan (2017). *Epidemiology of epithelial ovarian cancer*. DOI: 10.1016/j.bpobgyn.2016.08.006.

Weber, L. et al. (2017). "Activation of odorant receptor in colorectal cancer cells leads to inhibition of cell proliferation and apoptosis". In: *PLoS One* 12.3, e0172491. DOI: 10.1371/journal.pone.0172491.

Wei, F., A. Long, and Y. Wang (2019). *The Asprosin-OLFR734 hormonal signaling axis modulates male fertility*. DOI: 10.1038/s41421-019-0122-x.

White, E. A., H. A. Kenny, and E. Lengyel (2014). "Three-dimensional modeling of ovarian cancer". In: *Adv Drug Deliv Rev* 79-80, pp. 184–92. DOI: 10.1016/j.addr.2014.07.003.

Wicha, M. S. and D. F. Hayes (2011). "Circulating tumor cells: not all detected cells are bad and not all bad cells are detected". In: *J Clin Oncol* 29.12, pp. 1508–11. DOI: 10.1200/JCO.2010.34.0026.

Wiecek, M. et al. (2018). "Acute Anaerobic Exercise Affects the Secretion of Asprosin, Irisin, and Other Cytokines - A Comparison Between Sexes". In: *Front Physiol* 9, p. 1782. DOI: 10.3389/fphys.2018.01782.

Wu, L. et al. (2019). "Loss of Tyrosine Phosphatase Delta Promotes Gastric Cancer Progression via Signal Transducer and Activator of Transcription 3 Pathways". In: *Dig Dis Sci* 64.11, pp. 3164–3172. DOI: 10.1007/s10620-019-05637-z.

Wu, P.-Y. et al. (2020). "Real-World Study of Adding Bevacizumab to Chemotherapy for Ovarian, Tubal, and Peritoneal Cancer as Front-Line or Relapse Therapy (ROBOT): 8-Year Experience". In: *Front Oncol* 10, p. 1095. DOI: 10.3389/fonc.2020.01095.

Xia, P. and A. Dubrovska (2020). "Tumor markers as an entry for SARS-CoV-2 infection?" In: *FEBS J* 287.17, pp. 3677–3680. DOI: 10.1111/febs.15499.

Xiao, S. et al. (2017). "A microfluidic culture model of the human reproductive tract and 28-day menstrual cycle". In: *Nature Communications* 8.1, pp. 1–13. ISSN: 20411723. DOI: 10.1038/ncomms14584.

Xie, J. et al. (2014). "Beyond Warburg effect - Dual metabolic nature of cancer cells". In: *Scientific Reports* 4. ISSN: 20452322. DOI: 10.1038/srep04927.

Xie, Q., X. Meng, and Q. Liao (2022). "Oncologic outcomes of fertility-sparing surgery in early stage epithelial ovarian cancer: a population-based propensity score-matched analysis". In: *Archives of gynecology and obstetrics* 306.5. ISSN: 1432-0711. DOI: 10.1007/S00404-022-06536-X.

Xintaropoulou, C. et al. (2018). "Expression of glycolytic enzymes in ovarian cancers and evaluation of the glycolytic pathway as a strategy for ovarian cancer treatment". In: *BMC Cancer* 18.1. ISSN: 14712407. DOI: 10.1186/s12885-018-4521-4.

Yanagawa, H. et al. (2022). "The development of a novel antioxidant-based antiemetic drug to improve quality of life during anticancer therapy". In: *Biochem Biophys Rep* 32, p. 101363. DOI: 10.1016/j.bbrep.2022.101363.

Yang, Y.-P., T. M. Giret, and R. J. Cote (2021). "Circulating Tumor Cells from Enumeration to Analysis: Current Challenges and Future Opportunities". In: *Cancers (Basel)* 13.11. DOI: 10.3390/cancers13112723.

Yaryari, A. mohammad et al. (Mar. 2022). "Evaluation of serum levels of asprosin and other metabolic profiles in patients with idiopathic tonic-clonic generalized

epilepsy on treatment with valproic acid". In: *European journal of clinical pharmacology* 78 (3), pp. 393–403. ISSN: 1432-1041. DOI: 10.1007/S00228-022-03279-1.

Yu, H. et al. (2023). "Expert consensus on oncological [18F]FDG total-body PET/CT imaging (version 1)". In: *Eur Radiol* 33.1, pp. 615–626.

Yu, X. et al. (2017). "Protein tyrosine phosphatase receptor-type D acts as a negative regulator suppressing breast cancer". In: *Oncotarget* 8.58, pp. 98798–98811. DOI: 10.18632/oncotarget.22000.

Yu, Y. et al. (2020). "Placensin is a glucogenic hormone secreted by human placenta". In: *EMBO reports* 21.6. ISSN: 1469-221X. DOI: 10.15252/embr.201949530.

Zhai, X. et al. (2017). "Colon cancer recurrence-associated genes revealed by WGCNA co-expression network analysis". In: *Molecular Medicine Reports* 16.5, pp. 6499–6505. ISSN: 17913004. DOI: 10.3892/mmr.2017.7412.

Zhang, B. et al. (2018). *Advances in organ-on-a-chip engineering*. DOI: 10.1038/s41578-018-0034-7.

Zhang, G.-Q. et al. (2021). "Menopausal hormone therapy and women's health: An umbrella review". In: *PLoS Med* 18.8, e1003731.

Zhang, L. et al. (2019a). "Circulating asprosin concentrations are increased in type 2 diabetes mellitus and independently associated with fasting glucose and triglyceride". In: *Clin Chim Acta* 489, pp. 183–188. DOI: 10.1016/j.cca.2017.10.034.

– (2019b). "Circulating asprosin concentrations are increased in type 2 diabetes mellitus and independently associated with fasting glucose and triglyceride". In: *Clinica Chimica Acta* 489, pp. 183–188. ISSN: 18733492. DOI: 10.1016/j.cca.2017.10.034.

Zhang, R. et al. (2020). "Nobiletin Triggers Reactive Oxygen Species-Mediated Pyroptosis through Regulating Autophagy in Ovarian Cancer Cells". In: *J Agric Food Chem* 68.5, pp. 1326–1336. DOI: 10.1021/acs.jafc.9b07908.

Zhang, Z. et al. (2019c). "Asprosin improves the survival of mesenchymal stromal cells in myocardial infarction by inhibiting apoptosis via the activated ERK1/2-SOD2 pathway". In: *Life Sciences* 231. ISSN: 18790631. DOI: 10.1016/j.lfs.2019.116554.

Zhao, B. et al. (2022a). "TLR4 Agonist and Hypoxia Synergistically Promote the Formation of TLR4/NF-kB/HIF-1a Loop in Human Epithelial Ovarian Cancer". In: *Anal Cell Pathol (Amst)* 2022, p. 4201262. DOI: 10.1155/2022/4201262.

Zhao, E. et al. (2016). "Cancer mediates effector T cell dysfunction by targeting microRNAs and EZH2 via glycolysis restriction". In: *Nat Immunol* 17.1, pp. 95–103.

Zhao, H. et al. (2022b). "Fusion-inhibition peptide broadly inhibits influenza virus and SARS-CoV-2, including Delta and Omicron variants". In: *Emerg Microbes Infect* 11.1, pp. 926–937. DOI: 10.1080/22221751.2022.2051753.

Zhao, W. et al. (2013). "Decreased level of olfactory receptors in blood cells following traumatic brain injury and potential association with tauopathy". In: *Journal of Alzheimer's Disease* 34.2, pp. 417–429. ISSN: 18758908. DOI: 10.3233/JAD-121894.

Zhou, X. et al. (2021). "LINC02532 Contributes to Radiosensitivity in Clear Cell Renal Cell Carcinoma through the miR-654-5p/YY1 Axis". In: *Molecules (Basel, Switzerland)* 26.22. ISSN: 1420-3049. DOI: 10.3390/MOLECULES26227040.

Zietarska, M. et al. (2007). "Molecular description of a 3D in vitro model for the study of epithelial ovarian cancer (EOC)". In: *Molecular Carcinogenesis* 46.10, pp. 872–885. ISSN: 08991987. DOI: 10.1002/mc.20315.

Zou, J. et al. (2022). "Identification of key genes associated with polycystic ovary syndrome (PCOS) and ovarian cancer using an integrated bioinformatics analysis". In: *J Ovarian Res* 15.1, p. 30. DOI: 10.1186/s13048-022-00962-w.

Zozulya, S., F. Echeverri, and T. Nguyen (2001). "The human olfactory receptor repertoire." In: *Genome biology* 2.6, research0018.1. ISSN: 14656914. DOI: 10.1186/gb-2001-2-6-research0018.

Zucker, I. and A. K. Beery (June 2010). "Males still dominate animal studies". In: *Nature* 465 (7299), p. 690. ISSN: 1476-4687. DOI: 10.1038/465690A.